University of Ioannina

School of Sciences
Department of Physics

Division of Theoretical Physics

# Effective Field Theory as a probe for Physics Beyond the Standard Model

Konstantinos Mantzaropoulos

PhD Thesis

Ioannina 2024

Πανεπιστήμιο Ιωαννίνων

Σχολή Θετικών Επιστημών
Τμήμα Φυσικής

Τομέας Θεωρητικής Φυσικής

# Η Ενεργός Θεωρία Πεδίου ως Εργαλείο Εξερεύνησης Φυσικής πέρα από το Καθιερωμένο Πρότυπο

ΚΩΝΣΤΑΝΤΙΝΟΣ ΜΑΝΤΖΑΡΟΠΟΥΛΟΣ

ΔΙΔΑΚΤΟΡΙΚΗ ΔΙΑΤΡΙΒΗ

ΙΩΑΝΝΙΝΑ 2024

# *PhD Committee*

**Three-member PhD advisory committe**

- A. Dedes (Supervisor), Professor, Physics Department, University of Ioannina, Greece
- G. Leontaris, Professor Emeritus, Physics Department, University of Ioannina, Greece
- I. Rizos, Professor, Physics Department, University of Ioannina, Greece

**Seven-member PhD examination committee**

- A. Dedes (Supervisor), Professor, Physics Department, University of Ioannina, Greece
- G. Leontaris, Professor Emeritus, Physics Department, University of Ioannina, Greece
- I. Rizos, Professor, Physics Department, University of Ioannina, Greece
- L. Perivolaropoulos, Professor, Physics Department, University of Ioannina, Greece
- P. Kanti, Professor, Physics Department, University of Ioannina, Greece
- C. Foudas, Professor, Physics Department, University of Ioannina, Greece
- J. Rosiek, Professor, Faculty of Physics, University of Warsaw, Poland

# *Acknowledgements*

First and foremost, I would like to thank my PhD supervisor, Prof. Athanasios Dedes, for his guidance and support throughout this journey, as well as for numerous stimulating conversations about physics. I am also grateful to Prof. Janusz Rosiek. It was my pleasure to work alongside him and hear all about his trips. I would also like to warmly thank my friend and colleague, Lampros Trifyllis, without whom all those trips to workshops, schools, and conferences would have been dull. His numerous discussions and support throughout the PhD were invaluable. My gratitude also extends to all the funding bodies and individuals who financially supported those trips in one way or another. Finally, I would like to thank Ajdin Palavrić for his calculational prowess; together, we made fruitful efforts on projects, even if they did not ultimately come to fruition.

Apart from academic life, I would like to thank my partner, Vasiliki, for her support and understanding throughout these years. I also would like to thank all my friends and family who have put up with me, and I extend my apologies to them for not having a definite answer to the question of when this PhD will be completed.

Lastly, I would like to thank the Research Committee of the University of Ioannina for awarding me two scholarships at the start of my PhD, which greatly supported the initial stages of this thesis.

# *Abstract*

The main topic of this thesis is the study of Standard Model (SM) extensions within the framework of Effective Field Theory (EFT), where it is assumed that undiscovered particles exist at energies higher than those accessible to current experiments. There are two ways to utilize EFTs for making meaningful predictions. The first is the top-down approach, where the ultraviolet (UV) physics model is known, and our goal is to determine the effects of heavy particles in the low-energy (infrared, or IR) regime via a process known as matching. In contrast, the bottom-up approach is agnostic about the UV model; our starting point is the EFT Lagrangian, and our main concern is to constrain the free parameters in the low-energy EFT as much as possible using experimental data, thereby extracting hints about the dynamics that may describe the processes in the UV. Both approaches have their advantages and disadvantages, and this thesis aims to highlight their complementarity.

Specifically, there is a certain class of hypothetical particles called leptoquarks, which, as their name suggests, couple the leptonic doublet and the quark doublet to form new interactions. We have developed a universal formula for one-loop matching of all types of scalar leptoquarks onto the Standard Model Effective Field Theory (SMEFT) and have applied it to decouple an $SU(2)$ doublet and a triplet within this formalism. The effects of these new particles are studied in the IR regime, leading to phenomena such as the generation of neutrino masses and a sizeable contribution to the muon magnetic moment.

Additionally, following the first-ever evidence of the Higgs boson decaying into a $Z$-boson and a photon—and noting a mild discrepancy with the SM prediction—we study the Higgs sector observables using the bottom-up approach. We pinpoint the size of the Wilson coefficients (WCs) needed to account for the observed deviation. Moreover, we explore several single- and two-field scalar and fermionic extensions of the SM that could match the size of the WCs found in the model-independent analysis, highlighting the importance of the complementarity of both approaches.

In a similar vein, another discrepancy that had long persisted—but has recently diminished—lies in the lepton flavor universality ratios $R_K$ and $R_{K^*}$. Our main task was to calculate the maximum deviation obtainable within the Minimal Supersymmetric Standard Model

(MSSM) by matching it onto the Low Energy Effective Field Theory (LEFT). This approach allowed us to analyze these lepton flavor universality ratios within a consistent EFT framework.

# Περίληψη

Το κύριο θέμα αυτής της διατριβής είναι η μελέτη επεκτάσεων του Καθιερωμένου Μοντέλου (ΚΠ) στο πλαίσιο των Ενεργών Θεωριών Πεδίου (ΕΘΠ), που έχει ως κύρια παραδοχή ότι τα σωματίδια που δεν έχουν ακόμη ανακαλυφθεί υπάρχουν σε ενέργειες υψηλότερες από αυτές που είναι προσβάσιμες από τα τρέχοντα πειράματα. Υπάρχουν δύο τρόποι να χρησιμοποιηθούν οι ΕΘΠ για την παραγωγή ουσιαστικών προβλέψεων. Ο πρώτος είναι η προσέγγιση από πάνω προς τα κάτω, όπου το υπεριώδες μοντέλο φυσικής είναι γνωστό και στόχος μας είναι να καθορίσουμε τις επιδράσεις των βαρέων σωματιδίων στο χαμηλής ενέργειας (υπέρυθρο) καθεστώς μέσω μιας διαδικασίας γνωστής ως αντιστοίχιση. Αντιθέτως, η προσέγγιση από κάτω προς τα πάνω είναι αγνωστικιστική της προηγούμενης· το σημείο εκκίνησής μας είναι η Λαγκρανζιανή της ΕΘΠ, και ο κύριος στόχος μας είναι να περιορίσουμε όσο το δυνατόν περισσότερο τις ελεύθερες παραμέτρους στην ΕΘΠ χαμηλής ενέργειας χρησιμοποιώντας πειραματικά δεδομένα, εξάγοντας έτσι ενδείξεις για τη δυναμική που μπορεί να περιγράφει τις διαδικασίες στο υπεριώδες. Και οι δύο προσεγγίσεις έχουν τα πλεονεκτήματα και τα μειονεκτήματά τους, και αυτή η διατριβή υπογραμμίζει τη συμπληρωματικότητά τους.

Συγκεκριμένα, υπάρχει μια κατηγορία σωματιδίων που ονομάζονται λεπτοκουάρκς, τα οποία, όπως υποδηλώνει το όνομά τους, συζεύγουν την λεπτονική διπλέτα με τη διπλέτα των κουάρκ σχηματίζοντας έτσι νέες αλληλεπιδράσεις. Αναπτύξαμε μια καθολική φόρμουλα για την αντιστοίχιση σε επίπεδο ενός βρόχου όλων των βαθμωτών λεπτοκουάρκς στη ΕΘΠ του Καθιερωμένου Προτύπου και την εφαρμόσαμε για να αποσυζεύξουμε μια διπλέτα και μια τριπλέτα λεπτοκουάρκ, κάτω απο την συμμετρία βαθμίδος $SU(2)$, εντός αυτού του πλαισίου. Οι επιδράσεις αυτών των νέων σωματιδίων μελετώνται στο υπέρυθρο καθεστώς, οδηγώντας σε φαινόμενα όπως η δημιουργία μαζών για τα νετρίνα καθώς και μια σημαντική συμβολή στη μαγνητική ροπή του μιονίου.

Επιπλέον, μετά τα πρόσφατα δεδομένα για την πρώτη πειραματική ανακάλυψη της διάσπασης του μποζονίου Higgs σε ένα μποζόνιο $Z$ και ένα φωτόνιο—και σημειώνοντας μια ήπια απόκλιση από την πρόβλεψη του ΚΠ—μελετούμε τον τομέα του Higgs χρησιμοποιώντας την προσέγγιση από κάτω προς τα πάνω. Προσδιορίζουμε το μέγεθος των συντε-

λεστών Wilson (WCs) που απαιτούνται για να εξηγηθεί η παρατηρούμενη απόκλιση και επιπλέον, εξερευνούμε βαθμωτές και φερμιονικές επεκτάσεις του ΚΠ με ένα ή δύο πεδία που θα μπορούσαν να αντιστοιχούν στο μέγεθος των WCs που βρέθηκαν στην παραπάνω ανάλυση, αναδεικνύωντας έτσι τη σημασία της συμπληρωματικότητας των δύο προσεγγίσεων.

Με παρόμοιο τρόπο, μια άλλη απόκλιση που είχε παραμείνει για μεγάλο χρονικό διάστημα—αλλά πρόσφατα μειώθηκε—αφορά τους λόγους καθολικότητας λεπτονικής γεύσης $R_K$ και $R_{K^*}$. Υπολογίσαμε τη μέγιστη απόκλιση που μπορεί να επιτευχθεί εντός του Απλού Υπερσυμμετρικού Καθιερωμένου Προτύπου με την αντιστοίχισή του στην ΕΘΠ Χαμηλής Ενέργειας. Αυτή η προσέγγιση μας επέτρεψε να αναλύσουμε αυτούς τους λόγους καθολικότητας λεπτονικής γεύσης εντός ενός συνεπούς πλαισίου ενεργών θεωριών πεδίου.

# List of Tables

# List of Figures

# Contents

# *Preface*

I can vividly trace my interest in theoretical physics back to my undergraduate years, specifically to my first course in Quantum Mechanics, where I was introduced to this peculiar yet fascinating subject. It made a great impact on me—discovering how tiny particles, unseen by the naked eye, could possess such intriguing properties and behave in the most bizarre ways. My curiosity about the microcosmos was sparked. The study of quantum fields soon followed, and by that time, I was fully invested in the challenges this topic entails. The quantum theory of fields is vast; it not only serves as a framework for explaining a plethora of phenomena found in nature but also carries the foundational principles for building elegant theories about what our world is and could be.

The study of elementary particle physics began with the discovery of the electron, and since then, physics has come a long way. Over more than 100 years, the physics community has developed a theory to describe almost all known fundamental forces: the Standard Model (SM) of particle physics. The SM was consolidated in 2012 with the discovery of the Higgs boson, whose mechanism explains the generation of masses for all elementary particles. The SM has withstood the test of time through meticulous experimental verification and is capable of explaining physical phenomena in the microcosmos with remarkable accuracy. However, the persistence of the SM, coupled with a lack of recent evidence for deviations from it, presents a challenge for physicists seeking new discoveries. The SM cannot be the end of the story; there are unresolved topics that it cannot fully incorporate, such as dark matter, neutrino masses, and the unification of forces. Even though there is no clear way forward, the endeavor for a more complete theory of nature continues unabated.

This thesis explores what lies beyond the Standard Model, where it is believed that unknown force carriers and new particles reside, waiting to be discovered at energy scales that exceed the reach of our current experiments. The SM can be extended in multiple ways: augmenting the particle content directly, imposing new symmetries, or even postulating that particles are composed of tiny vibrating strings. However, in this thesis, we follow a different approach to systematically parameterize new physics through the separation of scales. This framework is known as Effective Field Theory (EFT).

Effective Field Theory leverages the principle of scale separation, where the influence of high-energy physics on low-energy phenomena is suppressed. This allows us to focus on low-energy processes by incorporating the effects of unknown high-energy physics into a set of free parameters in our theory. Consequently, we can make accurate predictions without detailed knowledge of the ultraviolet (UV) sector. There are two ways to approach EFT: either we hypothesize the underlying UV physics and work out the details of its effects at low-energy scales, or we acknowledge an unknown UV sector and construct a low-energy theory with several free parameters that encode the effects of the UV physics. Although these two approaches seem separate, in reality, they are complementary to each other. Studying this modern approach in physics is invaluable; it provides great insight into the dynamics of the UV phenomena we aim to explain and offers a systematic framework to enhance the accuracy of established theoretical calculations.

This thesis is organized into five chapters. In the first chapter, we provide a brief overview of elementary particle physics and the Standard Model, introducing the concept of effective field theories and highlighting the machinery of the two approaches outlined previously. The second chapter focuses on the extraction of Wilson coefficients (WCs) using the functional approach and delves deeper by considering a two-leptoquark model and its effect on observables at low-energy scales. In the third chapter, we investigate a timely issue regarding the observed deviation in the decay of the Higgs boson into a $Z$-boson and a photon. We conduct a model-independent statistical analysis within the framework of the Standard Model EFT, gauging the magnitude of the WCs capable of explaining this discrepancy. We also examine the phenomenon from a model-dependent perspective, considering several SM extensions that could provide a viable explanation for the observed deviation in the Higgs sector. Chapter 4 aims to provide an upper limit on the lepton flavor universality ratios $R_K$ and $R_{K^*}$ within the Minimal Supersymmetric Standard Model (MSSM) by considering several constraints from well-measured observables. Finally, in chapter five, we conclude and discuss the implications of these findings and suggest avenues for further research.

# Chapter 1

# Introduction

## 1.1 Elementary Particle Physics

Elementary particle physics is the field of study that seeks to understand the most fundamental constituents of the universe, those entities that are indivisible and govern the behavior of all matter and forces. At this scale, the principles of Quantum Mechanics (QM) dominate, rendering the classical mechanics of our everyday experiences obsolete. In the quantum realm, where particles exhibit wave-like behavior, the deterministic laws of classical physics give way to the probabilistic nature of quantum phenomena.

Given the minuscule size of elementary particles, they frequently travel at velocities approaching the speed of light, necessitating the incorporation of Special Relativity into their description. The union of Quantum Mechanics and Special Relativity leads to the framework of Quantum Field Theory (QFT), which provides a comprehensive description of the behavior of the fastest and smallest particles in nature. QFT is the theoretical bedrock of modern particle physics, allowing for the unification of particle and wave descriptions and offering profound insights into the fundamental interactions of particles.

Nature, as we currently understand it, is governed by four fundamental forces: the strong, electromagnetic, weak, and gravitational interactions. The advent of Quantum Mechanics revolutionized our understanding of these forces, particularly through the concept of force mediators. Each fundamental force is now associated with a specific type of particle that acts as its mediator, facilitating the interactions between other elementary particles. The Strong Force is mediated by *gluons* and is responsible for binding quarks together to form protons, neutrons, and other hadrons. It operates at the scale of atomic nuclei and is the most powerful of the fundamental forces. The Electromagnetic Force is mediated by *photons* and governs the interactions between charged particles. This force is responsible for the structure of atoms and molecules, as well as the behavior of electromagnetic waves, including light. The Weak Force is mediated by the $W^{\pm}$ and $Z$ bosons and is responsible for processes such as radioactive decay and neutrino interactions. It plays a crucial role in the fusion reactions that power stars.

The Gravitational Force, described by General Relativity, is mediated by the hypothetical graviton (which has yet to be discovered). While gravity is the most familiar force at macroscopic scales, in the microscopic realm of particle physics, it is exceedingly weak compared to the other forces. For example, the electromagnetic force between two elementary particles can exceed the gravitational force by nearly 40 orders of magnitude. Given its relative weakness, gravity is often neglected in particle physics. However, it is widely believed that at sufficiently high energy scales, approaching the so-called Planck scale ($M_P = 10^{16}$ TeV), gravitational interactions can no longer be ignored, and a quantum theory of gravity becomes essential.

The foundations of particle physics were laid with the discovery of the electron by J.J. Thomson in 1897, marking the first identification of a fundamental particle. This breakthrough was soon followed by Max Planck's work on blackbody radiation, where he introduced the revolutionary idea that electromagnetic energy is quantized, being emitted and absorbed in discrete packets called quanta. This was the first step in the quantization of electromagnetic interactions, leading to the birth of Quantum Mechanics. As experimental techniques advanced, a multitude of other particles were discovered, both fundamental, such as quarks and leptons, and composite, such as protons and neutrons. Over time, physicists meticulously tabulated the properties of these particles, including their mass, charge, and spin.

The culmination of decades of theoretical and experimental progress in elementary particle physics is the Standard Model (SM). The Standard Model is the most successful theory to date, describing the fundamental particles and their interactions (excluding gravity) with remarkable accuracy. The particle spectrum of the Standard Model can be divided into several categories.

- Matter Particles: These include quarks and leptons, which are the building blocks of matter. Quarks combine to form hadrons, such as protons and neutrons, while leptons include electrons, muons, taus, and neutrinos.
- Force Carriers: These are the mediators of the fundamental forces, including the gluon (for the strong force), the photon (for the electromagnetic force), and the W and Z bosons (for the weak force).
- The Higgs Boson: The only scalar boson in the Standard Model. The Higgs boson is a result of the mechanism called the Higgs mechanism of spontaneous electroweak symmetry breaking, which endows elementary particles with mass.

The Standard Model has been extraordinarily successful in explaining a wide range of experimental results and has withstood numerous experimental tests. However, it is widely acknowledged that the Standard Model is not the complete theory of fundamental interactions, as it does not incorporate gravity, nor does it account for neutrino masses, dark matter or dark energy. These limitations suggest that new physics lies beyond the Standard Model, waiting to be discovered as experiments probe ever higher energy scales and as theoretical advances continue to push the boundaries of our understanding.

## 1.2 The Standard Model of Particle Physics

Spacetime symmetries are fundamental to the way we understand the behavior of particles and fields within the framework of relativistic quantum field theory, the foundation upon which the Standard Model is built. At the heart of spacetime symmetries in the Standard Model is *Lorentz symmetry*, which is a cornerstone of Einstein's theory of special relativity. Lorentz symmetry dictates that the laws of physics are the same for all observers, regardless of their relative motion, provided they are in inertial (non-accelerating) frames of reference. This symmetry implies that physical phenomena do not depend on the orientation or the uniform motion of the observer in spacetime.

Lorentz symmetry can be mathematically described by the Lorentz group, which includes rotations in space and boosts (transformations related to changes in velocity). The Standard Model respects Lorentz symmetry, ensuring that the equations describing particles and their interactions are invariant under these transformations. This invariance leads to important physical consequences, such as the fact that the speed of light is constant in all inertial frames and that the mass of a particle is invariant, regardless of its velocity.

The *Poincaré* group extends the Lorentz group to include translations in space and time, reflecting the fact that the laws of physics are also invariant under shifts in position or time. This means that the physics described by the Standard Model does not depend on where or when an experiment is conducted, as long as the experiment is isolated from external influences. The Poincaré group encapsulates the full symmetry of flat spacetime in the context of special relativity, and it is this group that underlies the relativistic quantum field theories that describe the behavior of particles in the Standard Model [1–3].

Apart from the symmetries discussed above, which constitute external symmetries of the SM, there exist also internal symmetries that govern the particular interactions and the particle content of the SM. The SM from the standpoint of QFT is built upon the so called non-Abelian *gauge symmetries*, which are a type of local symmetry that applies to the fields associated with fundamental forces. The gauge group associated to the SM is,

$$G_{\mathrm{SM}} = SU(3)_c \times SU(2)_L \times U(1)_Y \ , \tag{1.1}$$

where each component corresponds to one of the fundamental forces.

The group of $SU(3)_c$ describes the mathematical framework which Quantum Chromodynamics (QCD) depends on, while the letter c stands for *color* which is a type of charge associated with quarks and gluons specific to strong interactions. The symmetry group reflects the invariance of QCD under rotations in the abstract space of color.

The rest of the SM gauge group, $SU(2)_L \times U(1)_Y$, embodies the theory of electroweak interactions, which unifies the electromagnetic and the weak nuclear force into a single force. The letter "L" stands for *left*, denoting that the symmetry applies only to left-handed particles, reflecting that chirality in the SM plays an important role. Lastly, the group $U(1)_Y$ refers to hypercharge, a quantum number related to the electric charge and the weak force.

A critical aspect of the Standard Model is spontaneous symmetry breaking, particularly as it relates to the Higgs mechanism. Although the underlying electroweak symmetry $SU(2)_L \times U(1)_Y$ would suggest that all these bosons should be massless, just like the photon, in nature, the W and Z bosons are massive, while the photon is not. This apparent discrepancy is resolved through the *Higgs mechanism*, where the Higgs field, a scalar field with its own dynamics, acquires a non-zero vacuum expectation value, spontaneously breaking the $SU(2)_L \times U(1)_Y$ symmetry down to the electromagnetic symmetry $U(1)_{\mathrm{EM}}$. This symmetry breaking imparts mass to the W and Z bosons, while the photon remains massless. The Higgs boson, discovered in 2012, is the quantum excitation of this field and serves as a direct confirmation of this

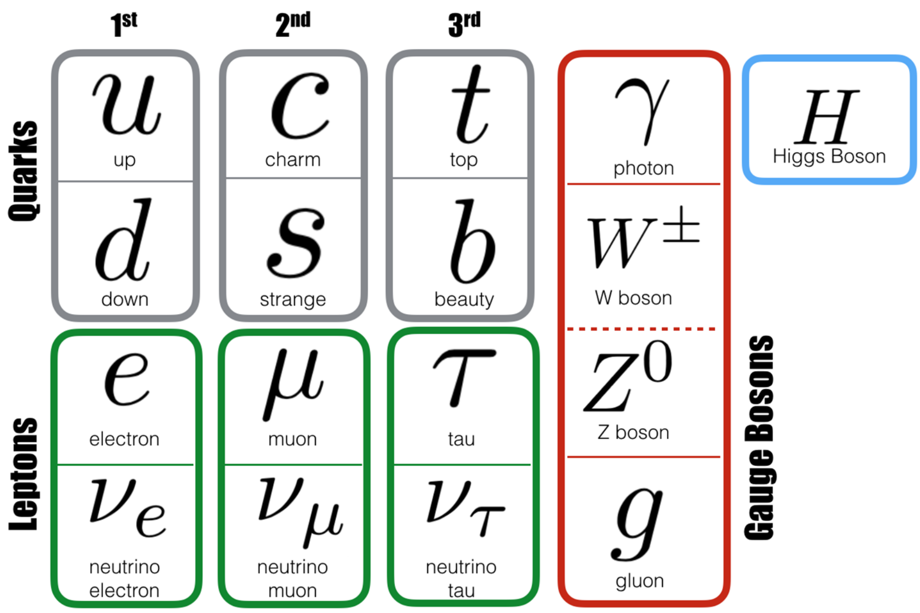


*Fig. 1.1: The building blocks of nature.*

mechanism. There are several textbooks covering the material of this chapter in more depth, the interested reader is referred to [4–6].

This concept of symmetry breaking is also pivotal in explaining the masses of the fermions (quarks and leptons) through their interactions with the Higgs field. The strength of these interactions (Yukawa couplings) determines the masses of the fermions, leading to the wide range of masses observed in nature, from the light electron to the much heavier top quark.

In defining the SM Lagrangian the local symmetry group $G_{\text{SM}}$ dictates that we introduce the following gauge bosons representations,

$$G^a_\mu \sim (8,1,0) \quad W^I_\mu \sim (1,3,0) \quad B_\mu \sim (1,1,0)\,. \tag{1.2}$$

As for the matter particles we introduce the following sets of fields under the $G_{\text{SM}}$ representation group,

$$q^i_L \sim \left(3,2,\frac{1}{6}\right), \quad \ell^i_L \sim \left(1,2,-\frac{1}{2}\right), \quad u^i_R \sim \left(3,1,\frac{2}{3}\right), \quad d^i_R \sim \left(3,1,-\frac{1}{3}\right), \quad e^i_R \sim (1,1,-1)\,, \tag{1.3}$$

where $i = 1,2,3$ denotes that there are three distinct generations for each field introduced above each of which the above representation is assigned. Lastly, the representation of the Higgs field under the SM gauge group reads,

$$\phi \sim \left(1,2,\frac{1}{2}\right). \tag{1.4}$$

Another important ingredient stemming from the SM gauge group is the covariant derivative defined as,

$$D_\mu = \partial_\mu - ig' B_\mu - ig\tau^I W^I_\mu - ig_s \lambda^a G^a_\mu, \tag{1.5}$$

where $g$, $g'$ and $g_s$, denote the couplings of each individual group of $G_{\text{SM}}$, while $\tau^I$ and $\lambda^a$ correspond to the generators of $SU(2)$ and $SU(3)$ respectively.

Having set all the necessary pieces we can now present the most general renormalizable Lagrangian that respects both the Poincaré group and the SM gauge group. We suppress chirality indices $L$ and $R$ of the fermionic fields for brevity,

$$\begin{aligned}\mathcal{L}_{\rm SM} = &-\frac{1}{4}F^{(i)}_{\mu\nu}F^{\mu\nu}_{(i)} - |D_\mu\phi|^2 + \mu^2\phi^\dagger\phi - \frac{\lambda}{2}\left(\phi^\dagger\phi\right)^2 \\ &+ i\bar{\psi}^{(i)}\not{D}\psi_{(i)} - \left(\bar{\ell}y_e e\phi + \bar{q}y_u u\tilde{\phi} + \bar{q}y_d d\phi\right) + \text{h.c.}\,,\end{aligned} \tag{1.6}$$

The first term in eq. (1.6) corresponds to the sum, denoted by $(i)$ of the kinetic terms of the three distinct field strength tensors of the gauge boson introduced in the paragraph above, while the second is the kinetic term of the Higgs boson. The rest of the expression constitutes the scalar potential which leads to the spontaneous symmetry breaking of the electroweak sector. On the second line the first terms implies the summation of the kinetic terms of all matter fields, while the rest denote the Yukawa sector which leads to the acquisition of mass for the matter particles upon symmetry breaking. Matrices $y_{(e,u,d)}$ are called the Yukawa couplings and are general $3\times 3$ matrices in flavor space.

*This elegant model of spontaneous symmetry breaking of the gauge group $SU(3)_c \times SU(2)_L \times U(1)$ can accommodate for almost all observed interactions and experimental data observed in elementary particle physics.*

Despite its successes, the SM is known to have significant limitations, both theoretical and experimental, which strongly suggest the existence of physics beyond the Standard Model (BSM). The remainder of this introduction will be devoted to a systematic exploration of the foundational concepts and theoretical frameworks that we will employ to address the known inconsistencies of the Standard Model (SM). By laying out these fundamental principles, we aim to establish a comprehensive understanding of the tools and methodologies that are pivotal in advancing beyond the current limitations of the SM.

Following this, we will introduce supersymmetry (SUSY), one of the most prominent theoretical extensions of the SM, which addresses several of the model's most pressing issues, such as the hierarchy problem. In parallel, we will explore the framework of effective field theory (EFT), a powerful tool that allows for the systematic study of new physics beyond the SM, even in the absence of a fully developed high-energy theory.

## 1.3 The Minimal Supersymmetric Standard Model

The following section serves as a brief introduction to the concept of Supersymmetry (SUSY), the interested reader may refer to ref. [7] for a detailed and robust review of SUSY.

Supersymmetry is one of the most compelling theoretical frameworks proposed as an extension of the Standard Model (SM) of particle physics. SUSY postulates a fundamental symmetry between fermions and bosons, two distinct classes of particles in quantum field theory. In a supersymmetric theory, every known particle in the SM has a corresponding superpartner: fermions are paired with bosons, and vice versa. These superpartners differ by half a unit of spin, meaning that a fermion has a bosonic superpartner and a boson has a fermionic superpartner.

The most widely studied and phenomenologically viable SUSY model is the Minimal Supersymmetric Standard Model (MSSM). It is a crucial framework for exploring the potential validity of SUSY in nature and serves as a cornerstone for many extensions and variations in high-energy physics. The MSSM's particle spectrum is significantly richer than that of the SM. It includes superpartners for each of the SM particles, as well as additional Higgs bosons necessary to maintain consistency within the SUSY framework. The main components of the MSSM particle spectrum are:

**Sfermions (squarks and sleptons)**:

- *Squarks* are the scalar superpartners of the SM quarks. Each quark flavor $q$ has two squarks associated with it $\tilde{q}_L$ and $\tilde{q}_R$.
- *Sleptons* are the scalar superpartners of the SM leptons. Each charged lepton flavor (electron, muon, tau) has two sleptons $\tilde{\ell}_L$ and $\tilde{\ell}_R$. Neutrinos also have corresponding sneutrinos $\tilde{\nu}$.

**Gauginos and Higgsinos**:

- *Gauginos* are the fermionic superpartners of the SM gauge bosons. They include the gluino $\tilde{g}$ (superpartner of the gluon, which depending on the SUSY-breaking mechanism, could be one of the heaviest superpartners in the MSSM), the Bino $\tilde{B}$ (superpartner of the $U(1)$ gauge boson) and the winos $\tilde{W}^{\pm}, \tilde{W}^0$ (superpartners of the $SU(2)$ gauge bosons).
- *Higgsinos* are the fermionic superpartners of the Higgs bosons. In the MSSM, there are two Higgs doublets, leading to four Higgsino states $\tilde{H}_u^0, \tilde{H}_d^0$ (neutral Higgsinos) and $\tilde{H}_u^+, \tilde{H}_d^-$ (charged Higgsinos).

These gauginos and Higgsinos mix to form the mass eigenstates known as **neutralinos** (four neutral particles, often denoted as $\tilde{\chi}_1^0, \tilde{\chi}_2^0, \tilde{\chi}_3^0, \tilde{\chi}_4^0$) and **charginos** (two charged particles $\tilde{\chi}_1^{\pm}, \tilde{\chi}_2^{\pm}$). The lightest neutralino $\tilde{\chi}_1^0$ is often considered the lightest supersymmetric particle (LSP) and a prime candidate for dark matter.

The MSSM also necessitates two Higgs doublets, resulting in five physical Higgs bosons. Two CP-even neutral Higgs bosons $h$ (lighter) and $H$ (heavier). One CP-odd neutral Higgs boson, $A^0$ and two charged Higgs bosons $H^{\pm}$. The introduction of an additional Higgs doublet allows the MSSM to address the hierarchy problem by maintaining SUSY and ensuring that the Higgs sector remains consistent with electroweak symmetry breaking.

In some SUSY models, the *gravitino*, the superpartner of the graviton, could be the LSP. It is an extremely weakly interacting particle, making it another dark matter candidate in scenarios where it is the LSP.

To name a few, the advantages of the MSSM are

- Resolution of the Hierarchy Problem: The hierarchy problem refers to the large discrepancy between the electroweak scale ($\sim 100$ GeV) and the Planck scale ($\sim 10^{19}$ GeV), at which gravitational interactions become significant. In the SM, the Higgs boson mass is extremely sensitive to quantum corrections, potentially driving it to very large values. SUSY provides a natural solution to this problem by introducing superpartners that cancel out the quadratic divergences in the Higgs mass, thereby stabilizing it at the electroweak scale.
- Gauge Coupling Unification: The MSSM predicts that the three gauge couplings of the SM—corresponding to the electromagnetic, weak, and strong forces—can unify at a

single energy scale ($\sim 10^{16}$ GeV) in a grand unified theory (GUT). This unification is not exact in the SM but is remarkably close in the MSSM, providing indirect evidence for the existence of SUSY at high energies.

- Dark Matter Candidate: In the MSSM, the lightest supersymmetric particle (LSP) is often stable due to a conserved quantum number called R-parity. If the LSP is electrically neutral, as is the case for the neutralino (a mixture of the superpartners of the photon, Z boson, and neutral Higgs bosons), it can serve as a viable dark matter candidate. This offers a potential explanation for the dark matter observed in the universe.

Despite its strengths, the MSSM also has limitations:

- Fine-Tuning: The MSSM still requires some degree of fine-tuning to explain the observed Higgs boson mass of 125 GeV. This has led to the exploration of alternative SUSY models or extensions of the MSSM.

- Lack of Direct Evidence: So far, no superpartners have been observed at the LHC, leading to increasingly stringent bounds on their masses and casting doubt on the simplest versions of the MSSM.

- Flavor and CP Problems: The MSSM introduces new sources of flavor and CP violation, which must be tightly constrained to avoid conflict with experimental observations, leading to additional model-building challenges.

The MSSM remains one of the most well-motivated extensions of the Standard Model, offering solutions to critical problems, we will explore the implications of the MSSM and flavor observables, in particular the contributions to the $R_K$, in Chapter 4.

## 1.4 Effective Field Theories

In this section, we introduce Effective Field Theory (EFT), a framework that plays an essential role in modern quantum field theory, particularly in addressing physics at different energy scales. The exposition closely follows the excellent review by A.V. Manohar [8], with additional references such as [9, 10]. Quantum field theories, in general, can be categorized into two large classes according to the renormalizability [1] of their interactions. These two classes are,

- **Renormalizable Field Theories**.

  Theories, such as the SM, fall into this category, where only need a finite number of counterterms are required to cancel their UV divergences arising from loop graphs. The Lagrangian of these theories include operators of mass dimension $\mathscr{D} \leq 4$, hence their interactions are renormalizable. In principle, renormalizable theories allow for calculations of observable quantities to infinite precision.

- **Non-Renormalizable Field Theories**.

  In these theories an infinite number of counterterms are needed to cancel the divergences from loop diagrams. The Lagrangian contains operators of higher mass dimension, $\mathscr{D} > 4$, adding up to the renormalizable ones. Although non-renormalizable theories require

[1] In this chapter we will assume the that the reader is familiar with renormalization theory. A good review on renormalization and effective field theories can be found in [11].

more complex treatment, they still allow for meaningful predictions within a specific energy scale.

*Effective Field Theories* (EFTs) fall into the second category. Although non-renormalizable, they are full fledged QFTs with both a regularization procedure and a renormalization scheme, just like ordinary QFTs. They, can make meaningful predictions up to some finite order defined by a power counting parameter $\delta$. Suppose we compute an observable to some order $\delta^n$, the error of our calculation would be of order $\delta^{n+1}$. Hence, *within the EFT framework we can compute experimental quantities to finite precision*.

In many cases the EFT is an approximation of a more complete theory, which is often called the *full theory*. There are two approaches to derive an EFT,

- **Top-down EFT**.

  In this method we "integrate out" the heavy degrees of freedom, related to the high energy scale $\Lambda$ of the full theory. As a result we obtain a set of *local* operators $\mathcal{O}_i^{\mathscr{D}}$ of dimension $\mathscr{D} > 4$ built from the fields of the low energy theory. The information of the full theory is encoded in a set of coefficients called the *Wilson coefficients*, $\mathcal{C}_i^{\mathscr{D}}$, multiplying their respective operators. These Wilson coefficients encode the impact of the high-energy physics on the low-energy observables.

- **Bottom-up EFT**.

  In this approach we add to a renormalizable theory higher dimensional operators, which respect *gauge invariance* and *locality*, promoting it to an EFT. The main difference with the top-down approach is that the Wilson coefficients of the theory and the UV scale $\Lambda$ are not known. This constitutes a model independent way to parametrize the effects of new physics arising from the scale $\Lambda$. By computing observables within the EFT comparing them against experimental data we can fix the values of a set of Wilson coefficients, thus providing indirect evidence for the nature of the high-energy physics.

Whether we use the top-down or bottom-up approach, both are constructed with a universal view, *to reproduce the same S-matrix element as the full theory*, this procedure is known as matching. In the first approach the matching is explicit while in the second one implicit, since the full theory is not known. In any case, this doesn't mean that the fields and parameters characterizing the full theory remain the same when going down to the EFT. On the contrary when computing in the EFT the fields and parameters are redefined according to redefinitions imposed by the decoupling of the heavy modes. This has also consequences in the RG flows, which are inherently different since the scale of the full theory and the EFT are not the same. One may then ask, "How does this reproduce the same S-matrix, since the fields are different?". The answer to this question lies in an important property of quantum field theory, *invariance of observables under field redefinitions*.

EFTs are not merely theoretical constructs but have proven invaluable in the study of a wide range of physical phenomena. Historically, the concept of EFTs emerged from the need to describe physical processes occurring at different energy scales. An EFT serves as a low-energy approximation to a more fundamental, high-energy theory, often referred to as the "full theory." The necessity of EFT arises in situations where it is either impractical or impossible to access the high-energy regime directly in experiments. This notion was first developed in low-energy QCD, leading to the creation of *chiral perturbation theory*, an EFT for QCD at low energies.

One of the major successes of EFTs in particle physics is the Fermi theory of weak interactions, which described an EFT valid at low energies before the electroweak theory emerged as a more fundamental theory. Similarly, Standard Model Effective Field Theory (SMEFT), which extends the Standard Model by including higher-dimensional operators, is an essential tool to study possible new physics beyond the current experimental reach. In SMEFT, the effects of new high-energy physics are suppressed by powers of the energy scale $\Lambda$, representing the scale at which new physics becomes important.

### 1.4.1 The EFT Lagrangian

Having established the foundational principles of effective field theory, we now turn to the technical construction of the EFT Lagrangian. In order to construct a Lagrangian we first have to identify the relevant degrees of freedom in the theory and impose symmetry constraints on the operators. We will begin by working out the dimensionality of the fields in $d$ dimensions.

The action of a theory must be dimensionless[2], in $d$ dimensions,

$$[\mathcal{S}] = \left[\int d^d x \; \mathcal{L}(x)\right] = 0 \,. \tag{1.7}$$

Given that $\left[d^d x\right] = -d$ the Lagrangian has mass dimension,

$$[\mathcal{L}(x)] = d \,. \tag{1.8}$$

Consider a Lagrangian built out of a scalar field $\phi(x)$, a spinor field $\psi(x)$ and a vector field $A_\mu(x)$ along with the partial derivative, $\partial_\mu$. The dimensionality of these fields can be worked out from their kinetic terms since $\left[\partial_\mu\right] = 1$. The dimensions of the relevant fields are,

$$[\psi] = \frac{d-1}{2} \,, \qquad [\phi] = \frac{d-2}{2} \,, \qquad \left[A_\mu\right] = \frac{d-2}{2} \,. \tag{1.9}$$

The gauge coupling's dimension $[g]$ is given by,

$$[g] = \frac{4-d}{2} \,, \qquad \text{such that} \qquad \left[D_\mu\right] = 1 \,. \tag{1.10}$$

A Lagrangian of any theory is composed as the sum of all *Lorentz* and *gauge* invariant operators,

$$\mathcal{L} = \sum_i c_i \mathcal{O}_i(x) \,. \tag{1.11}$$

The *renormalizable* part contains all operators with dimension $0 < \mathcal{D} \leq d$, while the non-renormalizable part consists of operators with $\mathcal{D} > d$. In the context of EFT, the Lagrangian can be organized as a formal expansion in powers of the operator dimension,

$$\mathcal{L}_{\text{EFT}} = \sum_{\mathcal{D}>d,\, i} \frac{c_i^{(\mathcal{D})} \mathcal{O}_i^{(\mathcal{D})}(x)}{\Lambda^{\mathcal{D}-d}} \,, \tag{1.12}$$

where $\Lambda$ is a high-energy scale characterizing the onset of new physics, and it is introduced to render the Wilson coefficients $c_i^{(\mathcal{D})}$ dimensionless. For example, in $d = 4$, the general Lagrangian takes the form,

$$\mathcal{L} = \mathcal{L}_{\mathcal{D}\leq 4} + \frac{\mathcal{L}_5}{\Lambda} + \frac{\mathcal{L}_6}{\Lambda^2} + \ldots \tag{1.13}$$

[2]We work in the natural system where $\hbar = c = 1$

The Lagrangian of eq. 1.13 should be treated as an expansion in powers of $1/\Lambda$ and should not be summed over to all orders as this would violate the EFT power counting rules. This expansion helps us organize the calculation of amplitudes in a systematic way.

The calculation of physical observables, such as scattering amplitudes, can be organized using a power counting scheme. Consider a general amplitude in $d$ dimensions. By dimensional analysis the contribution of an operator of dimension $\mathscr{D}$ to the amplitude will scale as,

$$\mathcal{A} \propto \left(\frac{E}{\Lambda}\right)^{\mathscr{D}-d} , \tag{1.14}$$

where E is the typical energy of the process. This corresponds to an insertion of a single operator of dimension $\mathscr{D} > d$. Multiple insertions of such operators lead to an amplitude of the form,

$$\mathcal{A} \propto \prod_i \left(\frac{E}{\Lambda}\right)^{\mathscr{D}_i-d} . \tag{1.15}$$

It is then convenient to define the power counting formula,

$$n = \sum_i (\mathscr{D}_i - d) , \tag{1.16}$$

with the sum running to all insertions of higher dimensional operators. Thus the amplitude turns out to be a power of $n$,

$$\mathcal{A} \propto \left(\frac{E}{\Lambda}\right)^{n} .$$

This formula illustrates the distinction between renormalizable and non-renormalizable theories. In renormalizable theories, only a finite number of operators contribute to physical amplitudes, while in EFTs, higher-dimensional operators provide corrections suppressed by powers of $E/\Lambda$.

To further illustrate the difference between renormalizable and EFT operators, consider a specific case in $d = 4$. Consider a graph with a single insertion of a $\mathscr{D} = 5$ operator. This will generate an amplitude of the form,

$$\mathcal{A} \propto \frac{E}{\Lambda} . \tag{1.17}$$

Inserting another operator of the same dimension we get an amplitude of the form,

$$\mathcal{A} \propto \left(\frac{E}{\Lambda}\right)^{2} , \tag{1.18}$$

which corresponds to the contribution of a dimension-$\mathscr{D} = 6$ operator. If these insertions occur in loop diagrams, the resulting amplitudes will be divergent, requiring counterterms from higher-dimensional operators, such as those in $\mathcal{L}_6$. This exemplifies how *we can generate arbitrarily high dimension operators that require an infinite amount of counterterms to cancel the UV divergences*. While the presence of an infinite number of higher-dimensional operators might seem problematic, it does not pose a practical issue for calculations. In an EFT, calculations are performed to a fixed order in $n$, meaning that only a finite number of operators contribute within a desired level of precision.

### 1.4.2 The Standard Model Effective Field Theory

We now turn to a particularly important example used in the precision calculation of observables: the Standard Model Effective Field Theory (SMEFT). The SMEFT framework extends the Standard Model (SM) by introducing higher-dimensional operators that encapsulate the effects of new physics beyond the SM. These operators respect the gauge symmetries of the SM but allow for interactions that arise at energy scales beyond the electroweak scale. It is expressed as:

$$\mathcal{L}_{\text{SMEFT}} = \mathcal{L}_{\text{SM}} + \sum_{n\geq 5}\sum_{i} \frac{C_i^{(n)}}{\Lambda^n} \mathcal{Q}_i^{(n)} = \mathcal{L}_{\text{SM}} + \sum_i \frac{C_i^{(5)}}{\Lambda} \mathcal{Q}_i^{(5)} + \sum_i \frac{C_i^{(6)}}{\Lambda^2} \mathcal{Q}_i^{(6)} + \mathcal{O}\left(\frac{1}{\Lambda^3}\right), \quad (1.19)$$

where $n$ indicates the dimension of the operator and $i$ runs to account for every operator of the respective dimension. This expansion organizes the effects of new physics in a power series of $\Lambda^{-1}$.

The construction of the SMEFT involves systematically listing all possible operators at each dimension that are consistent with the symmetries of the SM. This process requires careful consideration to avoid redundancies arising from equations of motion, integration by parts, and Fierz identities. The initial cataloging was performed in ref [12]. However, it was later realized that some operators in their basis were redundant due to equations of motion or could be eliminated through field redefinitions. This led to the development of the Warsaw basis in ref. [13], which provides a complete and non-redundant set of operators up to dimension six. The classification of operators of dimension seven and higher has been further explored in subsequent works, such as [14, 15].

At dimension five, there is a unique gauge-invariant operator that violates lepton number conservation by two units ($\Delta L = 2$). This operator is known as the Weinberg operator [16] and is responsible for generating Majorana masses for neutrinos after electroweak symmetry breaking. It is expressed as:

$$\mathcal{Q}^{(5)} = \epsilon_{jk}\epsilon_{mn} H^j H^m \left(l_{Lp}^k\right)^T \mathbb{C}\left(l_{Lr}^n\right), \quad (1.20)$$

where $\mathbb{C} = i\gamma^2\gamma^0$ the charge conjugation matrix. Indices $j, k, m, n$ are $SU(2)$ indices while $p, r$ are flavour indices. Upon spontaneous symmetry breaking, the Higgs field acquires a vacuum expectation value, and the Weinberg operator generates Majorana mass terms for neutrinos:

$$\mathcal{L}_{\nu\,\text{mass}} = -\frac{v^2}{2\Lambda} C_{pr}^{(5)} \left(\nu_p\right)^T \mathbb{C}\,\nu_r + \text{h.c.}, \quad (1.21)$$

where $v \approx 246\,\text{GeV}$ is the Higgs vev. Therefore, SMEFT provides us with tiny neutrino masses originated at the scale $\Lambda$.

At dimension six, the number of independent operators increases significantly. Assuming baryon number conservation and not counting flavor indices or Hermitian conjugates, there are 59 independent operators in the Warsaw basis. These operators modify various aspects of the SM. We write the Lagrangian of dim-6 operators as,

$$\mathcal{L}_{\text{SMEFT}}^{(6)} = \sum_X C^X \mathcal{Q}_X^{(6)} + \sum_f C^f \mathcal{Q}_f^{(6)}, \quad (1.22)$$

| $X^3$ | | $H^6$ and $H^4D^2$ | | $\psi^2H^3$ | |
|---|---|---|---|---|---|
| $\mathcal{Q}_G$ | $f^{ABC}G_\mu^{A\nu}G_\nu^{B\rho}G_\rho^{C\mu}$ | $\mathcal{Q}_H$ | $(H^\dagger H)^3$ | $\mathcal{Q}_{eH}$ | $(H^\dagger H)(\bar{l}_p e_r H)$ |
| $\mathcal{Q}_{\widetilde{G}}$ | $f^{ABC}\widetilde{G}_\mu^{A\nu}G_\nu^{B\rho}G_\rho^{C\mu}$ | $\mathcal{Q}_{H\Box}$ | $(H^\dagger H)\Box(H^\dagger H)$ | $\mathcal{Q}_{uH}$ | $(H^\dagger H)(\bar{q}_p u_r \widetilde{H})$ |
| $\mathcal{Q}_W$ | $\varepsilon^{IJK}W_\mu^{I\nu}W_\nu^{J\rho}W_\rho^{K\mu}$ | $\mathcal{Q}_{HD}$ | $(H^\dagger D^\mu H)^*(H^\dagger D_\mu H)$ | $\mathcal{Q}_{dH}$ | $(H^\dagger H)(\bar{q}_p d_r H)$ |
| $\mathcal{Q}_{\widetilde{W}}$ | $\varepsilon^{IJK}\widetilde{W}_\mu^{I\nu}W_\nu^{J\rho}W_\rho^{K\mu}$ | | | | |
| $X^2H^2$ | | $\psi^2XH$ | | $\psi^2H^2D$ | |
| $\mathcal{Q}_{HG}$ | $H^\dagger H G_{\mu\nu}^A G^{A\mu\nu}$ | $\mathcal{Q}_{eW}$ | $(\bar{l}_p\sigma^{\mu\nu}e_r)\tau^I H W_{\mu\nu}^I$ | $\mathcal{Q}_{Hl}^{(1)}$ | $(H^\dagger i\overleftrightarrow{D}_\mu H)(\bar{l}_p\gamma^\mu l_r)$ |
| $\mathcal{Q}_{H\widetilde{G}}$ | $H^\dagger H\widetilde{G}_{\mu\nu}^A G^{A\mu\nu}$ | $\mathcal{Q}_{eB}$ | $(\bar{l}_p\sigma^{\mu\nu}e_r)HB_{\mu\nu}$ | $\mathcal{Q}_{Hl}^{(3)}$ | $(H^\dagger i\overleftrightarrow{D}^I_\mu H)(\bar{l}_p\tau^I\gamma^\mu l_r)$ |
| $\mathcal{Q}_{HW}$ | $H^\dagger H W_{\mu\nu}^I W^{I\mu\nu}$ | $\mathcal{Q}_{uG}$ | $(\bar{q}_p\sigma^{\mu\nu}T^A u_r)\widetilde{H}G_{\mu\nu}^A$ | $\mathcal{Q}_{He}$ | $(H^\dagger i\overleftrightarrow{D}_\mu H)(\bar{e}_p\gamma^\mu e_r)$ |
| $\mathcal{Q}_{H\widetilde{W}}$ | $H^\dagger H\widetilde{W}_{\mu\nu}^I W^{I\mu\nu}$ | $\mathcal{Q}_{uW}$ | $(\bar{q}_p\sigma^{\mu\nu}u_t)\tau^I\widetilde{H}W_{\mu\nu}^I$ | $\mathcal{Q}_{Hq}^{(1)}$ | $(H^\dagger i\overleftrightarrow{D}_\mu H)(\bar{q}_p\gamma^\mu q_r)$ |
| $\mathcal{Q}_{HB}$ | $H^\dagger H B_{\mu\nu}B^{\mu\nu}$ | $\mathcal{Q}_{uB}$ | $(\bar{q}_q\sigma^{\mu\nu}u_r)\widetilde{H}B_{\mu\nu}$ | $\mathcal{Q}_{Hq}^{(3)}$ | $(H^\dagger i\overleftrightarrow{D}^I_\mu H)(\bar{q}_p\tau^I\gamma^\mu q_r)$ |
| $\mathcal{Q}_{H\widetilde{B}}$ | $H^\dagger H\widetilde{B}_{\mu\nu}B^{\mu\nu}$ | $\mathcal{Q}_{dG}$ | $(\bar{q}_p\sigma^{\mu\nu}T^A d_r)HG_{\mu\nu}^A$ | $\mathcal{Q}_{Hu}$ | $(H^\dagger i\overleftrightarrow{D}_\mu H)(\bar{u}_p\gamma^\mu u_r)$ |
| $\mathcal{Q}_{HWB}$ | $H^\dagger\tau^I H W_{\mu\nu}^I B^{\mu\nu}$ | $\mathcal{Q}_{dW}$ | $(\bar{q}_p\sigma^{\mu\nu}d_r)\tau^I H W_{\mu\nu}^I$ | $\mathcal{Q}_{Hd}$ | $(H^\dagger i\overleftrightarrow{D}_\mu H)(\bar{d}_p\gamma^\mu d_r)$ |
| $\mathcal{Q}_{H\widetilde{W}B}$ | $H^\dagger\tau^I H\widetilde{W}_{\mu\nu}^I B^{\mu\nu}$ | $\mathcal{Q}_{dB}$ | $(\bar{q}_p\sigma^{\mu\nu}d_r)HB_{\mu\nu}$ | $\mathcal{Q}_{Hud}$ | $(\widetilde{H}^\dagger iD_\mu H)(\bar{u}_p\gamma^\mu d_r)$ |

*Table 1.1: Dimension-6 operators except four-fermions as classified in [13].*

where $X = \left\{G_{\mu\nu}^A,\, W_{\mu\nu}^I,\, B_{\mu\nu}\right\}$ accounts for the bosonic only operators, while $\mathcal{Q}_f$ denotes operators containing fermion fields. The results of the independent operators excluding 4-fermions are shown in Table 1.1 as presented in [13]. Four-fermion operators are shown in Table 1.2

Many of the operators above change the standard definitions of the SM. For example, the operator $\mathcal{Q}_H$ shifts the vev of the Higgs field. The operator class $X^2H^2$ is phenomenologically important since it contributes to processes such as $h \to \gamma\,\gamma$ and $h \to Z\,\gamma$, which will eb the topic of Chapter 3. Operators of the class $\psi^2H^2$ redefine the Yukawa couplings of the SM interactions. These are only some changes imposed by dim-6 operators. The Feynman rules as well as the implications of spontaneous symmetry breaking in $R_\xi$-gauges have been worked out in Ref.[17]. The running of the Wilson coefficients have been calculated in a series of papers [18–20] and an extensive review of the SMEFT is given in Ref.[21]. As the operator dimension increases, the number of possible operators grows rapidly. The classification of dimension-7 operators has been explored in [14, 22], and dimension-8 operators in [15, 23]. The construction of these higher-dimensional operators involves advanced mathematical techniques (such as Hilbert series) due to the combinatorial complexity and the need to ensure operator independence.

## 1.5 Top-down EFTs

In the previous section we analyzed the structure of the Lagrangian of an EFT. In this section we will talk about the top-down approach of constructing the EFT by *decoupling* (or integrating out) a heavy particle with mass $M$ from the full theory. Schematically we may say that the particle exists in our theory when $\mu > M$ and at scales $\mu < M$ the particle doesn't have any dynamical degrees of freedom in our theory, where $\mu$ is the renormalization scale. The effects of this particle are encoded in the Lagrangian, where higher dimensional operators come into

| $(\bar{L}L)(\bar{L}L)$ | | $(\bar{R}R)(\bar{R}R)$ | | $(\bar{L}L)(\bar{R}R)$ | |
|---|---|---|---|---|---|
| $\mathcal{Q}_{ll}$ | $(\bar{l}_p\gamma_\mu l_r)(\bar{l}_s\gamma^\mu l_t)$ | $\mathcal{Q}_{ee}$ | $(\bar{e}_p\gamma_\mu e_r)(\bar{e}_s\gamma^\mu e_t)$ | $\mathcal{Q}_{le}$ | $(\bar{l}_p\gamma_\mu l_r)(\bar{e}_s\gamma^\mu e_t)$ |
| $\mathcal{Q}_{qq}^{(1)}$ | $(\bar{q}_p\gamma_\mu q_r)(\overline{ql}_s\gamma^\mu q_t)$ | $\mathcal{Q}_{uu}$ | $(\bar{u}_p\gamma_\mu u_r)(\bar{u}_s\gamma^\mu u_t)$ | $\mathcal{Q}_{lu}$ | $(\bar{l}_p\gamma_\mu l_r)(\bar{u}_s\gamma^\mu u_t)$ |
| $\mathcal{Q}_{qq}^{(3)}$ | $(\bar{q}_p\gamma_\mu\tau^I q_r)(\bar{q}_s\gamma^\mu\tau^I q_t)$ | $\mathcal{Q}_{dd}$ | $(\bar{d}_p\gamma_\mu d_r)(\bar{d}_s\gamma^\mu d_t)$ | $\mathcal{Q}_{ld}$ | $(\bar{l}_p\gamma_\mu l_r)(\bar{d}_s\gamma^\mu d_t)$ |
| $\mathcal{Q}_{lq}^{(1)}$ | $(\bar{l}_p\gamma_\mu l_r)(\bar{q}_s\gamma^\mu q_t)$ | $\mathcal{Q}_{eu}$ | $(\bar{e}_p\gamma_\mu e_r)(\bar{u}_s\gamma^\mu u_t)$ | $\mathcal{Q}_{qe}$ | $(\bar{q}_p\gamma_\mu q_r)(\bar{e}_s\gamma^\mu e_t)$ |
| $\mathcal{Q}_{lq}^{(3)}$ | $(\bar{l}_p\gamma_\mu\tau^I l_r)(\bar{q}_s\gamma^\mu\tau^I q_t)$ | $\mathcal{Q}_{ed}$ | $(\bar{e}_p\gamma_\mu e_r)(\bar{d}_s\gamma^\mu d_t)$ | $\mathcal{Q}_{qu}^{(1)}$ | $(\bar{q}_p\gamma_\mu q_r)(\bar{u}_s\gamma^\mu u_t)$ |
| | | $\mathcal{Q}_{ud}^{(1)}$ | $(\bar{e}_p\gamma_\mu u_r)(\bar{d}_s\gamma^\mu d_t)$ | $\mathcal{Q}_{qu}^{(8)}$ | $(\bar{q}_p\gamma_\mu T^A q_r)(\bar{e}_p\gamma^\mu T^A u_t)$ |
| | | $\mathcal{Q}_{ud}^{(8)}$ | $(\bar{u}_p\gamma_\mu T^A u_r)(\bar{d}_s\gamma^\mu T^A d_t)$ | $\mathcal{Q}_{qd}^{(1)}$ | $(\bar{q}_p\gamma_\mu q_r)(\bar{d}_s\gamma^\mu d_t)$ |
| | | | | $\mathcal{Q}_{qd}^{(8)}$ | $(\bar{q}_p\gamma_\mu T^A q_r)(\bar{d}_s\gamma^\mu T^A d_t)$ |

| $(\bar{L}R)(\bar{R}L)$ and $(\bar{L}R)(\bar{L}R)$ | | B-violating | |
|---|---|---|---|
| $\mathcal{Q}_{ledq}$ | $(\bar{l}_p^j e_r)(\bar{d}_s q_t^j)$ | $\mathcal{Q}_{duq}$ | $\epsilon^{\alpha\beta\gamma}\epsilon_{jk}\left[(d_p^\alpha)^T\mathbb{C}u_r^\beta\right]\left[(q_s^{\gamma j})^T\mathbb{C}l_t^k\right]$ |
| $\mathcal{Q}_{quqd}^{(1)}$ | $(\bar{q}_p^j u_r)\epsilon_{jk}(\bar{q}_s^k d_t)$ | $\mathcal{Q}_{qqu}$ | $\epsilon^{\alpha\beta\gamma}\epsilon_{jk}\left[(q_p^{\alpha j})^T\mathbb{C}q_r^{\beta k}\right]\left[(u_s^\gamma)^T\mathbb{C}e_t\right]$ |
| $\mathcal{Q}_{quqd}^{(8)}$ | $(\bar{q}_p^j T^A u_r)\epsilon_{jk}(\bar{q}_s^k T^A d_t)$ | $\mathcal{Q}_{qqq}$ | $\epsilon^{\alpha\beta\gamma}\epsilon_{jn}\epsilon_{km}\left[(q_p^{\alpha j})^T\mathbb{C}q_r^{\beta k}\right]\left[(q_s^{\gamma m})^T\mathbb{C}l_t^n\right]$ |
| $\mathcal{Q}_{lequ}^{(1)}$ | $(\bar{l}_p^j e_r)\epsilon_{jk}(\bar{q}_s^k u_t)$ | $\mathcal{Q}_{duu}$ | $\epsilon^{\alpha\beta\gamma}\left[(d_p^\alpha)^T\mathbb{C}u_r^\beta\right]\left[(u_s^\gamma)^T\mathbb{C}e_t\right]$ |
| $\mathcal{Q}_{lequ}^{(3)}$ | $(\bar{l}_p^j\sigma_{\mu\nu}e_r)\epsilon_{jk}(\bar{q}_s^k\sigma^{\mu\nu}u_t)$ | | |

*Table 1.2: Four-fermion operators, chiral indices are assumed in the operator class.*

play suppressed by the mass $M$ of the heavy particle. Another effect of the decoupling is the difference in the *beta functions* of the full and the effective theory, hence the couplings are affected as well. All of the above corrections, coming from the decoupling at some scale $M$ are referred as *threshold corrections*.

In constructing an EFT via to top-down approach one begins with a well defined UV model that describes physics at energy scales higher than a certain energy threshold. In order to systematically derive the EFT in the IR regime we follow the process of integrating out heavy degrees of freedom from the UV theory, this process is known as *matching*. The goal of this procedure is to obtain and effective theory that describes the dynamics of the light degrees of freedom in energy scales much lower than the mass scale of the full theory. Overall, the matching process boils down to the following statement, *the low-energy EFT and the full theory have to reproduce the same S-matrix elements.*

There are two methods for performing the matching, *diagrammatic matching*, through Feynman diagrams and *functional matching*, which directly deals with the path integral. Both methods aim for the same outcome but use different techniques to achieve it. Below, we will highlight how both approaches work and discuss their respective advantages.

In diagrammatic matching one calculates Green's functions in both the full theory and in the EFT using Feynman diagrams and by comparing the resulting computations the Wilson coefficients of the EFT are extracted that reproduce the same predictions as the low energy behavior of the UV theory. This can be done at any order in perturbation theory, our focus lies mainly in one loop matching. In order to achieve this one has to follow the steps outlined below.

- Draw all relevant Feynman diagrams up to one loop that do not contain any heavy degrees of freedom in the external legs. All heavy particles must circulate inside the loop and may be combined with light degrees of freedom also running in the loop.
- Calculate all relevant diagrams expanding the denominators in powers of $1/M$, where $M$ is the off-shell mass of the heavy particle, keeping the expansion up to the desired order. For example, if we want to include up to dimension 6 operators one has to cut-off the expansion to $1/M^2$ neglecting all other contributions suppressed by higher powers.
- Draw and calculate the corresponding diagrams in the EFT, which would include local operators without any heavy fields. Only light fields are allowed inside the loops. Note that Wilson coefficients are treated as unknown quantities in the EFT.
- Equate the amplitude at some desired scale $\mu$, and solve the system of equations for the Wilson coefficients.

Diagrammatic matching makes it easy to identify which diagrams contribute to a particular operator in the EFT and how different interactions affect observables. However, matching must be redone for each process or class of processes, which can be inefficient if one is interested in many observables or in extracting all WCs of the UV model.

In functional matching, one employs the path integral machinery along with the background field method to directly compute the effective action including the effects of heavy degrees of freedom. More specifically, we require the one-particle-irreducible (1PI) effective action to be the same as the one-light-particle-irreducible (1LPI) effective action stemming for the UV,

$$\Gamma^{\text{1PI}}_{\text{EFT}}[\phi] = \Gamma^{\text{1LPI}}_{\text{UV}}[\phi]\,, \tag{1.23}$$

where with $\phi$ we denote light degrees of freedom. At tree level one has to simply substitute in the UV Lagrangian, $\mathcal{L}_{\text{UV}}[\Phi,\phi]$, the equations of motion of the heavy particle $\Phi$, that is,

$$\mathcal{L}^{\text{tree}}_{\text{EFT}}[\phi] = \mathcal{L}[\Phi_c,\phi], \tag{1.24}$$

where $\Phi_c$ is the solution of the EOMs. At one-loop the computations are more involved but an elegant result arises in the end,

$$S^{\text{1-loop}}_{\text{EFT}} = \frac{i}{2}\,\text{STr}\log\left(-\left.\frac{\delta^2 S_{\text{UV}}}{\delta\phi^2}\right|_{\Phi=\Phi_c}\right)\Bigg|_{\text{hard}}\,, \tag{1.25}$$

where by “hard” we denote that all integrals in dimension regularization (DR) arising in the specific computations should be expanded in the region where $q \sim M_\Phi \gg m_\phi$. The second variations of the actions can be further decomposed in the following way as,

$$-\left.\frac{\delta^2 S_{\text{UV}}}{\delta\phi^2}\right|_{\Phi=\Phi_c} = \mathbf{K}-\mathbf{X}\,, \tag{1.26}$$

where $\mathbf{K}$ constitutes the inverse propagator while $\mathbf{X}$ denotes the interaction part. This lead to the following result,

$$S^{\text{1-loop}}_{\text{EFT}} = \frac{i}{2}\text{STr}\log\mathbf{K}\Big|_{\text{hard}} - \frac{i}{2}\sum_{n=1}^{\infty}\frac{1}{n}\,\text{STr}\left[\left(\mathbf{K}^{-1}\mathbf{X}\right)^n\right]\Big|_{\text{hard}}\,, \tag{1.27}$$

these two terms are known as "log-type" and "power-type" supertraces respectively. These can be systematically organized graphically. The method provides the complete set of effective operators and their coefficients without the need to consider specific processes. Although more general than diagrammatic matching functional methods involve sophisticated mathematical techniques that may be less intuitive than diagrammatic methods. The application of functional matching and its details is postponed until Chapter 2 of this thesis.

Since the results of functional matching are process independent they are universal in the sense that some part of the matching procedure can be calculated once and for all for many classes of UV model because they share common forms of **K** and **X** matrices. By assuming for example that any number of heavy scalar particles run in the loop one arrives at the so-called Universal One Loop Effective Action or UOLEA [24, 25]. Several other universal results have surfaced since then. The first graphical organization of function techniques is called *covariant diagrams* [26] which led to the extension of the UOLEA to include heavy-light contributions in the loop [27, 28]. Other results include the fermionic UOLEA [29, 30] and several other computations [31–34]. The go to workflow for functional matching is clearly described in [35].

However, if one follows the aforementioned prescription for one loop matching even for a simple SM extension the complexity of the calculations quickly rises and a by hand approach becomes tedious. For this reason there have been developed several automated packages to facilitate parts of the process of matching such as tree level matching [36], encoding the UOLEA to speed up calculations [37], calculating supertraces by applying the CDE technique [38, 39] all the way up to extracting the WCs through matching automatically [40, 41].

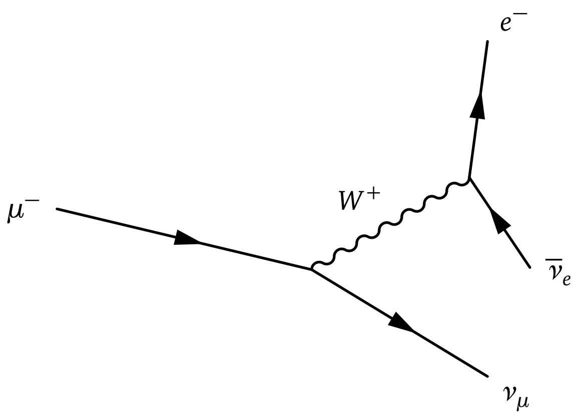


*Fig. 1.2: Tree level process $\mu \to \nu_\mu\, e\, \overline{\nu}_e$*

### 1.5.1 Fermi Theory

As a warm up example of a diagrammatic matching calculation we will introduce an EFT known as the *4-Fermi theory*, which is a low-energy description of the weak interactions. The Fermi theory was used for calculations of amplitudes well before the SM was discovered, the parameters of the SM were not essential to apply the theory. It gave a very accurate description of the phenomenology of weak interactions and by precision measurements at low energies, it gave constraints on the masses of the $W$ and $Z$ bosons.

We will derive the 4-Fermi theory from the weak interactions, by means of decoupling the

W-boson from the Green functions, i.e. Feynman diagrams. The weak charged current is,

$$J_\mu^+ = \frac{1}{\sqrt{2}}\left(\overline{\nu}_L^i \gamma_\mu e_L^i + V_{ij}\overline{u}_L^i \gamma_\mu d_L^j\right) . \tag{1.28}$$

The muon decay can be produced by this current and at tree-level it is described by the diagram in Fig.1.2. The amplitude, in unitary gauge, reads,

$$i\mathcal{A} = -\frac{g^2}{2}\left(\overline{e}_L \gamma^\mu \nu_{eL}\right)\frac{-i\left(g_{\mu\nu} - \frac{p_\mu p_\nu}{M_w^2}\right)}{p^2 - M_w^2}\left(\overline{\nu}_{\mu L}\gamma^\nu \mu_L\right) . \tag{1.29}$$

At low energies, $p^2 \ll M_w^2$, we can expand the propagator,

$$\frac{g_{\mu\nu} - \frac{p_\mu p_\nu}{M_W^2}}{p^2 - M_W^2} = -\frac{1}{M_W^2}\left[g_{\mu\nu} + \left(1 + \frac{p^2}{M_W^2}\right)\frac{p^2 g_{\mu\nu} - p_\mu p_\nu}{M_W^2} + \ldots\right] ,$$

keeping only the leading term we get the amplitude,

$$i\mathcal{A} = -i\frac{g^2}{2M_W^2}\left(\overline{e}_L \gamma^\mu \nu_{eL}\right)\left(\overline{\nu}_{\mu L}\gamma_\mu \mu_L\right) . \tag{1.30}$$

The Lagrangian describing this interaction is,

$$\mathcal{L}_{\text{4F}} = -\frac{4G_F}{\sqrt{2}}\left(\overline{\nu}_\mu \gamma^\mu P_L \mu\right)\left(\overline{e}\ \ \gamma_\mu P_L \nu_e\right) , \tag{1.31}$$

where we have defined,

$$\frac{4G_F}{\sqrt{2}} \equiv \frac{g^2}{2M_W^2} = \frac{2}{v^2} . \tag{1.32}$$

The procedure we have just used is known as *integrating out* a particle from the theory. The Lagrangian now describes a 4-fermion vertex as shown in Fig.1.3. We note that this Lagrangian does not mediate any heavy degrees of freedom such as the $W$-boson, and it only contains 4-fermion interactions. The muon decay lifetime in the limit $m_\mu \ll m_e$ in the Fermi theory is

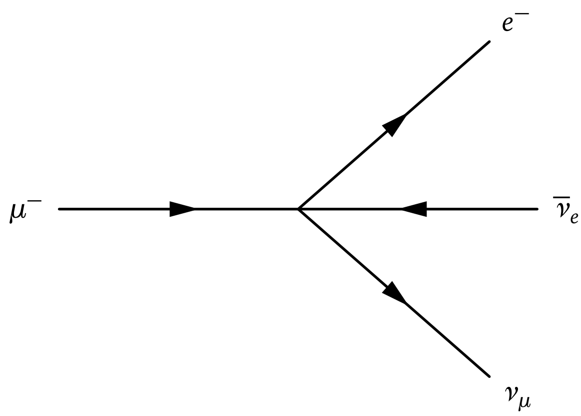


*Fig. 1.3: The muon decay in the 4-Fermi theory.*

easy to calculate and is given by,

$$\Gamma\left(\mu \to \nu_\mu e \overline{\nu}_e\right) = G_F^2 \frac{m_\mu^5}{192\pi^3} . \tag{1.33}$$

The experimental value of the muon lifetime is $\tau_\mu = 2.197\ \mu s$, this let us calculate $G_F$,

$$G_F = 1.166 \times 10^{-5}\ \text{GeV}^{-2} , \tag{1.34}$$

which, if we consider it to be the scale $1/\Lambda^2$ we get approximately the value $\Lambda \sim 300$ GeV, which indicates the scale at which the EFT admits a UV completion.

## 1.6 Bottom-up EFTs

Contrary to the top-down approach where the WCs are known in terms of couplings of the UV theory, in the bottom-up approach the WCs are treated as free parameters. In this approach we first construct a low energy EFT, without referring to any UV model of physics, and the values of the WCs are determined numerically by experimental data. To extract or constrain these WCs we employ statistical methods that compare theoretical predictions of observables with experimental data.

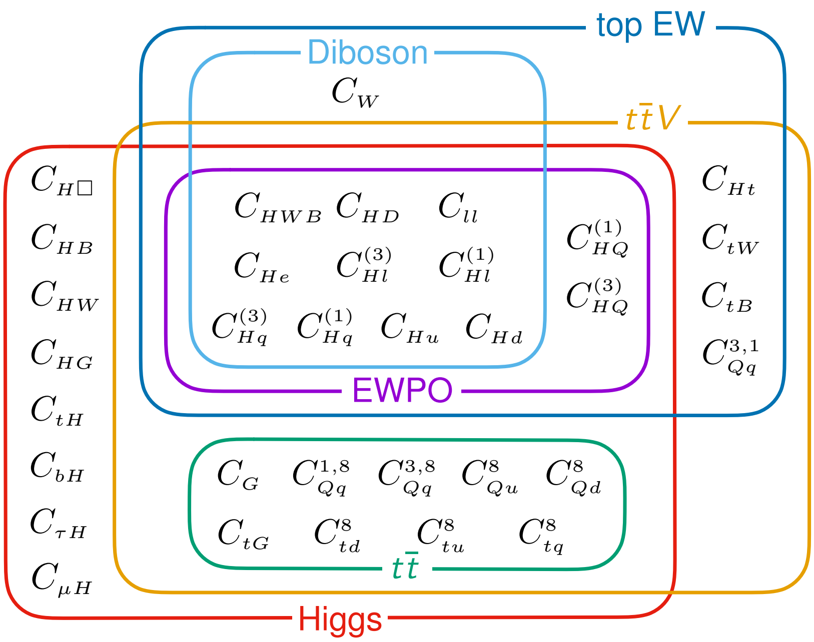


*Fig. 1.4: Different sectors of physical observables, related to the top-quark, and their corresponding dependence on WCs, taken from [42].*

The starting point is to postulate a Lagrangian, as our example EFT we will use the SMEFT, which part of it is also used in Chapter 3 to disentangle the Higgs sector. A very nice depiction of the various sectors and their dependence on the specific WCs can be seen in Fig.1.4. In order to constrain the WCs, we need precise theoretical predictions, calculated through the effective Lagrangian, for observables that are sensitive to higher dimensional operators. These observables may include, production and decay rates, cross sections, asymmetries and any other measurable quantity. Thus any set of observables $\mathcal{O}$ in principle can be written in the following form,

$$\mathcal{O}_{\text{theory}} = \mathcal{O}_{\text{SM}} + \delta\mathcal{O}_{\text{SMEFT}}\,, \tag{1.35}$$

where $O_{\text{SM}}$ contains the SM prediction while $\delta\mathcal{O}_{\text{SMEFT}}$ corresponds to the sum of WCs that affects the corresponding observable in the EFT. The next step is to collect a set of observables capable of constraining the aforementioned WCs, as an example, SMEFT, including flavor, consists of 2499 operators. The parameter space of dimension-6 WCs is huge and if we are to fairly bound each WCs an equal or larger amount of observables is required. The task is daunting but the effort has started through the use of computer packages such as `smelli` [43]. The set of observables $\mathcal{O}_{\text{exp}}$ is collected along with their associated uncertainties and correlations.

The chi-squared statistic is defined to quantify the discrepancy between the theoretical predictions and the experimental data,

$$\chi^2 = \left(\mathbf{O}_{\text{exp}} - \mathbf{O}_{\text{theory}}\right)^T \mathbf{V}^{-1} \left(\mathbf{O}_{\text{exp}} - \mathbf{O}_{\text{theory}}\right) , \tag{1.36}$$

where $\mathbf{O}_{\text{theory,exp}}$ are vectors denoting the set of theoretical predictions and experimental measurements respectively, while the *covariance* matrix $\mathbf{V}$ contains the relevant uncertainties and correlations of the measurements.

The main objective is to find the set of WCs, $\{C_i\}$, that minimize the $\chi^2$ function, thus providing the best fit to experimental data. The minimization is usually done by numerical optimization techniques, such as gradient descent and in some instances it can also be solved analytically, using matrix decomposition techniques such as Singular Value Decomposition (SVD), in the case where the theoretical predictions linearly depend on WCs, which is the case up until dimension-6 operators.

After obtaining the best-fit values of the Wilson coefficients, the next step is to assess the goodness of fit. This involves the examination of the minimum value the $\chi^2$ function has reached compared to the degrees of freedom relevant to the fit. In general the degrees of freedom are defined as the difference between the number of data points and the number of fitted parameters,

$$\nu = N_{\text{data}} - N_{\text{parameters}} , \tag{1.37}$$

To assess the goodness-of-fit we calculate the reduced chi-squared, $\chi^2_\nu = \chi^2_{\text{min}}/\nu$. A value close to one, $\chi_\nu \sim 1$, indicates that the theoretical model adopted can provide an acceptable fit to the data within uncertainties. A significantly larger value suggests that the model may not be able to accurately describe the data, potentially indicating the need for additional BSM physics to account for the discrepancies, or we may have underestimated the error variance of our data points. If on the other hand $\chi_\nu < 1$, the model *overfits* the data, indicating that the collection of data is too small and a larger set of observables is needed.

An important quantity to also consider is the *covariance* matrix of the fitted parameters, which provides information about the uncertainties and correlations of the WCs, defined as the inverse of the Hessian matrix of the $\chi^2$ function evaluated at it's minimum values,

$$(\text{Cov})_{ij} = \left( \frac{1}{2} \frac{\partial^2 \chi^2}{\partial C_i \, \partial C_j} \bigg|_{C^{\text{best-fit}}} \right)^{-1} , \tag{1.38}$$

where $C_{i,j}$ represent the various WCs of the chosen set. The diagonal elements of this matrix represent the variances of each individual WC, while the off-diagonal elements give the correlations between different WCs. These correlations deem important since they give information on how changes in one coefficient affects another when fitting the data. A neat graphical representation that shows the confidence regions of fitted parameters are *contour plots*, particularly useful when dealing with two or three parameters. They provide visual insight into the uncertainties and correlations between parameters, by showing levels of constant $\chi^2$ in the parameter space.

To create contour plots we chose two WCs out of the set of parameters to depict, e.g. $C_1$ and $C_2$ and fix the other to their best-fit values obtained by the $\chi^2$ minimization. Then, create a grid of data points around the best fit values of $C_1^{\text{best-fit}}$ and $C_2^{\text{best-fit}}$ and calculate the values of $\chi^2(C_1, C_2)$ for each grid point generated above keeping other parameters fixed. Lastly, determine the confidence intervals that you wish to show, e.g. when we draw $1\sigma$ contours this corresponds to 68.3% chance that a random point will land inside the contour plot region. To draw these values, evaluate the chi-squared distribution (inverse of the cumulative distribution) with two degrees of freedom, $\Delta\chi^2 = \chi^2 - \chi^2_{\rm min}$ to determine contours of constant $\chi^2$. For example, all points within $1\sigma$ will be inside the region defined by,

$$\chi^2(C_1, C_2) - \chi^2_{\rm min} \leq \Delta\chi^2(1\sigma) \Rightarrow \chi^2(C_1, C_2) - \chi^2_{\rm min} \leq 2.3\,. \tag{1.39}$$

Where the value of $\Delta\chi^2(1\sigma)$ can be found in tables or software for the chi-square distribution of two degrees of freedom.

Contour plots reveal crucial information about the parameters in a statistical analysis. The spread of the contours along each axis indicates the uncertainty in each parameter; narrow contours imply tight constraints, while wide contours suggest larger uncertainties. The orientation and shape of the contours show the correlations between parameters. If the contours are elongated along a diagonal, this indicates a strong correlation, meaning that changes in one parameter can be compensated by changes in the other without significantly affecting the $\chi^2$. Additionally, the regions enclosed by the contours represent parameter values consistent with the data at the specified confidence levels. Points outside these regions are excluded with a certain degree of confidence.

In effective field theories, contour plots are invaluable for several reasons. They provide insight into how the data constrain the parameters and reveal regions of parameter space consistent with experimental observations. By showing how parameters are correlated, contour plots help us understand the interplay between different operators in the EFT. Recognizing areas of parameter space with large uncertainties or strong correlations can motivate new measurements aimed at improving constraints. Additionally, contour plots facilitate the comparison of different theoretical models or scenarios by visually displaying how the allowed parameter regions change under different assumptions. All of these techniques outlined previously will be used to study a specific set of observables and WCs related to the Higgs sector in Chapter 3.

# Chapter 2

# Functional Matching of Scalar Leptoquarks

In this study we present a universal effective action for one-loop matching of all scalar leptoquarks. We use both the Universal One-Loop Effective Action (UOLEA) and covariant diagrams to evaluate the Wilson coefficients directly in the Green basis for up-to dimension-6 operators. On the technical side, we use the newly developed method of evaluating supertraces, to further validate the results stemming from the use of covariant diagrams. As an application, we perform a fully functional matching onto Standard Model Effective Field Theory (SMEFT) of a model with two scalar leptoquark fields: a weak isospin singlet and a doublet. We demonstrate its use by calculating several observables, such as lepton magnetic and electric dipole moments, neutrino masses, proton decay rate, while we comment upon fine tuning issues in this model. Apart from its phenomenological interest, this model generates the majority of dimension-6 operators and provides an EFT benchmark towards future matching automation. This chapter is based on ref [44].

## 2.1 Introduction

Effective field theory (EFT) [45–47] is an important part of our understanding of nature, it constitutes a robust way of dealing with new physics phenomena for Beyond the Standard Model (BSM) physics. One can obtain a low energy EFT action by integrating out heavy degrees of freedom from a, more general than the SM, UV-theory. At the end of the process we obtain an EFT Lagrangian with modified SM couplings and masses augmented by higher dimensional operators whose associated Wilson coefficients (Wcs) encode the information about the UV-theory [48]. The main technique to perform this kind of calculation has been Feynman diagrams. However, during the last decade, functional matching has seen a renewed interest.

The first steps were taken with the application of the covariant derivative expansion (CDE) in [49–51], while the revival of these techniques and methods was recently made in [32, 52]. A first universal result named UOLEA (Universal One Loop Effective Action) was developed in [24, 27, 28]. However, this result is not truly universal since it does not account for mixed statistics and open covariant derivatives, it can be used to decouple scalar particles only i.e. involving both heavy-heavy loops as well as heavy-light loops with the scalar particles running inside. Very recently the fermionic UOLEA was also constructed [29, 30] and the completion of the fermionic and scalar UOLEA was also developed [53] taking also mixed statistics into account.

Another approach to functional matching, which was used to derive the heavy-light part of the UOLEA, are the *covariant diagrams* [26], which mimic the usual Feynman diagrams but are at all steps gauge-covariant. This relatively new tool makes use of the expansion by regions [54, 55] and a simpler matching framework [33], which builds upon refs. [56, 57], to further simplify the matching procedure. An example application can be found in [25, 26]. The logic of these diagrams was taken a step forward with the development of *supertrace functional*-technique [35] which establishes a cleaner way to make up diagrammatic traces. Soon after that, an automated application of the CDE followed [38, 39] easing further matching calculations. Although aiming at a different direction, similar effective actions based on supertrace and Grassmannian techniques were derived in ref. [58] using a field-space supermanifold.

Briefly, the idea behind functional matching is to equate the generating functionals,

$$\Gamma_{\mathrm{EFT}}[\phi] = \Gamma_{\mathrm{L,UV}}[\phi]\,, \tag{2.1}$$

for the EFT and UV-theory with light fields ($\phi$) respectively. If $S$ is a heavy field, say a leptoquark field, with mass $M_S \gg m_\phi$, then the matching conditions at tree and one-loop level read:

$$\mathcal{L}^{(\mathrm{tree})}_{\mathrm{EFT}}[\phi] \quad = \quad \mathcal{L}_{\mathrm{UV}}[S,\phi]\Big|_{S=S_c[\phi]}\,, \tag{2.2}$$

$$\int d^d x\, \mathcal{L}^{(1-\mathrm{loop})}_{\mathrm{EFT}}[\phi] \quad = \quad \Gamma_{\mathrm{L,UV}}[\phi]\Big|_{\mathrm{hard}}\,. \tag{2.3}$$

Here $S_c[\phi]$ is the classical heavy field which solves the classical equations of motion (EOMs),

$$\left.\frac{\delta \mathcal{S}_{\mathrm{UV}}[S,\phi]}{\delta S}\right|_{S=S_c[\phi]} = 0\,. \tag{2.4}$$

Moreover, the evaluation of the loop-integral in the rhs of eq. (2.3) is performed in the (hard) region assuming momenta $q \sim M_S \gg m_\phi$ and has the form

$$\int d^d x\, \mathcal{L}_{\rm EFT}^{(1-{\rm loop})}[\phi] = \frac{i}{2}\, {\rm STr}\, \log \mathbf{K}\Big|_{\rm hard} - \frac{i}{2}\sum_{n=1}^{\infty}\frac{1}{n}\, {\rm STr}\big[(\mathbf{K}^{-1}\mathbf{X})^n\big]\Big|_{\rm hard}\,. \tag{2.5}$$

Therefore, the EFT Lagrangian is a sum of functional Supertraces through the log-function of the propagator $\mathbf{K}$ in field space and a power expansion of the operator $(\mathbf{K}^{-1}\mathbf{X})$, where $\mathbf{X}$ is a field operator - an interaction matrix - evaluated at $S = S_c[\phi]$. Basically, finding the $\mathbf{X}$-matrix, and evaluating the Supertrace functional at the desired order in the EFT Lagrangian is what is required for the master formula of eq. (2.5) to work. This is the functional approach mainly of refs. [26, 35] that we use in our work here in order to

1. derive a universal one-loop effective action up-to dimension-6 operators for all scalar leptoquark (LQ) extensions of the Standard Model (SM) [59].
2. apply the formalism in the decoupling of two heavy LQ fields, a coloured weak isospin singlet ($S_1$) and a coloured weak isospin doublet ($\tilde{S}_2$) and derive the full set of $d \leq 6$ operators, not resorting to Baryon or Lepton number conservation.
3. support the usefulness and clarity of functional matching over traditional Feynman diagrammatic methods or within functional methods, by comparing both supertrace and covariant diagrammatic techniques.

There are, various worked out examples functionally integrating out non-degenerate fields in refs. [24, 30, 53], however, with an exception of ref. [25] and to our knowledge, there is no other functional calculation with two-field decoupling and more general Yukawa interactions in the literature as the one we present here.[1] The renormalization scheme in our calculation is a (modified) mass independent one ($\overline{\rm MS}$) and we regulate the integrals with dimensional regularization. We match on to SMEFT operators within a redundant basis, referred to as *Green (or General) basis*, which consists of operators written before equations of motion for the light-fields are taken into account [63, 64]. Expressions for translating Wcs from Green to Warsaw basis [13] are given in ref. [64].

However, before taking up the above analysis, we first validated calculations performed with Feynman diagrammatic techniques. We started from matching a single charged singlet, the model of ref. [65] in SMEFT. We found full agreement apart from a missing operator [66]. Next, we applied functional covariant diagrams to a benchmark leptoquark model $S_1 + S_3$ of ref. [64], where we found perfect agreement with v4 of ref. [64]. Part of our functional calculation in this Chapter addresses this model too but now with the inclusion of Baryon number violating terms in the UV-Lagrangian. Finally, regarding the tree-level part of our calculation we found agreement with ref. [67].

We have chosen to study the decoupling of heavy scalar leptoquark fields for two main reasons: first, there is a plethora of interesting BSM phenomena associated to them, i.e. from neutrino masses and proton decay [68], to possible interpretation of recent flavour anomalies

[1] A complete one-loop functional matching of the singlet scalar extension of the SM exists in ref. [35] and very recently, there have also been two complete one loop, but one-field-type, matching calculations using functional methods, where ref. [60] matches the Type-I neutrino seesaw onto SMEFT, while ref. [61] matches the Higgs triplet extension of the electroweak gauge sector. Also recently, one-field heavy scalar decoupling has been classified in ref. [62] by using the code of ref. [37].

and enhanced anomalous magnetic moment of the muon [69–74], and second, leptoquark fields are naturally embedded in Grand Unified Theories (GUTs) which may be in turn linked to even more fundamental theories.

## 2.2 Universal One Loop Functional Matching for Scalar Leptoquarks

Leptoquarks ($S$) are hypothetical fields defined by their Yukawa interactions to both SM quarks and leptons via the Lagrangian,

$$\mathcal{L}_{\text{S–f}} \;=\; \bar{F}^c \boldsymbol{\lambda}_i^L F S_i \;+\; \bar{f}^c \boldsymbol{\lambda}_i^R f S_i \;+\; \bar{f}\, \tilde{\boldsymbol{\lambda}}_i F S_i \;+\; \text{h.c.}\,, \tag{2.6}$$

where fermion $F = \{q, \ell\}$ is a Left handed quark or lepton weak doublet field, while $f = \{u, d, e\}$ is a Right-handed fermion weak singlet field. $F^c, f^c$ denote charge-conjugated fermion fields. Gauge and flavour indices are all suppressed in (2.6), or otherwise encoded in the Yukawa couplings, $\boldsymbol{\lambda}^L, \boldsymbol{\lambda}^R$ and, $\tilde{\boldsymbol{\lambda}}$. Therefore, there are five different scalar leptoquark field representations in weak isospin space: three singlets, two doublets and one triplet. Their gauge quantum numbers under the SM gauge group, are shown in Table 2.1.[2] The LQ-flavour index $i$ in (2.6) takes the values $i = \{1, \tilde{1}, 2, \tilde{2}, 3\}$. [3] Obviously, by picking up only quarks from

| LQ-fields ($S$) | SU(3) | SU(2) | U(1) |
|---|---|---|---|
| $S_1$ | $\bar{3}$ | 1 | $\frac{1}{3}$ |
| $\tilde{S}_1$ | $\bar{3}$ | 1 | $\frac{4}{3}$ |
| $S_2$ | 3 | 2 | $\frac{7}{6}$ |
| $\tilde{S}_2$ | 3 | 2 | $\frac{1}{6}$ |
| $S_3$ | $\bar{3}$ | 3 | $\frac{1}{3}$ |

*Table 2.1: All possible representations of leptoquark fields under the SM gauge group.*

$F-$ (or from $f-$) fields we arrive at Baryon ($B$) and Lepton ($L$) number non-conservation LQ-interactions.

All five scalar LQs can interact with the SM Higgs-field[4] ($H$) through trilinear and quadratic terms of the form:

$$\mathcal{L}_{\text{S–H}} \;=\; (A_{ij} H^\dagger S_i S_j \;+\; \text{h.c.}) \;+\; \lambda_{Hi}(S_i^\dagger S_i)(H^\dagger H) \;+\; (\lambda_{3S} S_i S_j S_k H^\dagger + \text{h.c.}) \;+\; \dots\,, \tag{2.7}$$

where "..." mean other gauge invariant terms of the form $(SSHH)$ and $(SSSH)$. Their exact form is irrelevant for drawing the supertrace functional diagrams since their explicit details entered only at the end in **X**-matrices of (2.5). Note that the $A$-term of (2.7) has mass dimension one, there are only two options $HS_1\tilde{S}_2$ and $HS_3\tilde{S}_2$, and it plays an important role in the effective Lagrangian at $d \geq 5$ level as we shall see in the next section.

Furthermore, self-interactions among LQs read in general as

$$\mathcal{L}_{\text{S}} \;=\; -M_i^2 |S_i|^2 \;+\; A'_{ijk}(S_i^\dagger S_j S_k) \;+\; c_{ijkl}(S_i^\dagger S_j)(S_k^\dagger S_l) \;+\; \cdots\,, \tag{2.8}$$

[2] In notation of (2.6) some leptoquark fields from Table 2.1 may be their charge-conjugated fields.

[3] With apologies to the reader, the LQ-flavour indices-$i, j, k$ used throughout this section should not be confused with the colour indices-$i, j, k$ introduced in section 2.3.

[4] The hypercharge of the SM Higgs doublet is defined so that $Y_H = 1/2$.

where again "$\cdots$" refer to different internal gauge group invariant structure of terms not in our immediate interest in constructing the effective action. Again $A'$ is a mass dimension one parameter but break baryon and lepton numbers. Among the fields arranged in Table 2.1, there are three choices of $A'$-terms: $S_1^\dagger \tilde{S}_2 \tilde{S}_2$, $S_3^\dagger \tilde{S}_2 \tilde{S}_2$ and $\tilde{S}_1^\dagger S_2 \tilde{S}_2$. Masses $M_i$ in (2.8) are assumed much heavier than the electroweak scale $m_W$ but the dimension-full parameters introduced above could in general range within

$$0 \leq \{A/M_i, A'/M_i\} \lesssim 1 . \tag{2.9}$$

In total, the BSM Lagrangian is

$$\mathcal{L}_{\text{BSM}} = \mathcal{L}_{\text{S--f}} + \mathcal{L}_{\text{S--H}} + \mathcal{L}_{\text{S}} . \tag{2.10}$$

This "universal" way of writing down leptoquark interactions will be the stepping stone for the calculation of the effective action at tree and one-loop levels using eqs. (2.2),(2.3) and (2.5), respectively, since these will determine the dimensionality of the **X**-matrices that we will introduce shortly. Otherwise, the explicit form of $\mathcal{L}_{\text{BSM}}$ is given in Appendix A.

### 2.2.1 Tree level EFT, $\mathcal{L}_{\text{EFT}}^{(\text{tree})}$

We start out with the UV-Lagrangian $\mathcal{L}_{\text{UV}}[S,\phi] = \mathcal{L}_{\text{SM}}[\phi] + \mathcal{L}_{\text{BSM}}[S,\phi]$ and derive the EOMs (2.4) for the heavy fields $S_i$ in Table 2.1. We solve EOMs and substitute the solutions for the classical fields $S_{i,c}[\phi]$ back into $\mathcal{L}_{UV}$ in order to obtain the tree-level EFT from eq. (2.2). By expanding the classical field in inverse powers of heavy masses $M_i$

$$S_{i,c}[\phi] = S_{i,c}^{(3)} + S_{i,c}^{(4)} + \ldots , \tag{2.11}$$

we find

$$(S_{i,c}^{(3)})^\dagger = \frac{1}{M_i^2} \left( \bar{F}^c \boldsymbol{\lambda}_i^L F + \bar{f}^c \boldsymbol{\lambda}_i^R f + \bar{f} \tilde{\boldsymbol{\lambda}}_i F \right) , \tag{2.12}$$

$$(S_{i,c}^{(4)})^\dagger = \frac{1}{M_i^2} A_{ij} H^\dagger S_{j,c}^{(3)} . \tag{2.13}$$

The solutions $S_{i,c}^{(n)}$ contain operators with mass dimension $n$ which are suppressed by factors that scale like $M_i^{n-1}$. Plugging in this back to eqs. (2.6)-(2.8) we obtain the tree-level effective Lagrangian containing $d \leq 7$ operators

$$\mathcal{L}_{\text{EFT}}^{(\text{tree})}[\phi] = M_i^2 \, (S_{i,c}^{(3)})^\dagger \, (S_{i,c}^{(3)}) + (A_{ij} H^\dagger S_{i,c}^{(3)} S_{j,c}^{(3)} + \text{h.c.}) , \tag{2.14}$$

where $S_{i,c}^{(3)}$ is the hermitian conjugate of (2.12). Therefore, the tree-level EFT contains *only* four-fermion dimension-6 operators proportional to the product of couplings from the set $\{\boldsymbol{\lambda}^L, \boldsymbol{\lambda}^R, \tilde{\boldsymbol{\lambda}}\}$. On the other hand, *all* tree-level dimension-7 operators are proportional to the dimension-full combination of parameters $A \times \boldsymbol{\lambda}^2$. From eq. (2.7) we see that the parameters $\lambda_{Hi}$ and $\lambda_{3S}$ appear first to multiplying operators with dimensions-8 and 10, respectively, while from eq. (2.8), the parameters $A'$ and $c$ are associated with dimension-9 and 12, respectively. Although our main focus in this chapter is on operators with dimensions less or equal to six it is obvious that dimension-7 operators at tree-level may become equally important in the parameter region where $A \approx M_i$ and one other leptoquark mass is $M_j \approx \sqrt{v M_i}$, with $v$ being the electroweak vev.

### 2.2.2 K- and X-matrices

The neccessary steps for one loop matching are neatly outlined in [35] and are followed closely here. In performing the matching, the method of functional *supertraces* will be used as introduced in [35]. After collecting and constructing the supertraces, the application of the CDE (Covariant Derivative Expansion) is carried out automatically through two recently developed packages [38, 39]. We will be using mainly the package, `STrEAM` of [38].

The rationale of these diagrams comes from an earlier diagrammatic approach to matching which uses the so called covariant diagrams [26]. In Appendix B we make this comparison more explicit by presenting the equivalent covariant diagrams that match to the diagrammatic supertraces.

We begin by creating field multiplets, where we denote the five (heavy) leptoquark fields, listed in Table 2.1, as $\{S_i\} = \left\{S_1, \tilde{S}_1, S_2, \tilde{S}_2, S_3\right\}$. Additionally, to treat chiral fermions we introduce fictitious fields promoting Weyl fermions into Dirac and properly inserting projections operators to single-out the correct chirality of the fields in the end. For simplicity these projection operators are left implicit throughout the text. The field multiplets then read,

$$\varphi_S = \{\varphi_{S_i}\} = \left\{\begin{pmatrix} S_i \\ S_i^* \end{pmatrix}\right\} , \tag{2.15}$$

$$\varphi_H = \left\{\begin{pmatrix} H \\ H^* \end{pmatrix}\right\} , \tag{2.16}$$

$$\varphi_f = \left\{\varphi_\ell,\, \varphi_q,\, \varphi_u, \varphi_e,\, \varphi_d\right\} = \left\{\begin{pmatrix} \ell \\ \ell^c \end{pmatrix}, \begin{pmatrix} q \\ q^c \end{pmatrix}, \begin{pmatrix} u \\ u^c \end{pmatrix}, \begin{pmatrix} e \\ e^c \end{pmatrix}, \begin{pmatrix} d \\ d^c \end{pmatrix}\right\} , \tag{2.17}$$

$$\varphi_V = \{B,\, W,\, G\} \ . \tag{2.18}$$

We also introduce the conjugate field multiplets,

$$\bar{\varphi}_S = \left\{\bar{\varphi}_{S_i}\right\} = \left\{\begin{pmatrix} S_i^\dagger & S_i^T \end{pmatrix}\right\} , \tag{2.19}$$

$$\bar{\varphi}_H = \left\{\begin{pmatrix} H^\dagger & H^T \end{pmatrix}\right\} , \tag{2.20}$$

$$\bar{\varphi}_f = \left\{\bar{\varphi}_\ell,\, \bar{\varphi}_q,\, \bar{\varphi}_u, \bar{\varphi}_e,\, \bar{\varphi}_d\right\} = \left\{\begin{pmatrix} \bar{\ell} & \bar{\ell}^c \end{pmatrix}, \begin{pmatrix} \bar{q} & \bar{q}^c \end{pmatrix}, \begin{pmatrix} \bar{u} & \bar{u}^c \end{pmatrix}, \begin{pmatrix} \bar{e} & \bar{e}^c \end{pmatrix}, \begin{pmatrix} \bar{d} & \bar{d}^c \end{pmatrix}\right\} , \tag{2.21}$$

$$\bar{\varphi}_V = \{B,\, W,\, G\} \ . \tag{2.22}$$

These field multiplets are connected to the inverse propagator matrix-**K** and to interaction matrix-**X**, both needed for master formula (2.5), via the second variation of the action as

$$+\frac{1}{2}\,\delta\bar{\varphi}\,\mathbf{K}\,\delta\varphi \;-\; \frac{1}{2}\begin{pmatrix} \delta\bar{\varphi}_S & \delta\bar{\varphi}_L \end{pmatrix}\begin{bmatrix} X_{SS} & X_{SL} \\ X_{LS} & X_{LL} \end{bmatrix}\begin{pmatrix} \delta\varphi_S \\ \delta\varphi_L \end{pmatrix} . \tag{2.23}$$

We have gathered all *light* multiplets in $\varphi_L$ and we denote the whole field multiplet with $\varphi$ for brevity, while with $\delta\varphi$ we denote the variation of each respective multiplet. Matrix-**K** is block-diagonal with $(P^2 - m^2)$ for spin-0 fields, $(\not{P} - m)$ for spin-1/2 and $-\eta^{\mu\nu}(P^2 - m^2)$ for spin-1 fields in Feynman gauge. Here $P_\mu \equiv iD_\mu$ is basically the (Hermitian) covariant derivative. The **X**-matrix may contain potential-only interactions and/or terms with open covariant derivatives as well. It is evaluated with $S_i = S_{i,c}[\phi]$. Moreover, in the most general case,

$$\mathbf{X} \;=\; \mathbf{U} \;+\; P^\kappa \mathbf{Z}_\kappa \;+\; \bar{\mathbf{Z}}_\kappa P^\kappa \;+\; \ldots \tag{2.24}$$

where the dots contain terms with two or more open covariant derivatives, however these higher derivative terms do not appear in any renormalizable UV-model, such as the LQ-models under consideration and can be ignored.

The $\mathbf{X}$-interaction matrix structure in (2.23) is split into *heavy-heavy*, $\mathbf{X}_{SS}$, *light-light*, $\mathbf{X}_{LL}$ and *heavy-light (light-heavy)*, $\mathbf{X}_{SL}$ ($\mathbf{X}_{LS}$) sub-blocks. In terms of the expansion matrices of (2.24) these sub-blocks are organized in the following way,

$$(\mathbf{X}_{SS})_{10\times10} = \left(\left(U_{S_iS_j}\right)_{10\times10}\right), \tag{2.25}$$

$$(\mathbf{X}_{SL})_{10\times15} = \left(\left(U_{S_if}\right)_{10\times10} \quad \left(U_{S_iH}\right)_{10\times2} \quad \left(X_{S_iV}\right)_{10\times3}\right), \tag{2.26}$$

$$(\mathbf{X}_{LS})_{15\times10} = \begin{pmatrix} \left(U_{fS_i}\right)_{10\times10} \\ \left(U_{HS_i}\right)_{2\times10} \\ \left(X_{VS_i}\right)_{3\times10} \end{pmatrix}, \tag{2.27}$$

$$(\mathbf{X}_{LL})_{15\times15} = \begin{pmatrix} \left(U_{ff}\right)_{10\times10} & \left(U_{fH}\right)_{10\times2} & \left(U_{fV}\right)_{10\times3} \\ \left(U_{Hf}\right)_{2\times10} & \left(U_{HH}\right)_{2\times2} & \left(U_{HV}\right)_{2\times3} \\ \left(U_{Vf}\right)_{3\times10} & \left(U_{VH}\right)_{3\times2} & \left(U_{VV}\right)_{3\times3} \end{pmatrix}, \tag{2.28}$$

where with subscript we denote the respective matrix dimensionality for each generation of light fermions.

From the general interactions, eqs. (2.6),(2.7) and (2.8), of the scalar leptoquarks outlined in the previous subsection, we can now read the mass dimensions of the corresponding elements of $\mathbf{U}$-matrices. By schematically performing a second variation, for example on $S(\bar{f}f)$-terms,

$$\begin{aligned}\delta^2\left(S\bar{f}f\right) &\propto (\delta S)(\delta\bar{f})f + (\delta S)\bar{f}(\delta f) + S(\delta\bar{f})(\delta f) \\ &= (\delta\bar{f})U_{\bar{f}S}(\delta S) + (\delta S^T)U_{S^Tf}(\delta f) + (\delta\bar{f})U_{\bar{f}f}(\delta f),\end{aligned} \tag{2.29}$$

we can obtain the mass dimensions of the $\mathbf{X}$-matrices. Adding the h.c. of this interaction and doing again the exact calculation for the conjugate fermion fields, namely $S\bar{f}^cf^c$ + h.c., we can get the mass dimension of the matrices $[\mathbf{U}_{ff}] = 3$, $[\mathbf{U}_{S_if}] = 3/2$ and $[\mathbf{U}_{fS_i}] = 3/2$. Consequently, we arrive at the following mass dimensions for all involved matrices in notation of eqs. (2.25)-(2.28),

$$[\mathbf{X}_{SS}] = \left[(1,2,3,4,6)\right], \tag{2.30}$$

$$[\mathbf{X}_{SL}] = [\mathbf{X}_{LS}] = \left[3/2 \quad (3,4,6) \quad (3,4)\right], \tag{2.31}$$

$$[\mathbf{X}_{LL}] = [\mathbf{X}_{LL}]_{\text{SM}} + [\mathbf{X}_{LL}]_{\text{BSM}} = \begin{bmatrix} 1 & 3/2 & 3/2 \\ 3/2 & 2 & 2 \\ 3/2 & 2 & 2 \end{bmatrix} + \begin{bmatrix} 3 & 0 & 0 \\ 0 & 6 & 0 \\ 0 & 0 & 6 \end{bmatrix}, \tag{2.32}$$

where in parenthesis we denote all possible mass dimensions with $d \leq 6$ (starting from the lowest) of the $\mathbf{X}$-matrices.

For all scalar leptoquark interactions we need to calculate the explicit form of the $\mathbf{X}$-matrices in eqs. (2.25)-(2.28). This is done in Appendix A. As an application, we shall deploy those matrices in section 2.3, for a detailed functional matching procedure in a particular model for decoupling together two heavy LQ fields, the $S_1$ and the $\tilde{S}_2$.

### 2.2.3 Enumerating: UOLEA and supertraces

There are two contributions in the rhs of one-loop effective action [eq. (2.5)]: the log-type term, $\mathrm{STr}\log\mathbf{K}$, and the power-type, $\mathrm{STr}\left[(\mathbf{K}^{-1}\mathbf{X})^n\right]$. However, a great deal of contributions in eq. (2.5) are encoded in 19-UOLEA-terms [*c.f.* eq. (2.49)] for only-heavy scalars. These UOLEA terms include the full expressions of log-type terms and all power-type diagrams with *only heavy* scalars in the loop.

What remains to be added is all *heavy-light* diagrams. For those we use the technique of functional supertraces of ref. [35] and, as a cross check, the technique of covariant diagrams of ref. [26]. In fact, a detailed diagrammatic comparison of both techniques is given in Appendix B.

The **X**-matrices are the building blocks for the functional supertraces. In most of the cases only the **U**-matrices appear in the expansion (2.24). Different combinations of these matrices are inserted into diagrams and make up operators of up-to mass dimension-6. In what follows we list all diagrammatic supertraces along with the equivalent expressions that arise through this process (see [35] for details). Our notation in functional diagrams below is the following: heavy leptoquark fields $S_i$ with masses $M_i$ (double-dashed lines), $f, f', f'', f''' = q, u, d, \ell, e$ are the SM fermion fields (solid lines), $H$ is the SM Higgs-doublet (single dashed-lines), and $V = G, W, B$ are the SM gauge fields (wavy lines). Every circle indicates an insertion from $U$(or in general $X$)-matrices and $P_\mu$ is the covariant derivative. Furthermore, all SM fields are taken to be massless and $\eta^{\mu\nu} = (1, -1, -1, -1)$ is the metric tensor. With these definitions we obtain:

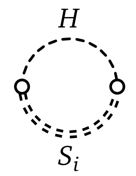


$$= \quad -\frac{i}{2}\,\mathrm{STr}\left[\frac{1}{P^2-M_i^2}U_{S_iH}\frac{1}{P^2}U_{HS_i}\right]\Bigg|_{\text{hard}}, \tag{2.33}$$

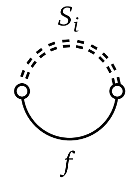


$$= \quad -\frac{i}{2}\,\mathrm{STr}\left[\frac{1}{P^2-M_i^2}U_{S_if}\frac{1}{\not{P}}U_{fS_i}\right]\Bigg|_{\text{hard}}, \tag{2.34}$$

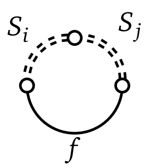


$$= \quad -\frac{i}{2}\,\mathrm{STr}\left[\frac{1}{P^2-M_i^2}U_{S_iS_j}\frac{1}{P^2-M_j^2}U_{S_jf}\frac{1}{\not{P}}U_{fS_i}\right]\Bigg|_{\text{hard}}, \tag{2.35}$$

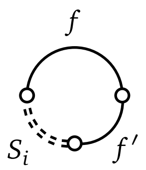


$$= \quad -\frac{i}{2}\,\mathrm{STr}\left[\frac{1}{P^2-M_i^2}U_{S_if}\frac{1}{\not{P}}U_{ff'}\frac{1}{\not{P}}U_{f'S_i}\right]\Bigg|_{\text{hard}}, \tag{2.36}$$

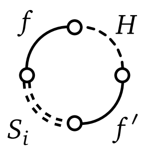


$$= \quad -\frac{i}{2}\,\mathrm{STr}\left[\frac{1}{P^2-M_i^2}U_{S_if}\frac{1}{\not{P}}U_{fH}\frac{1}{P^2}U_{Hf'}\frac{1}{\not{P}}U_{f'S_i}\right]\Bigg|_{\text{hard}}, \tag{2.37}$$

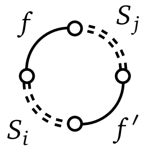


$$= \quad -\frac{i}{4}\,\mathrm{STr}\left[\frac{1}{P^2-M_i^2}U_{S_i f}\frac{1}{\not{P}}U_{f S_j}\frac{1}{P^2-M_j^2}U_{S_j f'}\frac{1}{\not{P}}U_{f' S_i}\right]\Bigg|_{\mathrm{hard}}, \tag{2.38}$$

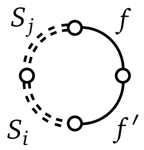


$$= \quad -\frac{i}{2}\,\mathrm{STr}\left[\frac{1}{P^2-M_i^2}U_{S_i S_j}\frac{1}{P^2-M_j^2}U_{S_j f}\frac{1}{\not{P}}U_{f f'}\frac{1}{\not{P}}U_{f' S_i}\right]\Bigg|_{\mathrm{hard}}, \tag{2.39}$$

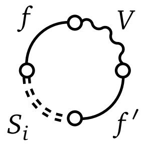


$$= \quad -\frac{i}{2}\,\mathrm{STr}\left[\frac{1}{P^2-M_i^2}U_{S_i f}\frac{1}{\not{P}}U^{\mu}_{fV}\frac{-\eta_{\mu\nu}}{P^2}U^{\nu}_{Vf'}\frac{1}{\not{P}}U_{f' S_i}\right]\Bigg|_{\mathrm{hard}}, \tag{2.40}$$

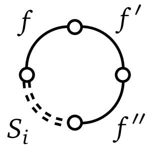


$$= \quad -\frac{i}{2}\,\mathrm{STr}\left[\frac{1}{P^2-M_i^2}U_{S_i f}\frac{1}{\not{P}}U_{f f'}\frac{1}{\not{P}}U_{f' f''}\frac{1}{\not{P}}U_{f'' S_i}\right]\Bigg|_{\mathrm{hard}}, \tag{2.41}$$

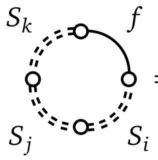


$$= \quad -\frac{i}{2}\,\mathrm{STr}\left[\frac{1}{P^2-M_i^2}U_{S_i S_j}\frac{1}{P^2-M_j^2}U_{S_j S_k}\frac{1}{P^2-M_k^2}U_{S_k f}\frac{1}{\not{P}}U_{f S_i}\right]\Bigg|_{\mathrm{hard}}, \tag{2.42}$$

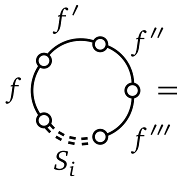


$$= \quad -\frac{i}{2}\,\mathrm{STr}\left[\frac{1}{P^2-M_i^2}U_{S_i f}\frac{1}{\not{P}}U_{f f'}\frac{1}{\not{P}}U_{f' f''}\frac{1}{\not{P}}U_{f'' f'''}\frac{1}{\not{P}}U_{f''' S_i}\right]\Bigg|_{\mathrm{hard}}, \tag{2.43}$$

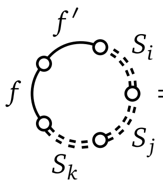


$$= \quad -\frac{i}{2}\,\mathrm{STr}\left[\frac{1}{P^2-M_i^2}U_{S_i S_j}\frac{1}{P^2-M_j^2}U_{S_j S_k}\frac{1}{P^2-M_k^2}U_{S_k f}\frac{1}{\not{P}}U_{f f'}\frac{1}{\not{P}}U_{f' S_i}\right]\Bigg|_{\mathrm{hard}}, \tag{2.44}$$

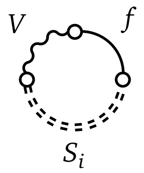


$$= \quad -\frac{i}{2}\,\mathrm{STr}\left[\frac{1}{P^2-M_i^2}X^{\mu}_{S_i V}\frac{-\eta_{\mu\nu}}{P^2}X^{\nu}_{Vf}\frac{1}{\not{P}}U_{f S_i}\right]\Bigg|_{\mathrm{hard}}, \tag{2.45}$$

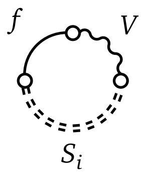


$$= \quad -\frac{i}{2}\,\mathrm{STr}\left[\frac{1}{P^2-M_i^2}U_{S_i f}\frac{1}{\not{P}}X^{\mu}_{fV}\frac{-\eta_{\mu\nu}}{P^2}X^{\nu}_{V S_i}\right]\Bigg|_{\mathrm{hard}}, \tag{2.46}$$

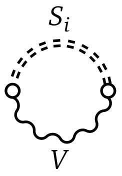


$$= \quad -\frac{i}{2}\,\mathrm{STr}\left[\frac{1}{P^2-M_i^2}X^{\mu}_{S_iV}\frac{-\eta_{\mu\nu}}{P^2}X^{\nu}_{VS_i}\right]\Bigg|_{\text{hard}} . \tag{2.47}$$

The total amount of *heavy-light* supertrace diagrams adds up to number 15.

In Appendix B one can find the explicit comparison between the number of covariant diagrams that match to a single Supertrace diagram. There the advantage of Supertraces is more evident.

### 2.2.4 Evaluating $\mathcal{L}_{\text{EFT}}^{(1-\text{loop})}$

The full 1-loop effective action is the sum of UOLEA for *heavy-heavy* loops and functional supertrace diagrams for *heavy-light* loops

$$\mathcal{L}_{\text{EFT}}^{(1-\text{loop})} = \mathcal{L}_{\text{UOLEA}} + \mathcal{L}_{\text{STr}}\,, \tag{2.48}$$

respectively. The UOLEA for *only-heavy* particles circulating in the loop, derived in Ref. [24] and then re-derived in Ref. [26], reads:

$$\begin{aligned}
\mathcal{L}_{\text{UOLEA}} = -ic_s\,\mathrm{tr}\,\Big\{ & f_2^{S_i}\,U_{S_iS_i} + f_3^{S_i}\,G'^{\mu\nu}_{S_i}G'_{\mu\nu,S_i} + f_4^{S_iS_j}\,U_{S_iS_j}U_{S_jS_i} \\
& + f_5^{S_i}\left(P^{\mu}G'_{\mu\nu,S_i}\right)\left(P_{\rho}G'^{\rho\nu}_{S_i}\right) + f_6^{S_i}\,G'^{\mu}_{\nu,S_i}G'^{\nu}_{\rho,S_i}G'^{\rho}_{\mu,S_i} + f_7^{S_iS_j}\,(P^{\mu}U_{S_iS_j})(P_{\mu}U_{S_jS_i}) \\
& + f_8^{S_iS_jS_k}\,U_{S_iS_j}U_{S_jS_k}U_{S_kS_i} + f_9^{S_i}\,U_{S_iS_i}G'^{\mu\nu}_{S_i}G'_{\mu\nu,S_i} \\
& + f_{10}^{S_iS_jS_kS_l}\,U_{S_iS_j}U_{S_jS_k}U_{S_kS_l}S_{S_lS_i} + f_{11}^{S_iS_jS_k}\,U_{S_iS_j}(P_{\mu}U_{S_jS_k})(P^{\mu}U_{S_kS_i}) \\
& + f_{12}^{S_iS_j}\,(P^2U_{S_iS_j})(P^2U_{S_jS_i}) + f_{13}^{S_iS_j}\,U_{S_iS_j}U_{S_jS_i}G'^{\mu\nu}_{S_i}G'_{\mu\nu,S_i} \\
& + f_{14}^{S_iS_j}\,(P_{\mu}U_{S_iS_j})(P_{\nu}U_{S_jS_i})G'^{\nu\mu}_{S_i} \\
& + f_{15}^{S_iS_j}\left(U_{S_iS_j}(P^{\mu}U_{S_jS_i}) - (P^{\mu}U_{S_iS_j})U_{S_jS_i}\right)(P^{\nu}G'_{\nu\mu,S_i}) \\
& + f_{16}^{S_iS_jS_kS_lS_m}\,U_{S_iS_j}U_{S_jS_k}U_{S_kS_l}U_{S_lS_m}U_{S_mS_i} \\
& + f_{17}^{S_iS_jS_kS_l}\,U_{S_iS_j}U_{S_jS_k}(P^{\mu}U_{S_kS_l})(P_{\mu}U_{S_lS_i}) \\
& + f_{18}^{S_iS_jS_kS_l}\,U_{S_iS_j}(P^{\mu}U_{S_jS_k})U_{S_kS_l}(P_{\mu}U_{S_lS_i}) \\
& + f_{19}^{S_iS_jS_kS_lS_mS_n}\,U_{S_iS_j}U_{S_jS_k}U_{S_kS_l}U_{S_lS_m}U_{S_mS_n}U_{S_nS_i}\Big\}\,,
\end{aligned} \tag{2.49}$$

where $G' = -[P_{\mu},P_{\nu}] = -igG_{\mu\nu}$ and $g$ is the coupling of the corresponding field strength tensor $G_{\mu\nu}$. $P_{\mu}$ is the covariant derivative that act to the right in every parenthesis. To get the correct contribution for Wilson coefficients we multiply these terms with $(-ic_s)$. Since we separate each complex scalar into a two component field multiplet, each component counts as a real degree of freedom, thus the correct value is, $c_s = 1/2$. We should note that after the term $f_9$ only the non-diagonal terms in $U_{SS}$ contribute and exclusively the mass dimension-1 terms of the Lagrangian. In this formula a summation over leptoquark fields $S_i$ from Table 2.1 is implied. The expressions for the coefficients, $f_1,\ldots,f_{19}$, can be found in ref. [26]. Appropriate limits of these expressions must be taken in case of degeneracies (i.e. more than one single $S$-field in the loop). Note that only **U**-matrices, calculated with $S_i = S_{i,c}[\phi]$, appear in (2.49).

We now need to calculate $\mathcal{L}_{\rm STr}$ in (2.48). For this purpose we use the package STrEAM [38] in order to calculate the relevant supertraces in (2.33)-(2.47). The main function of this package is the automation of the CDE application. As a result it computes local traces for further calculation inserting the explicit expressions of the **X**-matrices. We note that the option No$\gamma$inU removes *all* spinor indices from all matrices. However, in some instances the outer matrices contain spinor indices while the internal ones do not, or if they do, these matrices (anti)commute with $\gamma$-matrices. Therefore some manual intervention is necessary to obtain the final result.

The result of this procedure is given below. The traces are categorized depending on the number of $U$'s and $Z$'s involved in the respective diagram. The single term from the heavy-light UOLEA [(2.33)], derived in Refs. [27, 28], is also included here. The prefactor $-ic_s$ is omitted, $c_s = 1/2$ for complex scalars, and note that the matrix $U_{ff}$ contains only chirality projection operators $P_{(L,R)}$, which have been taken into account while anti-commuting $\gamma$-matrices. At the end, $\mathcal{L}_{\rm STr}$ in (2.48) is obtained from the equation,

$$\mathcal{L}_{\rm STr} = (-ic_s) \times (\text{sum of all contributions below}[\textit{c.f.}\ (2.51) - (2.77)])\,. \tag{2.50}$$

- $\underline{\mathcal{O}\left(U^2\right)}$

$$\left(1+\log\frac{\mu^2}{M_i^2}\right)\mathrm{tr}\left\{U_{S_iH}U_{HS_i}\right\}\,, \tag{2.51}$$

$$\frac{1}{2}\left(\frac{1}{2}+\log\frac{\mu^2}{M_i^2}\right)\mathrm{tr}\left\{U_{S_if}\gamma_\mu(P^\mu U_{fS_i})\right\}\,, \tag{2.52}$$

$$\frac{1}{12M_i^2}\,\mathrm{tr}\left\{U_{S_if}\gamma^\mu(P^2P_\mu U_{fS_i})+U_{S_if}\gamma^\mu(P_\mu P^2U_{fS_i})\right\}\,, \tag{2.53}$$

$$-\frac{1}{18M_i^2}\,\mathrm{tr}\left\{U_{S_if}\gamma_\nu U_{fS_i}(P_\mu G'^{\mu\nu}_{S_i})\right\}\,, \tag{2.54}$$

$$-\frac{1}{3M_i^2}\left(\frac{7}{12}+\log\frac{\mu^2}{M_i^2}\right)\mathrm{tr}\left\{U_{S_if}\gamma_\nu(P^\mu G'^{\mu\nu}_{f})U_{fS_i}\right\}\,, \tag{2.55}$$

$$\frac{i}{2M_i^2}\,\mathrm{tr}\left\{(P^\mu U_{S_if})\tilde{G}'_{\mu\nu}\gamma^\nu\gamma_5U_{fS_i}-U_{S_if}\tilde{G}'_{\mu\nu}\gamma^\nu\gamma_5(P^\mu U_{fS_i})\right\}\,. \tag{2.56}$$

- $\underline{\mathcal{O}\left(U^3\right)}$

$$\left(1+\log\frac{\mu^2}{M_i^2}\right)\mathrm{tr}\left\{U_{S_if}U_{ff'}U_{f'S_i}\right\}\,, \tag{2.57}$$

$$\frac{2\Delta_{ij}^2+(M_i^2+M_j^2)\log M_j^2/M_i^2}{4(\Delta_{ij}^2)^2}\,\mathrm{tr}\left\{(P^\mu U_{S_iS_j})U_{S_jf}\gamma_\mu U_{fS_i}\right\}\,, \tag{2.58}$$

$$\frac{1}{4\Delta_{ij}^2}\log\frac{M_j^2}{M_i^2}\,\mathrm{tr}\left\{U_{S_iS_j}U_{S_jf}\gamma_\mu(P^\mu U_{fS_i})-U_{S_iS_j}(P^\mu U_{S_jf})\gamma_\mu U_{fS_i}\right\}, \tag{2.59}$$

$$-\frac{1}{2M_i^2}\left(\frac{1}{2}+\log\frac{\mu^2}{M_i^2}\right)\mathrm{tr}\left\{U_{S_if}(P^2U_{ff'})U_{f'S_i}\right\}\,, \tag{2.60}$$

$$\frac{1}{2M_i^2}\,\mathrm{tr}\left\{U_{S_if}U_{ff'}(P^2U_{f'S_i})\right\}\ , \tag{2.61}$$

$$\frac{1}{2M_i^2}\,\mathrm{tr}\left\{U_{S_if}(P_\mu U_{ff'})(P^\mu U_{f'S_i})\right\}\ , \tag{2.62}$$

$$-\frac{1}{4M_i^2}\left(\frac{3}{2}+\log\frac{\mu^2}{M_i^2}\right)\mathrm{tr}\left\{U_{S_if}U_{ff'}i\sigma_{\mu\nu}G'^{\mu\nu}_{f'}U_{f'S_i}\right\}\ , \tag{2.63}$$

$$-\frac{1}{4M_i^2}\left(\frac{1}{2}+\log\frac{\mu^2}{M_i^2}\right)\mathrm{tr}\left\{U_{S_if}i\sigma_{\mu\nu}G'^{\mu\nu}_{f}U_{ff'}U_{fS_i}\right\}\ , \tag{2.64}$$

$$\frac{1}{2M_i^2}\,\mathrm{tr}\left\{U_{S_if}i\sigma_{\mu\nu}(P^\mu U_{ff'})(P^\nu U_{f'S_i})\right\}\ . \tag{2.65}$$

- $\underline{\mathcal{O}\left(U^4\right)}$

$$-\frac{1}{4M_i^2}\left(\frac{3}{2}+\log\frac{\mu^2}{M_i^2}\right)\mathrm{tr}\left\{U_{S_if}\gamma^\mu U_{fH}U_{Hf'}\gamma_\mu U_{f'S_i}\right\}\ , \tag{2.66}$$

$$-\frac{\log M_i^2/M_j^2}{4\Delta_{ij}^2}\,\mathrm{tr}\left\{U_{S_if}\gamma^\mu U_{fS_j}U_{S_jf'}\gamma_\mu U_{f'S_i}\right\}\ , \tag{2.67}$$

$$-\frac{\log M_i^2/M_j^2}{\Delta_{ij}^2}\,\mathrm{tr}\left\{U_{S_iS_j}U_{S_jf}U_{ff'}U_{f'S_i}\right\}\ , \tag{2.68}$$

$$-\frac{1}{4M_i^2}\left(\frac{3}{2}+\log\frac{\mu^2}{M_i^2}\right)\mathrm{tr}\left\{U_{S_if}\gamma^\mu U_{fV}U_{Vf'}\gamma_\mu U_{f'S_i}\right\}\ , \tag{2.69}$$

$$\begin{aligned}-\frac{1}{4M_i^2}\,\mathrm{tr}\Big\{&U_{S_if}U_{ff'}U_{f'f''}\gamma_\mu(P^\mu U_{f''S_i})\\ &-(P^\mu U_{fS_i})U_{ff'}U_{f'f''}\gamma_\mu U_{f''S_i}\Big\}\ ,\end{aligned} \tag{2.70}$$

$$\begin{aligned}-\frac{1}{2M_i^2}\left(1+\log\frac{\mu^2}{M_i^2}\right)\mathrm{tr}\Big\{&U_{fS_i}U_{ff'}(P^\mu U_{f'f''})\gamma_\mu U_{f''S_i}\\ &-U_{fS_i}(P^\mu U_{ff'})U_{f'f''}\gamma_\mu U_{f''S_i}\Big\}\ ,\end{aligned} \tag{2.71}$$

$$\begin{aligned}\mathcal{I}[q^2]^{1112}_{ijk0}\,\mathrm{tr}\Big\{&U_{S_iS_j}U_{S_jS_k}U_{S_kf}\gamma^\mu(P_\mu U_{fS_i})\\ &-U_{S_iS_j}U_{S_jS_k}(P^\mu U_{S_kf})\gamma_\mu U_{fS_i}\Big\}\ ,\end{aligned} \tag{2.72}$$

$$\begin{aligned}-\mathcal{I}[q^2]^{1211}_{ijk0}\,\mathrm{tr}\Big\{&U_{S_iS_j}(P^\mu U_{S_jS_k})U_{S_kf}\gamma_\mu U_{fS_i}\\ &-(P^\mu U_{S_iS_j})U_{S_jS_k}U_{S_kf}\gamma_\mu U_{S_if}\Big\}\ .\end{aligned} \tag{2.73}$$

- $\underline{\mathcal{O}\left(U^5\right)}$

$$\frac{1}{M_i^2}\left(1+\log\frac{\mu^2}{M_i^2}\right)\mathrm{tr}\left\{U_{S_if}U_{ff'}U_{f'f''}U_{f''f'''}U_{f'''S_i}\right\}\ , \tag{2.74}$$

$$4\mathcal{I}[q^2]^{1112}_{ijk0}\,\mathrm{tr}\left\{U_{S_iS_j}U_{S_jS_k}U_{S_kf}U_{ff'}U_{f'S_i}\right\}\ . \tag{2.75}$$

- $\underline{\mathcal{O}\left(Z^1\right)}$

$$\frac{1}{4}\left(\frac{3}{2}+\log\frac{\mu^2}{M_i^2}\right)\mathrm{tr}\left\{Z^\mu_{S_iV}U_{Vf}\gamma_\mu U_{fS_i}+U_{S_if}\gamma_\mu U_{fV}\bar{Z}^\mu_{VS_i}\right\}\ . \tag{2.76}$$

- $\underline{\mathcal{O}\left(Z^2\right)}$

$$\frac{M_i^2}{4}\left(\frac{3}{2}+\log\frac{\mu^2}{M_i^2}\right)\operatorname{tr}\left\{Z^{\mu}_{S_iV}\bar{Z}_{VS_i,\mu}\right\}\,. \tag{2.77}$$

In eqs. (2.51)-(2.77) above, the trace (tr) stands for a normal trace over the product of matrices-($U,Z$) that are direct products of spinor, gauge or flavour matrices. Also, with $\widetilde{G}$ we denote the usual dual tensor $\widetilde{G}'_{\mu\nu}=\frac{1}{2}\epsilon^{\mu\nu\rho\sigma}G'_{\rho\sigma}$. The $\mu$-parameter denotes the renormalization scale and the $\overline{MS}$-renormalization scheme with dimensional regularization is used throughout. Finally, the expressions for few integrals appearing before traces are ($\Delta_{ij}^2\equiv M_i^2-M_j^2$),

$$\mathcal{I}[q^2]^{1112}_{ijk0}=\frac{\log M_k^2/M_i^2}{4\Delta_{ij}^2\Delta_{ik}^2}-\frac{\log M_k^2/M_j^2}{4\Delta_{ij}^2\Delta_{jk}}\,, \tag{2.78}$$

$$\begin{aligned}\mathcal{I}[q^2]^{1211}_{ijk0}=&\frac{1}{4\Delta_{ij}^2}\left(\frac{3}{2}+\frac{M_i^2\log\mu^2/M_i^2+M_k^2\log\mu^2/M_k^2}{\Delta_{ik}^2}\right)\\&+\frac{\log\mu^2/M_j^2(M_i^2M_k^2-M_j^4)+M_k^2\log\mu^2/M_k^2(M_i^2-2M_j^2+M_k^2)}{4(\Delta_{ij}^2)^2(\Delta_{jk}^2)^2}\\&+\frac{2M_i^2-5M_j^2+3M_k^2}{8(\Delta_{ij}^2)^2\Delta_{jk}^2}\,.\end{aligned} \tag{2.79}$$

Following this general procedure, the operators extracted from $\mathcal{L}^{(1-\text{loop})}_{\text{EFT}}$ in (2.48) are given in a general operator basis, usually referred to as Green basis, which does not involve field EOMs in reducing the number operators, but only integration-by-parts. There is however, one more complication in writing down the Wilson coefficients even in Green basis. This is the appearance of the so-called *evanescent operators* [75, 76] that vanish in $d=4$ but do not vanish in general for $d\neq 4$ in certain four-fermion interactions. The effect of evanescent operators in SM EFT [64, 77, 78] is taken into account in the application we present in the next section.

It is easy to make the connection between eqs. (2.51)-(2.77) and the functional supertrace diagrams in eqs. (2.33)-(2.47). For example, say we want to find a diagram candidate for neutrino-mass generation operator $\ell\ell HH$. We need four interaction vertices, *i.e.* four $U$-matrices but no derivative ($P$) operators or $\gamma$-matrices. Looking at $\mathcal{O}(U^4)$ terms we see that only (2.68) satisfies this condition. Following the subscripts of $U$-matrices, in this case $S_i-S_j-f-f'-S_i$, we trivially see the corresponding diagram is that of (2.39). What is very nice in this approach is the fact that strict correlations between observables are now obvious, i.e., the operator resulting from (2.68) may be correlated with those containing the insertions $U_{S_iS_j}$, $U_{S_if}$ and $U_{ff'}$.

### 2.2.5 Summary

Our main formulae for the full 1-loop matching up-to dimension-6 order in EFT expansion for *all* scalar leptoquarks are:

1. Tree level matching: eq. (2.14),

2. One loop matching: eq. (2.48) = eq. (2.49) + eq. (2.50).

From now on we have to choose a specific model with heavy particles taken from Table 2.1, plug in the explicit X$(U,Z)$-matrices and operators will pop-out of the traces. The general form of interaction X$(U,Z)$-matrices is presented in Appendix A.

## 2.3 Application: The leptoquark model $S_1 + \tilde{S}_2$

In this section, we apply the machinery of functional matching onto a particular scalar leptoquark model. Consequently, we consider an extension of the SM consisting of two scalar colored leptoquarks, an isospin singlet and a doublet, $S_1$ and $\tilde{S}_2$, with masses $M_1$ and $\tilde{M}_2$, respectively. Their charges under the SM gauge group are shown in Table 2.2.

| Field/Group | SU(3) | SU(2) | U(1) |
|---|---|---|---|
| $S_1$ | $\bar{3}$ | 1 | $\frac{1}{3}$ |
| $\tilde{S}_2$ | 3 | 2 | $\frac{1}{6}$ |

*Table 2.2: Leptoquark charges under the SM gauge group for the $S_1 + \tilde{S}_2$ model.*

Interestingly, $S_1$ and $\tilde{S}_2$ belong to irreducible representations of an $SU(5)$ [or $SO(10)$] Grand Unified Theory (GUT). For example, $S_1$ may belong to $\bar{\mathbf{5}}, \overline{\mathbf{45}}, \overline{\mathbf{50}}$ and $\tilde{S}_2$ to $\mathbf{10}, \mathbf{15}$ irreps of minimal $SU(5)$, respectively. From the SM EFT operator content we derive below, we see that this model predicts fast proton decay and neutrino masses (and related $B$- and $L$-violating phenomena). Then it is natural for the two fields to have heavy masses $M_i \approx 10^{12}$ GeV which at the same time control the proton decay rate and generate neutrino masses consistent with experimental constraints [79–82].

On the other hand, one may apply a baryon parity where lepton, quark and therefore leptoquark fields, transform differently under a symmetry in order to protect the model from proton decay (although such a symmetry is not in general natural in GUTs as we argue below). In this case, $M_1$ and $\tilde{M}_2$ may be within the few-TeV range. Again, one may be able to account for radiative neutrino masses [83, 84], or current anomalous events such as the muon anomalous magentic moment [69, 84–86] and certain $B$-meson decays [69, 70].

In either cases, this $S_1 + \tilde{S}_2$-model seems to attract a certain phenomenological interest which motivates us for studying its effective operators and their matching onto the SM EFT Lagrangian. However, further than a functional matching demonstration, such as a detailed phenomenological consideration, are beyond the scope of this chapter.

### 2.3.1 Lagrangian and symmetries

We split the leptoquark Lagrangian into three parts,

$$\mathcal{L}_{\mathrm{BSM}} = \mathcal{L}_{\text{S-f}} + \mathcal{L}_{\text{S-H}} + \mathcal{L}_{\mathrm{S}} \,. \tag{2.80}$$

The first part refers to leptoquark-fermion interactions, the second one to leptoquark-Higgs interactions, while the last part contains self and mixed terms between the two leptoquarks. Explicitly the first part reads [64, 67],

$$\mathcal{L}_{\text{S-f}} = \Big[\Big(\lambda^{1L}_{pr}\Big)\bar{q}^c_{pi}\cdot\epsilon\cdot\ell_r + \Big(\lambda^{1R}_{pr}\Big)\bar{u}^c_i\, e_r\Big] S_{1i} + \text{h.c.}$$

$$+(\lambda^{\not{B}L}_{pr})\,S_{1i}\,\epsilon^{ijk}\,\bar{q}_{pj}\cdot\epsilon\cdot q^c_{rk}+(\lambda^{\not{B}R}_{pr})\,S_{1i}\,\epsilon^{ijk}\bar{d}_{pj}\,u^c_{rk}+\text{h.c.}$$
$$+(\tilde{\lambda}_{pr})\,\bar{d}_{pi}\tilde{S}^T_{2i}\cdot\epsilon\cdot\ell_r+\text{h.c.}\,, \tag{2.81}$$

where $\ell$ and $q$ are the lepton and quark field $SU(2)_L$-doublets while the singlets are denoted by $u,d,e$ in gauge basis[5] and $\epsilon$ is the antisymmetric tensor with $SU(2)_L$ indices. The matrix $\lambda^{\not{B}L}_{pr}$ is complex symmetric in flavor space while all other matrices in (2.81) are in general complex ones. From now on, we use the indices $p,r,s,t$ to denote *flavor* without making any distinction between quark and lepton flavors. We also use $i,j,k,l$ to label $SU(3)$ *fundamental* indices, while the dot-product denotes $SU(2)$ contractions in the fundamental representation. Later we will also use the letters $\alpha,\beta,\gamma,\delta$ for $SU(2)$ *fundamental* and $I,J,K,L$ for $SU(2)$ *adjoint* representation. Lastly, we use $A,B,C,D$ for the $SU(3)$ *adjoint* representation and suppress spinor-indices throughout.

The next part of the Lagrangian, namely leptoquark-Higgs interactions, reads [71],

$$\mathcal{L}_{\text{S-H}}=-\left(M_1^2+\lambda_{H1}|H|^2\right)|S_1|^2-\left(\tilde{M}_2^2+\tilde{\lambda}_{H2}|H|^2\right)|\tilde{S}_2|^2+\lambda_{\tilde{2}\tilde{2}}\,(\tilde{S}^\dagger_{2i}\cdot H)\,(H^\dagger\cdot\tilde{S}_{2i})$$
$$-A_{\tilde{2}1}\left(\tilde{S}^\dagger_{2i}\cdot H\right)S^\dagger_{1i}+\frac{1}{3}\lambda_3\epsilon^{ijk}\left(\tilde{S}^T_{2i}\cdot\epsilon\cdot\tilde{S}_{2j}\right)\left(H^\dagger\cdot\tilde{S}_{2k}\right)+\text{h.c.} \tag{2.82}$$

The last part containing leptoquark self-interactions is,

$$-\mathcal{L}_{\text{S}}=\frac{c_1}{2}\,(S_1^\dagger S_1)^2+\frac{\tilde{c}_2}{2}\,(\tilde{S}_2^\dagger\cdot\tilde{S}_2)^2+c^{(1)}_{1\tilde{2}}\,(S_1^\dagger S_1)(\tilde{S}_2^\dagger\cdot\tilde{S}_2)+c^{(2)}_{1\tilde{2}}(\tilde{S}^\dagger_{2\alpha}S_1)(S_1^\dagger\tilde{S}_{2\alpha})$$
$$+c^{(8)}_{\tilde{2}}(\tilde{S}^\dagger_{2i}\cdot\tilde{S}_{2j})\,(\tilde{S}^\dagger_{2j}\cdot\tilde{S}_{2i})+\left[A'S^\dagger_{1i}\,\epsilon^{ijk}\left(\tilde{S}^T_{2j}\cdot\epsilon\cdot\tilde{S}_{2k}\right)+\text{h.c.}\right]. \tag{2.83}$$

Our convention for the covariant derivative is,

$$D_\mu=\partial_\mu-ig'YB_\mu-igT^IW^I_\mu-ig_sT^AG^A_\mu\,, \tag{2.84}$$

where each $T$ represents the gauge-group generators of the corresponding representation of a generic field and $Y$ is its hypercharge. The field strength tensors for $U(1)_Y$, $SU(2)_L$ and $SU(3)_c$ gauge-fields are respectively,

$$B_{\mu\nu}=\partial_\mu B_\nu-\partial_\nu B_\mu\,, \tag{2.85}$$
$$W^I_{\mu\nu}=\partial_\mu W_\nu-\partial_\nu W_\mu+g\epsilon^{IJK}W^J_\mu W^K_\nu\,, \tag{2.86}$$
$$G^A_{\mu\nu}=\partial_\mu G_\nu-\partial_\nu G_\mu+g_sf^{ABC}G^B_\mu G^C_\nu\,. \tag{2.87}$$

Finally, the SM Yukawa couplings are defined as,

$$-\mathcal{L}_{\text{Y}}=(y_E)_{pr}\bar{\ell}_p\cdot H\,e_r+(y_U)_{pr}\,\bar{q}_{pi}\cdot\epsilon\cdot H^*\,u_{ri}+(y_D)_{pr}\,\bar{q}_{pi}\cdot H\,d_{ri}+\text{h.c.}\,, \tag{2.88}$$

while the Higgs potential is,

$$V_H=-m^2(H^\dagger\cdot H)+\frac{\lambda}{2}(H^\dagger H)^2\,. \tag{2.89}$$

It is always instructive in a given Lagrangian to check upon global symmetries such as Baryon ($B$) and Lepton ($L$) number, which may be broken by certain interaction parameters. For the $S_1+\tilde{S}_2$ model these are given in Table 2.3.

[5]Field redefinitions and flavour rotations to mass-basis are performed following ref. [17] after running the SM EFT parameters down to the EW scale.

| LQ-fields | $B$ | $L$ | $B-L$ |
|---|---|---|---|
| $S_1$ | -1/3 | -1 | 2/3 |
| $\tilde{S}_2$ | +1/3 | -1 | 4/3 |
| Parameters | | | |
| $\lambda^{\not{B}L}$ | +1 | +1 | 0 |
| $\lambda^{\not{B}R}$ | +1 | +1 | 0 |
| $A_{\tilde{2}1}$ | 0 | -2 | 2 |
| $A'$ | -1 | 1 | -2 |
| $\lambda_3$ | -1 | 3 | -4 |

*Table 2.3: B, L and $B-L$ quantum numbers for the fields $S_1$ and $\tilde{S}_2$ and parameters (promoted to fields). For normalization we take $B(q) = 1/3$ and $L(\ell) = 1$. All other parameters in eqs.* (2.81)*,*(2.82) *and* (2.83) *which are not quoted here, have zero B and L quantum numbers.*

Obviously, by assuming baryon and/or lepton number conservation we can eliminate all terms proportional to couplings ($\lambda^{\not{B}L}$, $\lambda^{\not{B}R}$,$A'$, $\lambda_3$) and/or $A_{\tilde{2}1}$, respectively. However, baryon and lepton symmetries cannot be well-defined gauge symmetries of a GUT model since they lead to chiral anomalies. On the other hand however, in SO(10)-GUTs for example (and also in the SM), $B-L$ is an anomaly free gauge symmetry and therefore we search for linear combinations of $B-L$-quantum numbers [87]. In this case, a $\mathbb{Z}_2$-symmetry $\exp(2\pi i(B-L)/2)$, does not exclude any of couplings above, a $\mathbb{Z}_3$-symmetry $\exp(2\pi i(B-L)/3)$, excludes $A_{\tilde{2}1}$,$A'$, $\lambda_3$, a $\mathbb{Z}_4$-symmetry $\exp(2\pi i(B-L)/4)$, excludes $A_{\tilde{2}1}$,$A'$, which is not desirable if we want to generate neutrino masses by loop-corrections. Therefore, there is no $B-L$ discrete symmetry that rejects terms proportional to $\lambda^{\not{B}L}$ (and $\lambda^{\not{B}R}$) which lead to proton decay. We conclude that in general, an extra (and possibly ad-hoc) symmetry should be in order if we are about to pick a combination of leptoquark fields with masses nearby the TeV scale. For a recent discussion the reader is referred to ref. [88].

### 2.3.2 Tree Level Matching

As is the case in EFTs, we assume that both leptoquarks masses, $M_i = \{M_1, \tilde{M}_2\}$, are heavier than any other scale in the theory. Moreover, the parameters $A_{\tilde{2}1}$, and $A'$ should lay in region (2.9). To match at *tree level* we need the equations of motion (2.4), in order to derive the classical fields,

$$S_{1i,c} = \frac{1}{M_1^2}\left[-(\lambda^{1L}_{pr})^\dagger \bar{\ell}_p \cdot \epsilon \cdot q^c_{ri} + (\lambda^{1R}_{pr})^\dagger \bar{e}_p u^c_{ri} + (\lambda^{\not{B}L}_{pr})^\dagger \epsilon^{ijk} \bar{q}^c_{pj} \cdot \epsilon \cdot q_{ri} - (\lambda^{\not{B}R}_{pr})^\dagger \epsilon^{ijk} \bar{u}^c_{pj} d_{rk}\right], \tag{2.90}$$

$$\tilde{S}_{2i\alpha,c} = \frac{1}{\tilde{M}_2^2}\left[-(\tilde{\lambda}_{pr})^\dagger \left(\bar{\ell}_p \cdot \epsilon\right)_\alpha d_{ri}\right]. \tag{2.91}$$

Substituting back into the Lagrangian [see (2.14)] we obtain the following Wilson coefficients that accompany $d = 6$-operators. In what follows, we split the Wilson coefficients to *tree* and *loop* contributions as $G = G^{(0)} + \frac{1}{(4\pi)^2} G^{(1)}$. The symbol $G$ denotes Wilson coefficients in Green basis, and we use exactly the same naming for operators as in ref. [64] that we append in Appendix C for complementarity purposes.

In summary, we find the following twelve $B$-number conserving tree-level coefficients

$$\left[G^{(1)}_{\ell q}\right]^{(0)}_{prst} = \frac{(\lambda^{1L}_{sp})^*(\lambda^{1L}_{tr})}{4M_1^2}\,, \qquad \left[G^{(3)}_{\ell q}\right]^{(0)}_{prst} = -\frac{(\lambda^{1L}_{sp})^*(\lambda^{1L}_{tr})}{4M_1^2}\,, \tag{2.92}$$

$$\left[G^{(1)}_{lequ}\right]^{(0)}_{prst} = \frac{(\lambda^{1L}_{sp})^*(\lambda^{1R}_{tr})}{2M_1^2}\,, \qquad \left[G^{(3)}_{\ell equ}\right]^{(0)}_{prst} = -\frac{(\lambda^{1L}_{sp})^*(\lambda^{1R}_{tr})}{8M_1^2}\,, \tag{2.93}$$

$$\left[G_{eu}\right]^{(0)}_{prst} = \frac{(\lambda^{1R}_{sp})^*(\lambda^{1R}_{tr})}{2M_1^2}\,, \qquad \left[G_{\ell d}\right]^{(0)}_{prst} = -\frac{(\tilde{\lambda}_{tp})^*(\tilde{\lambda}_{sr})}{2\tilde{M}_2^2}\,, \tag{2.94}$$

$$\left[G^{(1)}_{qq}\right]^{(0)}_{prst} = \frac{(\lambda^{\not{B}L}_{rt})^*(\lambda^{\not{B}L}_{sp})}{2M_1^2}\,, \qquad \left[G^{(3)}_{qq}\right]^{(0)}_{prst} = -\frac{(\lambda^{\not{B}L}_{rt})^*(\lambda^{\not{B}L}_{sp})}{2M_1^2}\,, \tag{2.95}$$

$$\left[G^{(1)}_{ud}\right]^{(0)}_{prst} = \frac{(\lambda^{\not{B}R}_{tr})^*(\lambda^{\not{B}R}_{sp})}{3M_1^2}\,, \qquad \left[G^{(8)}_{ud}\right]^{(0)}_{prst} = -\frac{(\lambda^{\not{B}R}_{tr})^*(\lambda^{\not{B}R}_{sp})}{M_1^2}\,, \tag{2.96}$$

$$\left[G^{(1)}_{quqd}\right]^{(0)}_{prst} = \frac{4}{3}\frac{(\lambda^{\not{B}R}_{ts})^*(\lambda^{\not{B}L}_{pr})}{M_1^2}\,, \qquad \left[G^{(8)}_{quqd}\right]^{(0)}_{prst} = -4\frac{(\lambda^{\not{B}R}_{ts})^*(\lambda^{\not{B}L}_{pr})}{M_1^2}\,, \tag{2.97}$$

and four $B$-number violating ones

$$\left[G_{qqq}\right]^{(0)}_{prst} = -2\frac{(\lambda^{\not{B}L}_{pr})^*(\lambda^{1L}_{st})}{M_1^2}\,, \qquad \left[G_{qqu}\right]^{(0)}_{prst} = \frac{(\lambda^{\not{B}L}_{pr})^*(\lambda^{1R}_{st})}{M_1^2}\,, \tag{2.98}$$

$$\left[G_{duq}\right]^{(0)}_{prst} = \frac{(\lambda^{\not{B}R}_{pr})^*(\lambda^{1L}_{st})}{M_1^2}\,, \qquad \left[G_{duu}\right]^{(0)}_{prst} = \frac{(\lambda^{\not{B}R}_{pr})^*(\lambda^{1R}_{st})}{M_1^2}\,. \tag{2.99}$$

As we see all tree-level dimension-six operators are four-fermion operators in the effective Lagrangian. Besides $M_i$, their strength is governed by products of leptoquark Yukawa couplings.

Finally for completeness, we present the five tree-level $d = 7$ Wilson coefficients in the basis of ref. [14]. They are,

$$\left[G^{(1)}_{LLQ\bar{d}H}\right]^{(0)}_{prst} = -\frac{A_{\tilde{2}1}}{M_1^2\tilde{M}_2^2}(\lambda^{1L}_{st})(\tilde{\lambda}_{pr})\,, \qquad \left[G^{(2)}_{LLQ\bar{d}H}\right]^{(0)}_{prst} = \frac{A_{\tilde{2}1}}{M_1^2\tilde{M}_2^2}(\lambda^{1L}_{st})(\tilde{\lambda}_{pr})\,, \tag{2.100}$$

$$\left[G_{Leu\bar{d}H}\right]^{(0)}_{prst} = \frac{A_{\tilde{2}1}}{2M_1^2\tilde{M}_2^2}(\lambda^{1R}_{tr})(\tilde{\lambda}_{sp})\,, \qquad \left[G_{LuddH}\right]^{(0)}_{prst} = \frac{A^*_{\tilde{2}1}}{M_1^2\tilde{M}_2^2}(\lambda^{\not{B}R}_{st})^\dagger(\tilde{\lambda}_{pr})^\dagger\,, \tag{2.101}$$

$$\left[G_{\bar{L}QQdH}\right]^{(0)}_{prst} = -2\frac{A^*_{\tilde{2}1}}{M_1^2\tilde{M}_2^2}(\lambda^{\not{B}L}_{st})^*(\tilde{\lambda}_{pr})^\dagger\,. \tag{2.102}$$

As noted in the paragraph below eq. (2.14), coefficients associated with $d = 7$ operators in eqs. (2.100)-(2.102) can be competitive to $d = 6$ ones in (2.98)-(2.99) if there is a certain hierarchy between the two scales involved, e.g., $M_1 \gg \tilde{M}_2$ and $A_{\tilde{2}1}v/\tilde{M}_2^2 \simeq 1$.

The appearance of products only $\lambda\cdot\lambda'$ with $|\Delta(B-L)| = 0$ and $A_{\tilde{2}1}\lambda\cdot\lambda'$ with $|\Delta(B-L)| = 2$ in coefficients for $d = 6$ and $d = 7$ tree-level EFT operators respectively, is not accidental. It follows from the $B, L$-numbers for the parameters quoted in Table 2.3, and an interesting connection [89, 90] between $\Delta B$ and $\Delta L$ with the minimum and possible dimensionality of operators

$$d_{\min} \quad \geq \quad \frac{9}{2}|\Delta B| + \frac{3}{2}|\Delta L|\,, \tag{2.103}$$

$$
\begin{aligned}
|\Delta(B-L)| &= 0,4,8,12,16,\ldots \qquad (d-\text{even})\,, && (2.104)\\
|\Delta(B-L)| &= 2,6,10,14,18,\ldots \qquad (d-\text{odd})\,. && (2.105)
\end{aligned}
$$

For example, a coefficient proportional to $A_{\tilde{2}1} \times (|\Delta(B-L)| = 0$ couplings) must necessarily be associated to odd-dimensional $d = 3,5,7,\ldots$ case which is confirmed here at tree and below at one-loop level. Similarly, the dimension-full parameter $A' \times (|\Delta(B-L)| = 0$ couplings) will be associated for the first time with $d = 7$-operators in EFT at 1-loop and at $d = 9$ at tree level; the dimensionless parameter $\lambda_3 \times (|\Delta(B-L)| = 0$ couplings) will appear first at $d = 10$ and so on.

### 2.3.3 One Loop Matching in the Green basis

As we explained in section 2.2.3, one loop matching is carried out in two steps. First, the original heavy-only UOLEA in eq. (2.49) is used to derive operators with heavy leptoquark fields (for this model $S_1$ and $\tilde{S}_2$) circulating in the loop. Second, we use the general results from evaluating functional Supertraces in (2.50) to calculate Wilson coefficients involving both heavy and light fields in the loop.

We list all one-loop Wilson coefficients produced both from the UOLEA and the Supertraces. As before, we split them in tree and loop level coefficients as $G_i = G_i^{(0)} + \frac{1}{(4\pi)^2} G_i^{(1)}$. Furthermore, for the quantities that renormalize $d = 4$ operators we write, $\lambda' = \lambda + \frac{1}{(4\pi)^2}\delta\lambda$, $m'^2 = m^2 + \frac{1}{(4\pi)^2}\delta m^2$, $y'_n = y_n + \frac{1}{(4\pi)^2}\delta y_n$, where $n = E,U,D$ and the wave function renormalization is $Z_k = 1 + \frac{1}{(4\pi)^2}\delta Z_k$ with $k = q,u,d,\ell,e$. For gauge bosons, we factor out of the resulting trace calculation the whole canonical kinetic term $-1/4 F_{\mu\nu}F^{\mu\nu}$, with $F_{\mu\nu}$ being a generic field strength tensor. Following an analogous naming scheme as in ref. [64] we define,

$$
L_i = \log\frac{\mu^2}{M_i^2}\,, \qquad \text{with} \quad i = 1,2\,, \tag{2.106}
$$

and the general $3\times 3$ matrices,

$$
\begin{aligned}
&\Lambda_\ell = (\lambda^{1\mathrm{L}})^\dagger \lambda^{1\mathrm{L}}\,, && \Lambda_q = (\lambda^{1\mathrm{L}})^*(\lambda^{1\mathrm{L}})^T\,, && \Lambda_u = (\lambda^{1\mathrm{R}})^*(\lambda^{1\mathrm{R}})^T\,, && (2.107)\\
&\Lambda_e = (\lambda^{1\mathrm{R}})^\dagger \lambda^{1\mathrm{R}}\,, && \tilde{\Lambda}_\ell = \tilde{\lambda}^\dagger\tilde{\lambda}\,, && \tilde{\Lambda}_d = \tilde{\lambda}\tilde{\lambda}^\dagger\,, && (2.108)\\
&\Lambda_q^{\not{B}} = \lambda^{\not{B}L}(\lambda^{\not{B}L})^\dagger\,, && \Lambda_u^{\not{B}} = (\lambda^{\not{B}R})^T(\lambda^{\not{B}R})^*\,, && \Lambda_d^{\not{B}} = \lambda^{\not{B}R}(\lambda^{\not{B}R})^\dagger\,, && (2.109)
\end{aligned}
$$

$$
\begin{aligned}
&Y_{1U}^{1L} = (\lambda^{1\mathrm{L}})^\dagger y_U^* \lambda^{1\mathrm{R}}\,, && Y_{1E}^{1L} = \left(\lambda^{1\mathrm{R}} y_E^\dagger (\lambda^{1\mathrm{L}})^\dagger\right)^T\,, && (2.110)\\
&Y_{2U}^{1L} = (\lambda^{1\mathrm{L}})^\dagger y_U^* y_U^T \lambda^{1\mathrm{L}}\,, && Y_{2D}^{1L} = (\lambda^{1\mathrm{L}})^\dagger y_D^* y_D^T \lambda^{1\mathrm{L}}\,, && (2.111)\\
&Y_{2U}^{1R} = (\lambda^{1\mathrm{R}})^\dagger y_U^T y_U^* \lambda^{1\mathrm{R}}\,, && Y_{2E}^{1R} = (\lambda^{1\mathrm{R}})^* y_E^T y_E^* (\lambda^{1\mathrm{R}})^T\,, && (2.112)\\
&Y_{3E}^{1L} = \left(\lambda^{1\mathrm{R}} y_E^\dagger y_E y_E^\dagger (\lambda^{1\mathrm{L}})^\dagger\right)^T && Y_{3U}^{1L} = (\lambda^{1\mathrm{L}})^\dagger y_U^* y_U^T y_U^* \lambda^{1\mathrm{R}}\,, && (2.113)\\
&\tilde{Y}_{2E} = \tilde{\lambda} y_E y_E^\dagger \tilde{\lambda}^\dagger\,, && \tilde{Y}_{2D} = \tilde{\lambda}^\dagger y_D^\dagger y_D \tilde{\lambda}\,, && (2.114)\\
&Y_{1D}^{\not{B}L} = \lambda^{\not{B}L} y_D^* (\lambda^{\not{B}R})^*\,, && Y_{1U}^{\not{B}L} = \lambda^{\not{B}L} y_U^* (\lambda^{\not{B}R})^\dagger\,, && (2.115)\\
&Y_{2U}^{\not{B}R} = \left((\lambda^{\not{B}R})^\dagger y_U^\dagger y_U \lambda^{\not{B}R}\right)^T\,, && Y_{2D}^{\not{B}R} = \left((\lambda^{\not{B}R})^\dagger y_D^\dagger y_D \lambda^{\not{B}R}\right)^T\,, && (2.116)\\
&Y_{2U}^{\not{B}L} = \left((\lambda^{\not{B}L})^\dagger y_U y_U^\dagger \lambda^{\not{B}L}\right)^T\,, && Y_{2D}^{\not{B}L} = \left((\lambda^{\not{B}L})^\dagger y_D y_D^\dagger \lambda^{\not{B}L}\right)^T\,, && (2.117)\\
&Y_{3D}^{\not{B}L} = \left((\lambda^{\not{B}R})^\dagger y_D^\dagger y_D y_D^\dagger \lambda^{\not{B}L}\right)^T\,, && Y_{3U}^{\not{B}L} = (\lambda^{\not{B}R})^* y_U^\dagger y_U y_U^\dagger \lambda^{\not{B}L}\,. && (2.118)
\end{aligned}
$$

Armed with those definitions we can now write the, lengthy but complete, one-loop Wilson coefficients associated to $d = 4$ (renormalizable operators) all the way up-to $d = 6$ operators in Green basis. All $d = 5$ and 6 operators and the categories they belong to are given in Appendix C. The hypercharges of $S_1$ and $\tilde{S}_2$ leptoquark fields are denoted as $Y_{S_1}$ and $Y_{\tilde{S}_2}$ respectively, and can be read from Table 2.1. $N_c$ is the number of colours and $C_F^G$ is the quadratic Casimir of fundamental representation of group $G$. Finally, we define the squared mass difference quantity $\Delta_{12}^2 \equiv M_1^2 - \tilde{M}_2^2$.

**Renormalizable Operators**

$$(\delta Z_B) = \frac{N_c}{3} g'^2 \left[ Y_{S_1}^2 L_1 + 2Y_{\tilde{S}_2}^2 L_2 \right] , \tag{2.119}$$

$$(\delta Z_W) = \frac{N_c}{6} g^2 L_2 , \tag{2.120}$$

$$(\delta Z_G) = \frac{N_c}{6} g_s^2 [L_1 + 2L_2] , \tag{2.121}$$

$$(\delta Z_\ell)_{pr} = \frac{N_c}{2} \left[ \left( \frac{1}{2} + L_1 \right) (\Lambda_\ell)_{pr} + \left( \frac{1}{2} + L_2 \right) (\tilde{\Lambda}_\ell)_{pr} \right] , \tag{2.122}$$

$$(\delta Z_e)_{pr} = \frac{N_c}{2} \left( \frac{1}{2} + L_1 \right) (\Lambda_e)_{pr} , \tag{2.123}$$

$$\left(\delta Z_q\right)_{pr} = \frac{1}{2} \left( \frac{1}{2} + L_1 \right) (\Lambda_q - 8\Lambda_q^{\not{B}})_{pr} , \tag{2.124}$$

$$(\delta Z_u)_{pr} = \frac{1}{2} \left( \frac{1}{2} + L_1 \right) (\Lambda_u + 2\Lambda_u^{\not{B}})_{pr} , \tag{2.125}$$

$$(\delta Z_d)_{pr} = \left( \frac{1}{2} + L_2 \right) (\tilde{\Lambda}_d)_{pr} + \left( \frac{1}{2} + L_1 \right) (\Lambda_d^{\not{B}})_{pr} , \tag{2.126}$$

$$(\delta Z_H) = N_c \left| A_{\tilde{2}1} \right|^2 \left[ \frac{M_1^2 + \tilde{M}_2^2}{2(\Delta_{12}^2)^2} + \frac{M_1^2 \tilde{M}_2^2 \log M_1^2/\tilde{M}_2^2}{(\Delta_{12}^2)^3} \right] , \tag{2.127}$$

$$(\delta y_E)_{pr} = -N_c(1 + L_1)(Y_{1U}^{1L})_{pr} , \tag{2.128}$$

$$(\delta y_U)_{pr} = -N_c(1 + L_1)(Y_{1E}^{1L})_{pr} - 4(Y_{1D}^{\not{B}L})_{pr}(1 + L_1) , \tag{2.129}$$

$$(\delta y_D)_{pr} = -4(Y_{1U}^{\not{B}L})_{pr}(1 + L_1) , \tag{2.130}$$

$$\begin{aligned}(\delta \lambda) = N_c \Bigg[ & \lambda_{H1}^2 L_1 + \left( \tilde{\lambda}_{H2}^2 + (\tilde{\lambda}_{H2} - \lambda_{\tilde{2}\tilde{2}})^2 \right) L_2 - |A_{\tilde{2}1}|^2 \lambda_{H1} \frac{\Delta_{12}^2 + \tilde{M}_2^2 \log \tilde{M}_2^2/M_1^2}{(\Delta_{12}^2)^2} \\ & + |A_{\tilde{2}1}|^2 (\tilde{\lambda}_{H2} - \lambda_{\tilde{2}\tilde{2}}) \frac{\Delta_{12}^2 + M_1^2 \log \tilde{M}_2^2/M_1^2}{(\Delta_{12}^2)^2} - \frac{1}{2} |A_{\tilde{2}1}|^4 \frac{2\Delta_{12}^2 + (M_1^2 + \tilde{M}_2^2) \log \tilde{M}_2^2/M_1^2}{(\Delta_{12}^2)^3} \Bigg] ,\end{aligned} \tag{2.131}$$

$$\begin{aligned}\left(\delta m^2\right) = N_c \Bigg[ & \lambda_{H1} M_1^2 (1 + L_1) + (2\tilde{\lambda}_{H2} - \lambda_{\tilde{2}\tilde{2}}) \tilde{M}_2^2 (1 + L_2) \\ & + |A_{\tilde{2}1}|^2 \left( 1 + \frac{M_1^2 \log \mu^2/M_1^2 - \tilde{M}_2^2 \log \mu^2/\tilde{M}_2^2}{\Delta_{12}^2} \right) \Bigg] .\end{aligned} \tag{2.132}$$

**Dimension-5 Operator**

$$[G_{\nu\nu}]_{pr}^{(1)} = N_c A_{\tilde{2}1} \left( (\lambda^{1L})^T y_D \tilde{\lambda} \right)_{pr} \frac{\log M_1^2/\tilde{M}_2^2}{M_1^2 - \tilde{M}_2^2} . \tag{2.133}$$

**Vector Bosons-Scalar Operators**

$X^3$

$$G_{3G}^{(1)} = \frac{g_s^3}{360}\left(\frac{1}{M_1^2} + \frac{2}{\tilde{M}_2^2}\right) , \tag{2.134}$$

$$G_{3W}^{(1)} = \frac{g^3 N_c}{360}\,\frac{1}{\tilde{M}_2^2} . \tag{2.135}$$

$X^2D^2$

$$G_{2B}^{(1)} = \frac{N_c}{30} g'^2 \left(\frac{Y_{S_1}^2}{M_1^2} + 2\frac{Y_{\tilde{S}_2}^2}{\tilde{M}_2^2}\right) , \tag{2.136}$$

$$G_{2W}^{(1)} = \frac{N_c}{60} g^2 \frac{1}{\tilde{M}_2^2} , \tag{2.137}$$

$$G_{2G}^{(1)} = \frac{1}{60} g_s^2 \left(\frac{1}{M_1^2} + \frac{2}{\tilde{M}_2^2}\right) . \tag{2.138}$$

$X^2H^2$

$$G_{HB}^{(1)} = N_c g'^2 \left[ Y_{S_1}^2 \left( \frac{\lambda_{H1}}{12M_1^2} - |A_{\tilde{2}1}|^2 \tilde{f}_{13}^{S_1\tilde{S}_2} \right) + Y_{\tilde{S}_2}^2 \left( \frac{(2\tilde{\lambda}_{H2} - \lambda_{\tilde{2}\tilde{2}})}{12\tilde{M}_2^2} - |A_{\tilde{2}1}|^2 \tilde{f}_{13}^{\tilde{S}_2 S_1} \right) \right] , \tag{2.139}$$

$$G_{HW}^{(1)} = N_c \frac{g^2}{4} \left( \frac{(\tilde{\lambda}_{H2} - \lambda_{\tilde{2}\tilde{2}})}{6\tilde{M}_2^2} - |A_{\tilde{2}1}|^2 \tilde{f}_{13}^{\tilde{S}_2 S_1} \right) , \tag{2.140}$$

$$G_{HG}^{(1)} = \frac{g_s^2}{2} \left[ \frac{\lambda_{H1}}{12M_1^2} + \frac{(2\tilde{\lambda}_{H2} - \lambda_{\tilde{2}\tilde{2}})}{12\tilde{M}_2^2} - |A_{\tilde{2}1}|^2 \left( \tilde{f}_{13}^{S_1\tilde{S}_2} + \tilde{f}_{13}^{\tilde{S}_2 S_1} \right) \right] , \tag{2.141}$$

$$G_{HWB}^{(1)} = -N_c\, g g' \left[ |A_{\tilde{2}1}|^2 \tilde{f}_{13}^{\tilde{S}_2 S_1} + Y_{\tilde{S}_2} \frac{\lambda_{\tilde{2}\tilde{2}}}{12\tilde{M}_2^2} \right] . \tag{2.142}$$

$H^2X^2D^2$

$$G_{BDH}^{(1)} = N_c |A_{\tilde{2}1}|^2 g' \left( Y_{S_1} + Y_{\tilde{S}_2} \right) \tilde{f}_{14}^{S_1\tilde{S}_2} , \tag{2.143}$$

$$G_{WDH}^{(1)} = N_c |A_{\tilde{2}1}|^2 \frac{g}{2} \tilde{f}_{14}^{\tilde{S}_2 S_1} . \tag{2.144}$$

$H^2D^4$

$$G_{DH}^{(1)} = 2N_c |A_{\tilde{2}1}|^2 \tilde{f}_{12}^{S_1\tilde{S}_2} . \tag{2.145}$$

$H^4D^2$

$$G_{H\Box}^{(1)} = -\frac{N_c}{12} \left( \frac{\lambda_{H1}^2}{M_1^2} + \frac{\tilde{\lambda}_{H2}^2}{\tilde{M}_2^2} \right) , \tag{2.146}$$

$$G_{HD}^{(1)} = -N_c \frac{\lambda_{\tilde{2}\tilde{2}}}{6\tilde{M}_2^2} + N_c \lambda_{\tilde{2}\tilde{2}} |A_{\tilde{2}1}|^2 (\tilde{f}_{11}^{\tilde{S}_2\tilde{S}_2 S_1} - 2\tilde{f}_{11}^{S_1\tilde{S}_2\tilde{S}_2}) - N_c |A_{\tilde{2}1}|^4 \left( \tilde{f}_{17}^{\tilde{S}_2 S_1} - 2\tilde{f}_{18}^{S_1\tilde{S}_2} \right) , \tag{2.147}$$

$$G_{HD}^{\prime(1)} = -N_c |A_{\tilde{2}1}|^2 \left( \lambda_{H1} \tilde{f}_{11}^{S_1 S_1 \tilde{S}_2} + \tilde{\lambda}_{H2} \tilde{f}_{11}^{\tilde{S}_2\tilde{S}_2 S_1} - 2\lambda_{\tilde{2}\tilde{2}} \tilde{f}_{11}^{S_1\tilde{S}_2\tilde{S}_2} \right) - N_c |A_{\tilde{2}1}|^4 \tilde{f}_{17}^{S_1\tilde{S}_2} , \tag{2.148}$$

$$\begin{aligned} G_{HD}^{\prime\prime(1)} = &-iN_c |A_{\tilde{2}1}|^2 \left( \lambda_{H1} \tilde{f}_{11}^{S_1\tilde{S}_2 S_1} + \tilde{\lambda}_{H2} \tilde{f}_{11}^{\tilde{S}_2 S_1 \tilde{S}_2} - \lambda_{\tilde{2}\tilde{2}} \tilde{f}_{11}^{S_1\tilde{S}_2\tilde{S}_2} \right) - iN_c |A_{\tilde{2}1}|^4 \tilde{f}_{18}^{S_1\tilde{S}_2} \\ &- \frac{iN_c}{12\tilde{M}_2^2} \left( 2\tilde{\lambda}_{H2} \lambda_{\tilde{2}\tilde{2}} - \lambda_{\tilde{2}\tilde{2}}^2 \right) . \end{aligned} \tag{2.149}$$

$H^6$

$$G_H^{(1)} = -\frac{N_c}{6}\left(\frac{\lambda_{H1}^3}{M_1^2} + 2\frac{\tilde{\lambda}_{H2}^3}{\tilde{M}_2^2}\right) + 2N_c|A_{\tilde{2}1}|^6\,\tilde{f}_{19}^{S_1\tilde{S}_2}\,. \tag{2.150}$$

**Two Fermion Operators**

$\psi^2 D^3$

$$[G_{\ell D}]_{pr}^{(1)} = -\frac{N_c}{6}\left[\frac{(\Lambda_\ell)_{pr}}{M_1^2} + \frac{(\tilde{\Lambda}_\ell)_{pr}}{\tilde{M}_2^2}\right], \tag{2.151}$$

$$[G_{eD}]_{pr}^{(1)} = -\frac{N_c}{6}\,\frac{(\Lambda_e)_{pr}}{M_1^2}\,, \tag{2.152}$$

$$\left[G_{qD}\right]_{pr}^{(1)} = -\frac{1}{6M_1^2}\left[(\Lambda_q)_{pr} - 8(\Lambda_q^{\not{\beta}})_{pr}\right], \tag{2.153}$$

$$[G_{uD}]_{pr}^{(1)} = -\frac{1}{6M_1^2}\left[2(\Lambda_u^{\not{\beta}})_{pr} + (\Lambda_u)_{pr}\right], \tag{2.154}$$

$$[G_{dD}]_{pr}^{(1)} = \frac{(\tilde{\Lambda}_d)_{pr}}{3\tilde{M}_2^2} - \frac{(\Lambda_d^{\not{\beta}})_{pr}}{3M_1^2}\,. \tag{2.155}$$

$\psi^2 XD$

$$[G_{W\ell}]_{pr}^{(1)} = -\frac{N_c}{6}\,g\left[\left(\frac{7}{12} + L_1\right)\frac{(\Lambda_\ell)_{pr}}{M_1^2} + \frac{(\tilde{\Lambda}_\ell)_{pr}}{6\tilde{M}_2^2}\right], \tag{2.156}$$

$$\left[G'_{\widetilde{W}\ell}\right]_{pr}^{(1)} = \frac{N_c}{4}\,g\,\frac{(\Lambda_\ell)_{pr}}{M_1^2}\,, \tag{2.157}$$

$$[G_{B\ell}]_{pr}^{(1)} = \frac{N_c}{3}\,g'\left[\left(\frac{7Y_q - 2Y_{S_1}}{12} + Y_q L_1\right)\frac{(\Lambda_\ell)_{pr}}{M_1^2} - \left(\frac{7Y_d + 2Y_{\tilde{S}_2}}{12} + Y_d L_2\right)\frac{(\tilde{\Lambda}_\ell)_{pr}}{\tilde{M}_2^2}\right], \tag{2.158}$$

$$\left[G'_{\widetilde{B}\ell}\right]_{pr}^{(1)} = -\frac{N_c}{2}\,g'\left[Y_q\frac{(\Lambda_\ell)_{pr}}{M_1^2} - Y_d\frac{(\tilde{\Lambda}_\ell)_{pr}}{\tilde{M}_2^2}\right], \tag{2.159}$$

$$[G_{Be}]_{pr}^{(1)} = \frac{N_c}{3}\,g'\left(\frac{7Y_u - 2Y_{S_1}}{12} + Y_u L_1\right)\frac{(\Lambda_e)_{pr}}{M_1^2}\,, \tag{2.160}$$

$$\left[G'_{\widetilde{B}e}\right]_{pr}^{(1)} = \frac{N_c}{2}\,g'\,Y_u\,\frac{(\Lambda_e)_{pr}}{M_1^2}\,, \tag{2.161}$$

$$\left[G_{Gq}\right]_{pr}^{(1)} = \frac{1}{18}\,g_s\,\frac{(\Lambda_q)_{pr}}{M_1^2} - \frac{4}{3}\,g_s\,\frac{(\Lambda_q^{\not{\beta}})_{pr}}{M_1^2}\left(\frac{3}{4} + L_1\right), \tag{2.162}$$

$$\left[G'_{\widetilde{G}q}\right]_{pr}^{(1)} = -2\,g_s\,\frac{(\Lambda_q^{\not{\beta}})_{pr}}{M_1^2}\,, \tag{2.163}$$

$$\left[G_{Wq}\right]_{pr}^{(1)} = -\frac{1}{6}\,g\left(\frac{7}{12} + L_1\right)\frac{(\Lambda_q)_{pr} + 8(\Lambda_q^{\not{\beta}})_{pr}}{M_1^2}\,, \tag{2.164}$$

$$\left[G'_{\widetilde{W}q}\right]_{pr}^{(1)} = \frac{1}{4}\,g\,\frac{(\Lambda_q)_{pr} - 8(\Lambda_q^{\not{\beta}})_{pr}}{M_1^2}\,, \tag{2.165}$$

$$\left[G_{Bq}\right]_{pr}^{(1)} = \frac{1}{3}\,g'\left[\left(\frac{7Y_\ell - 2Y_{S_1}}{12} + Y_\ell L_1\right)\frac{(\Lambda_q)_{pr}}{M_1^2} + \left(\frac{7Y_q + 2Y_{S_1}}{12} + Y_q L_1\right)\frac{8(\Lambda_q^{\not{\beta}})_{pr}}{M_1^2}\right], \tag{2.166}$$

$$\left[G'_{\widetilde{B}q}\right]^{(1)}_{pr} = -\frac{1}{2}\,g'\left[Y_\ell\frac{(\Lambda_\ell)_{pr}}{M_1^2} + Y_q\frac{8(\Lambda_q^{\not{B}})_{pr}}{M_1^2}\right], \tag{2.167}$$

$$[G_{Gu}]^{(1)}_{pr} = \frac{1}{18}g_s\frac{(\Lambda_u)_{pr}}{M_1^2} - \frac{1}{3}\,g_s\left(\frac{3}{4}+L_1\right)\frac{(\Lambda_u^{\not{B}})_{pr}}{M_1^2}\,, \tag{2.168}$$

$$\left[G'_{\widetilde{G}u}\right]^{(1)}_{pr} = -\frac{1}{2}\,g_s\,\frac{(\Lambda_u^{\not{B}})_{pr}}{M_1^2}\,, \tag{2.169}$$

$$[G_{Bu}]^{(1)}_{pr} = \frac{1}{3}\,g'\left[\left(\frac{7Y_e - 2Y_{S_1}}{12} + Y_e L_1\right)\frac{(\Lambda_u)_{pr}}{M_1^2} + \left(\frac{7Y_d + 2Y_{S_1}}{12} + Y_d L_1\right)\frac{2(\Lambda_u^{\not{B}})_{pr}}{M_1^2}\right], \tag{2.170}$$

$$\left[G'_{\widetilde{B}u}\right]^{(1)}_{pr} = \frac{1}{2}\,g'\left[Y_e\frac{(\Lambda_u)_{pr}}{M_1^2} + Y_d\frac{2(\Lambda_u^{\not{B}})_{pr}}{M_1^2}\right], \tag{2.171}$$

$$[G_{Gd}]^{(1)}_{pr} = \frac{1}{9}\,g_s\,\frac{(\tilde{\Lambda}_d)_{pr}}{\tilde{M}_2^2} - \frac{1}{3}\,g_s\left(\frac{3}{4}+L_1\right)\frac{(\Lambda_d^{\not{B}})_{pr}}{M_1^2}\,, \tag{2.172}$$

$$\left[G'_{\widetilde{G}d}\right]^{(1)}_{pr} = -\frac{1}{2}\,g_s\,\frac{(\Lambda_d^{\not{B}})_{pr}}{M_1^2}\,, \tag{2.173}$$

$$[G_{Bd}]^{(1)}_{pr} = -\frac{2}{3}\,g'\left[\left(\frac{7Y_\ell - 2Y_{S_1}}{12} + Y_\ell L_1\right)\frac{(\tilde{\Lambda}_d)_{pr}}{\tilde{M}_2^2} - \left(\frac{7Y_u + 2Y_{S_1}}{12} + Y_u L_1\right)\frac{(\Lambda_d^{\not{B}})_{pr}}{M_1^2}\right], \tag{2.174}$$

$$\left[G'_{\widetilde{B}d}\right]^{(1)}_{pr} = g'\left[2Y_\ell\frac{(\tilde{\Lambda}_d)_{pr}}{\tilde{M}_2^2} + Y_u\frac{(\Lambda_d^{\not{B}})_{pr}}{M_1^2}\right], \tag{2.175}$$

$$\left[G'_{Gq}\right]^{(1)}_{pr} = \left[G'_{Wq}\right]^{(1)}_{pr} = \left[G'_{Bq}\right]^{(1)}_{pr} = 0\,, \tag{2.176}$$

$$\left[G'_{Gu}\right]^{(1)}_{pr} = \left[G'_{Bu}\right]^{(1)}_{pr} = 0\,, \tag{2.177}$$

$$\left[G'_{Gd}\right]^{(1)}_{pr} = \left[G'_{Bd}\right]^{(1)}_{pr} = 0\,, \tag{2.178}$$

$$\left[G'_{W\ell}\right]^{(1)}_{pr} = \left[G'_{B\ell}\right]^{(1)}_{pr} = \left[G'_{Be}\right]^{(1)}_{pr} = 0\,. \tag{2.179}$$

$\psi^2 HD^2$

$$[G_{eHD1}]^{(1)}_{pr} = \frac{N_c}{2}\left(\frac{1}{2}+L_1\right)\frac{(Y_{1U}^{1L})_{pr}}{M_1^2}\,, \tag{2.180}$$

$$[G_{eHD2}]^{(1)}_{pr} = +\frac{N_c}{2}\frac{(Y_{1U}^{1L})_{pr}}{M_1^2}\,, \tag{2.181}$$

$$[G_{eHD3}]^{(1)}_{pr} = -\frac{N_c}{2}\frac{(Y_{1U}^{1L})_{pr}}{M_1^2}\,, \tag{2.182}$$

$$[G_{eHD4}]^{(1)}_{pr} = -\frac{N_c}{2}\frac{(Y_{1U}^{1L})_{pr}}{M_1^2}\,, \tag{2.183}$$

$$[G_{uHD1}]^{(1)}_{pr} = \frac{1}{2}\left(\frac{1}{2}+L_1\right)\frac{(Y_{1E}^{1L})_{pr} - 4(Y_{1D}^{\not{B}L})_{pr}}{M_1^2}\,, \tag{2.184}$$

$$\left[G_{uHD2}\right]^{(1)}_{pr} = \frac{(Y^{1L}_{1E})_{pr} - 4(Y^{\not{B}L}_{1D})_{pr}}{2M_1^2} \,, \tag{2.185}$$

$$\left[G_{uHD3}\right]^{(1)}_{pr} = -\frac{(Y^{1L}_{1E})_{pr} - 4(Y^{\not{B}L}_{1D})_{pr}}{2M_1^2} \,, \tag{2.186}$$

$$\left[G_{uHD4}\right]^{(1)}_{pr} = -\frac{(Y^{1L}_{1E})_{pr} - 4(Y^{\not{B}L}_{1D})_{pr}}{2M_1^2} \,, \tag{2.187}$$

$$\left[G_{dHD1}\right]^{(1)}_{pr} = -\frac{2}{M_1^2}\left(\frac{1}{2} + L_1\right)(Y^{\not{B}L}_{1U})_{pr} \,, \tag{2.188}$$

$$\left[G_{dHD2}\right]^{(1)}_{pr} = -\frac{2}{M_1^2}(Y^{\not{B}L}_{1U})_{pr} \,, \tag{2.189}$$

$$\left[G_{dHD3}\right]^{(1)}_{pr} = \frac{2}{M_1^2}(Y^{\not{B}L}_{1U})_{pr} \,, \tag{2.190}$$

$$\left[G_{dHD4}\right]^{(1)}_{pr} = \frac{2}{M_1^2}(Y^{\not{B}L}_{1U})_{pr} \,. \tag{2.191}$$

$\psi^2 XH$

$$\left[G_{eW}\right]^{(1)}_{pr} = -\frac{N_c}{8}\, g \left(\frac{1}{2} + L_1\right)\frac{(Y^{1L}_{1U})_{pr}}{M_1^2} \,, \tag{2.192}$$

$$\left[G_{eB}\right]^{(1)}_{pr} = \frac{N_c}{4}\, g' \left[(Y_q + Y_u)L_1 + \frac{1}{2}Y_q + \frac{3}{2}Y_u\right]\frac{(Y^{1L}_{1U})_{pr}}{M_1^2} \,, \tag{2.193}$$

$$\left[G_{uG}\right]^{(1)}_{pr} = g_s\,(1 + L_1)\,\frac{(Y^{\not{B}L}_{1D})_{pr}}{M_1^2} \,, \tag{2.194}$$

$$\left[G_{uW}\right]^{(1)}_{pr} = -\frac{1}{8}\, g \left[\left(\frac{1}{2} + L_1\right)\frac{(Y^{1L}_{1E})_{pr} - 4(Y^{\not{B}L}_{1D})_{pr}}{M_1^2}\right] \,, \tag{2.195}$$

$$\left[G_{uB}\right]^{(1)}_{pr} = \frac{1}{4}\, g' \left[(Y_\ell + Y_e)L_1 + \frac{1}{2}Y_\ell + \frac{3}{2}Y_e\right]\frac{(Y^{1L}_{1E})_{pr}}{M_1^2} \tag{2.196}$$

$$- g' \left[(Y_q + Y_d)L_1 + \frac{1}{2}Y_q + \frac{3}{2}Y_d\right]\frac{(Y^{\not{B}L}_{1D})_{pr}}{M_1^2} \,, \tag{2.197}$$

$$\left[G_{dG}\right]^{(1)}_{pr} = +g_s\,(1 + L_1)\,\frac{(Y^{\not{B}L}_{1U})_{pr}}{M_1^2} \,, \tag{2.198}$$

$$\left[G_{dW}\right]^{(1)}_{pr} = \frac{1}{2}\, g \left(\frac{1}{2} + L_1\right)\frac{(Y^{\not{B}L}_{1U})_{pr}}{M_1^2} \tag{2.199}$$

$$\left[G_{dB}\right]^{(1)}_{pr} = -g' \left[(Y_u + Y_q)L_1 + \frac{1}{2}Y_q + \frac{3}{2}Y_u\right]\frac{(Y^{\not{B}L}_{1U})_{pr}}{M_1^2} \,. \tag{2.200}$$

$\psi^2 DH^2$

$$\begin{aligned}\left[G^{(1)}_{H\ell}\right]^{(1)}_{pr} = &-\frac{N_c}{4}\left[(1 + L_1)\,\frac{(Y^{1L}_{2D})_{pr} - (Y^{1L}_{2U})_{pr}}{M_1^2} + (1 + L_2)\,\frac{2(\tilde{Y}_{2D})_{pr}}{\tilde{M}_2^2}\right] \\ &- \frac{N_c}{2}|A_{\tilde{2}1}|^2\left[\frac{1}{(\Delta_{12}^2)} + \frac{M_1^2 + \tilde{M}_2^2}{2(\Delta_{12}^2)^2}\log\frac{\tilde{M}_2^2}{M_1^2}\right]\frac{(\Lambda_\ell)_{pr} + (\tilde{\Lambda}_\ell)_{pr}}{\Delta_{12}^2} \,,\end{aligned} \tag{2.201}$$

$$\begin{aligned}
\left[G'^{(1)}_{H\ell}\right]^{(1)}_{pr} &= -\frac{N_c}{8}\Bigg[\frac{(Y^{1L}_{2U})_{pr}+(Y^{1L}_{2D})_{pr}+2\lambda_{H1}(\Lambda_\ell)_{pr}}{M_1^2} \\
&\quad +\frac{(2\tilde{\lambda}_{H2}-\lambda_{\tilde{2}\tilde{2}})(\tilde{\Lambda}_\ell)_{pr}+(\tilde{Y}_{2D})_{pr}}{\tilde{M}_2^2}\Bigg] \\
&\quad -\frac{1}{4}\frac{|A_{\tilde{2}1}|^2}{\Delta^2_{12}}\left[\frac{\log \tilde{M}_2^2/M_1^2}{\Delta^2_{12}}\Big((\Lambda_\ell)_{pr}+(\tilde{\Lambda}_\ell)_{pr}\Big)+\left(\frac{(\Lambda_\ell)_{pr}}{M_1^2}+\frac{(\tilde{\Lambda}_\ell)_{pr}}{\tilde{M}_2^2}\right)\right], \qquad (2.202)
\end{aligned}$$

$$\left[G^{(3)}_{H\ell}\right]^{(1)}_{pr} = \frac{N_c}{4}\left[(1+L_1)\,\frac{(Y^{1L}_{2D})_{pr}+(Y^{1L}_{2U})_{pr}}{M_1^2}\right], \qquad (2.203)$$

$$\left[G'^{(3)}_{H\ell}\right]^{(1)}_{pr} = \frac{N_c}{8}\left[\frac{(Y^{1L}_{2D})_{pr}-(Y^{1L}_{2U})_{pr}}{M_1^2}\right], \qquad (2.204)$$

$$\left[G_{He}\right]^{(1)}_{pr} = -\frac{N_c}{2}\,(1+L_1)\,\frac{(Y^{1R}_{2U})_{pr}}{M_1^2}-\frac{N_c}{2}|A_{\tilde{2}1}|^2\left[1+\frac{M_1^2+\tilde{M}_2^2}{2(\Delta^2_{12})}\log\frac{\tilde{M}_2^2}{M_1^2}\right]\frac{(\Lambda_e)_{pr}}{(\Delta^2_{12})^2}, \qquad (2.205)$$

$$\left[G'_{He}\right]^{(1)}_{pr} = -\frac{N_c}{4}\,\frac{(Y^{1R}_{2U})_{pr}+\lambda_{H1}(\Lambda_e)_{pr}}{M_1^2}-\frac{1}{4}|A_{\tilde{2}1}|^2\left[\frac{1}{M_1^2}+\frac{\log\tilde{M}_2^2/M_1^2}{\Delta^2_{12}}\right]\frac{(\Lambda_e)_{pr}}{\Delta^2_{12}}, \qquad (2.206)$$

$$\begin{aligned}
\left[G^{(1)}_{Hq}\right]^{(1)}_{pr} &= -\frac{1}{4}\left[(1+L_1)\,\frac{(Y^{1L}_{2E})_{pr}+8(Y^{\not{B}L}_{2D})_{pr}-8(Y^{\not{B}L}_{2U})_{pr}}{M_1^2}\right] \\
&\quad -\frac{1}{2}|A_{\tilde{2}1}|^2\left[\frac{1}{(\Delta^2_{12})}+\frac{M_1^2+\tilde{M}_2^2}{2(\Delta^2_{12})^2}\log\frac{\tilde{M}_2^2}{M_1^2}\right]\frac{(\Lambda_q)_{pr}-8(\Lambda^{\not{B}}_q)_{pr}}{\Delta^2_{12}}, \qquad (2.207)
\end{aligned}$$

$$\begin{aligned}
\left[G'^{(1)}_{Hq}\right]^{(1)}_{pr} &= -\frac{1}{8}\left[\frac{(Y^{1L}_{2E})_{pr}+2\lambda_{H1}(\Lambda_q)_{pr}+16\lambda_{H1}(\Lambda^{\not{B}}_q)_{pr}+8(Y^{\not{B}L}_{2D})_{pr}-8(Y^{\not{B}L}_{2U})_{pr}}{M_1^2}\right] \\
&\quad -\frac{1}{4}|A_{\tilde{2}1}|^2\left[\frac{1}{M_1^2}+\frac{\log\tilde{M}_2^2/M_1^2}{\Delta^2_{12}}\right]\frac{(\Lambda_q)_{pr}+8(\Lambda^{\not{B}}_q)_{pr}}{\Delta^2_{12}}, \qquad (2.208)
\end{aligned}$$

$$\left[G^{(3)}_{Hq}\right]^{(1)}_{pr} = \frac{1}{4}\left[(1+L_1)\,\frac{(Y^{1L}_{2E})_{pr}+8(Y^{\not{B}L}_{2D})_{pr}-8(Y^{\not{B}L}_{2U})_{pr}}{M_1^2}\right], \qquad (2.209)$$

$$\left[G'^{(3)}_{Hq}\right]^{(1)}_{pr} = \frac{1}{8}\left[\frac{(Y^{1L}_{2E})_{pr}+8(Y^{\not{B}L}_{2D})_{pr}-8(Y^{\not{B}L}_{2U})_{pr}}{M_1^2}\right], \qquad (2.210)$$

$$\begin{aligned}
\left[G_{Hu}\right]^{(1)}_{pr} &= \frac{1}{2}\,(1+L_1)\,\frac{(Y^{1R}_{2E})_{pr}+2(Y^{\not{B}R}_{2D})_{pr}}{M_1^2} \\
&\quad -\frac{1}{2}|A_{\tilde{2}1}|^2\left[\frac{1}{(\Delta^2_{12})}+\frac{M_1^2+\tilde{M}_2^2}{2(\Delta^2_{12})^2}\log\frac{\tilde{M}_2^2}{M_1^2}\right]\frac{(\Lambda_u)_{pr}-2(\Lambda^{\not{B}}_u)_{pr}}{\Delta^2_{12}}, \qquad (2.211)
\end{aligned}$$

$$\begin{aligned}
\left[G'_{Hu}\right]^{(1)}_{pr} &= -\frac{1}{4}\left[\frac{(Y^{1R}_{2E})_{pr}+\lambda_{H1}(\Lambda_u)_{pr}+2\lambda_{H1}(\Lambda^{\not{B}}_u)_{pr}+2(Y^{\not{B}R}_{2D})_{pr}}{M_1^2}\right] \\
&\quad -\frac{1}{4}|A_{\tilde{2}1}|^2\left[\frac{1}{M_1^2}+\frac{\log\tilde{M}_2^2/M_1^2}{\Delta^2_{12}}\right]\frac{(\Lambda_u)_{pr}+2(\Lambda^{\not{B}}_u)_{pr}}{\Delta^2_{12}}, \qquad (2.212)
\end{aligned}$$

$$\left[G_{Hd}\right]^{(1)}_{pr} = \frac{1}{2}\,(1+L_2)\,\frac{(\tilde{Y}_{2E})_{pr}}{\tilde{M}_2^2}-(1+L_1)\,\frac{(Y^{\not{B}R}_{2U})_{pr}}{M_1^2}$$

$$
-\frac{1}{2}|A_{\tilde{2}1}|^2\left[\frac{1}{(\Delta_{12}^2)}+\frac{M_1^2+\tilde{M}_2^2}{2(\Delta_{12}^2)^2}\log\frac{\tilde{M}_2^2}{M_1^2}\right]\frac{(\tilde{\Lambda}_d)_{pr}-2(\Lambda_d^{\not{B}})_{pr}}{\Delta_{12}^2}\,, \tag{2.213}
$$

$$
\begin{aligned}
\left[G'_{Hd}\right]^{(1)}_{pr} &= -\frac{1}{2}\frac{(Y_{2U}^{\not{B}R})_{pr}+\lambda_{H1}(\Lambda_d^{\not{B}})_{pr}}{M_1^2}-\frac{1}{4}\frac{(\tilde{Y}_{2E})_{pr}+(2\lambda_{H2}-\lambda_{\tilde{2}\tilde{2}})(\tilde{\Lambda}_d)_{pr}}{\tilde{M}_2^2}\\
&\quad -\frac{1}{4}\frac{|A_{\tilde{2}1}|^2}{\Delta_{12}^2}\left[\frac{\log\tilde{M}_2^2/M_1^2}{\Delta_{12}^2}\left((\tilde{\Lambda}_d)_{pr}+2(\Lambda_d^{\not{B}})_{pr}\right)+\left(\frac{(\tilde{\Lambda}_d)_{pr}}{M_1^2}+\frac{2(\Lambda_d^{\not{B}})_{pr}}{\tilde{M}_2^2}\right)\right]\,,
\end{aligned} \tag{2.214}
$$

$$
\left[G''_{H(d,u,e)}\right]^{(1)}_{pr}=\left[G''^{(1,3)}_{H\ell}\right]^{(1)}_{pr}=\left[G''^{(1,3)}_{Hq}\right]^{(1)}_{pr}=0\,. \tag{2.215}
$$

$\psi^2H^3$

$$
[G_{eH}]^{(1)}_{pr}=N_c\frac{(1+L_1)(Y_{3U}^{1L})_{pr}-\lambda_{H1}(Y_{1U}^{1L})_{pr}}{M_1^2}-N_c|A_{\tilde{2}1}|^2\left(\frac{1}{M_1^2}+\frac{\log\tilde{M}_2^2/M_1^2}{\Delta_{12}^2}\right)\frac{(Y_{1U}^{1L})_{pr}}{\Delta_{12}^2}\,, \tag{2.216}
$$

$$
\begin{aligned}
[G_{uH}]^{(1)}_{pr} &= \frac{(1+L_1)\left[(Y_{3E}^{1L})_{pr}-4(Y_{3D}^{\not{B}L})_{pr}\right]-\lambda_{H1}\left[(Y_{1E}^{1L})_{pr}-4(Y_{1D}^{\not{B}L})_{pr}\right]}{M_1^2}\\
&\quad -|A_{\tilde{2}1}|^2\left(\frac{1}{M_1^2}+\frac{\log\tilde{M}_2^2/M_1^2}{\Delta_{12}^2}\right)\frac{(Y_{1E}^{1L})_{pr}+4(Y_{1D}^{\not{B}L})_{pr}}{\Delta_{12}^2}\,,
\end{aligned} \tag{2.217}
$$

$$
\begin{aligned}
[G_{dH}]^{(1)}_{pr} &= -\frac{4(1+L_1)(Y_{3U}^{\not{B}L})_{pr}-4\lambda_{H1}(Y_{1U}^{\not{B}L})_{pr}}{M_1^2}\\
&\quad -4|A_{\tilde{2}1}|^2\left(\frac{1}{M_1^2}+\frac{\log\tilde{M}_2^2/M_1^2}{\Delta_{12}^2}\right)\frac{(Y_{1U}^{\not{B}L})_{pr}}{\Delta_{12}^2}\,.
\end{aligned} \tag{2.218}
$$

**Four Fermion Operators**

**Four Quarks**

$$
\begin{aligned}
\left[G^{(1)}_{qq}\right]^{(1)}_{prst} &= -\frac{1}{16}\frac{(\Lambda_q)_{pt}(\Lambda_q)_{sr}}{M_1^2}-\frac{4(\Lambda_q^{\not{B}})_{pr}(\Lambda_q^{\not{B}})_{st}+2(\Lambda_q^{\not{B}})_{pt}(\Lambda_q^{\not{B}})_{sr}}{M_1^2}\\
&\quad +\frac{2(\Lambda_q^{\not{B}})_{pr}(\Lambda_q)_{st}-2(\Lambda_q^{\not{B}})_{pt}(\Lambda_q)_{sr}}{M_1^2}\\
&\quad +\left[(1+N_c)(1+L_1)c_1+\frac{2\tilde{M}_2^2}{M_1^2}(1+L_2)\left(N_c c_{1\tilde{2}}^{(1)}+c_{1\tilde{2}}^{(2)}\right)\right.\\
&\quad \left.+\,8|A'|^2\,\frac{1}{M_1^2}L_2\right]\frac{(\lambda_{ps}^{\not{B}L})(\lambda_{rt}^{\not{B}L})^*}{2M_1^2}\\
&\quad -\frac{2(\lambda_{ps}^{\not{B}L})(\lambda_{rt}^{\not{B}L})^*}{M_1^2}\left[\left(g'^2Y_q^2-\frac{g_s^2}{12}-\frac{3g^2}{4}\right)\left(\frac{1}{2}+a_{\mathrm{ev}}\right)+\left(\frac{g_s^2}{6}+\frac{3g^2}{4}\right)(1+L_1)\right]\,,
\end{aligned} \tag{2.219}
$$

$$
\left[G^{(3)}_{qq}\right]^{(1)}_{prst}=-\frac{1}{16}\frac{(\Lambda_q)_{pt}(\Lambda_q)_{sr}}{M_1^2}-2\frac{(\Lambda_q^{\not{B}})_{pt}(\Lambda_q^{\not{B}})_{sr}}{M_1^2}
$$

$$
\begin{aligned}
&-\left[(1+N_c)(1+L_1)\,c_1+\frac{2\tilde{M}_2^2}{M_1^2}(1+L_2)\left(N_c c^{(1)}_{1\tilde{2}}+c^{(2)}_{1\tilde{2}}\right)\right.\\
&\left.+\,8|A'|^2\,\frac{1}{M_1^2}\,L_2\right]\frac{(\lambda^{\not{B}L}_{ps})(\lambda^{\not{B}L}_{rt})^*}{2M_1^2}\\
&+\frac{2(\lambda^{\not{B}L}_{ps})(\lambda^{\not{B}L}_{rt})^*}{M_1^2}\left[\left(g'^2Y_q^2-\frac{g_s^2}{12}-\frac{g^2}{4}\right)\left(\frac{1}{2}+a_{\rm ev}\right)+\left(\frac{g_s^2}{6}+\frac{g^2}{4}\right)(1+L_1)\right],
\end{aligned}
\tag{2.220}
$$

$$
\begin{aligned}
[G_{uu}]^{(1)}_{prst}&=-\frac{1}{8M_1^2}\left[(\Lambda_u)_{pt}(\Lambda_u)_{sr}+2(\Lambda_u^{\not{B}})_{pr}(\Lambda_u^{\not{B}})_{st}+2(\Lambda_u^{\not{B}})_{sr}(\Lambda_u^{\not{B}})_{pt}\right.\\
&\left.+4(\Lambda_u)_{pr}(\Lambda_u^{\not{B}})_{st}-4(\Lambda_u)_{pt}(\Lambda_u^{\not{B}})_{sr}\right],
\end{aligned}
\tag{2.221}
$$

$$
[G_{dd}]^{(1)}_{prst}=\frac{1}{4}\,\frac{(\tilde{\Lambda}_d)_{pt}(\tilde{\Lambda}_d)_{sr}-2(\Lambda_d^{\not{B}})_{pr}(\Lambda_d^{\not{B}})_{st}-2(\Lambda_d^{\not{B}})_{sr}(\Lambda_d^{\not{B}})_{pt}}{\tilde{M}_2^2}\,,
\tag{2.222}
$$

$$
\begin{aligned}
\left[G^{(1)}_{ud}\right]^{(1)}_{prst}&=\frac{(\Lambda_u)_{pr}(\Lambda_d^{\not{B}})_{st}}{3M_1^2}-\frac{3}{4}\,\frac{(\Lambda_u^{\not{B}})_{pr}(\Lambda_d^{\not{B}})_{st}}{M_1^1}\\
&+\left[(1+N_c)(1+L_1)\,c_1+\frac{2\tilde{M}_2^2}{M_1^2}(1+L_2)\left(N_c c^{(1)}_{1\tilde{2}}+c^{(2)}_{1\tilde{2}}\right)\right.\\
&\left.+\,8|A'|^2\,\frac{1}{M_1^2}\,L_2\right]\frac{(\lambda^{\not{B}R}_{ps})^T(\lambda^{\not{B}R}_{rt})^\dagger}{3M_1^2}\\
&+g'^2\frac{(\lambda^{\not{B}R}_{ps})^T(\lambda^{\not{B}R}_{tr})^*}{3M_1^2}\left[(Y_u-Y_d)^2\left(\frac{1}{2}+a_{\rm ev}\right)-(Y_u+Y_d+Y_{S_1})^2(1+L_1)\right]\\
&+g_s^2\left[\frac{4}{3}\left(\frac{1}{2}+a_{ev}\right)+\frac{5}{9}(1+L_1)\right]\frac{(\lambda^{\not{B}R}_{tr})^*(\lambda^{\not{B}R}_{sp})}{M_1^2}\,,
\end{aligned}
\tag{2.223}
$$

$$
\begin{aligned}
\left[G^{(8)}_{ud}\right]^{(1)}_{prst}&=-\frac{(\Lambda_u)_{pr}(\Lambda_d^{\not{B}})_{st}}{M_1^2}-\frac{(\Lambda_u^{\not{B}})_{pr}(\Lambda_d^{\not{B}})_{st}}{M_1^1}\\
&-\left[(1+N_c)(1+L_1)\,c_1+\frac{2\tilde{M}_2^2}{M_1^2}(1+L_2)\left(N_c c^{(1)}_{1\tilde{2}}+c^{(2)}_{1\tilde{2}}\right)\right.\\
&\left.+\,8|A'|^2\,\frac{1}{M_1^2}\,L_2\right]\frac{(\lambda^{\not{B}R}_{ps})^T(\lambda^{\not{B}R}_{rt})^\dagger}{M_1^2}\\
&-g'^2\frac{(\lambda^{\not{B}R}_{ps})^T(\lambda^{\not{B}R}_{tr})^*}{M_1^2}\left[(Y_u-Y_d)^2\left(\frac{1}{2}+a_{\rm ev}\right)-(Y_u+Y_d+Y_{S_1})^2(1+L_1)\right]\\
&+g_s^2\left[\frac{7}{6}\left(\frac{1}{2}+a_{ev}\right)+\frac{13}{6}(1+L_1)\right]\frac{(\lambda^{\not{B}R}_{tr})^*(\lambda^{\not{B}R}_{sp})}{M_1^2};,
\end{aligned}
\tag{2.224}
$$

$$
\begin{aligned}
\left[G^{(1)}_{qu}\right]^{(1)}_{prst}&=-\frac{1}{12}\,\frac{(\Lambda_q)_{pr}(\Lambda_u)_{st}}{M_1^2}-\frac{3(\Lambda_q^{\not{B}})_{pr}(\Lambda_u^{\not{B}})_{st}}{M_1^2}+\frac{(\Lambda_q)_{pr}(\Lambda_u^{\not{B}})_{st}-4(\Lambda_q^{\not{B}})_{pr}(\Lambda_u)_{st}}{3M_1^2}\\
&+\left(\frac{3}{2}+L_1\right)\frac{(y_D\lambda^{\not{B}R}+2\lambda^{\not{B}L}y_U^*)_{ps}(y_D^*(\lambda^{\not{B}R})^*+2(\lambda^{\not{B}L})^*y_U)_{rt}}{6M_1^2}\,,
\end{aligned}
\tag{2.225}
$$

$$
\left[G^{(8)}_{qu}\right]^{(1)}_{prst}=-\frac{1}{2}\,\frac{(\Lambda_q)_{pr}(\Lambda_u)_{st}}{M_1^2}-\frac{4(\Lambda_q^{\not{B}})_{pr}(\Lambda_u^{\not{B}})_{st}}{M_1^2}-\frac{(\Lambda_q)_{pr}(\Lambda_u^{\not{B}})_{st}-4(\Lambda_q^{\not{B}})_{pr}(\Lambda_u)_{st}}{M_1^2}
$$

$$-\left(\frac{3}{2}+L_1\right)\frac{(y_D\lambda^{\not{B}R}+2\lambda^{\not{B}L}y_U^*)_{ps}(y_D^*(\lambda^{\not{B}R})^*+2(\lambda^{\not{B}L})^*y_U)_{rt}}{2M_1^2}\,, \tag{2.226}$$

$$\left[G_{qd}^{(1)}\right]_{prst}^{(1)} = \frac{(\Lambda_q)_{pr}(\Lambda_d^{\not{B}})_{st}}{3M_1^2} - \frac{3(\Lambda_q^{\not{B}})_{pr}(\Lambda_d^{\not{B}})_{st}}{M_1^2} - \frac{1}{8}\frac{((\lambda^{1\mathrm{L}})^*\tilde{\lambda}^T)_{ps}(\tilde{\lambda}^*(\lambda^{1\mathrm{L}})^T)_{tr}}{M_1^2-\tilde{M}_2^2}\log\frac{M_1^2}{\tilde{M}_2^2}$$
$$-\left(\frac{3}{2}+L_1\right)\frac{(y_U(\lambda^{\not{B}R})^T+2\lambda^{\not{B}L}y_D^*)_{ps}(y_U^*(\lambda^{\not{B}R})^\dagger+2(\lambda^{\not{B}L})^*y_D)_{rt}}{6M_1^2}\,, \tag{2.227}$$

$$\left[G_{qd}^{(8)}\right]_{prst}^{(1)} = -\frac{(\Lambda_q)_{pr}(\Lambda_d^{\not{B}})_{st}}{M_1^2} - \frac{4(\Lambda_q^{\not{B}})_{pr}(\Lambda_d^{\not{B}})_{st}}{M_1^2}$$
$$+\left(\frac{3}{2}+L_1\right)\frac{(y_U(\lambda^{\not{B}R})^T+2\lambda^{\not{B}L}y_D^*)_{ps}(y_U^*(\lambda^{\not{B}R})^\dagger+2(\lambda^{\not{B}L})^*y_D)_{rt}}{2M_1^2}\,, \tag{2.228}$$

$$\left[G_{quqd}^{(1)}\right]_{prst}^{(1)} = \frac{4}{3}\Bigg[(1+N_c)(1+L_1)c_1 + \frac{2\tilde{M}_2^2}{M_1^2}(1+L_2)\left(N_c c_{1\tilde{2}}^{(1)} + c_{1\tilde{2}}^{(2)}\right)$$
$$+\,8|A'|^2\,\frac{1}{M_1^2}\,L_2\Bigg]\frac{(\lambda_{pr}^{\not{B}L})(\lambda_{st}^{\not{B}R})^\dagger}{M_1^2}$$
$$-\frac{4}{3}g'^2\frac{(\lambda_{ps}^{\not{B}L})(\lambda_{tr}^{\not{B}R})^*}{M_1^2}(1+L_1)\left[Y_q(Y_{S_1}+2Y_q)+Y_d(Y_d-Y_{S_1})\right]$$
$$+\frac{44}{9}g_s^2\frac{(\lambda_{tr}^{\not{B}R})^*(\lambda_{sp}^{\not{B}L})}{M_1^2}\left(\frac{8}{11}+L_1\right)\,, \tag{2.229}$$

$$\left[G_{quqd}^{(8)}\right]_{prst}^{(1)} = -4\Bigg[(1+N_c)(1+L_1)c_1 + \frac{2\tilde{M}_2^2}{M_1^2}(1+L_2)\left(N_c c_{1\tilde{2}}^{(1)} + c_{1\tilde{2}}^{(2)}\right)$$
$$+\,8|A'|^2\,\frac{1}{M_1^2}\,L_2\Bigg]\frac{(\lambda_{pr}^{\not{B}L})(\lambda_{st}^{\not{B}R})^\dagger}{M_1^2}$$
$$+4g'^2\frac{(\lambda_{ps}^{\not{B}L})(\lambda_{tr}^{\not{B}R})^*}{M_1^2}(1+L_1)\left[Y_q(Y_{S_1}+2Y_q)+Y_d(Y_d-Y_{S_1})\right]$$
$$+\frac{2}{3}g_s^2\frac{(\lambda_{tr}^{\not{B}R})^*(\lambda_{sp}^{\not{B}L})}{M_1^2}\,. \tag{2.230}$$

**Four Leptons**

$$\left[G_{\ell\ell}^{(1)}\right]_{prst}^{(1)} = -\frac{N_c}{8}\left[\frac{(\Lambda_\ell)_{pr}(\Lambda_\ell)_{st}}{M_1^2} + \frac{(\tilde{\Lambda}_\ell)_{pt}(\tilde{\Lambda}_\ell)_{sr}}{\tilde{M}_2^2}\right]\,, \tag{2.231}$$

$$[G_{ee}]_{prst}^{(1)} = -\frac{N_c}{8}\frac{(\Lambda_e)_{pr}(\Lambda_e)_{st}}{M_1^2}\,, \tag{2.232}$$

$$[G_{\ell e}]_{prst}^{(1)} = -\frac{N_c}{4}\frac{(\Lambda_\ell)_{pr}(\Lambda_e)_{st}}{M_1^2}\,. \tag{2.233}$$

**Semileptonic**

$$\left[G_{\ell q}^{(1)}\right]_{prst}^{(1)} = -\frac{1}{4}\frac{(\Lambda_\ell)_{pr}(\Lambda_q)_{st}}{M_1^2} - \frac{4(\Lambda_\ell)_{pr}(\Lambda_q^{\not{B}})_{st}}{M_1^2} + \frac{4(\lambda^{\not{B}L}\lambda^{1\mathrm{L}})_{tp}^*((\lambda^{1\mathrm{L}})^T\lambda^{\not{B}L})_{rs}}{M_1^2}$$
$$+\frac{1}{4}\left(\frac{3}{2}+L_2\right)\frac{(\tilde{\lambda}^\dagger y_D^\dagger)_{pt}(y_D\tilde{\lambda})_{sr}}{\tilde{M}_2^2}$$

$$
\begin{aligned}
&+\left[\frac{1+N_c}{4}\,(1+L_1)\,c_1+\frac{\tilde{M}_2^2}{2M_1^2}\,(1+L_2)\Big(N_c c^{(1)}_{1\tilde{2}}+c^{(2)}_{1\tilde{2}}\Big)\right.\\
&\left.+\,8|A'|^2\,\frac{1}{M_1^2}\,L_2\right]\frac{(\lambda^{1\mathrm{L}}_{ps})^\dagger(\lambda^{1\mathrm{L}}_{tr})}{M_1^2}\\
&+\frac{1}{4}\left(\frac{1}{2}+a_{\mathrm{ev}}\right)\left[g_s^2C_F^{\mathrm{SU}(3)}+g'^2(Y_q-Y_\ell)^2+3g^2\right]\frac{(\lambda^{1\mathrm{L}}_{ps})^\dagger\lambda^{1\mathrm{L}}_{tr}}{M_1^2}\,,
\end{aligned}
\tag{2.234}
$$

$$
\begin{aligned}
\left[G^{(3)}_{\ell q}\right]^{(1)}_{prst}=&\;\frac{4(\lambda^{\not{B}L}\lambda^{1\mathrm{L}})^*_{tp}((\lambda^{1\mathrm{L}})^T\lambda^{\not{B}L})_{rs}}{M_1^2}\\
&-\left[\frac{1+N_c}{4}\,(1+L_1)\,c_1+\frac{\tilde{M}_2^2}{2M_1^2}\,(1+L_2)\Big(N_c c^{(1)}_{1\tilde{2}}+c^{(2)}_{1\tilde{2}}\Big)\right.\\
&\left.+\,8|A'|^2\,\frac{1}{M_1^2}\,L_2\right]\frac{(\lambda^{1\mathrm{L}}_{ps})^\dagger(\lambda^{1\mathrm{L}}_{tr})}{M_1^2}\\
&-\frac{1}{4}\left(\frac{1}{2}+a_{\mathrm{ev}}\right)\left[g_s^2C_F^{\mathrm{SU}(3)}+g'^2(Y_q-Y_\ell)^2-3g^2\right]\frac{(\lambda^{1\mathrm{L}}_{ps})^\dagger\lambda^{1\mathrm{L}}_{tr}}{M_1^2}\,,
\end{aligned}
\tag{2.235}
$$

$$
\begin{aligned}
[G_{eu}]^{(1)}_{prst}=&\left[\frac{1+N_c}{2}\,(1+L_1)\,c_1+\frac{\tilde{M}_2^2}{M_1^2}\,(1+L_2)\Big(N_c c^{(1)}_{1\tilde{2}}+c^{(2)}_{1\tilde{2}}\Big)\right.\\
&\left.+\,8|A'|^2\,\frac{1}{M_1^2}\,L_2\right]\frac{(\lambda^{1\mathrm{R}}_{ps})^\dagger(\lambda^{1\mathrm{R}}_{tr})}{M_1^2}\\
&+\frac{1}{2}\left(\frac{1}{2}+a_{\mathrm{ev}}\right)\left[g_s^2C_F^{\mathrm{SU}(3)}+g'^2(Y_u-Y_e)^2+3g^2\right]\frac{(\lambda^{1\mathrm{R}}_{ps})^\dagger\lambda^{1\mathrm{R}}_{tr}}{M_1^2}+\frac{(\Lambda_e)_{pr}(\Lambda_u^{\not{B}})_{st}}{M_1^2}\,,
\end{aligned}
\tag{2.236}
$$

$$
[G_{ed}]^{(1)}_{prst}=\frac{(\Lambda_e)_{pr}(\Lambda_d^{\not{B}})_{st}}{M_1^2}-\frac{2(\lambda^{\not{B}R}\lambda^{1\mathrm{R}})^*_{tp}(\lambda^{\not{B}R}\lambda^{1\mathrm{R}})_{sr}}{M_1^2}-\frac{1}{2}\left(\frac{3}{2}-L_2\right)\frac{(y_E^\dagger\tilde{\lambda}^\dagger)_{pt}(\tilde{\lambda}y_E)_{sr}}{\tilde{M}_2^2}\,,
\tag{2.237}
$$

$$
\begin{aligned}
\left[G_{qe}\right]^{(1)}_{prst}=&-\frac{1}{4}\frac{(\Lambda_q)_{pr}(\Lambda_e)_{st}}{M_1^2}-\frac{4(\Lambda_q^{\not{B}})_{pr}(\Lambda_e)_{st}}{M_1^2}\\
&-\frac{1}{4}\left(\frac{3}{2}+L_1\right)\frac{((\lambda^{1\mathrm{L}})^*y_E^*-y_U(\lambda^{1\mathrm{R}})^*)_{ps}(\lambda^{1\mathrm{L}}y_E-y_U^*\lambda^{1\mathrm{R}})_{rt}}{M_1^2}\,,
\end{aligned}
\tag{2.238}
$$

$$
\begin{aligned}
[G_{\ell u}]^{(1)}_{prst}=&-\frac{1}{4}\frac{(\Lambda_\ell)_{pr}(\Lambda_u)_{st}}{M_1^2}+\frac{(\Lambda_\ell)_{pr}(\Lambda_u^{\not{B}})_{st}}{M_1^2}\\
&-\frac{1}{4}\left(\frac{3}{2}+L_1\right)\frac{((\lambda^{1\mathrm{L}})^\dagger y_U^*-y_E(\lambda^{1\mathrm{R}})^\dagger)_{ps}((\lambda^{1\mathrm{L}})^Ty_U-y_E^*(\lambda^{1\mathrm{R}})^T)_{rt}}{M_1^2}\\
&+\frac{1}{2}\frac{(\tilde{\lambda}^\dagger\lambda^{\not{B}R})_{ps}((\lambda^{\not{B}R})^\dagger\tilde{\lambda})_{tr}}{M_1^2-\tilde{M}_2^2}\log\frac{M_1^2}{\tilde{M}_2^2}\,,
\end{aligned}
\tag{2.239}
$$

$$
\begin{aligned}
[G_{\ell d}]^{(1)}_{prst}=&\;\frac{(\Lambda_\ell)_{pr}(\Lambda_d^{\not{B}})_{st}}{M_1^2}+\frac{1}{4}\frac{(\tilde{\Lambda}_\ell)_{pr}(\tilde{\Lambda}_d)_{st}}{M_1^2-\tilde{M}_2^2}\log\frac{M_1^2}{\tilde{M}_2^2}\\
&-\frac{1}{4}\left(\frac{3}{2}+L_1\right)\frac{((\lambda^{1\mathrm{L}})^\dagger y_D^*)_{ps}((\lambda^{1\mathrm{L}})^Ty_D)_{rt}}{M_1^2}
\end{aligned}
$$

$$
\begin{aligned}
&-\bigg[\frac{M_1^2}{\tilde{M}_2^2}(1+L_1)\Big(N_c c^{(1)}_{1\tilde{2}} + c^{(2)}_{1\tilde{2}}\Big) \\
&+\Big((1+2N_c)\,\tilde{c}_2 + (2+N_c)c^{(8)}_{\tilde{2}}\Big)(1+L_2)\bigg]\frac{\tilde{\lambda}^\dagger_{pt}\tilde{\lambda}_{sr}}{2\tilde{M}_2^2} \\
&-\frac{1}{2}\left(\frac{1}{2}+a_{\rm ev}\right)\left[g_2^2 C_F^{\rm SU(3)} + g^2 C_F^{\rm SU(2)} + g'^2(Y_\ell + Y_d)^2\right]\frac{(\tilde{\lambda}^*_{pt})(\tilde{\lambda}_{sr})}{\tilde{M}_2^2} \\
&-2|A'|^2\frac{(\tilde{\lambda}_{pt})^\dagger(\tilde{\lambda}_{sr})}{\tilde{M}_2^4}\left(1+\frac{M_1^2 L_1 - \tilde{M}_2^2 L_2}{\Delta_{12}^2}\right), \qquad (2.240)
\end{aligned}
$$

$$
\begin{aligned}
\left[G_{\ell edq}\right]^{(1)}_{prst} =& -\frac{6(\lambda^{\not{B}L}\lambda^{1\rm L})^*_{tp}(\lambda^{\not{B}R}\lambda^{1\rm R})_{sr}}{M_1^2} \\
&-\frac{1}{2}\left(\frac{3}{2}+L_1\right)\frac{((\lambda^{1\rm L})^\dagger y_D^*)_{ps}(\lambda^{1\rm L}y_E - y_U^*\lambda^{1\rm R})_{tr}}{M_1^2} \\
&+\frac{1}{2}\left(\frac{3}{2}+L_2\right)\frac{(\tilde{\lambda}^\dagger y_D^\dagger)_{pt}(\tilde{\lambda}y_E)_{sr}}{\tilde{M}_2^2}, \qquad (2.241)
\end{aligned}
$$

$$
\begin{aligned}
\left[G^{(1)}_{\ell equ}\right]^{(1)}_{prst} =& \bigg[\frac{1+N_c}{2}(1+L_1)\,c_1 + \frac{\tilde{M}_2^2}{M_1^2}(1+L_2)\Big(N_c c^{(1)}_{1\tilde{2}} + c^{(2)}_{1\tilde{2}}\Big) \\
&+8|A'|^2\,\frac{1}{M_1^2}\,L_2\bigg]\frac{(\lambda^{1\rm L}_{pt})^\dagger(\lambda^{1\rm R}_{sr})}{M_1^2} \\
&-\frac{3}{2}\left(\frac{3}{2}+L_1\right)\left[g_s^2 C_F^{\rm SU(3)} + g'^2(Y_q - Y_\ell)(Y_u - Y_e)\right]\frac{(\lambda^{1\rm L}_{ps})^\dagger\lambda^{1\rm R}_{tr}}{M_1^2}, \qquad (2.242)
\end{aligned}
$$

$$
\begin{aligned}
\left[G^{(3)}_{\ell equ}\right]^{(1)}_{prst} =& -\bigg[\frac{1+N_c}{8}(1+L_1)\,c_1 + \frac{\tilde{M}_2^2}{4M_1^2}(1+L_2)\Big(N_c c^{(1)}_{1\tilde{2}} + c^{(2)}_{1\tilde{2}}\Big) \\
&+8|A'|^2\,\frac{1}{M_1^2}\,L_2\bigg]\frac{(\lambda^{1\rm L}_{pt})^\dagger(\lambda^{1\rm R}_{sr})}{M_1^2} \\
&-\frac{1}{8}\left(\frac{3}{2}+L_1\right)\left[g_s^2 C_F^{\rm SU(3)} + g'^2(Y_q - Y_\ell)(Y_u - Y_e)\right]\frac{(\lambda^{1\rm L}_{ps})^\dagger\lambda^{1\rm R}_{tr}}{M_1^2}. \qquad (2.243)
\end{aligned}
$$

**B-violating**

$$
\begin{aligned}
\left[G_{duq}\right]^{(1)}_{prst} =& \bigg[(1+N_c)(1+L_1)\,c_1 + \frac{2\tilde{M}_2^2}{M_1^2}(1+L_2)\Big(N_c c^{(1)}_{1\tilde{2}} + c^{(2)}_{1\tilde{2}}\Big) \\
&+8|A'|^2\,\frac{1}{M_1^2}\,L_2\bigg]\frac{(\lambda^{\not{B}R}_{pr})^*(\lambda^{1\rm L}_{st})}{M_1^2} \\
&+(1+L_1)\left[g'^2\Big(Y_d(Y_q - Y_{S_1}) + Y_u(Y_\ell - Y_{S_1}) + Y_d(Y_u - Y_{S_1})\Big)\right]\frac{(\lambda^{\not{B}R}_{pr})^*(\lambda^{1\rm L}_{st})}{M_1^2} \\
&-\left(\frac{1}{2}+a_{ev}\right)(Y_\ell + Y_u)(Y_u + Y_d)\frac{(\lambda^{\not{B}R}_{pr})^*(\lambda^{1\rm L}_{st})}{M_1^2} \\
&+g_s^2\left[\frac{4}{3}\left(\frac{1}{2}+a_{ev}\right) - \frac{13}{6}(1+L_1)\right]\frac{(\lambda^{\not{B}R}_{pr})^*(\lambda^{1\rm L}_{st})}{M_1^2}
\end{aligned}
$$

$$
\begin{aligned}
&+\frac{((\tilde{\lambda})^*(\lambda^{1\mathrm{L}})^T)_{ps}((\lambda^{\not{B}R})^\dagger\tilde{\lambda})_{rt}}{M_1^2-\tilde{M}_2^2}\log\frac{M_1^2}{\tilde{M}_2^2}\\
&+\frac{(\lambda^{1\mathrm{L}}y_E+y_U^*\lambda^{1\mathrm{R}})_{pt}((\lambda^{\not{B}R})^\dagger y_D^\dagger+2y_U^T(\lambda^{\not{B}L})^*)_{sr}}{2M_1^2}\left(\frac{3}{2}+L_1\right), \qquad (2.244)
\end{aligned}
$$

$$
\begin{aligned}
\left[G_{qqu}\right]^{(1)}_{prst}=&\Bigg[(1+N_c)(1+L_1)c_1+\frac{2\tilde{M}_2^2}{M_1^2}(1+L_2)\left(N_c c^{(1)}_{1\tilde{2}}+c^{(2)}_{1\tilde{2}}\right)\\
&+8|A'|^2\,\frac{1}{M_1^2}L_2\Bigg]\frac{(\lambda^{\not{B}L}_{pr})^*(\lambda^{1\mathrm{R}}_{st})}{M_1^2}\\
&-(1+L_1)\left[4g'^2Y_{S_1}(2Y_q+Y_{S_1})\right]\frac{(\lambda^{\not{B}L}_{pr})^*(\lambda^{1\mathrm{R}}_{st})}{4M_1^2}\\
&+2g'^2\left(\frac{1}{2}+a_{ev}\right)Y_q(Y_e-Y_u)\frac{(\lambda^{\not{B}L}_{pr})^*(\lambda^{1\mathrm{R}}_{st})}{M_1^2}\\
&+g_s^2\frac{(\lambda^{\not{B}L}_{pr})^*(\lambda^{1\mathrm{R}}_{st})}{M_1^2}\left[\frac{2}{3}\left(\frac{1}{2}+a_{ev}\right)-\frac{5}{2}(1+L_1)\right]\\
&+\frac{(2(\lambda^{\not{B}L})^*y_D-y_U^*(\lambda^{\not{B}R})^\dagger)_{sp}(y_E^*(\lambda^{1\mathrm{R}})^T-(\lambda^{1\mathrm{L}})^Ty_U)_{tr}}{2M_1^2}\left(\frac{3}{2}+L_1\right)\\
&-\frac{(y_D^T\lambda^{1\mathrm{L}})_{pt}(2(\lambda^{\not{B}L})^*y_U+y_D^*(\lambda^{\not{B}R})^*)_{sr}}{2M_1^2}\left(\frac{3}{2}+L_1\right), \qquad (2.245)
\end{aligned}
$$

$$
\begin{aligned}
\left[G_{qqq}\right]^{(1)}_{prst}=&-\Bigg[(1+N_c)(1+L_1)c_1+\frac{2\tilde{M}_2^2}{M_1^2}(1+L_2)\left(N_c c^{(1)}_{1\tilde{2}}+c^{(2)}_{1\tilde{2}}\right)\\
&+8|A'|^2\,\frac{1}{M_1^2}L_2\Bigg]\frac{2(\lambda^{\not{B}L}_{pr})^*(\lambda^{1\mathrm{L}}_{st})}{M_1^2}\\
&+(1+L_1)\left[2g'^2Y_{S_1}(6Y_q+Y_\ell)\right]\frac{(\lambda^{\not{B}L}_{pr})^*(\lambda^{1\mathrm{L}}_{st})}{2M_1^2}\\
&+g_s^2\left(\frac{3}{2}+L_1\right)\frac{(\lambda^{\not{B}L}_{ps})^*(\lambda^{1\mathrm{L}}_{rt})}{12M_1^2}-\frac{5}{3}g_s^2\frac{(\lambda^{\not{B}L}_{pr})^*(\lambda^{1\mathrm{L}}_{st})}{M_1^2}\left(-\frac{3}{5}+L_1\right)\\
&+\frac{2g^2}{M_1^2}\left(\frac{3}{2}+L_1\right)\left[2(\lambda^{\not{B}L}_{ps})^*(\lambda^{1\mathrm{L}}_{rt})+(\lambda^{\not{B}L}_{rs})^*(\lambda^{1\mathrm{L}}_{tp})-(\lambda^{\not{B}L}_{pr})^*(\lambda^{1\mathrm{L}}_{st})\right], \qquad (2.246)
\end{aligned}
$$

$$
\begin{aligned}
\left[G_{duu}\right]^{(1)}_{prst}=&\Bigg[(1+N_c)(1+L_1)c_1+\frac{2\tilde{M}_2^2}{M_1^2}(1+L_2)\left(N_c c^{(1)}_{1\tilde{2}}+c^{(2)}_{1\tilde{2}}\right)\\
&+8|A'|^2\,\frac{1}{M_1^2}L_2\Bigg]\frac{(\lambda^{\not{B}R}_{pr})^*(\lambda^{1\mathrm{R}}_{st})}{M_1^2}\\
&-\Big[4(1+L_1)g'^2(2Y_u^2-2Y_eY_d-Y_eY_{S_1})\\
&+2g'^2Y_u(Y_d+3Y_u)-2g'^2Y_e(3Y_d-Y_u)\Big]\frac{(\lambda^{\not{B}R}_{pr})^*(\lambda^{1\mathrm{R}}_{st})}{4M_1^2}\\
&-2g'^2\frac{(\lambda^{\not{B}R}_{ps})^*(\lambda^{1\mathrm{R}}_{rt})}{M_1^2}\left(\frac{3}{2}+L_1\right)\left[Y_d(Y_e-Y_u)-Y_u(Y_e+Y_u)\right]\\
&-g_s^2\frac{1}{2}\left(\frac{7}{3}+L_1\right)\frac{(\lambda^{\not{B}R}_{pr})^*(\lambda^{1\mathrm{R}}_{st})}{M_1^2}. \qquad (2.247)
\end{aligned}
$$

In total, 109 out of 139 operators are generated in the Green basis which translates into 53 out of 59 operators in the Warsaw basis. The only operators not generated by the $S_1 + \tilde{S}_2$-model in the Warsaw basis are the CP violating ones, namely $Q_{3(\tilde{G},\tilde{W}),H(\tilde{B},\tilde{W},\tilde{G}),H\tilde{W}B}$, which are of course absent in the Green basis as well.

The UOLEA parameters $\tilde{f}_{11} - \tilde{f}_{19}$ appearing in Vector-Bosons-Scalar operators are given separately in Appendix D. The hypercharges of the SM chiral fermions and the Higgs are,

$$Y_\ell = -\frac{1}{2}\,, \quad Y_e = -1\,, \quad Y_q = \frac{1}{6}\,, \quad Y_u = \frac{2}{3}\,, \quad Y_d = -\frac{1}{3}\,, \quad \text{and} \quad Y_H = \frac{1}{2}\,, \tag{2.248}$$

respectively, while $Y_{S_1} = 1/3$ and $Y_{\tilde{S}_2} = 1/6$ for leptoquarks.

### 2.3.4 Theoretical Remarks

Further remarks on our findings for the complete set of $d \leq 6$ Wilson coefficients in Green basis at one-loop are in order.

#### Evanescent Operators

Evanescent operators appear in 4-point functions involving fermions. Treating the integrals in $d$-dimensions while using Fierz identities, that hold only in $d = 4$ or encountering higher order of $\gamma$-matrices products, give rise to evanescent operators that in general vanish in $d = 4$. The scheme we will be using for this type of structures is the introduction of local counterterms $a_{ev}, \ldots, f_{ev}$. For details the reader is referred to refs. [75–78, 91].

Although, strictly-speaking, not part of the actual matching calculation, in translating the raw results of the traces after substituting the $U$ matrices, one needs to choose a definite scheme to reduce the $\gamma$-matrix structure appearing in the subsequent equations and match it to a certain basis, such as the Green basis. In the model under consideration evanescent operators make their appearance in the Supertrace of (2.40) where both left and right projection operators appear in the same trace. We keep a general parameter $a_{ev}$ not resorting to any particular scheme. The usual scheme choice for evanescent operators, however, is $a_{ev} = \ldots = f_{ev} = 1$. The relevant Dirac-structures appearing in the model at hand are (in the NDR scheme $d = 4 - \epsilon$),

$$P_L\gamma_\mu\gamma_\nu P_L \otimes P_L\gamma^\mu\gamma^\nu P_L = 4\left(1 - \frac{\epsilon}{4}\right) P_L \otimes P_L - P_L\sigma_{\mu\nu}P_L \otimes P_L\sigma^{\mu\nu}P_L\,, \tag{2.249}$$

$$P_L\gamma_\mu\gamma_\nu P_L \otimes P_L\gamma^\nu\gamma^\mu P_L = 4\left(1 - \frac{\epsilon}{4}\right) P_L \otimes P_L + P_L\sigma_{\mu\nu}P_L \otimes P_L\sigma^{\mu\nu}P_L\,, \tag{2.250}$$

$$P_L\gamma^\mu\gamma^\nu P_L \otimes P_R\gamma^\mu\gamma^\nu P_R = 4\left(1 + a_{ev}\frac{\epsilon}{2}\right) P_L \otimes P_R + E^{(2)}_{LR}\,, \tag{2.251}$$

$$P_L\gamma^\mu\gamma^\nu P_L \otimes P_R\gamma^\nu\gamma^\mu P_R = 4\left[1 - \frac{\epsilon}{2}(1 + a_{ev})\right] P_L \otimes P_R + E^{(2)}_{LR}\,. \tag{2.252}$$

Plugging in a specific value for the coefficient $a_{ev}$, in our case, defines the evanescent operators $E^{(2)}_{LR}$.

#### RGE checks

As a further cross check of our results for Wilson coefficients we have calculated the Renormalization Group Equations (RGEs) for a certain set. For purely one-loop generated operators one has to just take the derivative with respect to the renormalization scale $\mu$ and extract the relevant $\beta$-function. For instance explicitly taking the derivative with respect to $\mu$ on $[C_{eW}]_{pr}$ we find,

$$\frac{d[C_{eW}]_{pr}}{d\ln\mu} = -N_c\, \frac{g}{4}\, \frac{(Y_{1U}^{1L})_{pr}}{M_1^2}\,. \tag{2.253}$$

Comparing with the $\beta$-functions from [18–20, 92],

$$[\beta_{eW}]_{pr} = 6\, g\, (y_U)^*_{st}\, \left[C^{(3)}_{\ell equ}\right]_{prst}\,, \tag{2.254}$$

after plugging in the value of the relevant Wc [eq. (2.93)], we get,

$$[\beta_{eW}]_{pr} = -\frac{3g}{4}\, \frac{(Y_{1U}^{1L})_{pr}}{M_1^2}\,, \tag{2.255}$$

which is in complete agreement, for $N_c = 3$, with the direct application of the derivative. The same procedure has been followed for every other purely one-loop generated Wcs and we have found no discrepancies in the comparison.

For operators generated at tree-level as well the picture is a bit different because at tree-level the coupling of the respective Wcs must be considered as running parameters due to shifts of the corresponding fields. However these exact shifts will cancel with the RG running due to wavefunction renormalization. For example, to bring back the lepton and quark doublet kinetic term we must make the following shift,

$$\ell_p \longrightarrow \ell_p - \frac{1}{2}\,(\delta Z_\ell)_{pp_1}\,\ell_{p_1}\,, \tag{2.256}$$

$$q_p \longrightarrow q_p - \frac{1}{2}\,(\delta Z_q)_{pp_1}\,q_{p_1}\,, \tag{2.257}$$

where $\delta Z_{(\ell,q)}$ correspond to eqs. (2.122) and (2.124), respectively. We have also suppressed all other indices apart from generation indices. In turn this produces a shift in the coupling $\lambda^{1\text{L}}_{pr}$. To absorb this shift we redefine the coupling as,

$$(\lambda^{1\text{L}}_{pr})^{\text{eff.}} = \lambda^{1\text{L}}_{pr} - \frac{1}{2}\lambda^{1\text{L}}_{pw}\,(\delta Z_\ell)_{wr} - \frac{1}{2}\lambda^{1\text{L}}_{wr}\,(\delta Z_q)_{wp}\,. \tag{2.258}$$

Taking the derivative w.r.t $\mu$-parameter we find the $\beta$-function for the effective running coupling,

$$\begin{aligned}[\beta_{\lambda^{1\text{L}}}]_{pr} = {}& \frac{N_c}{2}\,\left[\lambda^{1\text{L}}(\lambda^{1\text{L}})^\dagger\lambda^{1\text{L}} + \lambda^{1\text{L}}(\tilde{\lambda})^\dagger\tilde{\lambda}\right]_{pr} \\ &+\frac{1}{2}\,\left[(\lambda^{1\text{L}})^T(\lambda^{1\text{L}})^*(\lambda^{1\text{L}})^T - 8(\lambda^{1\text{L}})^T\lambda^{\not{B}L}(\lambda^{\not{B}L})^\dagger\right]_{pr}\,. \end{aligned} \tag{2.259}$$

The same of course can be done for the complex conjugate coupling,

$$[\beta_{(\lambda^{1\text{L}})^\dagger}]_{pr} = [\beta_{\lambda^{1\text{L}}}]^\dagger_{pr}\,. \tag{2.260}$$

These two will contribute, for instance, in the RG evolution of the operator $C^{(1)}_{\ell q}$. Ignoring finite parts, and for the clarity of the cancellation considering only the part produced by the shifts in the fermion fields, we find

$$[C^{(1)}_{\ell q}]_{prst} \propto [C^{(1)}_{\ell q}]^{(0)}_{prst} - \frac{1}{2}\left\{(\delta Z_\ell)_{pw}\,[C^{(1)}_{\ell q}]^{(0)}_{wrst} + (\delta Z_\ell)_{rw}\,[C^{(1)}_{\ell q}]^{(0)}_{pwst}\right.$$

$$+(\delta Z_q)_{sw}\,[C_{\ell q}^{(1)}]_{prwt}^{(0)} + (\delta Z_q)_{tw}\,[C_{\ell q}^{(1)}]_{prsw}^{(0)}\Big\}$$
$$+\left[c_1\,L_1 + \frac{\tilde{M}_2^2}{2M_1^2}\,L_2\,(3c_{1\tilde{2}}^{(1)} + c_{1\tilde{2}}^{(2)}) + 8|A'|^2\,\frac{1}{M_1^2}\,L_2\right]\frac{(\lambda_{ps}^{1\mathrm{L}})^\dagger(\lambda_{tr}^{1\mathrm{L}})}{M_1^2}\,. \tag{2.261}$$

Schematically for the operator above we have,

$$\frac{d[C_{\ell q}^{(1)}]_{prst}}{d\ln\mu} \propto \frac{d[C_{\ell q}^{(1)}]_{prst}^{(0)}}{d\ln\mu} - \frac{1}{2}\frac{d}{d\ln\mu}\Big\{(\delta Z_\ell)_{pw}\,[C_{\ell q}^{(1)}]_{wrst}^{(0)} + (\delta Z_\ell)_{rw}\,[C_{\ell q}^{(1)}]_{pwst}^{(0)}$$
$$+(\delta Z_q)_{sw}\,[C_{\ell q}^{(1)}]_{prwt}^{(0)} + (\delta Z_q)_{tw}\,[C_{\ell q}^{(1)}]_{prsw}^{(0)}\Big\}$$
$$+\left[2c_1 + \frac{\tilde{M}_2^2}{M_1^2}\,(3c_{1\tilde{2}}^{(1)} + c_{1\tilde{2}}^{(2)}) + 16|A'|^2\,\frac{1}{M_1^2}\right]\frac{(\lambda_{ps}^{1\mathrm{L}})^\dagger(\lambda_{tr}^{1\mathrm{L}})}{M_1^2}\,. \tag{2.262}$$

On the other hand the derivative of the tree-level operator reads,

$$\frac{d[C_{\ell q}^{(1)}]_{prst}^{(0)}}{d\ln\mu} = \frac{(\lambda_{ps}^{1\mathrm{L}})^\dagger}{4M_1^2}\,(\beta_{\lambda^{1\mathrm{L}}})_{tr} + \frac{(\lambda^{1\mathrm{L}})_{tr}}{4M_1^2}\,(\beta_{(\lambda^{1\mathrm{L}})^\dagger})_{ps} - \frac{(\lambda_{ps}^{1\mathrm{L}})^\dagger(\lambda^{1\mathrm{L}})_{tr}}{4M_1^2}\,\gamma_{M_1^2}\,, \tag{2.263}$$

where $\gamma_{M_1^2} = d\ln M_1^2/d\ln\mu$ is the anomalous dimension of the leptoquark mass. The last term in (2.263) will cancel with the last line of (2.262). In contrast to the coupling, this cancellation is not captured by the matching procedure, where we have assumed no heavy-external-field legs.

The remaining terms inside the curly brackets in (2.262), due to the redefintion of the fermion fields, exactly cancel the contributions to the $\beta$-function from the tree-level result (2.263). Cancellations aside, by taking the explicit derivative of the whole set of Wcs we can cross-check the logarithmic part of our results. Comparing the $\beta$-functions produced by our model, with the relevant parts of [18–20, 92], we find complete agreement.

### 2.3.5 Phenomenological Aspects

In this section we present some interesting phenomenological aspects arising from the $S_1 + \tilde{S}_2$ LQ-model whose one-loop effective Lagrangian derived previously in this section.

#### Lepton magnetic and electric dipole moments

There is some evidence for a deviation of the muon anomalous magnetic moment. FNAL experiment [93] confirmed previous results by BNL experiment [94] and found a $4.2\sigma$ excess w.r.t the SM, $\Delta a_\mu = a_\mu^{\exp} - a_\mu^{\mathrm{SM}} = (251 \pm 59) \times 10^{-11}$ [93]. As a demonstration of our one-loop effective Lagrangian we work out the contribution to $\Delta a_\mu$ from the decoupling of $S_1 + \tilde{S}_2$-leptoquarks, and compare it with the fixed order one-loop calculation.

Within functional approach, contributions to magnetic moments of fermions arise from eqs. (2.63) and (2.64). The corresponding functional supertrace diagram and its expression is displayed in (2.36). The above contributions along with the insertion of the tree-level operator $[\mathcal{O}_{\ell equ}^{(3)}]$, associated with $[C_{\ell equ}^{(3)}]$ given in eq. (2.93), in a one-loop diagram computed for example in ref. [95] constitute the full EFT formula in this model. The dominant new physics contributions to the anomalous magnetic moment of the $\ell$-generation lepton are thus

$$\Delta a^{\ell} \;=\; \frac{4m_{\ell}v}{\sqrt{2}}\left[\frac{1}{g'}\mathfrak{Re}[\mathcal{C}_{eB}] - \frac{1}{g}\mathfrak{Re}[\mathcal{C}_{eW}]\right]_{\ell\ell} + \frac{2N_c}{3\pi^2}\sum_{q} m_{\ell}m_q \log\left(\frac{\mu^2}{m_q^2}\right)\mathfrak{Re}\left\{[\mathcal{C}^{(3)}_{\ell equ}]_{\ell\ell qq}\right\}\,, \tag{2.264}$$

where $v$ is the vev, $m_\ell$ is the $\ell = e, \mu, \tau$ lepton mass and $m_q$ is the quark mass running in the loop with $q = t, c, u$. We note for later, that when evolving down to the top quark mass, $m_t$, the dominant part of the last term vanishes, hence we can neglect all other sub-leading terms in the sum. Therefore, we are left with the first two terms in the square bracket. The coefficients $\mathcal{C}_{eB}$ and $\mathcal{C}_{eW}$ are defined at low energies in mass basis of ref. [17]. They are related to the Warsaw gauge basis coefficients, $C_{eB}$ and $C_{eW}$, through the expressions,

$$\mathcal{C}_{eB} = U^{\dagger}_{e_L} C_{eB} U_{e_R}\,, \qquad \mathcal{C}_{eW} = U^{\dagger}_{e_L} C_{eW} U_{e_R}\,, \tag{2.265}$$

where the unitary matrices $U_{e_{L,R}}$ diagonalize the lepton mass matrices, $U^{\dagger}_{e_L} y_E U_{e_R} = \hat{y}_E = diag(y_e, y_\mu, y_\tau)$. Since our results are given in Green basis we need a translation from Green to Warsaw basis. This translation is nicely given in ref. [64]. After a little algebra, we find the coefficients at renormalization scale $\mu$ (still gauge basis in $3 \times 3$ matrix notation) to be

$$[C_{eB}]^{(1)}(\mu) \;=\; \frac{g' N_c}{16\pi^2}\left\{\frac{5}{24}\left[\log\left(\frac{\mu^2}{M_1^2}\right) + \frac{19}{10}\right]\frac{Y^{1L}_{1U}}{M_1^2} - \frac{1}{24}\frac{y_E\cdot\Lambda_e}{M_1^2} - \frac{1}{48}\frac{\tilde{\Lambda}_\ell\cdot y_E}{\tilde{M}_2^2}\right\}\,, \tag{2.266}$$

$$[C_{eW}]^{(1)}(\mu) \;=\; \frac{g N_c}{16\pi^2}\left\{-\frac{1}{8}\left[\log\left(\frac{\mu^2}{M_1^2}\right) + \frac{3}{2}\right]\frac{Y^{1L}_{1U}}{M_1^2} + \frac{1}{24}\frac{\Lambda_\ell\cdot y_E}{M_1^2} - \frac{1}{48}\frac{\tilde{\Lambda}_\ell\cdot y_E}{\tilde{M}_2^2}\right\}\,, \tag{2.267}$$

where "$\cdot$" means matrix multiplication. These results are in agreement with ref. [95]. The parameters $Y^{1L}_{1U}, \Lambda_e, \tilde{\Lambda}_\ell$ and $\Lambda_\ell$ are defined in eqs. (2.110),(2.108) and (2.107), respectively. We then use the RGE running of the coefficients $C_{eB}, C_{eW}$ from the heavy leptoquark mass scale $M_1$ down to the top-quark mass scale $m_t$ and plug the result into (2.264) to find at leading-log approximation (for $N_c = 3$):[6]

$$\begin{aligned}\Delta a_\ell^{(S_1+\tilde{S}_2)} = &\sum_{q=u,c,t}\frac{m_\ell}{4\pi^2}\frac{m_q}{M_1^2}\left[\log\left(\frac{m_t^2}{M_1^2}\right) + \frac{7}{4}\right]\mathfrak{Re}(\hat{\lambda}^{1L*}_{q\ell}\hat{\lambda}^{1R}_{q\ell}) \\ &- \frac{m_\ell^2}{32\pi^2 M_1^2}\left(\hat{\lambda}^{1L*}_{q\ell}\hat{\lambda}^{1L}_{q\ell} + \hat{\lambda}^{1R*}_{q\ell}\hat{\lambda}^{1R}_{q\ell}\right)\,,\end{aligned} \tag{2.268}$$

where all parameters and masses are to be evaluated at $m_t$ and the "hatted" couplings are defined in mass basis as,

$$\hat{\lambda}^{1L} = U^{T}_{u_L}\lambda^{1L}U_{e_L}\,, \quad \hat{\lambda}^{1R} = U^{T}_{u_R}\lambda^{1R}U_{e_R}\,, \quad \hat{\tilde{\lambda}} = U^{\dagger}_{d_R}\tilde{\lambda}\,U_{eL}\,, \tag{2.269}$$

with $U^{\dagger}_{u_L} y_U U_{u_R} = \hat{y}_U = \mathrm{diag}(y_u, y_s, y_t)$ being the up-quark fermion Yukawa couplings. Note that, as it should, the one-loop expression (2.268) agrees with the fixed order calculation of ref. [69] for the $S_1$-leptoquark decoupling. Also obvious from (2.268) is a natural enhancement of $O(m_t/m_\ell)$ due to $S_1$-decoupling, while there is no effect from the $\tilde{S}_2$-particle decoupling. However, a similar enhancement is shown in eq. (2.128), for the one-loop corrections to the Yukawa coupling of the leptons, and subsequently to the lepton mass itself.

[6] To leading-log order the result is the same by setting $\mu = m_t$ in (2.266) and (2.267) and then take the difference in (2.264), and neglecting the contribution from light quark masses.

Moreover, a bound on electron Electric Dipole Moment (eEDM), $|d_e| < 1.1 \times 10^{-29}\mathrm{e}\cdot\mathrm{cm}$ at 90% CL, anounced by ACME collaboration [96] in year 2018. Our complete 1-loop functional matching LQs renders the calculation of eEDM very easy. As mentioned previously, in the model at hand ($S_1 + \tilde{S}_2$), bosonic operators of the form $H^2 F\tilde{F}$ and $F^3$ are not induced, therefore the only effect at one-loop arises from the Warsaw-basis operators $Q_{eB}$, $Q_{eW}$ and $Q^{(3)}_{\ell equ}$ as before. Basically, the calculation is the same with the lepton magnetic moments we performed above. Again, neglecting the contribution from $C^{(3)}_{\ell equ}$ since the evaluation is at $\mu = m_t$, the eEDM reads,

$$\frac{d_e}{e}(m_t) \;=\; \sqrt{2}\,v \left[\frac{1}{g'}\mathfrak{Im}[\mathcal{C}_{eB}(m_t)] \;-\; \frac{1}{g}\mathfrak{Im}[\mathcal{C}_{eW}(m_t)]\right]_{11} . \tag{2.270}$$

Plugging into (2.270) the imaginary parts of eqs. (2.266) and (2.267) after substituting $\mu = m_t$, we find

$$\frac{d_e}{e} \;=\; \frac{1}{8\pi^2}\frac{m_t}{M_1^2}\left[\log\left(\frac{m_t^2}{M_1^2}\right) + \frac{7}{4}\right]\mathfrak{Im}(\hat{\lambda}^{1L\,*}_{31}\hat{\lambda}^{1R}_{31}) . \tag{2.271}$$

This result agrees with the fixed order 1-loop calculation, up to $\mathcal{O}(m_t^2/M_1^4)$-terms, obtained by applying the general one-loop formula for lepton EDMs from ref. [97] onto the particular $S_1 + \tilde{S}_2$ LQ-model. The leading-log term of (2.271) also agrees with the one obtained in refs. [68, 98].

The reader should note that this is a SMEFT calculation, i.e. we have chosen $\mu = m_t$. Ideally it's more appropriate to match onto Low Energy Effective Field Theory (LEFT) and perform the calculation of dipole moments at lower scales, which is beyond the scope of this chapter. For a thorough EFT analysis of leptonic magnetic and electric dipole moments along these lines the reader is referred to refs. [95, 99].

### Radiative Neutrino masses

A nice feature of the $S_1 + \tilde{S}_2$ model is that neutrino masses are induced radiatively at one-loop. The single dimension-5 operator $Q_{\nu\nu}$, defined in Appendix C, arises in the effective Lagrangian from the supertrace functional diagram (2.39) which after calculation provides us the associated Wilson coefficient $G_{\nu\nu} = C_{\nu\nu}$ (2.133) in both Green and Warsaw basis. The result is finite and agrees with ref. [71]. Then going to the mass basis SMEFT Lagrangian of ref. [17] we have for the diagonal neutrino mass matrix

$$m_\nu \;=\; -v^2\, U^T_{\nu_L}\, C_{\nu\nu}\, U_{\nu_L} . \tag{2.272}$$

By using the tree level definitions of CKM and MNS matrices[7], as $K_{\mathrm{CKM}} = U^\dagger_{u_L} U_{d_L}$ and $U_{\mathrm{MNS}} = U^\dagger_{e_L} U_{\nu_L}$ and eq. (2.269) we obtain

$$m_\nu \;=\; -\frac{\sqrt{2}}{16\pi^2}\frac{vA_{\tilde{2}1}}{M_1^2 - \tilde{M}_2^2}\left[U^T_{\mathrm{MNS}}\,(\hat{\lambda}^{1L})^T\, K_{\mathrm{CKM}}\, m_d\, \hat{\tilde{\lambda}}\, U_{\mathrm{MNS}}\right]\log\left(\frac{M_1^2}{\tilde{M}_2^2}\right) , \tag{2.273}$$

where $m_d$ is the diagonal down quark mass matrix. The neutrino masses clearly follow a "down-quark" mass hierarchy with the couplings $\hat{\lambda}^{1L}$, $\hat{\tilde{\lambda}}$ and the CKM matrix defining off-diagonal transitions. Obviously, depending on the value of the parameter $A_{\tilde{2}1}$ that mixes both leptoquarks with the Higgs boson, we can probe two different mass scales: (i) $A_{\tilde{2}1}/max(M_1, M_2) \simeq 1$, and (ii) $A_{\tilde{2}1}/max(M_1, M_2) \to 0$. In case (i) correct order of magnitude of neutrino mass,

[7] There is no "pollution" to CKM or MNS matrices from other tree level operators in this model.

$m_\nu \lesssim 0.1$ eV, and $\lambda \sim O(1)$ requires $M_1 \approx M_2 \gtrsim 10^{13}$ GeV and this is currently consistent with proton decay bounds (see below), whereas in case (ii) $M_1 \approx M_2 \simeq 1$ TeV requires $A_{\tilde{2}1} \approx 10^{-7}$ GeV which is technically natural in terms of a $\mathbb{Z}_3$ (or $\mathbb{Z}_4$) softly broken discrete symmetry discussed in section 2.3 (but still baryon number violating couplings, $\lambda^{\not{B}L}$ and $\lambda^{\not{B}R}$, are allowed and have to be set to zero by another symmetry in order to avoid fast proton decay).

### Proton decay

Baryon number is violated in the $S_1 + \tilde{S}_2$ model. *All* $d = 6$ baryon number violating (BNV) operators appear already at tree level in the effective Lagrangian [eqs. (2.98),(2.99)], after the decoupling of $S_1$-field. From these expressions and Table 2.3 we easily see they have $\Delta B = \Delta L = 1$ consistent with eqs. (2.103) and (2.104). Rotating fermion fields into the mass basis of ref. [17] we find for the tree-level Wilson-coefficients

$$
\begin{aligned}
[C^{qqu}]^{(0)}_{f_1 f_2 f_3 f_4} &= \frac{1}{M_1^2}\,[K^T_{\rm CKM}\,(\lambda^{\hat{\not{B}}L})^*]_{f_1 f_2}\,(\hat{\lambda}^{1R})_{f_3 f_4}\,, &(2.274)\\
\big[C^{duq}\big]^{(0)}_{f_1 f_2 f_3 f_4} &= \frac{1}{M_1^2}\,(\lambda^{\hat{\not{B}}R})^*_{f_1 f_2}\,[K^T_{\rm CKM}\,\hat{\lambda}^{1L}]_{f_3 f_4}\,, &(2.275)\\
\big[C^{duu}\big]^{(0)}_{f_1 f_2 f_3 f_4} &= \frac{1}{M_1^2}\,(\lambda^{\hat{\not{B}}R})^*_{f_1 f_2}\,(\hat{\lambda}^{1R})_{f_3 f_4}\,, &(2.276)\\
[C^{qqq}]^{(0)}_{f_1 f_2 f_3 f_4} &= -\frac{2}{M_1^2}\,[K^T_{\rm CKM}\,(\lambda^{\hat{\not{B}}L})^*]_{f_1 f_2}\,[K^T_{\rm CKM}\hat{\lambda}^{1L}]_{f_3 f_4}\,, &(2.277)
\end{aligned}
$$

where the “hatted" couplings are given in eq. (2.269) in addition to

$$
\lambda^{\hat{\not{B}}L} = U^\dagger_{u_L}\,\lambda^{\not{B}L}\,U^*_{d_L}\,, \qquad \lambda^{\hat{\not{B}}R} = U^\dagger_{d_R}\,\lambda^{\not{B}R}\,U^*_{u_R}\,. \tag{2.278}
$$

Obviously, due to lepton and baryon quantum numbers arranged in Table 2.3, only one BNV-coupling, $\lambda^{\not{B}L}$ or $\lambda^{\not{B}R}$, appear for $\Delta L = \Delta B = 1$. Plugging these into the Feynman Rules of ref. [17] we derive decay rates for general nucleon decay processes.

To date, proton decay has not been observed and Super Kamiokande has increased the proton lifetime limits up to $\sim 10^{34}$ years with bounds [100, 101]

$$
\tau(p \to e^+ \pi^0) > 1.6 \times 10^{34}\ \text{yrs}\,, \qquad \tau(p \to \bar{\nu} K^+) > 0.59 \times 10^{34}\ \text{yrs}\,, \tag{2.279}
$$

being the most sensitive ones to BSM physics [102]. Based on the first of these bounds we derive constraints on the following products of couplings:

$$
2(\lambda^{\hat{\not{B}}R})^*_{11}\hat{\lambda}^{1R}_{11}\,,\quad 2(\lambda^{\hat{\not{B}}R})^*_{11}\hat{\lambda}^{1L}_{11}\,,\quad 2(\lambda^{\hat{\not{B}}L})^*_{11}\hat{\lambda}^{1R}_{11}\,,\quad 4(\lambda^{\hat{\not{B}}L})^*_{11}\hat{\lambda}^{1L}_{11} \lesssim 10^{-6}\left(\frac{M_1}{3\times 10^{12}}\right)^2 . \tag{2.280}
$$

Note that although the CKM-matrix, $K_{\rm CKM}$, appears explicitly in tree expressions (2.274)-(2.277), it disappears completely from the relevant BNV vertices of ref. [17] for physical fields. In summary, $M_1 \gtrsim 3 \times 10^{12}$ GeV and first generation $\hat{\lambda}^{1L,1R} \sim O(1)$ and $\lambda^{\not{B}L}$ and $\lambda^{\not{B}R}$ of the order of electron yukawa coupling is, currently, a safe combination.

At tree level, the proton decay constraints in eq. (2.280) apply on the 11 entries of $\lambda$-matrices. This changes by going to higher orders where in principle all flavour structure of those matrices are getting involved through the CKM-matrix. One loop contributions to BNV

Wilson coefficients are given in eqs. (2.244)-(2.247). For example, by just looking at $[G_{qqq}]^{(1)}$ and the term proportional to the strong QCD coupling, $g_s^2(\lambda_{ps}^{\not{B}L})^*(\lambda_{st}^{1L})$ we find a contribution to the $p \to e^+\pi^0$ amplitude of the form $g_s^2(\hat{\lambda}^{\not{B}L}K^\dagger_{\text{CKM}})_{11}(K^T_{CKM}\hat{\lambda}^{1L})_{11}$ which, although CKM-suppressed, displays a certain sensitivity in the off-diagonal $\lambda_{1i}$ entries under the strong proton decay bounds of (2.279). A partial list of dedicated studies on proton decay in leptoquark-like models are given in refs. [81, 103–105] and related reviews in refs. [82, 102].

In summary, unless there is a symmetry to prohibit BNV-couplings, the mass $M_1$ must be bigger than the "intermediate" scale $\sim 10^{12}$ GeV. As we discuss in the next paragraph, this will bring every other leptoquark masses e.g. $\tilde{M}_2$, at around that scale unless unnatural fine tuning is called upon in the Higgs sector.

**Perturbativity and Fine Tuning**

An interesting interplay between the LQ masses can be explored in some operators that contain the ratio of the two masses. We can thus put some bounds on the ratio $M_1/\tilde{M}_2$ so that perturbation theory is not violated. For example, for the operator $G_{\ell d}$ adding the tree, eq.(2.94), and one-loop level, eq.(2.240) that depends on the LQ mass ratio, we have,

$$[G_{\ell d}]_{prst} \propto -\frac{\tilde{\lambda}^*_{tp}\tilde{\lambda}_{sr}}{2\tilde{M}_2^2}\left(1+\frac{1}{16\pi^2}\frac{M_1^2}{\tilde{M}_2^2}(N_c c^{(1)}_{1\tilde{2}} + c^{(2)}_{1\tilde{2}})(1+L_1)\right). \tag{2.281}$$

Other operators depend on the inverse mass ratio $\tilde{M}_2/M_1$. For instance, adding eq.(2.95) and eq.(2.219), we have,

$$\left[G^{(1)}_{\ell q}\right]_{prst} \propto \frac{(\lambda^{1L})^*_{sp}(\lambda^{1L}_{tr})}{4M_1^2}\left(1+\frac{2}{16\pi^2}\frac{\tilde{M}_2^2}{M_1^2}(N_c\, c^{(1)}_{1\tilde{2}} + c^{(2)}_{1\tilde{2}})(1+L_2)\right). \tag{2.282}$$

For perturbation theory to work, loop level contributions have to be way smaller than tree level ones. Then we can get a combined constrain for the ratio of the masses,

$$2\frac{N_c c^{(1)}_{1\tilde{2}} + c^{(2)}_{1\tilde{2}}}{16\pi^2}(1+L_2) < \frac{M_1^2}{\tilde{M}_2^2} < \frac{16\pi^2}{(1+L_1)(N_c\, c^{(1)}_{1\tilde{2}} + c^{(2)}_{1\tilde{2}})}, \tag{2.283}$$

which depends explicitly on parameters of the self interactions of the leptoquarks. Next, we define the following quantities,

$$r^2 \equiv \frac{M_1^2}{\tilde{M}_2^2}, \qquad \alpha \equiv \frac{N_c\, c^{(1)}_{1\tilde{2}} + c^{(2)}_{1\tilde{2}}}{16\pi^2}. \tag{2.284}$$

The inequality then becomes,

$$2\alpha(1+L_2) < r^2 < \frac{1}{\alpha(1+L_1)}. \tag{2.285}$$

Which can be written in the following form,

$$\frac{\mu^2}{\tilde{M}_2^2}\exp\left(1-\frac{1}{\alpha r^2}\right) < r^2 < \frac{M_1^2}{\mu^2}\exp\left(\frac{r^2}{2\alpha}-1\right). \tag{2.286}$$

From here on we will pick up a renormalization scale, first we will pick $\mu = M_1$ and then $\mu = \tilde{M}_2$. As for the parameters $c^{(1,2)}_{1\tilde{2}}$ we will take them first of order unity and second to a fine tuned value of the order of $10^{-4}$. Plugging these numbers into eq.(2.284) we get $\alpha = 1/4\pi^2$ and $\alpha = 10^{-4}/4\pi^2$ for each respective value of c's. Both these values will be used for both cases of the renormalization scale and extract some bounds for the masses.

- For the first case, $\mu = M_1$. In this case the combined inequality reads, for $N_c = 3$,

$$r^2 \exp\left(1 - \frac{1}{\alpha r^2}\right) < r^2 < \exp\left(\frac{r^2}{2\alpha} - 1\right) . \tag{2.287}$$

The right inequality is always satisfied, while from the left one we can get that,

$$r^2 < \frac{1}{\alpha} . \tag{2.288}$$

Considering the two distinct values of $\alpha$, we can get $M_1 < (2\pi,\, 2\pi \times 10^2)\, \tilde{M}_2$.

- For the second case $\mu = \tilde{M}_2$. The inequality becomes,

$$\exp\left(1 - \frac{1}{\alpha r^2}\right) < r^2 < r^2 \exp\left(\frac{r^2}{2\alpha} - 1\right) . \tag{2.289}$$

The right part gives, $r^2 > 2\alpha$, while the left part is always true.

If we combine the two results we can get the following bound,

$$2\alpha < r^2 < \frac{1}{\alpha} . \tag{2.290}$$

Plugging the values of $\alpha$ we get,

$$\frac{1}{\sqrt{2\pi}}\,(1,\, 10^{-2}) < \frac{M_1}{\tilde{M}_2} < 2\pi\,(1,\, 10^2) . \tag{2.291}$$

Therefore, we can conclude that when couplings $c^{(1,2)}_{1\tilde{2}}$ are of $\mathcal{O}(1)$ the masses can be taken to be of similar magnitude without violating perturbation theory. If we fine tune the couplings to even smaller values we can further increase the mass ratio giving us more room to tune the numerical values of the masses.

Noteworthy, the situation we just described for the Wcs, $G^{(1)}_{\ell d}$ and $G^{(1)}_{\ell q}$, share the same characteristics with the Higgs mass hierarchy problem which is of course evident in LQ-models. Indeed, by performing the matching procedure we have assumed that the Higgs mass $m$ is zero i.e., the Higgs field is part of the low energy EFT. Therefore, one-loop contributions to the Higgs mass found in (2.132) have to be of the order of the EW scale. For this to happen there are two cases *(i)* LQ-masses are of the order of the TeV-scale and Higgs couplings naturally of order $\mathcal{O}(1)$ or *(ii)* LQ-masses are heavier but Higgs couplings e.g. $\lambda_{H1}, \tilde{\lambda}_{H2}, \lambda_{\tilde{2}\tilde{2}}$ together with $A_{\tilde{2}1}/M_1$ are small enough, although there is no known symmetry to naturally accommodate all these limits.

## 2.4 Conclusions

The resurgence of functional techniques to matching has led to a fair amount of universal results and compact formulae over the last few years. In this chapter we explored the matching of all scalar leptoquark representations that can be constructed under the SM gauge group. We have extracted through the use of *Supertrace functional techniques* [35] a universal formula, eq. (2.14) for tree level and eq. (2.48) for one-loop matching plus all **X**-matrices in Appendix A, for the decoupling of all scalar leptoquarks and put it to use in two distinct models. First we cross-tested it with the Feynman diagrammatic approach of the $S_1 + S_3$ model [64]. Then we applied it to the, phenomenologically richer, $S_1 + \tilde{S}_2$ model taking also baryon number violating couplings into account. In total, the latter model generates the single dimension-5 Weinberg operator at one loop, which gives rise to radiative neutrino masses. At dimension-6, 109 operators are generated in the Green basis while in the translation to Warsaw basis we are left with 53 (out of 59) operators thus covering almost the entire spectrum of dimension-6 operators, the only exception being the set of 6 bosonic CP-violating ones. Our results of the given Wilson coefficients, derived in section 2.3, have been also cross checked with the one loop RGEs finding complete agreement.

On the phenomenological side, we have briefly explored several distinct observables. First, we studied the implications to the lepton magnetic and electric dipole moments where there has been recent experimental advances. With this example we demonstrated the use of the matching in arriving at known results from fixed order calculations. Secondly, we have investigated possible regions of leptoquark masses, at the scale of a few TeV and at a high scale, as well as their coupling with the Higgs field, to generate radiatively the order of magnitude of neutrino masses through the Weinberg operator. Furthermore, we were able to put certain bounds in the combinations of BNV and non-BNV couplings, through the investigation of proton decay at tree level and one-loop. Last but not least, we have constructed a combined inequality for the ratio of the two LQ masses so that perturbation theory is not violated and briefly discussed the hierarchy problem in LQ-models.

As a concluding remark we would like to point out that models covering almost the entirety of the given operator basis spectrum, can serve as excellent *benchmarks* for various codes that will perform the matching automatically. The main reason for this argument is that within matching one needs to apply a fair amount of identities ranging from group theoretic, to Fierz identities and also accounting for evanescent operators arising from higher number of $\gamma$-matrix structures. All of the above have been encountered in the models that have been investigated in this chapter, ultimately, adding up to the number of fully worked out examples of one loop matching.

# Chapter 3

# Disentagling SMEFT and UV contributions in $h \to Z\gamma$ and $h \to \gamma\gamma$ decays

LHC searches have revealed that the Higgs boson decay to a photon pair is nearly consistent with the Standard Model (SM), whereas recently, there is evidence for the decay of the Higgs boson to a $Z$-boson and a photon. These observables are governed by the same set of Wilson-coefficients at the tree level in Standard Model Effective Field Theory (SMEFT). In this study, we attempt to explain a potential discrepancy between the decays $h \to \gamma\gamma$ and $h \to Z\gamma$. We conduct a model-independent analysis in SMEFT to determine the magnitude and features of the Wilson coefficients needed to explain a distinction between the two signal strengths. These assumptions are then considered at a top-down approach where we consider all single and two field extensions of the SM, including scalars and fermions, as candidates for novel interactions. We perform the matching of these models to one loop using automated packages and compare the models' predictions about $h \to Z\gamma$. This chapter is based on ref [106].

## 3.1 Introduction

Building upon the foundations established in the previous chapters, we now turn our attention to exploring how new physics can manifest in the properties and decays of the Higgs boson. In Chapter 1, more specifically in Sections 1.4 through 1.6, we introduced the concept of Effective Field Theories (EFTs) and discussed both the top-down and bottom-up approaches to constructing them. The top-down approach involves starting from a well-defined ultraviolet (UV) model and systematically integrating out heavy degrees of freedom to derive an EFT that captures the low-energy dynamics. This process, known as matching, ensures that the low-energy EFT reproduces the same S-matrix elements as the full theory. We highlighted how matching can be performed either diagrammatically, using Feynman diagrams, or through functional matching, which directly utilizes the path integral formalism.

In Chapter 2, we delved deeper into functional matching techniques, emphasizing their advantages over diagrammatic methods. Functional matching provides a process-independent way to derive the complete set of effective operators and their Wilson coefficients (WCs) without the need to consider specific processes. We applied these techniques to the decoupling of heavy scalar leptoquark fields, demonstrating how functional methods can efficiently handle complex interactions and generate universal results. This set the stage for understanding how new heavy particles can influence low-energy observables through their contributions to the WCs in the Standard Model Effective Field Theory (SMEFT).

With this theoretical groundwork in place, Chapter 3 aims to investigate the impact of new physics on the Higgs boson's properties and decay channels, specifically focusing on the recent observations in the $h \to Z\gamma$ decay mode.

Since the discovery of the Higgs particle by the LHC [107, 108] and the absence of any new smoking gun event our attention is increasingly turning to studying in detail the properties and the couplings of the Higgs particle. Its decay and production can be affected by particles that have not yet been discovered or hinted at, and are thus elusive. If these new particles are heavy the Standard Model Effective Field Theory (SMEFT) (for reviews we refer the reader to Refs. [21, 52, 109]) provides a framework to study the effects of particles that are found above the electroweak (EW) scale, namely $v \sim$ 245 GeV. The constituents of this framework are higher dimensional operators that respect the SM gauge group, thus we add to the SM Lagrangian the sum of terms with mass dimension greater than 4,

$$\mathcal{L} = \mathcal{L}_{\rm SM} + \frac{C^5 \mathcal{O}^5}{\Lambda} + \frac{C^6 \mathcal{O}^6}{\Lambda^2} + \dots , \tag{3.1}$$

where as a superscript the mass dimension of each respective operator is denoted and $\Lambda$ serves as the scale of new (UV) physics. Each operator is accompanied by its respective coefficient known as Wilson coefficient (Wc) which encodes the effects of UV physics.

Deviations from the SM values of decay and production channels are encoded in the so called signal strength. These are calculated as the ratio,

$$\mu_{h\to X} = \frac{\Gamma(\text{SMEFT}, h \to X)}{\Gamma(\text{SM}, h \to X)} = 1 + \frac{\Gamma(\text{BSM}, h \to X)}{\Gamma(\text{SM}, h \to X)} , \tag{3.2}$$

where with $\Gamma$(BSM) we denote the decay rate that is affected only by physics beyond the SM (BSM). The signal strengths are split in the following manner $\mu_{h\to X} = 1 + \delta R_{h\to X}$, where

$\delta R_{h\to X} = \Gamma(\text{BSM}, h \to X)/\Gamma(\text{SM}, h \to X)$. Hence new physics that contributes to each respective channel would shift $\mu_{h\to X}$ to values different than one. The decays of the Higgs into two gauge bosons have been measured with high precision and in agreement with the SM are $WW^*, ZZ^*, \gamma\gamma$ [110–116]. A detailed analysis of the properties, the decay and production as well as future directions for Higgs physics can be found in [117, 118]. Although most of the aforementioned decays are in agreement with the SM a recent analysis by the ATLAS and the CMS collaboration [119] found evidence for the decay of $h \to Z\gamma$, which was an elusive decay up to now. Additionally, they reported a mild excess of around $\sim 2\sigma$ with respect to the SM value, the measured signal strength is,

$$\mu_{h\to Z\gamma} = 2.2 \pm 0.7\,. \tag{3.3}$$

Subtracting the SM value of the signal strength $\mu^{\text{SM}}_{h\to Z\gamma} = 1$, this implies that contributions from new physics must account for $\mu^{\text{BSM}}_{h\to Z\gamma} = 1.2 \pm 0.7$, under the assumption that all uncertainties originate from the UV sector. This study aims to answer this question, which UV model could account for such an excess in the $h \to Z\gamma$ decay?

To address this question, we explore both the top-down and bottom-up approaches within the SMEFT framework, building upon the methodologies discussed in Chapter 1, more specifically in Sections 1.4 to 1.6 and on Chapter 2, Section 2.2. The values of the WCs that affect the Higgs boson's properties can be calculated through the matching process in the top-down approach. In this procedure, WCs are derived from a complete UV model, and their analytic expressions depend on the couplings and scales of the model. This matching can be performed either diagrammatically or directly through the path integral, as detailed in Chapter 2. Functional matching, in particular, has gained renewed interest due to new techniques [26, 35] and the emergence of universal results [24, 27–31, 33, 53, 120], even at two-loop order [34]. The automation of these techniques has evolved to encompass a broad spectrum of methods, from SuperTrace calculations [38, 39] to the efficient computation of WCs directly from the Lagrangian [37, 40, 41, 44, 121].

Alternatively, the bottom-up approach offers a model-agnostic method where the WCs remain unknown and their values are determined by fitting a set of observables to these coefficients. Throughout this chapter, we will use the Warsaw basis [13] to study the effects of UV-independent WCs on the relevant decays of the Higgs boson. We will consider operators up to dimension-6, as the only dimension-5 operator in the Warsaw basis (found in Table C.1) relates to neutrino masses and is irrelevant to the observables considered here. This approach allows us to gauge the magnitude of new physics that may affect each WC individually and may provide hints about the structure of the UV model.

However, a downside of the bottom-up approach is the unknown correlations between WCs that may arise from specific UV models. As discussed in Chapters 1, sections 1.4-1.6 and Chapter 2, the bottom-up and top-down approaches should be seen as complementary. While the bottom-up approach can highlight which WCs are most relevant for explaining the observed excess in $h \to Z\gamma$, the top-down approach can provide the correlations and constraints among WCs imposed by the UV theory, since the number of couplings in the UV model is typically fewer than the number of independent WCs in the Warsaw basis. Moreover, the SMEFT predicts that the $h \to \gamma\gamma$ decay receives contributions from almost the same set of operators as $h \to Z\gamma$, with similar governing expressions, as explored in Section 3.2. Therefore, it is crucial to investigate these two decays under the same scope and attempt to disentangle the contributions that could lead to an excess in $h \to Z\gamma$ without conflicting with the precise measurements of $h \to \gamma\gamma$.

Several recent studies have addressed this question by varying the field content or extending the gauge group of the SM [122–125]. Other works have explored enhancements of $h \to Z\gamma$ through renormalization group effects of tree-level generated dimension-8 operators, including massive vector-boson fields [126], which are not considered in this chapter. Contributions from the Minimal Supersymmetric Standard Model (MSSM) to $h \to Z\gamma$ can be found in Ref. [127], and the decay $h \to Z\gamma$ has been proposed as a probe to test the compositeness of the Higgs boson within the EFT framework [128].

The structure of this chapter is as follows. In Section 3.2, we study the Higgs decays $h \to \gamma\gamma$ at one-loop order within the SMEFT, using the bottom-up approach. We make several rescalings of WCs to account for their tree-level and one-loop-level contributions. After identifying the major contributions to their signal strengths, we fit all relevant WCs to a set of observables related to the Higgs sector and compare the values of WCs needed to account for the observed data. In Section 3.3, we shift our focus to possible UV-complete models that could account for the values of WCs found in the fit. We consider all colorless single-field extensions of the SM that respect the gauge group, as tabulated in the tree-level dictionary [67]. We assess their ability to generate the necessary WCs through matching procedures. In Section 3.4, we categorize interactions based on their loop functions and devise a scheme to tabulate two-field models that generate WCs relevant to the Higgs decays. We match all models to the Warsaw basis using automated packages and perform a constrained minimization to find the best values for the couplings and masses of each respective model. We leave the signal strength of the decay $h \to Z\gamma$ as a prediction of each model and compare the results to the $h \to \gamma\gamma$ decay. Finally, in Section 3.5, we summarize our findings, discuss their implications for new physics scenarios, and suggest directions for future research.

## 3.2 Model independent analysis in SMEFT

There are two Higgs decays in SMEFT that are of interest to us currently, namely, $h \to \gamma\gamma$ and $h \to Z\gamma$. Their semi-numerical expressions, at one-loop order, of the signal strengths, in the input scheme $\{G_F, M_W, M_Z\}$, and in units of TeV$^{-2}$, are [129–131],

$$
\begin{aligned}
\delta R_{h\to Z\gamma} \simeq\, & 0.18\left(C^{\ell\ell}_{1221} - C^{\phi\ell(3)}_{11} - C^{\phi\ell(3)}_{22}\right) + 0.12\left(C^{\phi\Box} - C^{\phi D}\right) \\
& - 0.01\left(C^{d\phi}_{33} - C^{u\phi}_{33}\right) + 0.02\left(C^{\phi u}_{33} + C^{\phi q(1)}_{33} - C^{\phi q(3)}_{33}\right) \\
& + \left[14.99 - 0.35\log\frac{\mu^2}{M_W^2}\right] C^{\phi B} - \left[14.88 - 0.15\log\frac{\mu^2}{M_W^2}\right] C^{\phi W} + \left[9.44 - 0.26\log\frac{\mu^2}{M_W^2}\right] C^{\phi WB} \\
& + \left[0.10 - 0.20\log\frac{\mu^2}{M_W^2}\right] C^{W} - \left[0.11 - 0.04\log\frac{\mu^2}{M_W^2}\right] C^{uB}_{33} + \left[0.71 - 0.28\log\frac{\mu^2}{M_W^2}\right] C^{uW}_{33} \\
& - 0.01\, C^{uW}_{22} - 0.01\, C^{dW}_{33} + \dots\,,
\end{aligned}
\tag{3.4}
$$

$$
\begin{aligned}
\delta R_{h\to\gamma\gamma} \simeq\, & 0.18\left(C^{\ell\ell}_{1221} - C^{\phi\ell(3)}_{11} - C^{\phi\ell(3)}_{22}\right) + 0.12\left(C^{\phi\Box} - 2C^{\phi D}\right) \\
& - 0.01\left(C^{e\phi}_{22} + 4C^{e\phi}_{33} + 5C^{u\phi}_{22} + 2C^{d\phi}_{33} - 3C^{u\phi}_{33}\right) \\
& - \left[48.04 - 1.07\log\frac{\mu^2}{M_W^2}\right] C^{\phi B} - \left[14.29 - 0.12\log\frac{\mu^2}{M_W^2}\right] C^{\phi W} + \left[26.17 - 0.52\log\frac{\mu^2}{M_W^2}\right] C^{\phi WB}
\end{aligned}
$$

$$+\left[0.16-0.22\log\frac{\mu^2}{M_W^2}\right]C^W+\left[2.11-0.84\log\frac{\mu^2}{M_W^2}\right]C^{uB}_{33}+\left[1.13-0.45\log\frac{\mu^2}{M_W^2}\right]C^{uW}_{33}$$
$$-\left[0.03-0.01\log\frac{\mu^2}{M_W^2}\right]C^{uB}_{22}-\left[0.01-0.00\log\frac{\mu^2}{M_W^2}\right]C^{uW}_{22}+\left[0.03-0.01\log\frac{\mu^2}{M_W^2}\right]C^{dB}_{33}$$
$$-\left[0.02-0.01\log\frac{\mu^2}{M_W^2}\right]C^{dW}_{33}+\left[0.02-0.00\log\frac{\mu^2}{M_W^2}\right]C^{eB}_{33}-\left[0.01-0.00\log\frac{\mu^2}{M_W^2}\right]C^{eW}_{33}+\ldots, \tag{3.5}$$

where the dots denote terms whose contributions are lower than $0.01\times C$ and $\mu$ is the renormalization scale. We are restricting ourselves to contributions without CP-violation. These operators are heavily constrained by Electric Dipole Moments (EDMs), and would contribute with tiny corrections to the observables and the problem we are trying to tackle in this chapter.

At a first glance we can naively say that the main contributions in these two observables originate from the same three operators, $\{C^{\phi B}, C^{\phi W}, C^{\phi WB}\}$, however in the tree-level dictionary [67] these operators arise only from one-loop processes, assuming that the UV-Lagrangian contains terms only up to dimension 4, and restrict ourselves to UV models containing only scalars and/or fermions. If we consider the presence of operators with dimension greater than 4 in the UV Lagrangian, or if we incorporate vector fields into the analysis, these operators can also be generated at tree level.

One way to disentangle the tree and loop level contributions is to split the coefficients into their tree and loop level parts as follows, $C = C^{[0]} + \frac{1}{16\pi^2}C^{[1]} \simeq C^{[0]} + 0.6\times 10^{-2}C^{[1]}$. From what was discussed in the previous paragraph, we shall set $C^{[0]\phi B}$, $C^{[0]\phi W}$ and $C^{[0]\phi WB}$ to zero. This re-scales all coefficients so that we can easily compare between contributions of different operators. Apart from the tree-loop split, for the case of the three Wilson coefficients mentioned above, we can do another re-scaling, $C^{\phi B}\to g'^2\hat{C}^{\phi B}$, $C^{\phi W}\to g^2\hat{C}^{\phi W}$, $C^{\phi WB}\to g' g\hat{C}^{\phi WB}$. We immediately see that in both expressions the operators $C^{(e,u,d)(B,W)}$, $C^W$, are small since they occur at one-loop in the SMEFT. We can also observe that the combination of the three Wcs $C^{\ell\ell}_{1221}$, $C^{\phi\ell(3)}_{11,22}$ constitutes the correction of SMEFT to the Fermi constant, which is known to high accuracy. The corrections of the Fermi constant in the SMEFT read [17, 132], $G_F^{\text{SMEFT}} = G_F + \delta G_F$, where $G_F = 1.1663787(6)\times 10^{-5}\,\text{GeV}^{-2}$ and $\delta G_F = -\frac{1}{\sqrt{2}}\left(C^{\ell\ell}_{1221} - C^{\phi\ell(3)}_{11} - C^{\phi\ell(3)}_{22}\right)$. So, we re-write the formulas with the re-scaled contributions, setting the renormalization scale to $\mu = \Lambda = 1$ TeV and the Fermi constant correction, in order to compare the coefficients again,

$$\begin{aligned}\delta R_{h\to Z\gamma} \simeq & -0.25\,\delta G_F + 0.12\left(C^{[0]\phi\Box} - C^{[0]\phi D}\right)\\ & +0.01\hat{C}^{[1]\phi B} - 0.04\,\hat{C}^{[1]\phi W} + 0.01\,\hat{C}^{[1]\phi WB}\\ & -0.01\left(C^{[0]d\phi}_{33} - C^{[0]u\phi}_{33}\right)+\ldots,\end{aligned} \tag{3.6}$$

$$\begin{aligned}\delta R_{h\to\gamma\gamma} \simeq & -0.25\,\delta G_F + 0.12\left(C^{[0]\phi\Box} - 2C^{[0]\phi D}\right)\\ & -0.03\,\hat{C}^{[1]\phi B} - 0.04\,\hat{C}^{[1]\phi W} + 0.03\,\hat{C}^{[1]\phi WB}\\ & -0.01\left(C^{[0]e\phi}_{22} + 4C^{[0]e\phi}_{33}\right)\\ & -0.01\left(5C^{[0]u\phi}_{22} + 2C^{[0]d\phi}_{33} - 3C^{[0]u\phi}_{33}\right)+\ldots.\end{aligned} \tag{3.7}$$

Disentangling the formulas in such a way provides us with more insight on the values of the couplings that we can expect in the UV. With this procedure we have also narrowed down a multitude of contributing operators to just a handful of them making the study of these two observables easier.

A few remarks are in order.

- The largest contribution to $\delta R_{h\to\gamma\gamma}$ no longer originates from the operator $C^{\phi B}$ even though initially that was the case. The most dominant Wcs are $C^{\ell\ell}_{1221}$, $C^{\phi\ell(3)}_{11}$, $C^{\phi\ell(3)}_{22}$, while next in magnitude are the Wcs $C^{\phi D}$ and $C^{\phi\Box}$. Incidentally, these five operators contribute maximally to $\delta R_{h\to Z\gamma}$ as well.

- The model in question must not generate large corrections to the Fermi constant, whose SMEFT expression depends on $C^{\ell\ell}_{1221}$, $C^{\phi\ell(3)}_{11}$, $C^{\phi\ell(3)}_{22}$, which is excluded, unless we tune down its couplings to minuscule values to reach a correction of the order of $10^{-6}$. Additionally, Wilson coefficients $C^{\phi\Box}$ and $C^{\phi D}$ could cancel each other out in $h \to \gamma\gamma$ if $C^{\phi\Box} = 2C^{\phi D}$ and that could boost $h \to Z\gamma$, unless they are not generated at tree level and are suppressed by a loop factor. However, in the case of a cancellation both $C^{\phi D}$ and $C^{\phi\Box}$ would be heavily constrained by the $T$-parameter, since the coefficients are directly related to each other.

- What values of Wcs would it take to boost $h \to Z\gamma$ while simultaneously these Wcs would destructively contribute in $h \to \gamma\gamma$? Ideally we would like to avoid generating the dominant tree level Wcs mentioned in the two previous bullets because they equally contribute to both observables and there is no apparent way to cancel each other out. Our main goal is to restore the dominance of $C^{\phi(B,W,WB)}$ Wcs.

- For both signal strengths their expressions are almost identical with the only difference being the Wc $C^{e\phi}_{pp}$ which contributes only to $\delta R_{h\to\gamma\gamma}$, however operators of such kind arising from the tree level are usually suppressed by the Yukawa coupling of the corresponding fermion and are thus suppressed for the most part. For this reason we will keep from now on only contributions from the third generation of quarks.

- In the expressions in eq.(3.4) and eq.(3.5) for the signal strengths all Wcs are considered at the renormalization scale $\mu$, $C(\mu)$. Since we have split the operators in the tree and loop counterparts the RG mixing of loop level operators constitutes a two loop effect and is neglected. Since we have set $\mu = \Lambda = 1$ TeV, all Wcs are from now on considered at $C(\mu) = C(\Lambda)$.

We construct a chi-square function to explore further the correlations and the required numerical values that these three coefficients need to take to accommodate an excess in one over the other observable. The observables that we choose to add are the decay and production signal strengths of the Higgs boson which can fairly constrain all Wcs in our study. We consider the decays of the Higgs boson tabulated in the first column of Table 3.1 and the for the production modes we include gluon fusion (ggF), vector boson fusion (VBF), associated production with a vector boson (Wh, Zh) and lastly, associated production with a pair of top quakrs (tth). Apart from these we also add the oblique parameters $S$ and $T$, since they highly constrain $C^{\phi WB}$ and $C^{\phi D}$ respectively. In the $\{G_F, M_W, M_Z\}$ scheme, these two expressions read,

$$\Delta S = \frac{2\pi}{G_F^2 M_W \sqrt{M_Z^2 - M_W^2}} \frac{C^{\phi WB}}{\Lambda^2} , \tag{3.8}$$

$$\Delta T = \frac{\pi}{4G_F^2} \frac{M_Z^2}{M_W^2 (M_Z^2 - M_W^2)} \frac{C^{\phi D}}{\Lambda^2} \tag{3.9}$$

Substituting the relevant values and setting $\Lambda = 1\,\text{TeV}$, we get the semi-numerical expression,

$$\Delta S = 0.0199\, \hat{C}^{[1]\phi WB} , \tag{3.10}$$

$$\Delta T = -4.0083\, C^{\phi D} . \tag{3.11}$$

The experimental values of decay and production channels that we are using to construct the $\chi^2$ function are shown in Table 3.1. For $S$ and $T$ parameters we have the following two experimental values and corresponding uncertainties, $S_{\text{exp}} = -0.02 \pm 0.07$ and $T_{\text{exp}} = 0.04 \pm 0.06$ [133].

| Decay | Experiment | Production | Experiment |
|---|---|---|---|
| $\delta R_{h\to\gamma\gamma}$ | $0.10 \pm 0.07$ | $\delta R_{ggF}$ | $-0.03 \pm 0.08$ |
| $\delta R_{h\to Z\gamma}$ | $1.20 \pm 0.70$ [119] | $\delta R_{VBF}$ | $-0.20 \pm 0.12$ |
| $\delta R_{h\to ZZ^*}$ | $0.02 \pm 0.08$ | $\delta R_{Wh}$ | $0.44 \pm 0.26$ |
| $\delta R_{h\to WW^*}$ | $0.00 \pm 0.08$ | $\delta R_{Zh}$ | $0.29 \pm 0.25$ |
| $\delta R_{h\to\mu^+\mu^-}$ | $0.21 \pm 0.35$ | $\delta R_{tth}$ | $-0.06 \pm 0.20$ |
| $\delta R_{h\to\tau^+\tau^-}$ | $-0.09 \pm 0.09$ | | |
| $\delta R_{h\to b\bar{b}}$ | $0.01 \pm 0.12$ | | |

*Table 3.1: Numerical values used to construct the $\chi^2$ function to be minimized. The decay channel values were taken from [133], except for the $h \to Z\gamma$ decay. The production channel experimental values were taken from CMS[117].*

We define the $\chi^2$,

$$\chi^2 = \left(O^{\text{SMEFT}} - O^{\text{exp}}\right)^T \left(\sigma^2\right)^{-1} \left(O^{\text{SMEFT}} - O^{\text{exp}}\right) , \tag{3.12}$$

where $O^{\text{exp}}$ is the column vector that contains the central values of the experimental measurements of the corresponding signal strengths of Table 3.1, while in this case $\sigma^2$ is a $N_{\text{obs}} \times N_{\text{obs}}$ diagonal matrix containing the relevant uncertainties, where we have neglected theory uncertainties and assumed that all measurements are uncorrelated. The quantity $O^{\text{SMEFT}}$ can be decomposed into two pieces, a purely SM piece, $O^{\text{SM}}$ and a purely BSM piece, $O^{\text{BSM}}$. Since the SM piece is a pure number we subtract it from the experimental values and we define $O^{\delta} = O^{\text{SM}} - O^{\text{exp}}$. We use Singular Values Decomposition (SVD) technique as described in [134] to solve this least squares problem and we cross-check the results by also minimizing the chi-square function. The set of Wcs we consider here are

$$\left\{C^{\phi B},\ C^{\phi W},\ C^{\phi WB},\ C^{\phi\Box},\ C^{\phi D},\ C_{33}^{u\phi},\ C_{33}^{d\phi}\right\} , \tag{3.13}$$

where we neglect the Wcs that affect corrections to the Fermi constant.

The best-fit values for the Wilson coefficients that we obtain, for $\Lambda = 1\,\text{TeV}$ are,

$$\hat{C}^{[1]\phi B} = 23.75 \pm 3.03 , \tag{3.14}$$

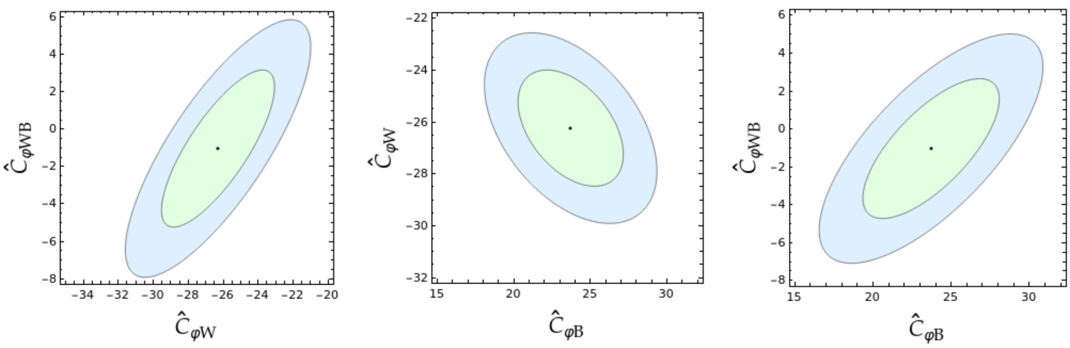


*Fig. 3.1: Error ellipses drawn by setting each respective coefficient to its best-fit value while varying the other two. Green and light blue contours represent, 1$\sigma$ and 2$\sigma$ respectively.*

$$\hat{C}^{[1]\phi W} = -26.26 \pm 2.68\,, \tag{3.15}$$
$$\hat{C}^{[1]\phi WB} = -1.07 \pm 3.63\,, \tag{3.16}$$
$$C^{\phi\Box} = -0.18 \pm 0.40\,, \tag{3.17}$$
$$C^{\phi D} = 0.01 \pm 0.01\,, \tag{3.18}$$
$$C^{u\phi}_{33} = -0.83 \pm 1.21\,, \tag{3.19}$$
$$C^{d\phi}_{33} = 0.001 \pm 0.03\,. \tag{3.20}$$

We also note the values of the first three Wcs before rescalings to be, $C^{\phi B} = 0.018 \pm 0.002$, $C^{\phi W} = -0.071 \pm 0.007$ and $C^{\phi WB} = -0.0015 \pm 0.005$. Comparing the results of our SMEFT analysis it can be seen that within the marginalised values reported in refs. [42, 135] our own values fall within the ranges given in the aforementioned references. However, if we consider the individual cases where only one Wc contributes to observables the values that we obtain fall short of the ranges obtained in the global fits. This deviation could be justified by the amount of observables contained in the global fits, while in this study we focus dominantly on the Higgs sector observables.

The correlation matrix for these coefficients, is,

| Wcs | $C^{\phi B}$ | $C^{\phi W}$ | $C^{\phi WB}$ | $C^{\phi\Box}$ | $C^{\phi D}$ | $C^{u\phi}_{33}$ | $C^{d\phi}_{33}$ |
|---|---|---|---|---|---|---|---|
| $C^{\phi B}$ | 1. | 0.268 | 0.633 | 0.073 | −0.013 | 0.192 | 0.032 |
| $C^{\phi W}$ | | 1. | 0.613 | 0.539 | −0.007 | 0.335 | 0.205 |
| $C^{\phi WB}$ | | | 1. | 0.003 | 0 | 0.001 | 0.001 |
| $C^{\phi\Box}$ | | | | 1. | 0.03 | 0.33 | 0.374 |
| $C^{\phi D}$ | | | | | 1. | 0.006 | 0.007 |
| $C^{u\phi}_{33}$ | | | | | | 1. | 0.157 |
| $C^{d\phi}_{33}$ | | | | | | | 1. |

(3.21)

From the covariance matrix of the coefficients we can also draw the error ellipses, as shown in Figure 3.1. In each of the plots we have set each respective coefficient that is not drawn to its best-fit values and have drawn error ellipses of the other two. For example, in the first plot we have set every coefficient but $C_{\phi W}$ and $C_{\phi WB}$ to is best-fit value and have plotted the error ellipses of the other two.

Let us now establish the criteria that UV models must meet in order to be considered viable for further study:

1. The most important relation that needs to hold is that $C^{\phi B}$ and $C^{\phi W}$ need to have a definite sign difference. This means that the UV model has to generate both. It alone could accommodate for an excess in $h \to Z\gamma$ if no other Wc that affects the two observables equally is generated.

2. We also notice that if $C^{\phi WB}$ is generated it's value would need to be small, even accounting for uncertainties because of the direct relation to the $S$-parameter.

3. Some models could also generate a pair of $C^{\phi\Box}$ and $C^{\phi D}$, if they are generated together at tree level they are proportional to each other. From the fit we see that including uncertainties it could be possible to accommodate this possibility.

## 3.3 Single field UV models

In the following sections we examine the single field extensions of the tree level dictionary [67, 136] as well as some potential two field cases. To get all the expressions of the relevant generated operators we use the package SOLD [121], which contains all information on Wcs exclusively generated at one-loop order from scalar and vector like fermion extensions, while for tree-level generated operators we use the package MatchMakerEFT [40] and cross-check with the expressions found in ref. [67]. We refrain from including or discussing massive vector bosons for several reasons. First, no automated package exists up to date that could give us immediately Wcs and facilitate our study. Second and most important, we would need to account for the gauge boson mass, which would require the inclusion of a spontaneous symmetry breaking mechanism able to explain the origin of the mass. Additionally, if we consider vector bosons the Wcs that are of interest, namely $C^{\phi(B,W,WB)}$, are generated at tree level and are either coming from already non renormalizable interactions of dimension greater than four, or in some cases even if these operators are coming from interactions of dimension less or equal to four there is never a sign difference between Wcs $C^{\phi B}$ and $C^{\phi W}$ [67]. The inclusion of vector boson extensions is outside the scope of this study. Additionally, barring vector boson extensions, CP-violating operators come from interactions of already non-renormalizable operators in the models that we investigate, we restrict ourselves to interactions of the original Lagrangian up to mass dimension four.

### 3.3.1 The case for BSM scalars

To examine some viable scenarios we list in Table 3.2 all scalar fields that serve as extensions of the SM, that also have a linear coupling with the SM particle content. We also list the tree level operators that they generate as well as the subset of loop level operators that are interesting for our case study. We exclude colored fields, as they induce the operator $\mathcal{O}^{\phi G}$, which significantly impacts the production rate of $ggF$. Given that this production channel is precisely measured, we aim to avoid constraints associated with this bound. In the following bullets all cases of Table 3.2 will be investigated if they could account for the values of the Wcs obtained in the SMEFT analysis. In the matching calculations only the necessary operators for our discussion are provided, all other operators not presented are either zero or generated at loop-level and their contributions is deemed too small as has been discussed in Section 3.2. In the results presented below the notation of the tree-level dictionary [67] is being followed, the Lagrangian used for scalars can be found in Appendix A.2 of the aforementioned reference. For clarity however, the subset of the Lagrangian where the operator is being induced from is also presented. The mass terms of the new scalars are denoted by $M_i$, where $i = \{\mathcal{S}, \mathcal{S}_1, \mathcal{S}_2, \varphi, \Xi, \Xi_1, \Theta_1, \Theta_3\}$.

| Fields | Irrep | Tree level operators | Loop level operators |
|---|---|---|---|
| $\mathcal{S}$ | $(1,1)_0$ | $\mathcal{O}^{\phi\Box}$ | $\mathcal{O}_{\phi B}, \mathcal{O}_{\phi W}, \mathcal{O}_{\phi WB}$ |
| $\mathcal{S}_1$ | $(1,1)_1$ | $\mathcal{O}^{\ell\ell}$ | $\mathcal{O}_{\phi B}$ |
| $\mathcal{S}_2$ | $(1,1)_2$ | $\mathcal{O}^{ee}$ | $\mathcal{O}_{\phi B}$ |
| $\varphi$ | $(1,2)_{1/2}$ | $\mathcal{O}^{(e,u,d)\phi}$ | $\mathcal{O}_{\phi B}, \mathcal{O}_{\phi W}, \mathcal{O}_{\phi WB}$ |
| $\Xi$ | $(1,3)_0$ | $\mathcal{O}^{\phi D}, \mathcal{O}^{\phi\Box}, \mathcal{O}^{(e,u,d)\phi}$ | $\mathcal{O}_{\phi B}, \mathcal{O}_{\phi W}$ |
| $\Xi_1$ | $(1,3)_1$ | $\mathcal{O}^{\phi D}, \mathcal{O}^{\phi\Box}, \mathcal{O}^{(e,u,d)\phi}$ | $\mathcal{O}_{\phi B}, \mathcal{O}_{\phi W}, \mathcal{O}_{\phi WB}$ |
| $\Theta_1$ | $(1,4)_{1/2}$ | $\mathcal{O}^{\phi}$ | $\mathcal{O}_{\phi B}, \mathcal{O}_{\phi W}, \mathcal{O}_{\phi WB}$ |
| $\Theta_3$ | $(1,4)_{3/2}$ | $\mathcal{O}^{\phi}$ | $\mathcal{O}_{\phi B}, \mathcal{O}_{\phi W}, \mathcal{O}_{\phi WB}$ |

*Table 3.2: Tree and relevant loop level operators generated by new scalar field extensions of the SM. The first column follows the naming convention of ref. [67], while in the second one the representation of each field is denoted as $(SU(3), SU(2))_{U(1)}$.*

- Field $\mathcal{S}$, a neutral scalar generates all the necessary operators. The subset Lagrangian reads,

$$\Delta\mathcal{L} \supset (\kappa_{\mathcal{S}})\mathcal{S}\,\phi^\dagger\phi\ . \tag{3.22}$$

The expressions of the Wcs are,

$$C^{\phi\Box} = -\frac{(\kappa_{\mathcal{S}})^2}{2M_{\mathcal{S}}^4}\,, \tag{3.23}$$

$$\hat{C}^{[1]\phi WB} = 2\,\hat{C}^{[1]\phi B} = 2\,\hat{C}^{[1]\phi W} = \frac{(\kappa_{\mathcal{S}})^2}{6M_{\mathcal{S}}^4}\,. \tag{3.24}$$

This set of Wcs would be impossible to explain a possible deviation because of the universal contribution to $C^{\phi\Box}$ and additionally $C^{\phi B} = C^{\phi W}$.

- Fields $\mathcal{S}_{1,2}$, charged singlets do no generate the required set of operators necessary for our purposes. Additionally, $\mathcal{S}_1$, gives $C_{\ell\ell}$ which would potentially contribute strongly to Fermi constant. For completeness, the expressions of the Wcs are

$$\mathcal{S}_1:\quad \left(C^{\ell\ell}\right)_{ijkl} = \frac{(y_{\mathcal{S}_1})^*_{jl}(y_{\mathcal{S}_1})_{ik}}{M_{\mathcal{S}_1}^2}\,, \tag{3.25}$$

$$\hat{C}^{[1]\phi B} = -\frac{\lambda_{\mathcal{S}_1}}{12M_{\mathcal{S}_1}^2}\,, \tag{3.26}$$

$$\mathcal{S}_2:\quad \left(C^{ee}\right)_{ijkl} = \frac{(y_{\mathcal{S}_2})^*_{lj}(y_{\mathcal{S}_2})_{ki}}{2M_{\mathcal{S}_2}^2}\,, \tag{3.27}$$

$$\hat{C}^{[1]\phi B} = -\frac{\lambda_{\mathcal{S}_2}}{3M_{\mathcal{S}_2}^2}\,, \tag{3.28}$$

where the Lagrangian for the relevant couplings reads,

$$\Delta\mathcal{L} \supset \lambda_{\mathcal{S}_1}(\mathcal{S}_1^\dagger\mathcal{S}_1)(\phi^\dagger\phi) + \lambda_{\mathcal{S}_2}(\mathcal{S}_2^\dagger\mathcal{S}_2)(\phi^\dagger\phi)$$

$$(y_{\mathcal{S}_1})_{ij}\mathcal{S}_1^\dagger \bar{l}_{Li} i\sigma^2 l_{Lj}^c + (y_{\mathcal{S}_2})_{ij}\mathcal{S}_2^\dagger \bar{e}_{Ri} e_{Rj}^c + \text{h.c.}\,, \tag{3.29}$$

where $i, j$ are flavor indices. So, we exclude these two single fields as well.

- Next is the 2HDM, where a recent work [137] also explores the matching of this model and fits to relevant Higgs observables. Field $\varphi$ generates the correct set. The interaction Lagrangian is presented below along with terms not contained in the tree-level dictionary (as were generated by SOLD),

$$\begin{aligned}\Delta\mathcal{L} \supset & \kappa_{\varphi^2\phi^2}\, \phi_\alpha^\dagger \varphi_\beta^\dagger \phi_\gamma \varphi_\delta C^{(1)}_{\alpha\beta\gamma\delta} + \lambda_{\varphi^2\phi^2}\, \phi_\alpha^\dagger \varphi_\beta^\dagger \phi_\gamma \varphi_\delta C^{(2)}_{\alpha\beta\gamma\delta} \\ & (y_{e\varphi})_{ij}\varphi^\dagger \bar{e}_{Ri} l_{Lj} + (y_{d\varphi})_{ij}\varphi^\dagger \bar{d}_{Ri} q_{Lj} + \text{h.c.} & (3.30) \\ & (y_{u\varphi})_{ij}\varphi^\dagger i\sigma^2 \bar{q}_{Li}^T u_{Rj} + \lambda_\varphi (\varphi^\dagger\phi)(\phi^\dagger\phi) + \text{h.c.}\,, & (3.31)\end{aligned}$$

where a summation of the indices $\alpha, \beta, \gamma, \delta$ is implied, which represent SU(2) indices ranging $\alpha, \beta, \gamma, \delta = 1, 2$, while $C$'s are the Clebsh-Gordan (CG) tensors of the coupling. The superscript T denotes transposition in SU(2) space. The non-zero elements of the corresponding CG tensors are,

$$C^{(1)}_{1111} = C^{(1)}_{2222} = 2\,, \tag{3.32}$$
$$C^{(1)}_{1212} = C^{(1)}_{1221} = C^{(1)}_{2121} = C^{(1)}_{2112} = 1\,, \tag{3.33}$$
$$C^{(2)}_{1212} = C^{(2)}_{2121} = -C^{(2)}_{1221} = -C^{(2)}_{2112} = 1\,. \tag{3.34}$$

The expressions of the Wcs are,

$$\hat{C}^{[1]\phi B} = \hat{C}^{[1]\phi W} = -\frac{3\kappa_{\varphi^2\phi^2} + 2\lambda_{\varphi^2\phi^2}}{96\, M_\varphi^2}\,, \tag{3.35}$$
$$\hat{C}^{[1]\phi WB} = -\frac{\kappa_{\varphi^2\phi^2} - 2\lambda_{\varphi^2\phi^2}}{48\, M_\varphi^2}\,, \tag{3.36}$$
$$\left(C^{e\phi}\right)_{ij} = \frac{\lambda_\varphi\, (y_{e\varphi})^*_{ji}}{M_\varphi^2} \tag{3.37}$$
$$\left(C^{d\phi}\right)_{ij} = \frac{\lambda_\varphi\, (y_{d\varphi})^*_{ji}}{M_\varphi^2} \tag{3.38}$$
$$\left(C^{u\phi}\right)_{ij} = -\frac{\lambda_\varphi^*\, (y_{u\varphi})_{ji}}{M_\varphi^2}\,. \tag{3.39}$$

The Higgs-gauge boson operators are generated but the two most important ones are equal. For this reason we exclude this model.

- Next we consider electroweak triplets. First $\Xi$ generates the following operators,

$$C^{\phi\Box} = -\frac{1}{4}C^{\phi D} = \frac{\kappa_\Xi^2}{2M_\Xi^4}\,, \tag{3.40}$$
$$\hat{C}^{[1]\phi B} = \frac{\kappa_\Xi^2}{16M_\Xi^4}\,, \tag{3.41}$$
$$\hat{C}^{[1]\phi W} = -\frac{1}{4}\,\hat{C}^{[1]\phi B} + \frac{\lambda_\Xi}{6\sqrt{6}M_\Xi^2}\,, \tag{3.42}$$
$$\left(C^{e\phi}\right)_{ij} = \frac{\kappa_\Xi^2\, (y_e)^*_{ji}}{M_\Xi^4} \tag{3.43}$$

$$\left(C^{d\phi}\right)_{ij} = \frac{\kappa_\Xi^2 (y_d)^*_{ji}}{M_\Xi^4} \tag{3.44}$$

$$\left(C^{u\phi}\right)_{ij} = -\frac{\kappa_\Xi^2 (y_u)^*_{ji}}{M_\Xi^4}\,, \tag{3.45}$$

where $y_{(e,u,d)}$ are the Yukawa coupling of the SM defined in eq.(A.1) of ref [67]. The corresponding Lagrangian for the rest of the couplings reads,

$$\Delta\mathcal{L} \supset (\kappa_\Xi)\,\phi^\dagger \Xi^a \sigma^a \phi + \lambda_\Xi\, \Xi^a \Xi^a\, (\phi^\dagger \phi)\,, \tag{3.46}$$

where a summation of the index $a$ is implied. The index denotes SU(2) triplets taking values $a = 1, 2, 3$. Although the model appears promising as it generates all the necessary Wilson coefficients (Wcs), these Wcs are strongly correlated. We can express these correlations through the following relations:, $C^{\phi\Box} = -C^{\phi D}/4 = 8\,C^{\phi B}$, $(C^{(e,d)\phi})_{ij} = 2(y_{(e,d)})^*_{ji}\,C^{\phi\Box}$ and $(C^{u\phi})_{ij} = -2(y_u)^*_{ji}\,C^{\phi\Box}$. The most stringent constraint for this model comes from the $T$-parameter which is proportional to $C^{\phi D}$ and forces us to a small value for this Wc which is related to $C^{\phi B}$ which needs to have a large value. To provide a clearer picture, we can express the following observables, where we retain only the top Yukawa coupling and neglect other contributions due to their insignificance:

$$\Delta T = -8.016\frac{\kappa_\Xi^2}{M_\Xi^4}\,, \tag{3.47}$$

$$\delta R_{h\to\gamma\gamma} = 0.508\,\frac{\kappa_\Xi^2}{M_\Xi^4} - 0.0025\,\frac{\lambda_\Xi}{M_\Xi^2}\,, \tag{3.48}$$

$$\delta R_{h\to Z\gamma} = 0.2912\,\frac{\kappa_\Xi^2}{M_\Xi^4} - 0.0026\,\frac{\lambda_\Xi}{M_\Xi^2}\,. \tag{3.49}$$

In order to satisfy the bound for the $T$-parameter, which in our case needs to be negative and by taking the lower bound of the experimental value at $T_{\text{exp}} \geq -0.02$, we get the bound for the coupling to mass ratio $\kappa_\Xi^2/M_\Xi^4 \geq 25 \times 10^{-4}$, substituting these values into eqs. (3.48) and (3.49) we get,

$$\delta R_{h\to\gamma\gamma} = 0.0013 - 0.0025\,\frac{\lambda_\Xi}{M_\Xi^2}\,, \tag{3.50}$$

$$\delta R_{h\to Z\gamma} = 0.0007 - 0.0026\,\frac{\lambda_\Xi}{M_\Xi^2}\,. \tag{3.51}$$

These contributions are insufficient, leaving only the universal effect of the triplet's quartic coupling with the Higgs, which cannot serve the purpose of splitting apart the two observables. We rule this model out as well.

- The next triplet, $\Xi_1$ is charged and the corresponding Wcs are,

$$C^{\phi\Box} = \frac{1}{2}C^{\phi D} = \frac{2|\kappa_{\Xi_1}|^2}{M_{\Xi_1}^4}\,, \tag{3.52}$$

$$\hat{C}^{[1]\phi WB} = -\frac{5|\kappa_{\Xi_1}|^2}{12 M_{\Xi_1}^4} - \frac{\lambda'_{\Xi_1}}{6\sqrt{3}M_{\Xi_1}^2}\,, \tag{3.53}$$

$$\hat{C}^{[1]\phi B} = -\frac{|\kappa_{\Xi_1}|^2}{4 M_{\Xi_1}^4} + \frac{\lambda_{\Xi_1}}{4\sqrt{6}M_{\Xi_1}^2}\,, \tag{3.54}$$

$$\hat{C}^{[1]\phi W} = -\frac{|\kappa_{\Xi_1}|^2}{12M_{\Xi_1}^4} + \frac{\lambda_{\Xi_1}}{6\sqrt{6}M_{\Xi_1}^2} \,, \tag{3.55}$$

$$\left(C^{e\phi}\right)_{ij} = \frac{2|\kappa_{\Xi_1}|^2 \,(y_e)^*_{ji}}{M_{\Xi_1}^4} \,, \tag{3.56}$$

$$\left(C^{d\phi}\right)_{ij} = \frac{2|\kappa_{\Xi_1}|^2 \,(y_d)^*_{ji}}{M_{\Xi_1}^4} \tag{3.57}$$

$$\left(C^{u\phi}\right)_{ij} = -\frac{2|\kappa_{\Xi_1}|^2 \,(y_u)^*_{ji}}{M_{\Xi_1}^4} \,. \tag{3.58}$$

The Lagrangian is,

$$\begin{aligned}\Delta\mathcal{L} \supset & \lambda_{\Xi_1}(\Xi_1^{a\dagger}\Xi^a)(\phi^\dagger\phi) + \lambda'_{\Xi_1} f_{abc}\,(\Xi_1^{a\dagger}\Xi^b)(\phi^\dagger\sigma^c\phi) \\ & (\kappa_{\Xi_1})\,\Xi_1^{a\dagger}(i\sigma^2\phi^*\sigma^a\phi) + \text{h.c.}\,,\end{aligned} \tag{3.59}$$

where $f_{abc} = i/\sqrt{2}\varepsilon_{abc}$ and $\varepsilon_{abc}$ is the totally antisymmetric tensor.

In this case, the operators are directly related to each other, we can rewrite $C^{\phi W}$ as follows, $\hat{C}^{[1]\phi W} = \hat{C}^{[1]\phi B}/3 + \frac{\lambda_{\Xi_1}}{12\sqrt{6}M_{\Xi_1}^2}$, this relation shows that we cannot easily change the sign of these two operators since they are directly related. Also strong constraints for the coupling $\kappa_{\Xi_1}$ come from the $T$-parameter. Substituting the values of the Wcs we have,

$$\Delta T = 16.033\,\frac{|\kappa_{\Xi_1}|^2}{M_{\Xi_1}^4} \,, \tag{3.60}$$

$$\Delta S = -0.008\,\frac{|\kappa_{\Xi_1}|^2}{M_{\Xi_1}^4} - 0.0019\,\frac{\lambda'_{\Xi_1}}{M_{\Xi_1}^2} \,, \tag{3.61}$$

$$\begin{aligned}\delta R_{h\to\gamma\gamma} = {} & 0.720\,\frac{|\kappa_{\Xi_1}|^2}{M_{\Xi_1}^4} \\ & - \frac{0.0067\lambda_{\Xi_1} + 0.0033\lambda'_{\Xi_1}}{M_{\Xi_1}^2} \,,\end{aligned} \tag{3.62}$$

$$\begin{aligned}\delta R_{h\to Z\gamma} = {} & 0.244\,\frac{|\kappa_{\Xi_1}|^2}{M_{\Xi_1}^4} \\ & - \frac{0.0015\lambda_{\Xi_1} + 0.0011\lambda'_{\Xi_1}}{M_{\Xi_1}^2} \,.\end{aligned} \tag{3.63}$$

Setting the T-parameter to be of the order of $T \sim 10^{-2}$, we can get a bound for the ratio $|\kappa_{\Xi_1}|^2/M_{\Xi}^4 \sim 0.6 \times 10^{-3}$ and we rewrite the rest,

$$\Delta S \simeq -0.19 \times 10^{-2}\,\frac{\lambda'_{\Xi_1}}{M_{\Xi_1}^2} \,, \tag{3.64}$$

$$\delta R_{h\to\gamma\gamma} \simeq -10^{-2}\,\frac{0.67\lambda_{\Xi_1} + 0.33\lambda'_{\Xi_1}}{M_{\Xi_1}^2} \,, \tag{3.65}$$

$$\delta R_{h\to Z\gamma} \simeq -10^{-2}\,\frac{0.15\lambda_{\Xi_1} + 0.11\lambda'_{\Xi_1}}{M_{\Xi_1}^2} \,. \tag{3.66}$$

From these relation we can see that the two signal strengths cannot be separated. This model is also explored in ref [126]. The same conclusion is reached and can be seen in their Figure 6 panel (c), where the difference $\delta R_{h\to\gamma\gamma} - \delta R_{h\to Z\gamma}$ is plotted.

- Moving on the last two scalar fields we have a charged field labeled $\Theta_1$ in the 4-representation of $SU(2)$. The Wc expressions read,

$$\hat{C}^{[1]\phi B} = \frac{\lambda_{\Theta_1}}{16\, M_{\Theta_1}^2}\,, \quad \hat{C}^{[1]\phi W} = 4\, \hat{C}^{[1]\phi B}\,, \tag{3.67}$$

$$\hat{C}^{[1]\phi WB} = -\frac{\lambda'_{\Theta_1^2\phi^2}}{6\, M_{\Theta_1}^2}\,. \tag{3.68}$$

It is evident that we cannot under any circumstance get opposite signs for $C^{\phi B}$ and $C^{\phi W}$. Apart from the Lagrangian found in eq.(A.7) of ref. [67] we also have the additional interaction term,

$$\Delta\mathcal{L} \supset \lambda'_{\Theta_1^2\phi^2}\, \phi_\alpha^\dagger \Theta_{1I}^\dagger \phi_\beta \Theta_{1J}\, C^{(3)}_{\alpha I\beta J}\,, \tag{3.69}$$

where summation of the indices is implied. Indices range is for $\alpha, \beta = 1, 2$ while for $I, J = 1, 2, 3$. The only non-zero values of the CG tensor read

$$C^{(3)}_{1112} = C^{(3)}_{1223} = C^{(3)}_{2213} = C^{(3)}_{2221} = i\,, \tag{3.70}$$

$$C^{(3)}_{1123} = C^{(3)}_{2311} = -C^{(3)}_{1321} = -C^{(3)}_{2113} = -1\,, \tag{3.71}$$

$$C^{(3)}_{1211} = C^{(3)}_{1322} = C^{(3)}_{2122} = C^{(3)}_{2312} = -i\,. \tag{3.72}$$

- The same situation stands for the other charged field labeled, $\Theta_3$, but we list here the generated operators for completeness. Part of the Lagrangian can be found on eq.(A.7) of ref. [67] and the additional part is the same as in the previous bullet, but with the substitution $\Theta_1 \to \Theta_3$ and $C^{(3)}_{\alpha I\beta J} \to C^{(4)}_{\alpha I\beta J}$. The same relations hold for $C^{(4)}_{\alpha I\beta J}$ too. The Wcs read,

$$\hat{C}^{[1]\phi B} = \frac{9\, \lambda_{\Theta_3}}{16\, M_{\Theta_3}^2}\,, \quad \hat{C}^{[1]\phi W} = \frac{8}{27}\, \hat{C}^{[1]\phi B}\,, \tag{3.73}$$

$$\hat{C}^{[1]\phi WB} = -\frac{\lambda'_{\Theta_3^2\phi^2}}{4\, M_{\Theta_3}^2}\,. \tag{3.74}$$

### 3.3.2 The case for vector-like fermions

Barring chiral fermions, where constraints from multiple Higgs observables have ruled out this scenario [125], we can extend the fermion content of the SM by the fields shown in Table 3.3.

The case here is clearer than the scalars because we will always need two fermions to make up interactions with the Higgs and this saturates the dimension of the corresponding operator fast. For completeness we list the generated Wcs for each fermion listed in Table 3.3 although none of them can accommodate to the splitting of the observables because their Wcs are proportional and the dominant ones i.e. $C^{\phi B}$ and $C^{\phi W}$ come also with the same sign:

$$N:\ \hat{C}^{[1]\phi B} = \hat{C}^{[1]\phi W} = \frac{1}{2}\, \hat{C}^{[1]\phi WB} = \frac{|\lambda_N|^2}{24 M_N^2}\,, \tag{3.75}$$

| Fields | Irrep | Tree level operators | Loop level operators |
|---|---|---|---|
| $N$ | $(1,1)_0$ | $\mathcal{O}_5$, $\mathcal{O}_{\phi\ell}^{(1,3)}$ | $\mathcal{O}_{\phi B}$, $\mathcal{O}_{\phi W}$, $\mathcal{O}_{\phi WB}$ |
| $E$ | $(1,1)_{-1}$ | $\mathcal{O}_{e\phi}$, $\mathcal{O}_{\phi\ell}^{(1,3)}$ | $\mathcal{O}_{\phi B}$, $\mathcal{O}_{\phi W}$, $\mathcal{O}_{\phi WB}$ |
| $\Delta_1$ | $(1,2)_{-1/2}$ | $\mathcal{O}_{e\phi}$, $\mathcal{O}_{\phi e}$ | $\mathcal{O}_{\phi B}$, $\mathcal{O}_{\phi WB}$ |
| $\Delta_3$ | $(1,2)_{-3/2}$ | $\mathcal{O}_{e\phi}$, $\mathcal{O}_{\phi e}$ | $\mathcal{O}_{\phi B}$, $\mathcal{O}_{\phi WB}$ |
| $\Sigma$ | $(1,3)_0$ | $\mathcal{O}_5$, $\mathcal{O}_{e\phi}$, $\mathcal{O}_{\phi\ell}^{(1,3)}$ | $\mathcal{O}_{\phi B}$, $\mathcal{O}_{\phi W}$, $\mathcal{O}_{\phi WB}$ |
| $\Sigma_1$ | $(1,3)_{-1}$ | $\mathcal{O}_{e\phi}$, $\mathcal{O}_{\phi\ell}^{(1,3)}$ | $\mathcal{O}_{\phi B}$, $\mathcal{O}_{\phi W}$, $\mathcal{O}_{\phi WB}$ |

*Table 3.3: Tree level operators generated by new vector-like fermions.*

$$E:\ \hat{C}^{[1]\phi B} = 3\,\hat{C}^{[1]\phi W} = -\frac{3}{4}\,\hat{C}^{[1]\phi WB} = \frac{|\lambda_E|^2}{8M_E^2}\,, \tag{3.76}$$

$$\Delta_1:\ \hat{C}^{[1]\phi B} = -3\,\hat{C}^{[1]\phi WB} = \frac{|\lambda_{\Delta_1}|^2}{4M_{\Delta_1}^2}\,,\ \hat{C}^{[1]\phi W} = 0\,, \tag{3.77}$$

$$\Delta_3:\ \hat{C}^{[1]\phi B} = 5\,\hat{C}^{[1]\phi WB} = \frac{5\,|\lambda_{\Delta_3}|^2}{12M_{\Delta_3}^2}\,,\ \hat{C}^{[1]\phi W} = 0\,, \tag{3.78}$$

$$\Sigma:\ \hat{C}^{[1]\phi B} = \frac{3}{7}\,\hat{C}^{[1]\phi W} = -\frac{1}{2}\,\hat{C}^{[1]\phi WB} = \frac{|\lambda_\Sigma|^2}{32M_\Sigma^2}\,, \tag{3.79}$$

$$\Sigma_1:\ \hat{C}^{[1]\phi B} = \frac{9}{7}\,\hat{C}^{[1]\phi W} = \frac{9}{8}\,\hat{C}^{[1]\phi WB} = \frac{3|\lambda_{\Sigma_1}|^2}{32M_{\Sigma_1}^2}\,. \tag{3.80}$$

The Lagrangian used to obtain the Wcs for all fermions can be found in eq.(A.12) of ref. [67], where all relevant coupling are defined. The masses of the heavy fermions are denoted by $M_i$, where $i = \{N,\, E,\, \Delta_1,\, \Delta_3,\, \Sigma,\, \Sigma_1\}$

Summing up, we presented all relevant Wcs, both tree and loop level, of single field extensions, of scalars and fermions, that primarily affect the signal strengths $\delta R_{h\to\gamma\gamma}$ and $\delta R_{h\to Z\gamma}$. We have found that no single field can accommodate a potential excess in one observable over the other. We must also mention that we can extend this list of fields with particles that do not have any linear coupling with the SM and leave the hypercharge as a general parameter that can be fit to find a suitable value. However, these contributions arise from the quartic interactions with the Higgs and cannot yield values that align with the single-field framework previously discussed. They become relevant when considering two-field extensions, as will be addressed in Section 3.4.

As a general observation, it is important to note that the value of the Wc we aim to achieve is significantly higher than what is produced in the single-field scenarios. The coefficients that scale with the coupling-to-mass ratio vary from ideally $10^{-1}$ to $10^{-3}$, these values need to be increased by one or two orders of magnitude to satisfy the requirements established in the SMEFT analysis. Addressing this challenge is complex, as the mass of the heavy field cannot be reduced significantly without compromising the convergence of the EFT, and the coupling cannot exceed $4\pi$ due to perturbativity constraints. Consequently, we are constrained to consider models involving additional fields, with the hope that their contributions may accumulate to achieve the desired effect.

## 3.4 Two-field models

In the two field case scenarios we have a plethora of combinations to work with. We can combine scalars (fermions) with scalars (fermions) and scalars with fermions and analyze each model that shows some promising characteristics on Wcs. In order to tackle the number of models that arise from these combinations we can rely on the single field results and add on top of that new scalar and/or fermion fields that could amend the situation.

In disentangling the two-field models we will aim to categorize the interactions and their corresponding Wcs systematically, by borrowing results from functional matching techniques which directly deal with the path integral and contain a form of universality in the results, independent of the specific interaction of UV physics. In particular, when the matching at one loop is performed, and only heavy scalars run in the loop the resulting effective action is called Universal One Loop Effective Action (UOLEA) first introduced in ref. [24]. Functional matching results have also been expanded to include heavy-light particles in the loop as well as fermions [27–31, 35, 44, 53, 120]. For our purposes we will resort to results from the original UOLEA and the heavy-light UOLEA.

In order to generate the operators $C^{\phi(B,W,WB)}$, we need the functional traces to contain $G'_{\mu\nu}G'_{\mu\nu}$, where $G'_{\mu\nu} = -igG_{\mu\nu}$ where $g$ is the corresponding coupling of the field strength tensor $G_{\mu\nu}$, which directly relates to the gauge group representations of the field. If the fields have representations under several groups a summation over the different strength tensors is understood. There are two such traces in the heavy-only UOLEA and another two in the heavy-light UOLEA for scalar fields. The first two terms have also been presented in Chapter 2, eq. (2.49), while the last two terms can be found in [28],

$$\tilde{f}_i^{9}\,\mathrm{tr}\left\{U^H_{ii}\,G'_{i,\mu\nu}G'_{i,\mu\nu}\right\}\,, \tag{3.81}$$

$$\tilde{f}_{ij}^{13}\,\mathrm{tr}\left\{U^H_{ij}U^H_{ji}\,G'_{i,\mu\nu}G'_{i,\mu\nu}\right\}\,, \tag{3.82}$$

$$\tilde{f}_i^{13A}\,\mathrm{tr}\left\{U^{HL}_{ii'}U^{LH}_{i'i}\,G'_{i,\mu\nu}G'_{i,\mu\nu}\right\}\,, \tag{3.83}$$

$$\tilde{f}_i^{13B}\,\mathrm{tr}\left\{U^{LH}_{i'i}U^{HL}_{ii'}\,G'_{i',\mu\nu}G'_{i',\mu\nu}\right\}\,, \tag{3.84}$$

where the coefficients $\tilde{f}$ read,

$$\tilde{f}_i^{9} = -\frac{1}{12M_i^2}\,, \tag{3.85}$$

$$\tilde{f}_{ij}^{13} = \frac{2M_i^4 + 5M_i^2M_j^2 - M_j^4}{12M_i^2(\Delta_{ij}^2)^3} - \frac{M_i^2M_j^2}{2(\Delta_{ij}^2)^4}\log\left(\frac{M_i^2}{M_j^2}\right)\,, \tag{3.86}$$

$$\tilde{f}_i^{13A} = \frac{1}{6M_i^4}\,, \tag{3.87}$$

$$\tilde{f}_i^{13B} = -\frac{1}{4M_i^4}\,, \tag{3.88}$$

where $M_i$ denotes the mass of the heavy scalar field. The coefficients are defined as $\tilde{f} = 16\pi^2 f$ and are obtained through integration of Feynman integrals over momentum. They are labelled as universal coefficients because they factor out the mass dependence of the UV physics. The unprimed indices of the $U$-matrices denote the set of heavy fields, while the primed indices denote the set of light fields. We have also labeled the mass difference of the heavy fields as $\Delta^2_{ij} = M_i^2 - M_j^2$ for brevity. The $U$-matrices are nothing more than differentiation of the Lagrangian with respect to the fields that the subscript indices denote, hence they contain both fields and couplings which in the end need to be traced throughout all available spaces of the fields (i.e. flavor, SU(2), Lorentz etc.).

We can now categorize the interactions needed to produce our Wcs of interest through the terms in eqs. (3.81-3.84). For example, in the first term (3.81) the mass dimension of $U$ is $[U^H_{ii}] = 2$, which must contain two Higgs fields to produce the desired operators, and it has been differentiated two times with respect to the heavy field, thus we can schematically write down the Lagrangian term as, $\Delta\mathcal{L} \sim X_i X_i H^\dagger H$. Following the same line of thought for the other two terms we can then write the correspondence,

$$\tilde{f}_i^9 \,\mathrm{tr}\left\{U^H_{ii}\, G'_{i,\mu\nu} G'_{i,\mu\nu}\right\} \longrightarrow \Delta\mathcal{L} \sim X_i X_i H^\dagger H \,, \tag{3.89}$$

$$\tilde{f}_{ij}^{13} \,\mathrm{tr}\left\{U^H_{ij} U^H_{ji}\, G'_{i,\mu\nu} G'_{i,\mu\nu}\right\} \longrightarrow \Delta\mathcal{L} \sim X_i X_j H + \mathrm{h.c.} \,, \tag{3.90}$$

$$\left.\begin{array}{l} \tilde{f}_i^{13A} \,\mathrm{tr}\left\{U^{HL}_{ii'} U^{LH}_{i'i}\, G'_{i,\mu\nu} G'_{i,\mu\nu}\right\} \\ \tilde{f}_i^{13B} \,\mathrm{tr}\left\{U^{LH}_{i'i} U^{HL}_{ii'}\, G'_{i',\mu\nu} G'_{i',\mu\nu}\right\} \end{array}\right\} \longrightarrow \Delta\mathcal{L} \sim X_i X_{i'} H + \mathrm{h.c.} \,. \tag{3.91}$$

We note that for (3.91), the only light scalar in the SM is the Higgs thus $X_{i'} = H$ and the interaction becomes $\Delta\mathcal{L} \sim X_i H^\dagger H$ and the only suitable fields have hypercharge $Y_i = 0$ and correspond to the neutral singlet $S$ and the triplet $\Xi$, which were previously discussed. We can then pair up these two fields with any other one to give us the desired operators. Next, eq.(3.89) conserves the hypercharge universally, that is this term is going to be present even if the value of the hypercharge is arbitrary. Lastly, eq.(3.90) is a linear coupling of the Higgs and the heavy fields so the hypercharge of the corresponding new fields have to obey the following rule, if we suppose that we leave $Y_i$ free, the hyperchage of $X_j$ is going to take the value $Y_j = Y_i + Y_H$ with $Y_H = 1/2$. In Table 3.4 we present the two-field models that could generate the operators $C^{\phi(B,W,WB)}$. We split the table depending on the field content, either we have two scalars labelled as $(SS)$, a scalar and a fermion labeled as $(SF)$ or two fermions labeled as $(FF)$.

Our strategy to determine the most we can get in the decay $h \to Z\gamma$ will be to construct a $\chi^2$ with all observables mentioned in Table 3.1, excluding $h \to Z\gamma$ and leaving it as prediction for each model. The main reason for substituting the decay $h \to Z\gamma$ from a constraint to a prediction is that we want more freedom in the parameter space of each model, and leaving this specific decay as a models' prediction is more suitable for our purpose. Meanwhile, it yields slightly better results than having it as a constraint. Seeking a sign difference in the fashion of Section 3.3 is not an option for this procedure in certain models that we are going to investigate. The reason behind this, is that Wcs expressions in specific cases become much more complex and an automated procedure is deemed more useful. Also, Wcs serve as a medium for the couplings of each UV model. Since we are now considering UV physics with definite couplings it is more appropriate to discuss couplings directly related to physical observables instead of Wcs.

We set bounds to the relevant couplings and masses and perform a constrained minimization of the $\chi^2$ for each model. In the minimization we bound the couplings of each model to a range of $\lambda \sim [-2, 2]$ so as to account for perturbativity and for the masses we set the lowest values to be $M_{S(F)} \geq 0.7\,\mathrm{TeV}$ to avoid issues with the EFT validity, since the lowest scale is the

| Model # | Field 1 | Field 2 | Tree Level |
|---|---|---|---|
| $SS_{101Y_2}$ | $S_a \to (1,1,0)$ | $S_b \to (1,1,Y_2)$ | $\mathcal{O}^{\phi\Box}$ |
| $SS_{102Y_2}$ | $S_a \to (1,1,0)$ | $S_b \to (1,2,Y_2)$ | $\mathcal{O}^{\phi\Box}$ |
| $SS_{103Y_2}$ | $S_a \to (1,1,0)$ | $S_b \to (1,3,Y_2)$ | $\mathcal{O}^{\phi\Box}$ |
| $SS_{302Y_2}$ | $S_a \to (1,3,0)$ | $S_b \to (1,2,Y_2)$ | $\mathcal{O}^{\phi\Box}$, $\mathcal{O}^{\phi D}$, $\mathcal{O}^{(e,u,d)\phi}$ |
| $SS_{303Y_2}$ | $S_a \to (1,3,0)$ | $S_b \to (1,3,Y_2)$ | $\mathcal{O}^{\phi\Box}$, $\mathcal{O}^{\phi D}$, $\mathcal{O}^{(e,u,d)\phi}$ |
| $SS_{1Y_1 2Y_2}$ | $S_a \to (1,1,Y_1)$ | $S_b \to (1,2,Y_1+1/2)$ | - |
| $SS_{2Y_1 1Y_2}$ | $S_a \to (1,2,Y_1)$ | $S_b \to (1,1,Y_1+1/2)$ | - |
| $SS_{2Y_1 3Y_2}$ | $S_a \to (1,2,Y_1)$ | $S_b \to (1,3,Y_1+1/2)$ | - |
| $SS_{3Y_1 2Y_2}$ | $S_a \to (1,3,Y_1)$ | $S_b \to (1,2,Y_1+1/2)$ | - |
| $SF_{101Y_2}$ | $S_a \to (1,1,0)$ | $F_b \to (1,1,Y_2)$ | $\mathcal{O}^{\phi\Box}$ |
| $SF_{102Y_2}$ | $S_a \to (1,1,0)$ | $F_b \to (1,2,Y_2)$ | $\mathcal{O}^{\phi\Box}$ |
| $SF_{103Y_2}$ | $S_a \to (1,1,0)$ | $F_b \to (1,3,Y_2)$ | $\mathcal{O}^{\phi\Box}$ |
| $SF_{302Y_2}$ | $S_a \to (1,3,0)$ | $F_b \to (1,2,Y_2)$ | $\mathcal{O}^{\phi\Box}$, $\mathcal{O}^{\phi D}$, $\mathcal{O}^{(e,u,d)\phi}$ |
| $SF_{303Y_2}$ | $S_a \to (1,3,0)$ | $F_b \to (1,3,Y_2)$ | $\mathcal{O}^{\phi\Box}$, $\mathcal{O}^{\phi D}$, $\mathcal{O}^{(e,u,d)\phi}$ |
| $FF_{1Y_1 2Y_2}$ | $F_a \to (1,1,Y_1)$ | $F_b \to (1,2,Y_1+1/2)$ | - |
| $FF_{2Y_1 1Y_2}$ | $F_a \to (1,2,Y_1)$ | $F_b \to (1,1,Y_1+1/2)$ | - |
| $FF_{2Y_1 3Y_2}$ | $F_a \to (1,2,Y_1)$ | $F_b \to (1,3,Y_1+1/2)$ | - |
| $FF_{3Y_1 2Y_2}$ | $F_a \to (1,3,Y_1)$ | $F_b \to (1,2,Y_1+1/2)$ | - |

*Table 3.4: Two field models, all singlets under SU(3), that can generate $C^{\phi(B,W,WB)}$. We have established the following naming convention for the models. Capital letters denote field content as described in the text. The first two subscript indices denote gauge quantum numbers under $SU(2)\times U(1)$ for the first field shown in column 2 (Field 1), while the last two denote the gauge quantum numbers under $SU(2)\times U(1)$ for the field in column 3 (Field 2). In the subscripts we refrain from denoting $SU(3)$ since all field under consideration are singlets under this gauge group. In columns 2 and 3, the full representation of the gauge group, under $SU(3)\times SU(2)\times U(1)$ is shown for the fields considered in the model of column 1. In total there are 18 candidate models.*

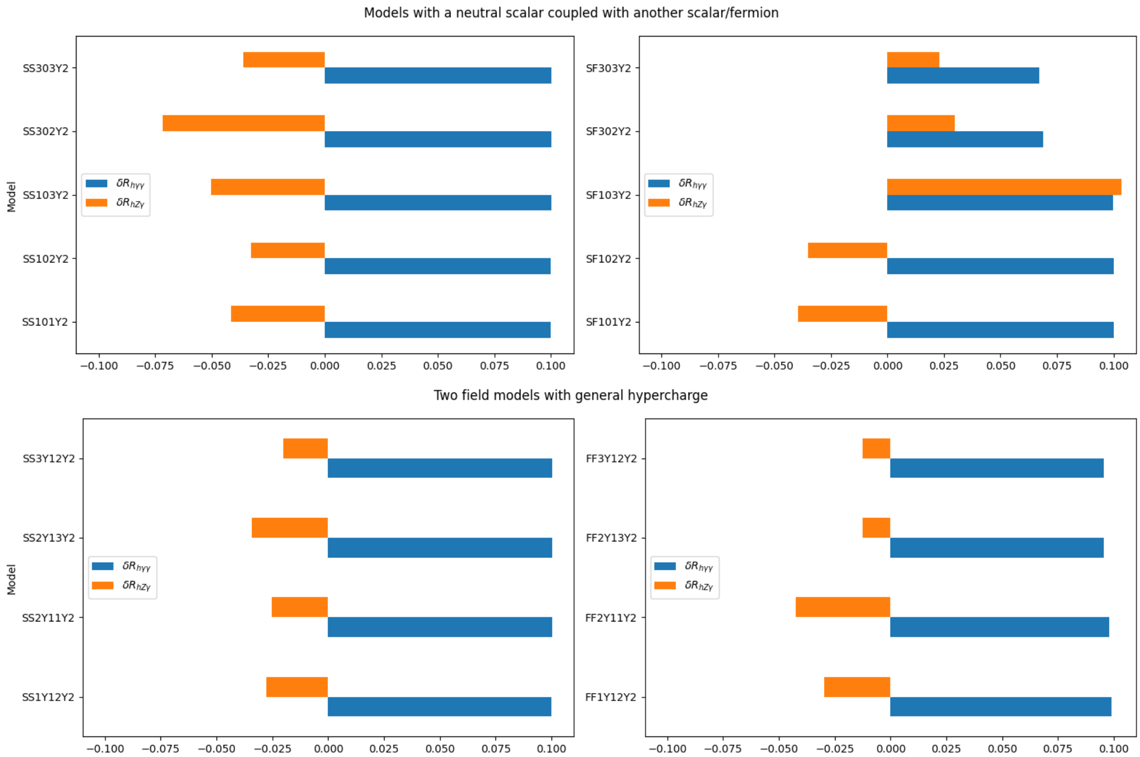


*Fig. 3.2: The orange color represents the prediction of $h \to Z\gamma$ for each model while blue represents the values of $h \to \gamma\gamma$ obtained from the minimization of the couplings and masses (in the non-degenerate limit).*

Higgs vev. In the models where the hypercharge relation obeys $Y_j = Y_i + 1/2$, the minimization with respect to the masses is more involved since there is also the degenerate mass limit that needs to be accounted for. In the non-degenerate case we restrict the mass difference to be greater than 0.1 TeV keeping of course the lowest bound of 0.7 TeV for both masses. We have also explored the degenerate mass limit, where in some cases we saw a slight improvement while in other cases we saw the gap between the two observables widen. Finally, we substitute the best fit values into $\delta R_{h\to Z\gamma}$ to get the models' prediction. The values of the corresponding Wcs at both tree and loop-level are matched with MatchMakerEFT [40] and, for exclusively loop generated operators, the expressions from MatchMakerEFT are also cross-checked with the package SOLD [121].

In Figure 3.2 we present the results of the minimization procedure along with the prediction of $h \to Z\gamma$ of each respective model and the value of $h \to \gamma\gamma$ obtained by this minimization. We observe that only one model predicts the value of $\delta R_{h\to Z\gamma}$ to be greater than that of $\delta R_{h\to\gamma\gamma}$. The only model capable to boost the one over the other observable, albeit with a negligible difference is $SF_{103Y_2}$, containing a neutral scalar singlet and a fermion triplet. The masses of the particles provided by the minimization subject to the constrains mentioned previously are for the scalar $M_S = 1.62$ TeV and for the fermion $M_F = 0.7$ TeV, with a hypercharge $Y_2 = 0$. The exact values of the prediction is $\delta R_{h\to\gamma\gamma} = 0.099$ and $\delta R_{h\to Z\gamma} = 0.104$. Their difference is of the order $\sim 0.5\%$ with respect to the SM signal strength $\mu = 1$ and with the assumptions we have made on the models it can never reach the observed difference of the two signal strengths.

## 3.5 Conclusions

Following the first evidence of the Higgs boson decaying into a photon and a Z-boson by the ATLAS and CMS collaborations, we addressed the reported excess of $\sim 2\sigma$ [119]. We conducted a model-independent analysis in the SMEFT, incorporating various observables in both the decay and production channels of the Higgs boson. By performing a $\chi^2$-minimization, we found the best-fit values for each Wilson coefficient. This procedure reveals the most general relations among the Wcs to account for any discrepancy. Our main finding is that the Wilson coefficients $C^{\phi B}$ and $C^{\phi W}$ need to have opposite signs and have comparable magnitudes, while $C^{\phi WB}$ needs to be small since it's heavily constrained by the $S$-parameter.

Using a model-independent approach, we identified the necessary characteristics that UV models must possess to account for the excess in $h \to Z\gamma$. We considered all scalar and fermion single-field extensions of the SM that respect the SM gauge group but found that none could accommodate the data. Subsequently, we examined two-field models combining scalars and/or fermions. The candidate models were categorized based on their content and their universal loop-integral coefficient using the UOLEA.

We matched all UV models using automated packages and constructed a new $\chi^2$ function, which we minimized with respect to model parameters. As shown in Figure 3.2, out of the 18 model families, only one specific model, which includes a neutral scalar singlet and a neutral fermion triplet, can boost $h \to Z\gamma$ while preserving the $h \to \gamma\gamma$ decay. However, this model still cannot fully accommodate the observed discrepancy in the data.

While our analysis primarily focused on scenarios where new physics can be integrated out and treated within the SMEFT framework, it is insightful to consider the possibility of going beyond the EFT approach. If the new particles are light, with masses comparable to the electroweak scale, they cannot be integrated out, and their effects must be treated explicitly in the theory. For instance, introducing a light scalar and a light fermion triplet directly into the SM would require us to consider their direct contributions to Higgs decays at the loop level. These particles could potentially contribute significantly to the $h \to Z\gamma$ while keeping the $h \to \gamma\gamma$ decay within experimental bounds. This approach necessitates extending the SM to include these particles explicitly and performing a detailed analysis of their impact on Higgs observables and other precision measurements, ensuring consistency with experimental constraints such as electroweak precision tests and flavor physics. While this is beyond the scope of the present study, it represents a promising avenue for future research that could potentially explain the observed excess in $h \to Z\gamma$ decay.

In summary, this study is valuable for providing the values and characteristics of Wcs capable of generating an enhancement in the decay channel $h \to Z\gamma$ over $h \to \gamma\gamma$. Moreover, the exploration of various two-field model families, surpassing the limitations of single-field models, provides insightful perspectives into potential UV physics behind this mild excess in $h \to Z\gamma$. If future data confirm this excess, our attention can pivot towards the investigation of alternative UV physics as the source of the discrepancy.

In the following chapter, we shift our focus to the flavor sector. Specifically, we investigate how the Minimal Supersymmetric Standard Model, can impact lepton flavor universality ratios like $R_K$ and $R_{K^*}$ in an exact manner making approximations only in the full 1-loop expansion of the theory. We aim to determine whether the MSSM can produce significant deviations in these ratios without conflicting with existing experimental constraints.

# Chapter 4

# The $R_K$ in the MSSM

We examine if the MSSM with a general flavour structure is capable of explaining the long-standing anomalies in $b \to s\ell^+\ell^-$ transitions, considering the latest LHCb measurements from 2022 where previous anomalies in the lepton flavor universality (LFU) ratios $R_K$ and $R_{K^*}$ have diminished. After carefully analyzing the potentially important supersymmetric contributions, we find that large effects can arise in the region of parameter space with a light wino, a light muon sneutrino, a relatively light left stop, and sizable mixing among left-handed squarks of the 2$^{\text{nd}}$ and 3$^{\text{rd}}$ generation. It is shown that even though the constraints from $B_s$–$\bar{B}_s$ mixing and $B \to X_s\gamma$ can be avoided, the maximal effect in $R(K^{(*)})$, taking into account LHC constraints, is below 5%. This chapter is based on unpublished work in collaboration with Andreas Crivellin, Athanasios Dedes and Janusz Rosiek.

## 4.1 Introduction

Building upon the methods and insights of previous Chapters, Chapter 4 shifts focus to another area where new physics may manifest: flavor-changing neutral currents (FCNCs) in semileptonic $b \to s\ell^+\ell^-$ transitions. These processes are highly sensitive to contributions from physics beyond the SM, making them excellent probes for new particles and interactions at the TeV scale. In particular, we examine the potential of the Minimal Supersymmetric Standard Model (MSSM) to account for observed anomalies in these transitions.

In the SM, FCNCs are highly suppressed due to the Glashow–Iliopoulos–Maiani (GIM) mechanism [138]. The GIM mechanism arises from the unitarity of the Cabibbo Kobayashi Maskawa (CKM) matrix and the specific structure of quark couplings to the weak interaction. It ensures that flavor-changing processes occur only at the loop level, with significant cancellations among contributions from different quark generations. Specifically, in the SM, the absence of tree-level FCNCs is a consequence of the universality of the weak interaction and the alignment of flavor eigenstates.

For the $b \to s\ell^+\ell^-$ transitions, the dominant SM contributions come from electroweak penguin and box diagrams involving the exchange of virtual $W$ and $Z$ gauge bosons as well as photons. The leading-order diagrams are loop-induced and involve internal top quarks and $W$ gauge bosons. Due to the GIM mechanism, contributions from different quark generations interfere destructively, leading to a suppression of the overall amplitude.

Importantly, these SM contributions are lepton flavor universal. This means that the interaction strength is the same for all three lepton flavors (electron, muon, and tau), aside from negligible effects due to differences in lepton masses. As a result, the SM predicts that the ratios should be very close to unity. The experimental measurements of these ratios thus provide a sensitive test of lepton flavor universality (LFU). Any significant deviation from $R_K = R_{K^*} = 1$ would indicate new physics that violates LFU.

Semileptonic $b \to s\ell^+\ell^-$ transitions have garnered significant attention in recent years due to observed tensions between experimental measurements and SM predictions. Notably, anomalies have been reported in observables such as the angular observable $P_5'$ [139–142] and the branching ratios of $B \to K\mu^+\mu^-$ and $B_s \to \phi\mu^+\mu^-$ [143–146]. These discrepancies suggest potential violations of lepton flavor universality (LFU), which is a key feature of the SM.

Previously, hints of LFU violation were also observed in the ratios $R(K)$ and $R(K^*)$, defined as:

$$R_K = \frac{\mathrm{Br}(B \to K\mu^+\mu^-)}{\mathrm{Br}(B \to Ke^+e^-)}\,, \tag{4.1}$$

$$R_{K^*} = \frac{\mathrm{Br}(B \to K^*\mu^+\mu^-)}{\mathrm{Br}(B \to K^*e^+e^-)}\,, \tag{4.2}$$

which were measured to deviate from the SM predictions. However, the latest measurements by the LHCb collaboration [147, 148] have shown these ratios to be consistent with the SM:

$$R_K^{\mathrm{LHCb}} = 0.949^{+0.042+0.022}_{-0.041-0.022}\,, \tag{4.3}$$

$$R_{K^*}^{\mathrm{LHCb}} = 1.027^{+0.072+0.027}_{-0.068-0.026}\,, \tag{4.4}$$

reducing the significance of LFU violation in these observables. Additionally, the latest measurement of $B_s \to \phi\mu^+\mu^-$ from CMS [149] is in agreement with the SM prediction [150]. Despite this, global fits still indicate tensions in the $b \to s\mu^+\mu^-$ sector, particularly in observables sensitive to the Wilson coefficient $C_9$ [151–154]. A multitude of studies have attempted to explain these anomalies through various extensions of the SM, including new gauge bosons ($Z'$) [155–160], leptoquarks [161–163], and loop effects from generic new physics [164–167]. Extensions of the MSSM have also been considered, such as the R-parity violating MSSM [168–170], gauge group extended MSSM [171–175], and the MSSM with right-handed neutrinos [176].

The discovery of the Higgs boson in 2012 at the Large Hadron Collider (LHC) [177, 178] provided a crucial confirmation of the SM but also raised questions about the stability of the electroweak scale against radiative corrections from higher energy scales. Supersymmetry, and specifically the MSSM [7, 179, 180], offers a solution by stabilizing the Higgs boson mass through the introduction of superpartners for each SM particle. Each superpartner has been introduced in Chapter 1, and more specifically Section 1.3. However, supersymmetric particles can introduce new sources of flavor violation that are not aligned with the SM flavor structure, potentially affecting FCNC processes. If these supersymmetric particles are not too heavy, they can be produced directly at the LHC and can lead to observable effects in precision measurements.

However, the question remains whether the minimal R-parity conserving MSSM, with a general flavor structure, can account for the observed anomalies in $b \to s\ell^+\ell^-$ transitions. Previous analyses have yielded conflicting conclusions: Ref.[181] suggested that no sizable effect is possible within the MSSM, while the more recent study in Ref.[182] claimed that substantial modifications of $R_K$ and $R_{K^*}$ can be achieved.

In this chapter, we aim to clarify the maximal possible size of new physics contributions to $b \to s\ell^+\ell^-$ transitions within the R-parity conserving MSSM. By employing the techniques discussed in previous chapters, we will analyze how the MSSM's additional particles and interactions can affect LFU observables, such as $R_K$ and $R_{K^*}$, as well as LFU-conserving observables sensitive to FCNCs.

We begin by introducing the operator basis of the Low Energy Effective Field Theory (LEFT) in Section 4.2, which is appropriate for energies below the electroweak scale. We review the extraction of the key observables $R_K$ and $R_{K^*}$ and discuss the relevant WCs within this framework. In Section 4.3, we perform a detailed phenomenological analysis using the `SUSY_FLAVOR` package [183–185]. We explore the parameter space of the MSSM, considering general sources of flavor violation, and evaluate the impact on $b \to s\ell^+\ell^-$ observables. We pay special attention to the constraints from other flavor processes and precision measurements to ensure the viability of the scenarios considered. Finally, in Section 4.4, we summarize our findings and discuss their implications for the MSSM and potential extensions. Appendix F provides the analytic formulas derived using the Flavour Expansion Theorem [186], supporting the calculations performed in the main text.

By applying the methods of EFT and matching procedures from earlier chapters, we extend our investigation of new physics effects beyond the Higgs sector to the flavor sector. The techniques of integrating out heavy particles and determining their contributions to low-energy observables through WCs are equally applicable here. This approach allows us to systematically assess the MSSM's capacity to account for the observed anomalies in $b \to s\ell^+\ell^-$ transitions and to identify the key parameters and interactions responsible for any potential effects.

Moreover, the complementary use of both top-down and bottom-up perspectives, as emphasized in previous chapters, enables us to explore the MSSM both as a UV-complete theory and through its low-energy effective interactions. This dual approach provides a comprehensive understanding of how supersymmetric particles might influence flavor observables and helps to elucidate the potential for discovering new physics in upcoming experiments.

This chapter thus serves as a continuation of our exploration into the ways in which EFTs and matching techniques can be utilized to probe physics beyond the SM, as were exemplified in Chapters 2 and 3. By focusing on the flavor sector and the MSSM, we aim to shed light on one of the most intriguing areas in particle physics, where hints of new physics continue to emerge and challenge our understanding of fundamental interactions.

## 4.2 Results

### 4.2.1 Operator Bases

Taking into account the LHC constraints [187], we can safely assume that the sparticles are much heavier than the $B$-meson mass and use an effective Lagrangian for $b \to s\ell^{K+}\ell^{K-}$ ($\ell^K = e, \mu, \tau$ for $K = 1, 2, 3$) transitions, which is usually written as [188],

$$\mathcal{L}_{\text{eff}} = \frac{4G_F}{\sqrt{2}} V_{ts}^* V_{tb} \frac{e^2}{16\pi^2} \sum_{i,K} C_i^{K(\prime)} \mathcal{O}_i^{K(\prime)} . \tag{4.5}$$

Here $V_{ij}$ are the CKM matrix elements, $G_F = 1/(\sqrt{2}v^2)$ is the Fermi coupling constant (with $v \approx 246\,\text{GeV}$), $e$ the electric charge and $C_i^{(\prime)}(\mu)$ the Wilson coefficients of the corresponding dimension-6 operators $O_i^{(\prime)}(\mu)$. We will match the MSSM on this effective theory at the scale $\mu = M_W$ (thus neglecting RGE effects from the SUSY to the EW scale) and then evolve the coefficients down to the scale $\mu \sim m_b$ of the processes. Since we are focusing primarily on $R_{K,K^{*0}}$ observables, the relevant operators in Eq. (4.5) are [189–191]

$$\mathcal{O}_9^{K(\prime)} = \left(\bar{s}\gamma_\mu P_{L(R)} b\right)\left(\bar{\ell^K}\gamma^\mu \ell^K\right) , \qquad \mathcal{O}_{10}^{K(\prime)} = \left(\bar{s}\gamma_\mu P_{L(R)} b\right)\left(\bar{\ell^K}\gamma^\mu\gamma_5 \ell^K\right) . \tag{4.6}$$

Note that we did not consider scalar operators here, which, due to their enhanced effect in $B_s \to \mu^+\mu^-$ [192–195] are not capable of given a sizable effect in $R_{K,K^{*0}}$ [196]. This means that we will also disregard the Higgs effects in the MSSM and thus work in the low $\tan\beta$ limit.

Most MSSM calculations have been carried out with the use of chiral basis of Ref. [197]

$$\mathcal{L}_{\text{eff}} = -\frac{1}{16\pi^2} \sum_{X,Y=L,R} C_{VXY}\, O_{VXY} , \tag{4.7}$$

more natural for this model. Writing down explicitly the flavour indices ($I, J$ for quarks and $K, L$ for leptons), one has

$$\mathcal{O}_{VXY}^{IJKL} = \left(\bar{q}^J \gamma^\mu P_X q^I\right)\left(\bar{\ell}^L \gamma_\mu P_Y \ell^K\right) . \tag{4.8}$$

Exemplifying the notation, the coefficient $C_{VLL}^{3222}$ multiplies the operator $(\bar{s}\gamma_\mu P_L b)(\bar{\mu}\gamma^\mu P_L \mu)$ and so on. By comparing Eq. (4.7) to Eq. (4.5) we obtain the respective relation of Wilson coefficients in both bases (with $\lambda = -4G_F e^2 V_{ts}^* V_{tb}/\sqrt{2}$),

$$C_9^K = \frac{1}{2\lambda}\left(C_{VLR}^{32KK} + C_{VLL}^{32KK}\right), \tag{4.9}$$

$$C_9^{K\prime} = \frac{1}{2\lambda}\left(C_{VRL}^{32KK} + C_{VRR}^{32KK}\right), \tag{4.10}$$

$$C_{10}^K = \frac{1}{2\lambda}\left(C_{VLR}^{32KK} - C_{VLL}^{32KK}\right), \tag{4.11}$$

$$C_{10}^{K\prime} = \frac{1}{2\lambda}\left(C_{VRR}^{32KK} - C_{VRL}^{32KK}\right). \tag{4.12}$$

Note that numerically $1/(2\lambda) \approx 3.7\times 10^6$ GeV$^{-2}$. For example, a quick estimate for $|C_9| \sim O(1)$ with $|C_{VLL}^{3222}| \sim e^4 \delta_{23}/M_{SUSY}^2$ results in soft SUSY breaking masses of about $M_{SUSY} \lesssim 300$ GeV, with maximal flavour squark mixing (defined as the ratio of off-diagonal to diagonal entries in squark mass matrix) $\delta_{23} \sim O(1)$. This naive estimate shows that there is a need for a careful examination of the size of one-loop MSSM contributions, as well as of the current experimental constraints from indirect and direct SUSY searches on MSSM parameter space.

### 4.2.2 Observables

Following Ref. [189], the contributions to $R_K$ and $R_{K^*}$ can be (approximately) captured by the interference terms between SM and the MSSM contributions ($\Delta_\pm$) as well as by pure MSSM ones ($\Sigma_\pm$),

$$R_K \simeq 1 + \Delta_+ + \Sigma_+ , \tag{4.13}$$

$$R_{K^{*0}} \simeq 1 + p(\Delta_- - \Delta_+ + \Sigma_- - \Sigma_+) + \Delta_+ + \Sigma_+ , \tag{4.14}$$

where

$$\Delta_\pm = 2\,\mathrm{Re}\left[\frac{C_{VLL}^{\mu} \pm C_{VRL}^{\mu}}{C_{VLL}^{\mathrm{SM}}} - (\mu \to e)\right], \tag{4.15}$$

$$\Sigma_\pm = \frac{|C_{VLL}^{\mu} \pm C_{VRL}^{\mu}|^2 + |C_{VLR}^{\mu} \pm C_{VRR}^{\mu}|^2}{|C_{VLL}^{\mathrm{SM}}|^2} - (\mu \to e). \tag{4.16}$$

Some remarks regarding the simplification of our notation are in order. The Wilson coefficient $C_{VLL}^{\mathrm{SM}}$ refers to the SM contribution $C_{VLL}^{3222}$ (in the SM this is equal to $C_{VLL}^{3211}$) while coefficients like $C_{VLL}^{\mu}$ are *pure* supersymmetric contributions, e.g. $C_{VLL}^{\mu} \equiv C_{VLL}^{3222\,(\mathrm{SUSY})}$. The parameter $p$ in Eq. (4.14) is the polarization fraction of transverse parallel and longitudinal contributions to $B \to K^* \ell^+ \ell^-$ and its value is close to unity - for our numerical analysis, we will use $p \simeq 0.86$ [198]. As from Eq. (4.15) it is clear that any CP-violating effects will only maginally affect the MSSM predictions for $R_K$ and $R_{K^{0*}}$, we will assume real SUSY parameters throughout this chapter.[1]

[1] Although in our numerical analysis we shall use the full expressions of Eqs. (4.13) and (4.14), a less precise (up to 10% error) approximation is to assume that NP contributions are much smaller w.r.t. SM ones and ignore $\Sigma_\pm$, further set $p = 1$ and therefore get $R_K \approx 1 + \Delta_+$ and $R_{K^{*0}} \approx 1 + \Delta_-$.

### 4.2.3 Analytical SUSY contributions

In the MSSM, contributions to $R_{K,K^{*0}}$ arise at one-loop level, like in the SM. The full expressions for the coefficients $C_{VXY}$, using exact diagonalization of the mass matrices, have been presented in Ref. [197] (except for the photon-mediated diagram $F_{\gamma L,R}$ listed here in Appendix F). These contributions can be decomposed as

$$C_{VLL}^{IJKL} = B_{VLL}^{IJKL} - \frac{e(1-4s_W^2)}{2s_W c_W M_Z^2}\delta^{KL}\left(F_{ZL}^{JI} - \frac{e(1-2s_W^2/3)}{2s_W c_W}\left(\Sigma_{dV}^{JI} - \Sigma_{dA}^{JI}\right)\right) + e^2 F_{\gamma L}^{JI}\delta^{KL}\,, \tag{4.17}$$

$$C_{VLR}^{IJKL} = B_{VLR}^{IJKL} + \frac{e\,s_W^2}{s_W c_W M_Z^2}\delta^{KL}\left(F_{ZL}^{JI} - \frac{e(1-2s_W^2/3)}{2s_W c_W}\left(\Sigma_{dV}^{JI} - \Sigma_{dA}^{JI}\right)\right) + e^2 F_{\gamma L}^{JI}\,\delta^{KL}\,, \tag{4.18}$$

$$C_{VRR}^{IJKL} = B_{VRR}^{IJKL} + \frac{e\,s_W^2}{s_W c_W M_Z^2}\delta^{KL}\left(F_{ZR}^{JI} + \frac{e s_W}{3c_W}\left(\Sigma_{dV}^{JI} + \Sigma_{dA}^{JI}\right)\right) + e^2 F_{\gamma R}^{JI}\delta^{KL}\,, \tag{4.19}$$

$$C_{VRL}^{IJKL} = B_{VRL}^{IJKL} - \frac{e\,(1-2s_W^2)}{2s_W c_W M_Z^2}\delta^{KL}\left(F_{ZR}^{JI} + \frac{e s_W}{3c_W}\left(\Sigma_{dV}^{JI} + \Sigma_{dA}^{JI}\right)\right) + e^2 F_{\gamma R}^{JI}\delta^{KL}\,, \tag{4.20}$$

containing the contributions from box-diagrams ($B_{VXY}$), $Z$-penguins ($F_{ZL(R)}$), and off-shell photon-penguins ($F_{\gamma L(R)}$). Note that while the $Z-$ and photon-contributions affect in general $b \to s\ell^+\ell^-$ transitions, their effect in $R_{K,K^{*0}}$ drops out, in eqs. (4.15), as they are lepton flavour universal.

#### Chargino box contributions

The box diagram containing chargino-squark-sneutrino in the loop gives

$$(B_{VLL}^{IJKL})_C = \frac{e^2}{4s_W^2} Z_+^{1n} Z_+^{1m*}\, Z_{\tilde{\nu}}^{LN} Z_{\tilde{\nu}}^{KN*}\, V_{dUC,L}^{Jln*}\, V_{dUC,L}^{Ilm}\, D_2(m_{C_m}^2, m_{C_n}^2, m_{U_l}^2, m_{\tilde{\nu}_N}^2)\,, \tag{4.21}$$

where the quark-chargino-up-squark vertices are defined in Appendix F, Eq. (F.6), with $Z_+, Z_{\tilde{\nu}}, Z_U$ being the rotation matrices diagonalizing the chargino, sneutrino, and up-squark mass matrices, respectively. We consistently follow the notation for vertices from Refs. [199, 200] where $K$ is defined to be the CKM-matrix and $D_2$ is a loop function, defined in Appendix G, eq. (G.2), with the arguments, $m_{C_n}, m_{U_l}, m_{\tilde{\nu}_N}$ being the physical masses of charginos, up-squarks and sneutrinos, respectively.

However, from Eq. (4.21) it is difficult to understand the origin and importance of the effects. To that end, a very useful method, called Flavour Expansion Theorem (FET), has been developed in Ref. [186] which algebraically connects the amplitudes calculated in the mass basis of a Lagrangian to the corresponding expressions in the gauge-basis without performing any diagrammatic calculations. We note here that, especially for the chargino box diagrams, after expanding each term in mass-Insertions (MIs) in first order using FET *we are only left with the* $(B_{VLL})_C$ *terms*. The other terms, $(B_{VLR})_C, (B_{VRL})_C$, and $(B_{VRR})_C$, in the expansion are suppressed by higher powers of quark masses or are of higher MI order. Therefore, we will use $(B_{VLR})_C \approx 0$ below.

By expanding (4.21) using the FET to the first order in MI approximation we obtain (summation over repeating generation indices is always assumed in all subsequent formulae, even if they repeat more than two times)

$$(B^{IJKL}_{VLL})_C = \frac{e^4}{4s_W^4} K^{NJ*} K^{NI}\, \delta_{KL}\, D_2(\,|M_2|^2, |M_2|^2, (\mathcal{M}_U^2)^N_{LL}, (\mathcal{M}_\nu^2)^K\,) \tag{4.22}$$

$$+ \frac{e^4}{4s_W^4} K^{NJ*} K^{MI}\, \delta_{KL}\, (\widehat{\mathcal{M}}_U^2)^{NM}_{LL}\, E_2(|M_2|^2, |M_2|^2, (\mathcal{M}_U^2)^N_{LL}, (\mathcal{M}_U^2)^M_{LL}, (\mathcal{M}_\nu^2)^K) \tag{4.23}$$

$$+ \frac{e^4}{4s_W^4} K^{NJ*} K^{NI}\, (\widehat{\mathcal{M}}_\nu^2)^{KL}\, E_2(|M_2|^2, |M_2|^2, (\mathcal{M}_U^2)^N_{LL}, (\mathcal{M}_\nu^2)^K, (\mathcal{M}_\nu^2)^L)\,, \tag{4.24}$$

where $M_2$ is the wino mass, $(\mathcal{M}_U^2)_{LL}$ the left-handed $3\times 3$ up-squark squared mass matrix[2] and $(\mathcal{M}_\nu^2)$ the sneutrino squared mass matrix.[3] Following the notation of Ref. [186], in (4.24) and throughout the rest of chapter the hatted mass-matrices contain only off-diagonal elements, i.e. have zeros in the diagonal. Finally, $D_2$ and $E_2$ are loop functions defined in (G.2) and (G.3), respectively.

The first line in Eq. (4.22), contains only CKM effects which is typical in mSUGRA scenarios leading to so-called Minimal Flavor Violating (MFV) version of the MSSM. The second line of Eq. (4.23) contain squark-mass mixing effects, which is typical in a general flavour MSSM scenario. The last line, Eq. (4.24), contains only Lepton-Flavour Violating (LFV) effects, absent for $R_K$ or $R_{K^{*0}}$ but certainly contributing to decays like $B \to \mu e$ or $B \to \mu\tau$ [201] – they have been written here just for complimentary reasons, connecting to the idea of correlations between lepton flavor conserving and flavor violating decays [202].

In order to have sizable deviations of $R_K$ or $R_{K^{*0}}$ from unity we need to have a large mismatch of contributions between the electrons and muons in the final state, i.e. $B^{3222}_{VLL} - B^{3211}_{VLL} \approx B^{3222}_{VLL}$, as an effect with opposite sign is not possible, and non-universal sneutrino masses are required (also due to the bounds from $\mu \to e\gamma$ [203]). This is a non-common situation and is associated with the supersymmetry breaking scenario at hand. It can certainly not be a gauge-mediated or an anomaly mediated soft susy-breaking scenario, i.e., $(\mathcal{M}_\nu^2)^1 >> (\mathcal{M}_\nu^2)^2$ or $(\mathcal{M}_\nu^2)^2 >> (\mathcal{M}_\nu^2)^1$.

In order to grasp the effect, let's assume, without loss of generality regarding the maximal effect on $R_K$, the former limit together with the case (forbidden by Tevatron and LHC) of light squarks, $(\mathcal{M}_U)^K_{LL} \sim v$, where $v$ is the Higgs vev. The SUSY contributions are normally small (they are loop induced) therefore it is enough to keep the linear term in $R_K$, i.e, $R_K \approx 1 + \Delta_+$. By plugging into the result for $B^{3222}_{VLL}$ from (4.22), and set the SM value for $C_9^{\rm SM} = 4.2$, for the chargino contribution we get in the MFV-like scenario, i.e. for the vanishing squark flavor mass insertions

$$R_{K,K^{*0}}(\chi^\pm)\big|_{\rm MFV} \approx 1 - 0.02 \left(\frac{v}{M_{SUSY}}\right)^2 , \tag{4.25}$$

where we took, just for estimate purposes, equal masses for particles in the loop, $D_2(x,x,x,x) = 1/(3x^2)$. Even in the hypothetical scenario of SUSY masses at the EW scale, the chargino loop with only CKM flavour effects and large hierarchy of sleptons (or squarks) are similar to the theoretical error [204] from just the SM QED corrections! Concluding, squark flavour blind MSSM gives, to a good approximation, ignorable contributions to $R_K$ and $R_{K^{0*}}$.

[2] The subscript "LL" in $(\mathcal{M}_U^2)_{LL}$ is part of its name, not summed indices.

[3] As long as the neutrinos are massless, $\mathcal{M}_\nu^2$ equals $\mathcal{M}_L^2$ appearing later, *c.f.* Eq. (4.30), in neutralino expansion.

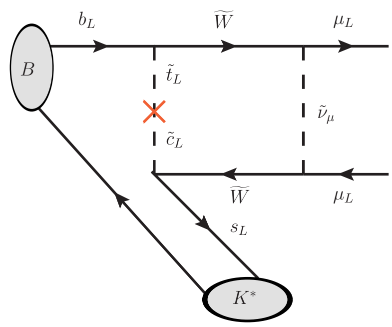


*Fig. 4.1: The main supersymmetric diagram contributing to $R_K$ and $R_{K^{*0}}$.*

Let's now examine the contributions of (4.23) and take heavy (say few TeV) and common diagonal up squark mass matrix elements, $(\mathcal{M}_U^2)_{LL}^K = M_{\rm SUSY}^2$ but at the same time a comparably large off-diagonal $(\mathcal{M}_U^2)_{LL}^{23}$ matrix element. In such case, all but one eigenvalues stay heavy while the smallest one (we call it light stop mass[2], $m_{\tilde{t}}^2$) can become very small. Of course in this case one has to resume higher order corrections in FET until convergence reached. In practice, one can prove[4] that this can be easily achieved by replacing the diagonal squark masses in gauge basis, $(\mathcal{M}_U)_{LL}^K$, by their physical (mass-basis) eigenvalues, $m_{\tilde{t}_i}$. For $m_{\tilde{t}} \sim M_2 \sim (\mathcal{M}_\nu)^{22} \ll (\mathcal{M}_U^2)_{LL}^K \sim (\mathcal{M}_{\tilde{\nu}})^{11}$, we find,

$$R_{K,K^{*0}}(\chi^\pm)\big|_{\rm MSSM} \approx 1 - \frac{\pi \alpha_{em}}{6 s_W^4} \frac{\delta_{LL}^{23}}{|K_{ts}^* K_{tb}|} \frac{v^2}{m_{\tilde{t}}^2} \frac{1}{C_9^{\rm SM}} \approx 1 - 0.4 \left(\frac{v^2}{m_{\tilde{t}}^2}\right) \delta_{LL}^{23} \,, \tag{4.26}$$

where we have defined the squark mixing parameter as

$$(\delta_U)_{LL}^{23} = \delta_{LL}^{23} = \frac{(\mathcal{M}_U^2)_{LL}^{23}}{(\mathcal{M}_U^2)_{LL}^K} \,. \tag{4.27}$$

In (4.26) we used the fact that $E_2(x,x,y,x,x) \simeq 1/(3x^2y^2)$ for $y \gg x$. Now the corrections are by a factor of 200 bigger than before for $\delta_{LL}^{23} \sim 1$. The real reason behind this enhancement is that now the squark mixing parameter $\delta_{LL}^{23}$ in (4.26) is divided by the small product of CKM matrices $|K_{ts}^* K_{td}| \approx 0.04$. The value $\delta_{LL}^{23} \approx 1$, is of course a maximal limit (otherwise we have a tachyonic squark!). In fact, as we shall see next, eq. (4.26), the chargino-stop-muon sneutrino box diagram shown in Fig. 4.1, is the dominant contribution to $R_K$.

#### Neutralino box contributions

The neutralino - down squark - slepton box diagram gives for $C_{VLL}$ in (4.17) [197]:

$$\begin{aligned}(B_{VLL}^{IJKL})_N = &+ \frac{1}{4} V_{dDN,L}^{Jln*} V_{dDN,L}^{Ilm} \, V_{lLN,L}^{Lom*} V_{lLN,L}^{Kon} \, D_2(m_{N_m}^2, m_{N_n}^2, m_{D_l}^2, m_{L_o}^2) \\ &+ \frac{1}{2} V_{dDN,L}^{Jln*} V_{dDN,L}^{Ilm} \, V_{lLN,L}^{Lon*} V_{lLN,L}^{Kom} \, m_{N_m} m_{N_n} \, D_0(m_{N_m}^2, m_{N_n}^2, m_{D_l}^2, m_{L_o}^2) \,,\end{aligned} \tag{4.28}$$

where $D_0$ and $D_2$ are loop functions defined in (G.1) and (G.2) with arguments physical masses, $m_{N_m}, m_{D_l}, m_{L_o}$ for neutralinos, down-squarks and sleptons, respectively. The corresponding interaction vertex $V_{dDN,L}$ is defined in (F.8) and

$$V_{lLN,L}^{Iij} = \frac{e}{\sqrt{2} s_W c_W} Z_L^{Ii} \left( Z_N^{1j} s_W + Z_N^{2j} c_W \right) + Y_l^I Z_L^{(I+3)i} Z_N^{3j} \,, \tag{4.29}$$

[4] In the case of Hermitian matrix that contains $2\times2$ block diagonal sub-matrices one can resume MI to all orders and arrive at this result. A. Dedes, *unpublished notes*.

with $Z_N, Z_D, Z_L$ being rotation matrices from flavour to mass basis as given in Ref. [199, 200]. By neglecting the terms proportional to small down quark masses and terms diagonal in squark flavour (which are negligible following our discussion that led to eq. (4.25)) the FET expanded result is[5],

$$
\begin{aligned}
(B_{VLL}^{IJKL})_N = &\frac{e^4}{48 c_W^4 s_W^4}\,\delta^{KL}(\widehat{\mathcal{M}_D^2})^{IJ}_{LL} \\
&\Big\{9c_W^4\Big[E_2(|M_2|^2,|M_2|^2,(\mathcal{M}_D^2)^I_{LL},(\mathcal{M}_D^2)^J_{LL},(\mathcal{M}_L^2)^K_{LL}) \\
&-\frac{2}{3}D_0(|M_2|^2,(\mathcal{M}_D^2)^I_{LL},(\mathcal{M}_D^2)^J_{LL},(\mathcal{M}_L^2)^K_{LL})\Big] \\
&+s_W^4\Big[E_2(|M_1|^2,|M_1|^2,(\mathcal{M}_D^2)^I_{LL},(\mathcal{M}_D^2)^J_{LL},(\mathcal{M}_L^2)^K_{LL}) \\
&-\frac{2}{3}D_0(|M_1|^2,(\mathcal{M}_D^2)^I_{LL},(\mathcal{M}_D^2)^J_{LL},(\mathcal{M}_L^2)^K_{LL})\Big] \\
&-2s_W^2c_W^2\Big[2\mathrm{Re}(M_1M_2^*)E_0(|M_1|^2,|M_2|^2,(\mathcal{M}_D^2)^I_{LL},(\mathcal{M}_D^2)^J_{LL},(\mathcal{M}_L^2)^K_{LL}) \\
&\quad+E_2(|M_1|^2,|M_2|^2,(\mathcal{M}_D^2)^I_{LL},(\mathcal{M}_D^2)^J_{LL},(\mathcal{M}_L^2)^K_{LL})\Big]\Big\}\,.
\end{aligned}
\tag{4.30}
$$

Notice that for neutralinos, it is down-squark off-diagonal matrix elements $(\widehat{\mathcal{M}_D^2})^{32}_{LL}$ that matter. Out of the terms in the square brackets in (4.30), the first one seems to be the dominant because of the prefactor $9c_W^4$ relative to the others that have the suppression of $s_W^2c_W^2$ (or even worse, $s_W^4$). However, there is a leading order cancellation between the PV-functions when we replace their arguments with physical squark masses as we did before, that is

$$
E_2(x,x,x,y,x)-\frac{2}{3}D_0(x,x,y,x)\simeq\frac{1}{3y^4}\left[\frac{5}{2}-\log(\frac{y^2}{x^2})\right]\,,\qquad y\gg x\,. \tag{4.31}
$$

This $1/y^4$ behaviour is effectively of a higher order than the chargino one which scales like $\sim 1/(x^2y^2)$. Therefore, *neutralino box-diagrams are not really enhanced even for extreme squark mass mixing*. We shall check this conclusion numerically below (*c.f.* Fig. 4.2).

Moreover, in the case of neutralinos there are also contributions from $B_{VRL}$ even at first order in FET expansion. These enter at the leading order in the expressions for $R_K$ and $R_{K^{*0}}$, (4.13) and (4.14) respectively, and have to be analyzed. We find (neglecting terms suppressed by down quark masses) that,

$$
\begin{aligned}
B_{VRL}^{IJKL} = &-\frac{e^4\delta^{KL}}{12c_W^4 s_W^2}(\widehat{\mathcal{M}_D^2})^{IJ}_{RR}\big[E_2(|M_1|^2,|M_1|^2,(\mathcal{M}_D^2)^I_{RR},(\mathcal{M}_D^2)^J_{RR},(\mathcal{M}_L^2)^K_{LL}) \\
&-\frac{2}{3}D_0(|M_1|^2,(\mathcal{M}_D^2)^I_{RR},(\mathcal{M}_D^2)^J_{RR},(\mathcal{M}_L^2)^K_{LL})\Big]\,.
\end{aligned}
\tag{4.32}
$$

The relevant to $R_K$ contribution is now proportional to RH squark mixing, $(\widehat{\mathcal{M}_D^2})^{23}_{RR}$ but its contribution to $B_{VRL}^{IJKL}$ are again naturally tiny because of the cancellation (4.31). Additionally, there is now a division of loop functions by a factor of, $12s_W^2$ whereas the chargino diagram is divided by $4s_W^4$.

This smallness of LR terms is important for the correlation between observables $R_K$ and $R_{K^{0*}}$: since $C_{VRL}\approx 0$ we conclude from (4.15) that $\Delta_+\approx\Delta_-$. Furthermore, from Eqs. (4.13)

[5] We used the code MassToMI [205] in applying FET to all analytical formulae of [197]. We are only focusing on potentially large effects here and avoid displaying long expressions with subdominant contributions.

and (4.14) we conclude that *the observables $R_K$ and $R_{K^{0*}}$ in MSSM are predicted to be equal to a good approximation (in EFT language, we could say up-to dimension* 8 *contributions)*. Therefore, from now on, we only focus on the results for the $R_K$.

#### Charged-Higgs box contributions

There are no box diagram contributions with charged-Higgs and $u$-quark to $B_{VLL}$ and $B_{VRL}$ and therefore to $R_K$ in leading approximation (4.15). There are however, universal contributions to $B_{VLR}$ and $B_{VRR}$ contributing to $C_9^{(\prime)}$ and $C_{10}^{(\prime)}$. All these contributions are suppressed by small lepton Yukawa couplings.

#### Summary of SUSY contributions to $R_K$

Out of all complicated box diagrams relevant to $R_K$ observables in the MSSM, only the chargino one, shown in Fig. 4.1, is qualified to produce significant effects (i.e. more than few percent) and only to $C_{VLL}$ coefficient. Although eq. (4.26) is an extreme limit, the seemingly large contribution to $R_K$ (perhaps also to $C_9$ via eq. (4.10)) encourages us to proceed further by checking its compatibility with direct and indirect searches. Before going to the exact numerical results lets summarize our strategy in getting maximal $R_K$ ($\approx R_{K^{*0}}$):

- Large mass hierachy between the muon sneutrino and the electron sneutrino,
- Large left up-squark mixing, $\delta_{LL}^{23}$, of order $\mathcal{O}(1)$,
- Wino, stop and a muon sneutrino masses as close as allowed by the experimental searches to the EW scale.

## 4.3 Phenomenological analysis

### 4.3.1 Direct SUSY searches

It is important to note that the dominant SUSY effect in $R_{K^*}$, see Eq. (4.26), does not depend on the Higgsino mixing parameter $\mu$, nor the Bino mass $M_1$. Therefore, one can use these parameters as “jockers" in evading some experimental constraints, such as searches for electroweak SUSY particles. Moreover, the parameters of the Higgs sector, such as the CP-odd Higgs mass $M_A$, the ratio of the two vevs $\tan\beta$, the holomorphic or non-holomorphic trilinear soft breaking couplings $A_t$ and $A'_t$, do not enter in MSSM's $R_K$ at leading order: they can be used however to set the light Higgs boson mass to the experimental value, $m_h \approx 125$ GeV. For the figures below, we have chosen, $\tan\beta = 5, M_A = 2$ TeV as reference values.

Recent ATLAS searches [206] for long-lived charginos based on disappearing track signatures reveal that chargino masses up to 660 (210) GeV are excluded in scenarios where the chargino is a pure wino (higgsino). In addition, the same analysis excludes chargino masses below 300 GeV for a gluino mass below 2.1 TeV. These two suggest heavy gluino and bino LSP. However, the process most important to us is the Wino/Bino like case where there is a direct production of $\chi_1^\pm \chi_2^0$ where $\chi_1^\pm$ and $\chi_2^0$ are mass-degenerate (pure) Winos and $\chi_1^0$ is a pure bino state. Then they further decay as $\chi_1^\pm \to W^\pm \chi_1^0$ and $\chi_2^0 \to Z\chi_1^0$. This decay pattern has been studied in Ref. [207]. We adopt the mass parameters, for $M_1 = 0.1$ TeV, $M_2 = 0.2$ TeV which are allowed in this compressed spectrum. For $M_2 \gtrsim 350$ GeV, this area is easily allowed but the predicted $R_K$ turns out to be 2-3% smaller than the case of $M_2 = 200$ GeV which we adopt as a eference value in the figures below.

Furthermore, the gluino mass is taken to be $m_{\tilde{g}} = 2.5$ TeV, consistent with ATLAS and CMS searches [208]. The Higgsino mass parameter is crucial for $b \to s\gamma$ as we shall see below in section 4.3.2. We choose two cases: $\mu = 0.5$ TeV [*c.f.* Fig. 4.2] and $\mu = 3$ TeV [*c.f.* Fig. 4.3].

Another parameter of interest for $R_K$ is the left-handed muon sneutrino mass (to a good approximation equal to the left-handed smuon mass). This is constrained from early LHC studies [209] from $\tilde{\mu}_L^- \to \mu^-\chi_1^0$ decay to be approximately above 300 GeV. First generation sleptons, the selectrons, must be much heavier in order to obtain appreciable impact on $R_K \neq 1$. Therefore, in our numerics below, we choose large mass hierarchy between first and second generation of sleptons, $(\mathcal{M}_\nu)^{K=1,3} = 3$ TeV and $(\mathcal{M}_\nu)^{K=2} = 0.3$ TeV, respectively.

As we showed before in (4.26), big effects on $R_K$ arise because of large $\delta_{LL}^{23} \sim 1$ and because at this limit the light stop runs quickly towards a zero mass. Direct production of the light top squark through gluon exchange is not affected by the mixing. The most relevant to us here is the decay mode of the light top-squark to chargino and bottom quark, $\tilde{t}_1 \to b + \chi_1^+$. The chargino then decays to the neutralino LSP and an off-shell $W$-boson, $\chi_1^+ \to W^{+(*)} + \chi_1^0$. Within pMSSM assumptions used in the ATLAS analysis [210] and $m_{\chi_1^0} = m_{\chi_1^\pm}$, it is highly unlikely there is a (left) top-squark mass below 550 GeV. A CMS analysis [211], goes even higher in top-squark masses. In this study, the flavour changing stop decay, $\tilde{t} \to c + \chi_1^0$ has been also searched for. The bounds this time are in the vicinity of 1.2 TeV or so. However, in a very recent complementary analysis, ATLAS searches for top squark pair production exclude top squark masses up to 1.25 TeV, considering different decay channels, which can be seen from Fig. 2 in ref. [212]. We must however note that, to the best of our knowledge, there are no dedicated top squark mass bound analyses in terms of the MSSM with $\mathcal{O}(1)$-mixing between 2nd and 3rd generation. We therefore, choose a common scale for the left-up squark masses at 2.5 TeV and vary the squark mixing parameter, $\delta_{LL}^{23}$ of (4.27) in the region [-1:1] while forbidding light stop masses with $m_{\tilde{t}} \lesssim 1.25$ TeV.

When $\delta_{LL}^{23} \approx 1$ the left sbottom mass is also running to small values, as the light stop mass does. LHC searches [213, 214] on direct bottom squark production and subsequent decays $\tilde{b} \to b + \chi_1^0$ reveal a bound of approximately 1.4 TeV. However, the light stop bound is saturated first, and therefore we plot exclusion area only from stop searches in our figures.

The MSSM prediction[6] for $R_K$ when varying the squark mixing parameter $\delta_{LL}^{23}$ and other parameters optimized as discussed above is given in Fig. 4.2. As displayed in this figure, the neutralino loop contribution is small (as we analytically proved before), never exceeding a few percent. The dominant contribution comes from the chargino-up squark loop and the effect on $R_K$ can be as large as $\pm 25\%$ for the aforementioned input set of parameters and before experimental constraints on top-squark. $R_K$ is very sensitive to the value of $M_2$: for example, taken a wino-LSP with the bound of 660 GeV we observe negligible deviations from $R_K = 1$. Similar effects arise when varying the smuon mass parameter. The choice of the MSSM parameter space we adopt here should be regarded as an optimum for large SUSY effects on the $R_K$ observable.

The increase of squark mixing $|\delta_{LL}^{23}|$ in (4.27), increases the (23) element of the left-squark

[6] We use `SUSY_FLAVOR (v2.54)`-code [183–185] throughout. This code takes carefully into account the convergence and ressumation effects in $b \to s\gamma$ due to large squark mixing.

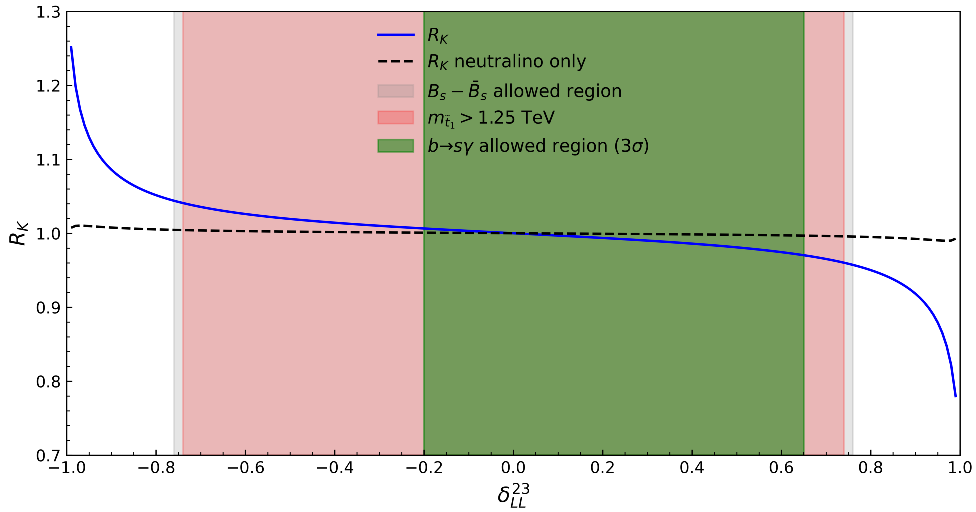


*Fig. 4.2: $R_K$ vs. left-squark mass mixing, $\delta_{LL}^{23}$ defined in eq. (4.27), with $M_2 = 200$ GeV and $\mu = 0.5$ TeV. The blue line is the full MSSM prediction to $R_K$ whereas the black line indicates only the neutralino contribution. The light red area corresponds to $m_{\tilde{t}} \gtrsim 1.25$ TeV whereas the light-grey area to the allowed area by $\Delta M_{Bs}^{\rm NP} \leq 20\%$ constraint. The area drawn with green is allowed by the by $B \to X_s\gamma$ constraint at $3\sigma$.*

mass matrix and therefore reduces its lightest eigenvalue as $|\delta_{LL}^{23}|$ becomes bigger and bigger. The LHC bound denoted in Fig. 4.2 reduces the available effect on $|R_K|$ which cannot be bigger than $\pm4\%$ (note that it is almost symmetric under $\delta_{LL}^{23} \to -\delta_{LL}^{23}$).

### 4.3.2 $\Delta M_s$ and $B \to X_s\gamma$

The variation of $\delta_{LL}^{23}$ has a moderate impact on $\Delta M_s$ but a great impact on $B \to X_s\gamma$ (or equivalently on $C_7$, see below). In calculating those and all other observables in our analysis, we include all chirally enhanced effects in Yukawa couplings and CKM by following Ref. [215]. All these effects have been implemented in `SUSY_FLAVOR v2.54` program, where our numerical outcomes result from.

By taking the $2\sigma$ bound from the experimental observation on $\Delta M_s = 1.1688(14) \times 10^{-11}$ GeV [216] we see from Figs. 4.2, 4.3 that effects on $|R_K|$ cannot be bigger than $\pm5\%$ for both $\mu = 0.5$ TeV and $\mu = 3$ TeV,

$$|\Delta R_K|_{\rm (MSSM)}^{\Delta M_s} \lesssim 5\% \, . \tag{4.33}$$

Supersymmetric effects on $B \to X_s\gamma$ are very well known [217–220]. The operators dominating the $B \to X_s\gamma$ process are the dipole operators

$$\mathcal{O}_7^{(\prime)} = \frac{m_b}{e} \left(\bar{s}\, \sigma_{\mu\nu} P_{R(L)}\, b\right) F^{\mu\nu} \, . \tag{4.34}$$

The associated Wilson coefficient to $\mathcal{O}_7$ is[7]

$$C_7 = \frac{e^2}{m_b} \left( F_{7\gamma}^{32} + m_s F_{7\gamma R}^{32} + m_b F_{7\gamma L}^{32} \right) , \tag{4.35}$$

[7] Similarly for $C_7'$ by changing $L \longleftrightarrow R$.

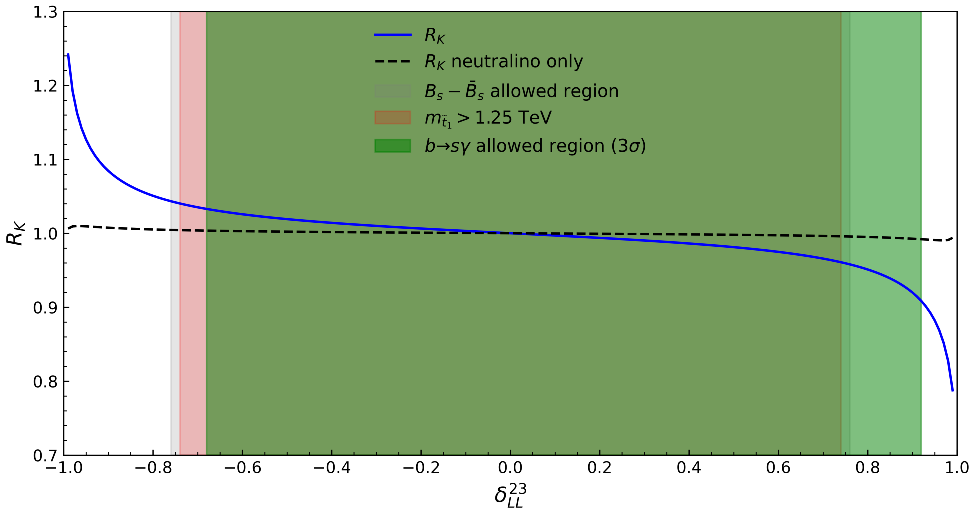


*Fig. 4.3: Similar with Fig. 4.2 but with $\mu = 3$ TeV. The allowed (green) region from $b \to s\gamma$ now reaches large values of $\delta_{LL}^{23}$.*

where $F_{7\gamma}^{JI}$ are the relevant one-loop contributions. The function $F_{\gamma L}^{32}$ contains exactly the same vertices as the one appear in (4.21) for $(B_{VLL})_C$ and subsequently for $R_K$ in eq. (4.13). We have expanded by using FET the chargino/neutralino/gluino corrections to $C_7$ in (4.35) and nailed down the dominant contribution (when the $R_K$ is enhanced of course) to $B \to X_s\gamma$. This arises from the chargino-squark loop. It reads,

$$\begin{aligned}(C_7)_C \;&\propto (\widehat{M}_U^2)_{LL}^{32}\left[\mathcal{F}(|M_2|^2,\{(\mathcal{M}_U^2)_{LL}^{22},(\mathcal{M}_U^2)_{LL}^{33}\})\right.\\ &\left.+|\mu|^2\left(1+\frac{M_2\mu}{|\mu|^2}\tan\beta\right)\mathcal{F}(\{|\mu|^2,|M_2|^2\},(\mathcal{M}_U^2)_{LL}^{22},(\mathcal{M}_U^2)_{LL}^{33}\})\right]. \end{aligned} \tag{4.36}$$

The function $\mathcal{F}(x,y,z)$ is a combination of Passarino-Veltman functions [221], details of which are not important for our qualitative discussion here.[8] Curly brackets denote divided differences of first order, e.g. $\mathcal{F}(x,\{y,z\}) \equiv \frac{\mathcal{F}(x,y)-\mathcal{F}(x,z)}{y-z}$ or second order, e.g $\mathcal{F}(\{x,y\},\{z,w\}) = \frac{\mathcal{F}(x,\{z,w\})-\mathcal{F}(y,\{z,w\})}{x-y}$ and so on. One can read definitions and properties of divided differences from Refs. [186, 203]. As we obtain from (4.36), for similar values of $M_2$ and $\mu$ the effect from $\delta_{LL}^{32} = \delta_{LL}^{23} = O(1)$ onto $b \to s\gamma$, grows even larger with $\tan\beta$.

The $3\sigma$ allowed region from $\mathcal{B}(B \to X_s\gamma)$ when varying $\delta_{LL}^{23}$ with $\mu = 500$ GeV is presented in Fig. 4.2 – it is denoted in green colored area. Even within $3\sigma$ of the experimental observation for $\mathcal{B}(B \to X_s\gamma) = (3.32 \pm 0.15) \times 10^{-4}$ [216], the squark mixing is constrained to be between $-0.2 \lesssim \delta_{LL}^{23} \lesssim 0.7$. By setting this bound in Fig. 4.2 we obtain

$$|\Delta R_K|_{(\mathrm{MSSM})}^{b\to s\gamma} \lesssim 3\%\,, \quad \text{for } |\mu| = 500 \text{ GeV}\,. \tag{4.37}$$

There is however a cancellation/suppression mechanism that takes place in (4.36) for large values of Higgsino mass $|\mu|$. In this case and because of the limit
$\lim_{x->\infty}\mathcal{F}(\{x,y\},\{z,w\}) = -\frac{\mathcal{F}(y,\{z,w\})}{x}$ we get

$$(C_7)_C \;\propto (\widehat{M}_U^2)_{LL}^{32}\left(\frac{M_2}{\mu}\tan\beta\right)\mathcal{F}(|M_2|^2,\{(\mathcal{M}_U^2)_{LL}^{22},(\mathcal{M}_U^2)_{LL}^{33}\}) \to 0\,, \quad |\mu| \gg M_2\tan\beta\,. \tag{4.38}$$

[8] Of course in our numerical results and in figures, exact formulae are taken into account in `SUSY_FLAVOR` program.

Hence there is more room for $R_K$ now. For example, for $\mu = 3$ TeV and keeping $\tan\beta = 5$ throughout we obtain from Fig. 4.3 that the LL squark mixing lies in the region $-0.7 \lesssim \delta_{LL}^{23} \lesssim 0.9$ and this translates in[9]

$$|\Delta R_K|_{(\mathrm{MSSM})}^{b\to s\gamma} \lesssim 10\% \,, \quad \text{for } |\mu| = 3 \text{ TeV} \,. \tag{4.39}$$

Other cancellation mechanisms [222] may result from varying $\delta_{RR}^{23}$ and $\delta_{LR}^{23}$ which affect $F_{7\gamma R}$ and $F_{7\gamma}$ functions respectively. As a consequence, fine cancellation between these and $\delta_{LL}^{23}$ effects on $b\to s\gamma$ may occur. One can switch on effects from other squark mixings, in particular $\delta_{LR}^{23}$, But since $\delta_{LL}^{23} \approx 1$, we need to have an exceedingly fine tuned situation with other squark mixings, $\delta_{LR}^{23}, \delta_{RR}^{23}$, of order one. Even though such a case could occur in multi-parametric scans, it is unlikely to survive due to other $B$-observable constraints, such as $B_s - \bar{B}_s$ mixing, and $B_s \to \mu^+\mu^-$. Therefore, we believe that the limit of large $\mu$ is the only solution in relaxing the $b\to s\gamma$ constraint when $\delta_{LL}^{23} = O(1)$ allowing for more room in $R_K$ MSSM predictions [see eq. (4.39)].

### Muon anomalous magnetic moment

Because the muon slepton and the Wino/Bino masses are nearby the EW scale, it is tempting to discuss here another anomaly, the muon $(g-2)$ anomaly. Recent BNL measurements [223] show a $4.2\sigma$ deviation from the SM if data driven dispersion relations are adopted: $\Delta a_\mu = a_\mu^{\mathrm{exp}} - a_\mu^{\mathrm{SM}} = (251 \pm 59) \times 10^{-11}$. The FET expansion to various contributions has been performed in App. E.1 of Ref. [203]. The fact that we need large $\mu \gg M_2 \tan\beta$ for $R_K$ in order to avoid the $b\to s\gamma$ constrain, amusingly results to completely analogous suppression for $\Delta a_\mu$! For the input parameters of Fig. 4.4 we obtain $\Delta a_\mu \approx 14 \times 10^{-11}$ which is far too small to explain the current deviation.

### MSSM $C_9$ and $C_{10}$ in our analysis

It is customary to present the global fits from all possibly relevant observables in terms of the low energy Wilson coefficients $C_9$ and $C_{10}$ defined in eqs. (4.10) and (4.12). A partial list of recent reference analyses is given in our introduction section. Although $R_K$ is entirely driven by the box MSSM diagram in Fig. 4.1, for $b\to s\mu^+\mu^-$, the MSSM predictions for $C_9$ may not be large due to cancellations between penguin and box diagrams. In fact, this is what exactly happens here for the $R_K$-optimized parameter space we studied and displayed in Fig. 4.4: There is a partial cancellation between the photon penguin[10], and the box-diagrams. The $Z$-penguin turns out to be numerically subdominant for $C_9$ since it is proportional to, $(1-4s_W^2)$ as it is obvious from eq. (4.17).

After applying the FET in relevant box and photon penguin diagrams, we find the dominant contribution that again arises from the chargino-up-squark loop. For equal masses of $M_2 = M_{\tilde{\mu}} = m_{\tilde{t}} \ll m_{\tilde{q}}$ we find for the Wilson coefficients of $C_9$ and $C_{10}$ contributing to the process $b\to s\mu^+\mu^-$

$$C_9^{(\mathrm{MSSM})} \simeq -\left(\frac{\pi\alpha_{\mathrm{em}}}{12 s_W^4}\right)\left(\frac{v^2}{m_{\tilde{t}}^2}\right)\left(\frac{\delta_{LL}^{23}}{|K_{ts}^* K_{tb}|}\right)\left(1-\frac{7}{3}s_W^2\right) ,$$

[9]Note that for $\mu = -3$ TeV we obtain a bound $-0.9 \lesssim \delta_{LL}^{23} \lesssim 0.7$ and hence the bound in (4.39) is for absolute $R_K$ and $\mu$ values.

[10]The photon-penguin is calculated and expanded with FET in App. F.

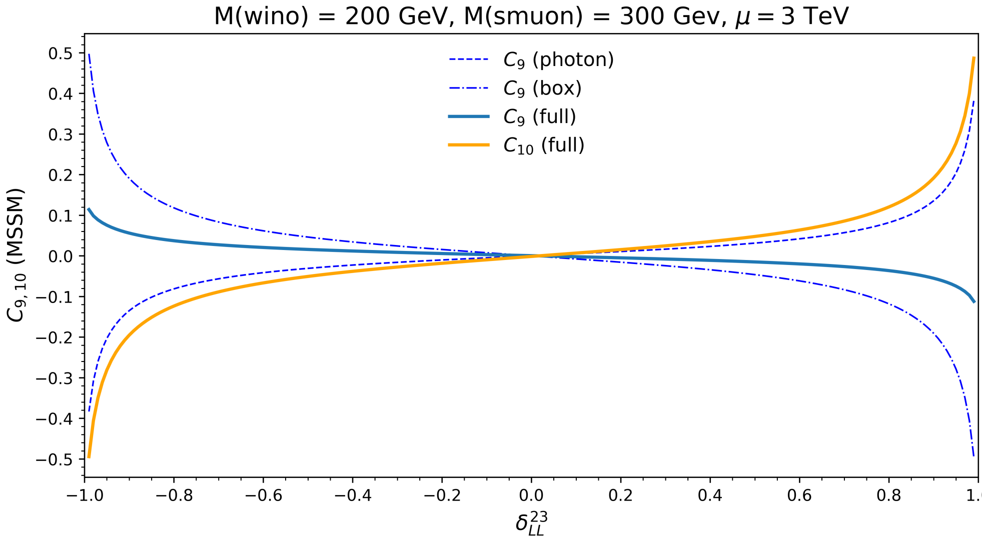


*Fig. 4.4: MSSM contributions to $C_9$ and $C_{10}$ for the same inputs as in Fig. 4.3.*

$$C_{10}^{(\mathrm{MSSM})} \simeq \left(\frac{\pi\alpha_{\mathrm{em}}}{12 s_W^4}\right)\left(\frac{v^2}{m_{\tilde{t}}^2}\right)\left(\frac{\delta^{23}_{LL}}{|K^*_{ts}K_{tb}|}\right).$$

Obviously, $C_9$ and $C_{10}$ are not equal in absolute values. The partial cancellation in $C_9$ cannot be mitigated by varying the parameters within the MSSM. It is important to emphasize that the parameter space we have explored is specifically chosen to optimize the observables $R_K$ and $R_{K^{0*}}$; it is not a comprehensive or general scan of the entire parameter space of the MSSM. Within this parameter space, even the maximum values for $C_9$ and $C_{10}$ shown in Fig. 4.4 are not able to explain all $B$-anomalies combined but $R_K$ and $R_{K^{0*}}$ can be brought not further off than current experimental values. Combined analyses are useful but require careful attention.

### Another Interesting Scenario

In the recent summarizing plot by ATLAS, see Fig. 2 of [212], instead of bounding the stop to be above 1.25 TeV, one may consider the region where the stop mass is around 600 GeV and the neutralino mass is around 400 GeV. In this section, we will try to extract the maximum effect in the $R_K$ from this region, which for brevity we call the 'ATLAS gap'. To achieve this, we will resort to scanning the $m_{\tilde{t}_1} - m_{\tilde{\chi}^0_1}$ plane and draw contours of the values of $R_K$ on this plane, since this will be more illuminating on the points that fall into this region.

Our initial strategy is to find optimal values for $\delta^{23}_{LL}$, i.e. that give the largest contribution to the $R_K$, while simultaneously avoiding constraints from direct searches and the experimental observables, $b \to s\gamma$ and $\Delta M_s$. More specifically, for the scan we set all diagonal squark mass matrices to take equal values inside the range $[1, 13]$ TeV, with a step of 0.1 TeV, and we co-vary the Bino and Wino masses, with an increment of 10 GeV, always keeping a 50 GeV mass gap from each other. Finally, we scan for large values of $\delta^{23}_{LL}$, in the range $\delta^{23}_{LL} = [0.90, 0.99]$ in 0.01 bins. The rest details of the scan as well as the numerical values of the other parameters are shown in the table below. The code `SUSY_FLAVOR` outputs the mass eigenstates, of the stop, the neutralino and the values of the $R_K$ during the scan. Then the allowed values of the $R_K$, by experimental bounds, are plotted on top of the ATLAS exclusion region, for each specific $\delta^{23}_{LL}$ in Fig. 4.5.

| Parameter | Value |
|---|---|
| $M_A$ | 2 TeV |
| $\tan\beta$ | 4 |
| $\mu$ | 3 TeV |
| $M_1$ | $[300, 600]$ GeV |
| $M_2$ | 600 GeV |
| $M_3$ | 6 TeV |
| $(\mathcal{M}_L)^{22}_{LL}$ | 600 GeV |
| $(\mathcal{M}_L)^{II}_{LL}, I = 1,3$ | 3 TeV |
| $(\mathcal{M}_L)^{II}_{RR}, I = 1,\ldots 3,$ | 3 TeV |
| $(\mathcal{M}_{U,D})^{II}_{XX}, I = 1,\ldots 3, X = L,R$ | $[1, 10]$ TeV |
| $(\delta_U)^{33}_{LR}$ | 0.35 |
| $\delta^{23}_{LL}$ | 0.99 |

*Table 4.1: Initialized parameters for scanning the stop-neutralino plane.*

One of the most stringent constraint comes from $B_s - \bar{B}_s$ mixing. For that reason we first plot the allowed regions from that bound. The largest value of $\delta^{23}_{LL}$ to open up the region into the ATLAS 'gap' is found at $\delta^{23}_{LL} = 0.96$. Since we can safely land $B_s - \bar{B}_s$ mixing in the ATLAS 'gap' we turn our attention to the second most stringent constraint, which comes from $b \to s\gamma$. Motivated by the need to allow as much parameter space as possible we fix the value of the off-diagonal element at $\delta^{23}_{LL} = 0.96$ and instead, scan for a range of $(\delta_D)^{23}_{LR}$ values, where a known enhancement of $b \to s\gamma$ exists [224]. The range of the scan is $(\delta_D)^{23}_{LR} = [-0.99, 0.99]$ with an increment of 0.01, which from now on we denote as $(\delta_D)^{23}_{LR} = \delta^{32}_{LR}$. The rest of the parameters are left the same as in the table above. Again, we plot the, allowed by $b \to s\gamma$ bound, $R_K$ regions in the the calculated neutralino-stop plane on top of the ATLAS exclusion regions, for various $\delta^{23}_{LR}$. We find that this bound can be safely avoided and a large region in the parameter space opens up, including the ATLAS gap.

In the contour plot below Fig. 4.5 we show how the parameter space in the stop-neutralino plane opens up into the ATLAS gap before and after allowing for LR-mixing between the squarks. We find that the $R_K$ deviates more for LR mixing values in the region $\delta^{23}_{LR} = [0.3, 0.4]$. Even though this specific region in the parameter space is fully allowed the difference doesn't exceed the value shown below,

$$|\Delta R_K|^{\text{gap}}_{\text{(MSSM)}} \lesssim 5\% \,, \qquad (4.40)$$

which is what we have achieved in the previous scenario as well, enforcing the case of just a 5% difference even more.

## 4.4 Conclusions

After clearing up analytically the complicated form of several SUSY contributions by using the Flavour Expansion Theorem (FET) we find that large $R_K$ happens when the stop, chargino and muon-sneutrino are close to the electroweak scale and the left-squark mixing of second

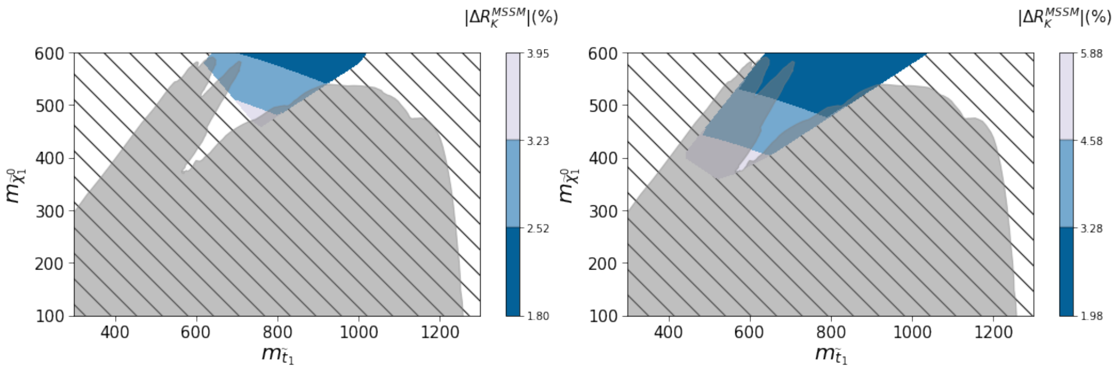


*Fig. 4.5: The final result of our last scenario is presented here for $\delta_{LL}^{23} = 0.96$. On the left plot we have $\delta_{LR}^{23} = 0$, while on the right a stark difference can be seen for $\delta_{LR}^{23} = 0.30$. By allowing LR squark mixing we have opened up a considerable amount of points in the parameter space inside the allowed gap of the ATLAS exclusion region.*

and third generation is close to unity. In principle, MSSM can result in up-to 45% corrections on $R_K$ as it is shown analytically in (4.26). However, this is a heavily constrained region by direct LHC SUSY searches. Moreover, $R_K$ is further constrained by flavour observables too, mainly from the $B \to X_s \gamma$ process since $\mathcal{B}(B \to X_s \gamma)$ is affected by similar Feynman diagrams as $R_K$ does. The conclusion is that, in the region of heavy Higgsino mass parameter $\mu$ where $\mathcal{B}(B \to X_s \gamma)$ is suppressed, MSSM effects on $R_K$ and $R_{K^{0*}}$, in both scenarios that we examined, can reach a $\pm 5\%$. Therefore, the MSSM prediction, $R_K = R_{K^{0*}} = 1 \pm 0.05$, closes down within current experimental values, (4.3) and (4.4).

# Chapter 5

# Conclusions and future directions

This thesis aimed to investigate the effects of new interactions in the low-energy regime through the lens of Effective Field Theory (EFT). Specifically, we sought to demonstrate the complementarity of employing both the top-down and bottom-up approaches in EFTs. We leveraged statistical techniques by utilizing both experimental data and theoretical calculations, while also developing methods and universal results through the abstract mathematical structures in the functional matching formalism using the path integral. From a physics standpoint, we addressed timely issues such as neutrino masses, signal strength deviations in Higgs boson decays, as well as lepton flavor universality ratios.

In Chapter 2, we derived a universal one-loop matching formula for all scalar leptoquark extensions using functional methods. We successfully decoupled heavy modes from a non-trivial model within SMEFT, comprising an $SU(2)$ doublet and a triplet, both carrying color charge under $SU(3)$. This enabled us to analyze their contributions to low-energy observables, revealing notable effects on neutrino mass generation through the dimension-five Weinberg operator, the anomalous magnetic moment of the muon, and electric dipole moments. Furthermore, we placed strict bounds on baryon number-violating couplings to avoid proton decay and explored the perturbativity and EFT validity of the model. Lastly, this procedure generates the majority of the operators in SMEFT, serving as an excellent benchmark for several automated packages that perform the matching.

In Chapter 3, utilizing the bottom-up approach, we conducted a model-independent statistical analysis within SMEFT to pinpoint the values of the Wilson coefficients required to explain the observed deviation in the decay $h \to Z\gamma$. We constructed a chi-squared, $\chi^2$, statistical framework incorporating covariance matrices and contour plots to analyze the parameter space of the Wilson coefficients. Our analysis revealed that certain dimension-six operators, specifically those modifying the Higgs-gauge boson couplings, must have Wilson coefficients of particular magnitudes to reconcile the experimental data with theoretical predictions. We explored several single- and two-field scalar and fermionic extensions of the SM, such as adding new scalar singlets or doublets and vector-like fermions, to assess their viability in matching the required Wilson coefficients. These models were analyzed using both the top-down approach, through explicit matching onto SMEFT, and the bottom-up approach, by comparing their predictions with experimental constraints. Only a two-field model was able to produce an excess in the data; however, it still did not fully match the experimentally observed deviation.

In Chapter 4, We investigated the lepton flavor universality ratios $R_K$ and $R_{K^*}$, which had previously exhibited deviations from SM predictions but have recently shown diminished discrepancies. By matching the MSSM onto LEFT, we calculated the maximum deviations in these ratios that the MSSM could accommodate without conflicting with existing experimental constraints. Our findings indicated that, within the parameter space allowed by current data, the MSSM can produce only minimal deviations in these ratios. This suggests that the MSSM, in its minimal form, is unlikely to fully account for significant deviations in lepton flavor universality ratios, highlighting the need to consider extended models or alternative explanations.

This thesis makes several contributions to the field of particle physics. The development of a universal one-loop matching formula for scalar leptoquarks enhances the theoretical toolkit available for studying new physics scenarios. It allows for systematic and consistent incorporation of leptoquark effects into SMEFT analyses, facilitating comparisons between different models and experimental data, and adds to the collection of fully worked-out matching examples in SMEFT. Our work on Higgs boson decays provides valuable insights into how deviations from SM predictions can be interpreted within the EFT framework. By constraining the Wilson coefficients and exploring viable SM extensions, we contribute to the understanding of possible new physics in the Higgs sector and provide guidance for model-building. The analysis of lepton flavor universality ratios within the MSSM offers important perspectives on the model's capabilities and limitations. It underscores the challenges in explaining flavor anomalies within minimal supersymmetric frameworks and highlights the need for alternative models or mechanisms. By employing both the top-down and bottom-up approaches, this thesis demonstrates their complementarity in exploring new physics. The top-down approach allows for detailed model-specific predictions, while the bottom-up approach provides model-independent constraints essential for guiding theoretical developments.

While this research advances our understanding, several limitations should be acknowledged. The conclusions drawn from specific SM extensions are inherently dependent on the chosen models and their parameter spaces; other viable models or parameter choices not explored in this thesis could offer alternative explanations. The EFT approach relies on the assumption that new physics effects can be captured by higher-dimensional operators suppressed by a high-energy scale $\Lambda$. If new physics lies at energy scales close to current experimental reach, or if the operator expansion does not converge rapidly, the EFT framework may be less effective. The analyses involve uncertainties from both experimental measurements and theoretical calculations. Statistical uncertainties in experimental data, as well as approximations made in theoretical computations (e.g., neglecting higher-loop corrections), can impact the precision of the results.

In conclusion, this thesis contributes to the ongoing effort to uncover physics beyond the Standard Model by providing new methods, analyses, and insights. The development of a universal matching formula for scalar leptoquarks and the application of both top-down and bottom-up approaches enrich the theoretical landscape and offer pathways for interpreting experimental observations. Our work underscores the importance of EFT as a powerful framework for bridging the gap between high-energy theories and low-energy phenomenology.

The findings presented here not only enhance our understanding of specific phenomena, such as Higgs boson decays and lepton flavor universality ratios, but also illustrate the broader utility of combining different theoretical approaches. As experimental precision continues to improve and new data become available, the methods and results of this thesis will serve as valuable resources for further investigations into the fundamental laws governing the universe.

Building on the research conducted in this thesis, several avenues for future work are proposed. Investigate the impact of two-loop and higher-order corrections in the matching procedures for leptoquarks and other new particles. This would improve the precision of theoretical predictions and potentially reveal subtle effects not captured at one-loop order. Extend the analysis to include other beyond-the-Standard-Model scenarios, such as models with vector leptoquarks. This could provide a more comprehensive understanding of possible new physics effects. Utilize new data from the Large Hadron Collider (LHC) and future colliders to refine the constraints on Wilson coefficients and test the viability of proposed models. Improved measurements of Higgs boson properties, flavor observables, and rare decays will be particularly valuable. Create computational tools and software packages that implement the universal matching formulas and statistical analysis frameworks developed in this thesis. This would facilitate broader use by the research community and enable more efficient exploration of parameter spaces. Incorporate advanced statistical methods, such as Bayesian inference or machine learning algorithms, to improve the analysis of experimental data and the extraction of constraints on theoretical models.

The pursuit of physics beyond the Standard Model remains one of the most exciting and challenging endeavors in modern science. This thesis contributes to this quest by offering new tools and perspectives that aid in the interpretation of experimental results and the development of theoretical frameworks. As we continue to probe the frontiers of particle physics, the synergy between theoretical innovation and experimental exploration will be essential. It is our hope that the work presented here will inspire further research and ultimately contribute to a deeper understanding of the fundamental constituents of matter and their interactions.

# APPENDICES

# Appendix A

# Lagrangian and X-matrices for scalar leptoquarks

We append here the general Lagrangian for all scalar leptoquarks and the relevant **X**-matrices needed to construct the EFT Lagrangian at one-loop. It can be split into three parts, in eqs. (2.6),(2.7) and (2.8). The notation for LQs is given in Table 2.1.

The LQ-SM fermion interactions are,

$$\begin{aligned}\mathcal{L}_{\text{LQ-f}} = & \left[\left(\lambda^{1\mathrm{L}}_{pr}\right)\bar{q}^c_{pi}\cdot\epsilon\cdot\ell_r + \left(\lambda^{1\mathrm{R}}_{pr}\right)\bar{u}^c_i\,e_r\right]S_{1i} + \text{h.c.} \\ & + \left[(\lambda^{\not{B}L}_{pr})\,\epsilon^{ijk}\,\bar{q}_{pj}\cdot\epsilon\cdot q^c_{rk} + (\lambda^{\not{B}R}_{pr})\,\epsilon^{ijk}\bar{d}_{pj}\,u^c_{rk}\right]S_{1i} + \text{h.c.} \\ & + \left[(\tilde{\lambda}^{1}_{pr})\,\bar{d}^c_{pi}\,e_r + (\tilde{\lambda}^{1\not{B}}_{pr})\,\epsilon^{ijk}\,\bar{u}_{pj}\,u^c_{rk}\right]\tilde{S}_{1i} + \text{h.c.} \\ & + \left[(\lambda^{2LR}_{pr})\,\bar{q}_{pi\alpha}e_r - (\lambda^{2RL}_{pr})\,\bar{u}_{pi}\,\ell_{r\beta}\,\epsilon^{\beta\alpha}\right]S_{2i\alpha} + \text{h.c.} \\ & + (\tilde{\lambda}_{pr})\,\bar{d}_{pi}\tilde{S}^T_{2i}\cdot\epsilon\cdot\ell_r + \text{h.c.} \\ & + \left[(\lambda^{3L}_{pr})\,\bar{q}^c_{pi}\cdot\epsilon\cdot\sigma^I\cdot\ell_r + (\lambda^{3\not{B}}_{pr})\,\epsilon^{ijk}\,\bar{q}_{pj}\cdot\sigma^I\cdot\epsilon\cdot q^c_{rk}\right]S^I_{3i} + \text{h.c.}\,. \end{aligned} \tag{A.1}$$

The LQ-Higgs interactions read,

$$\begin{aligned}\mathcal{L}_{\text{LQ-H}} = & -\sum_n\left(M_n^2 + \lambda_{Hn}\,|S_n|^2\right)|H|^2 + \sum_{n=2,\tilde{2}}\lambda_{nn}\,(S^\dagger_{ni}\cdot H)(H^\dagger\cdot S_{ni}) \\ & \big[-A_{\tilde{2}1}\,S^\dagger_{1i}\,(\tilde{S}^\dagger_{2i}\cdot H) + A_{\tilde{2}3}\,S^{I\dagger}_{3i}\,(\tilde{S}^\dagger_{2i}\cdot\sigma^I\cdot H) \\ & + \lambda_{2\tilde{2}}\,(S^\dagger_{2i}\cdot H)(H^T\cdot\epsilon\cdot\tilde{S}_{2i}) + \lambda_{3\tilde{1}}\,\tilde{S}^\dagger_{1i}\,(H^T\cdot\epsilon\cdot\sigma^I\cdot H)S^I_{3i} \\ & + \lambda_{H13}\,(H^\dagger\cdot\sigma^I\cdot H)\,S^{I\dagger}_{3i}\,S_{1i} + \text{h.c.}\big] \\ & - i\lambda_{\epsilon H3}\,\epsilon^{IJK}\,(H^\dagger\cdot\sigma^I\cdot H)S^{J\dagger}_{3i}\,S^{K\dagger}_{3i}\,. \end{aligned} \tag{A.2}$$

Where the index $n$ runs through, $n = 1,\tilde{1},2,\tilde{2},3$ in one to one correspondence to the sets $\{S_1,\tilde{S}_1,S_2,\tilde{S}_2,S_3\}$, $\{M_1,\tilde{M}_1,M_2,\tilde{M}_2,M_3\}$ and $\{\lambda_{H1},\tilde{\lambda}_{H1},\lambda_{H2},\tilde{\lambda}_{H2},\lambda_{H3}\}$.

Finally, self-interactions among scalar leptoquarks are

$$\mathcal{L}_{\text{S}} = -V(S)\,, \tag{A.3}$$

where $V(S)$ is the tree-level potential that is built from gauge group invariant combinations among LQ fields. In general $V(S)$ for all LQs is quite lengthy. For combinations $S_1 + \tilde{S}_2$, the potential $V(S_1, \tilde{S}_2)$ can be read from (2.83), for $S_1 + S_3$ from eq. (2.3) of ref. [64] while the most general one in eqs. (46) and (49) of ref. [225]. Note that $X(U)$-matrices are constructed solely from simple second field derivatives of $V(S)$ and there is no need to be written down explicitly.

In what follows we reserve letters $i, \alpha, p, \mu, A$ and $I$ to denote the respective field indices in the *left* hand side multiplet $\bar{\varphi} = (\bar{\varphi}_S, \bar{\varphi}_L)$, while the letters $j, \beta, r, \nu, B, J$ are used for the *right* hand side multiplet $\varphi = (\varphi_S, \varphi_L)$ and we suppress spinor indices. Each letter represents the respective gauge group representation given in Table 2.1. Additionally, the chirality projection operators regarding the Weyl to Dirac conversion of fermions mentioned in the main text, are left implicit.

## A.1 $\mathbf{X_{SS}}$

$\underline{\mathbf{U_{S_1 S_1}}}$

$$U_{S_1^\dagger S_1} = \lambda_{H1} |H|^2 \delta_{ij} + \frac{\partial^2 V}{\partial S_{1i}^\dagger \, \partial S_{1j}} \,, \tag{A.4}$$

$$U_{S_1 S_1^\dagger} = \lambda_{H1} |H|^2 \delta_{ij} + \frac{\partial^2 V}{\partial S_{1i} \, \partial S_{1j}^\dagger} \,. \tag{A.5}$$

$\underline{\mathbf{U_{S_1 \tilde{S}_2}}}$

$$U_{S_1 \tilde{S}_2} = A_{\tilde{2}1}^* H_\beta^* \delta_{ij} + \frac{\partial^2 V}{\partial S_{1i} \, \partial \tilde{S}_{2j\beta}} \,, \tag{A.6}$$

$$U_{S_1^\dagger \tilde{S}_2^*} = A_{\tilde{2}1} H_\beta \delta_{ij} + \frac{\partial^2 V}{\partial S_{1i}^\dagger \, \partial \tilde{S}_{2j\beta}^*} \,. \tag{A.7}$$

$\underline{\mathbf{U_{S_1 S_3}}}$

$$U_{S_1^\dagger S_3} = \lambda_{H13}^* \, \delta_{ij} \, (H^\dagger \sigma^J H) + \frac{\partial^2 V}{\partial S_{1i}^\dagger \, \partial S_{3j}^J} \,, \tag{A.8}$$

$$U_{S_1 S_3^*} = \lambda_{H13} \, \delta_{ij} \, (H^\dagger \sigma^J H) + \frac{\partial^2 V}{\partial S_{1i} \, \partial S_{3j}^{I*}} \,. \tag{A.9}$$

$\underline{\mathbf{U_{\tilde{S}_1 \tilde{S}_1}}}$

$$U_{\tilde{S}_1^\dagger \tilde{S}_1} = \tilde{\lambda}_{H1} |H|^2 \delta_{ij} + \frac{\partial^2 V}{\partial \tilde{S}_{1i}^\dagger \, \partial \tilde{S}_{1j}} \,, \tag{A.10}$$

$$U_{\tilde{S}_1 \tilde{S}_1^\dagger} = \tilde{\lambda}_{H1} |H|^2 \delta_{ij} + \frac{\partial^2 V}{\partial \tilde{S}_{1i} \, \partial \tilde{S}_{1j}^\dagger} \,. \tag{A.11}$$

$\underline{\mathbf{U_{\tilde{S}_1 S_3}}}$

$$U_{\tilde{S}_1^\dagger S_3} = -\lambda_{3\tilde{1}}\,\delta_{ij}\,(H^T\cdot\epsilon\cdot\sigma^J\cdot H) + \frac{\partial^2 V}{\partial\tilde{S}_{1i}^\dagger\,\partial S_{3j}^J}\,, \tag{A.12}$$

$$U_{\tilde{S}_1 S_3^*} = \lambda_{3\tilde{1}}^*\,\delta_{ij}\,(H^\dagger\cdot\sigma^J\cdot\epsilon\cdot H^*) + \frac{\partial^2 V}{\partial\tilde{S}_{1i}\,\partial S_{3j}^{J*}}\,. \tag{A.13}$$

$\underline{\mathbf{U_{S_2S_2}}}$

$$U_{S_2^\dagger S_2} = \delta_{ij}\delta_{\alpha\beta}\lambda_{H2}|H|^2 - \lambda_{22}\,\delta_{ij}\,H_\alpha H_\beta^* + \frac{\partial^2 V}{\partial S_{2i\alpha}^\dagger\,\partial S_{2j\beta}}\,, \tag{A.14}$$

$$U_{S_2^T S_2^*} = \delta_{ij}\delta_{\alpha\beta}\lambda_{H2}|H|^2 - \lambda_{22}\,\delta_{ij}\,H_\alpha^* H_\beta + \frac{\partial^2 V}{\partial S_{2i\alpha}^T\,\partial S_{2j\beta}^*}\,. \tag{A.15}$$

$\underline{\mathbf{U_{S_2\tilde{S}_2}}}$

$$U_{S_2^\dagger\tilde{S}_2} = \lambda_{2\tilde{2}}\,\delta_{ij}\,H_\alpha\,(\epsilon\cdot H)_\beta^T + \frac{\partial^2 V}{\partial S_{2i\alpha}^\dagger\,\partial\tilde{S}_{2j\beta}}\,, \tag{A.16}$$

$$U_{S_2^T\tilde{S}_2^*} = \lambda_{2\tilde{2}}\,\delta_{ij}\,H_\alpha^*\,(\epsilon\cdot H^*)_\beta + \frac{\partial^2 V}{\partial S_{2i\alpha}^T\,\partial\tilde{S}_{2j\beta}^*}\,. \tag{A.17}$$

$\underline{\mathbf{U_{\tilde{S}_2\tilde{S}_2}}}$

$$U_{\tilde{S}_2^\dagger\tilde{S}_2} = \delta_{ij}\delta_{\alpha\beta}\tilde{\lambda}_{H2}|H|^2 - \lambda_{\tilde{2}\tilde{2}}\,\delta_{ij}\,H_\alpha H_\beta^* + \frac{\partial^2 V}{\partial\tilde{S}_{2i\alpha}^\dagger\,\partial\tilde{S}_{2j\beta}}\,, \tag{A.18}$$

$$U_{\tilde{S}_2^T\tilde{S}_2} = \frac{2}{3}\lambda_5\epsilon^{ijk}\left[\epsilon^{\alpha\alpha_1}\tilde{S}_{2j\alpha_1}H_\beta^* + \tilde{S}_{2k\alpha_1}\epsilon^{\alpha_1\beta}H_\alpha^* - \epsilon^{\alpha\beta}(H^\dagger\cdot\tilde{S}_{2k})\right] + \frac{\partial^2 V}{\partial\tilde{S}_{2i\alpha}^T\,\partial\tilde{S}_{2j\beta}}\,, \tag{A.19}$$

$$U_{\tilde{S}_2^\dagger\tilde{S}_2^*} = \frac{2}{3}\lambda_5\epsilon^{ijk}\left[\epsilon^{\alpha\alpha_1}\tilde{S}_{2k\alpha_1}H_\beta + \tilde{S}_{2k\alpha_1}\epsilon^{\alpha_1\beta}H_\alpha - \epsilon^{\alpha\beta}(\tilde{S}_{2k}^\dagger\cdot H)\right] + \frac{\partial^2 V}{\partial\tilde{S}_{2i\alpha}^\dagger\,\partial\tilde{S}_{2j\beta}^*}\,, \tag{A.20}$$

$$U_{\tilde{S}_2^T\tilde{S}_2^*} = \delta_{ij}\delta_{\alpha\beta}\tilde{\lambda}_{H2}|H|^2 - \lambda_{\tilde{2}\tilde{2}}\,\delta_{ij}\,H_\alpha^* H_\beta + \frac{\partial^2 V}{\partial\tilde{S}_{2i\alpha}^T\,\partial\tilde{S}_{2j\beta}^*}\,. \tag{A.21}$$

$\underline{\mathbf{U_{\tilde{S}_2S_1}}}$

$$U_{\tilde{S}_2^T S_1} = A_{\tilde{2}1}^* H_\alpha^*\delta_{ij} + \frac{\partial^2 V}{\partial\tilde{S}_{2i\alpha}^T\,\partial S_{1j}}\,, \tag{A.22}$$

$$U_{\tilde{S}_2^\dagger S_1^\dagger} = A_{\tilde{2}1} H_\alpha\delta_{ij} + \frac{\partial^2 V}{\partial\tilde{S}_{2i\alpha}^\dagger\,\partial S_{1j}^\dagger}\,. \tag{A.23}$$

$\underline{\mathbf{U_{\tilde{S}_2S_2}}}$

$$U_{\tilde{S}_2^\dagger S_2} = \lambda_{2\tilde{2}}\,\delta_{ij}\,H_\beta^*\,(\epsilon\cdot H^*)_\alpha + \frac{\partial^2 V}{\partial\tilde{S}_{2i\alpha}^*\,\partial S_{2j\beta}}\,, \tag{A.24}$$

$$U_{\tilde{S}_2^T S_2^*} = \lambda_{2\tilde{2}}\,\delta_{ij}\,H_\beta\,(\epsilon\cdot H)_\alpha^T + \frac{\partial^2 V}{\partial\tilde{S}_{2i\alpha}\,\partial S_{2j\beta}^*}\,. \tag{A.25}$$

$\underline{\mathbf{U_{\tilde{S}_2S_3}}}$

$$U_{\tilde{S}_2^\dagger S_3^*} = A_{\tilde{2}3}\,\delta_{ij}\,(\sigma^J \cdot H)_\alpha + \frac{\partial^2 V}{\partial \tilde{S}^*_{2i\alpha}\,\partial S^{J*}_{3j}}\,, \tag{A.26}$$

$$U_{\tilde{S}_2^T S_3} = A^*_{\tilde{2}3}\,\delta_{ij}\,(\sigma^J \cdot H^*)^T_\alpha + \frac{\partial^2 V}{\partial \tilde{S}_{2i\alpha}\,\partial S^{J}_{3j}}\,. \tag{A.27}$$

<u>**$\mathbf{U_{S_3S_3}}$**</u>

$$U_{S_3^\dagger S_3} = \lambda_{H3}\,\delta_{ij}\,\delta^{IJ}\,|H|^2 + i\lambda_{\epsilon H3}\,\epsilon^{IJK}\,(H^\dagger\sigma^K H)\,\delta_{ij} + \frac{\partial^2 V}{\partial S^{I*}_{3i}\,\partial S^{J}_{3j}}\,, \tag{A.28}$$

$$U_{S_3^T S_3} = \lambda_{H3}\,\delta_{ij}\,\delta^{IJ}\,|H|^2 - i\lambda_{\epsilon H3}\,\epsilon^{IJK}\,(H^\dagger\sigma^K H)\,\delta_{ij} + \frac{\partial^2 V}{\partial S^{I}_{3i}\,\partial S^{J*}_{3j}}\,. \tag{A.29}$$

<u>**$\mathbf{U_{S_3S_1}}$**</u>

$$U_{S_3^\dagger S_1} = \lambda_{H13}\,\delta_{ij}\,(H^\dagger\sigma^I H) + \frac{\partial^2 V}{\partial S^{I*}_{3i}\,\partial S_{1j}}\,, \tag{A.30}$$

$$U_{S_3^T S_1^*} = \lambda^*_{H13}\,\delta_{ij}\,(H^\dagger\sigma^I H) + \frac{\partial^2 V}{\partial S^{I}_{3i}\,\partial S^*_{1j}}\,. \tag{A.31}$$

<u>**$\mathbf{U_{S_3\tilde{S}_1}}$**</u>

$$U_{S_3^\dagger \tilde{S}_1} = \lambda^*_{3\tilde{1}}\,\delta_{ij}\,(H^\dagger \cdot \sigma^I \cdot \epsilon \cdot H^*) + \frac{\partial^2 V}{\partial S^{I*}_{3i}\,\partial \tilde{S}_{1j}}\,, \tag{A.32}$$

$$U_{S_3^T \tilde{S}_1^*} = -\lambda_{3\tilde{1}}\,\delta_{ij}\,(H^T \cdot \epsilon \cdot \sigma^I \cdot H^*) + \frac{\partial^2 V}{\partial S^{I}_{3i}\,\partial \tilde{S}^*_{1j}}\,. \tag{A.33}$$

<u>**$\mathbf{U_{S_3\tilde{S}_2}}$**</u>

$$U_{S_3^\dagger \tilde{S}_2^*} = -A_{\tilde{2}3}\,\delta_{ij}\,(\sigma^I \cdot H)_\beta + \frac{\partial^2 V}{\partial S^{I*}_{3i}\,\partial \tilde{S}^*_{2j\beta}}\,, \tag{A.34}$$

$$U_{S_3^T \tilde{S}_2} = -A^*_{\tilde{2}3}\,\delta_{ij}\,(\sigma^I \cdot H^*)^T_\beta + \frac{\partial^2 V}{\partial S^{I}_{3i}\,\partial \tilde{S}_{2j\beta}}\,. \tag{A.35}$$

<u>**Matrix Structure**</u>

$$\mathbf{U_{S_nS_m}} = \begin{pmatrix} U_{S_n^\dagger S_m} & U_{S_n^\dagger S_m^*} \\ U_{S_n^T S_m} & U_{S_n^T S_m^*} \end{pmatrix}\,, \tag{A.36}$$

with $n,m = 1,\tilde{1},2,\tilde{2},3$. All combinations make up the whole matrix structure of the heavy-only $\mathbf{U_{SS}}$. Here we have listed all terms involving the Higgs field as well. There are also terms coming from the potential of all leptoquarks which are found by the general formula,

$$U_{S_n^\dagger S_m} = \frac{\partial V}{\partial S_n^\dagger\,\partial S_m}\,,\quad U_{S_n^\dagger S_m^*} = \frac{\partial V}{\partial S_n^\dagger\,\partial S_m^*}\,,\quad U_{S_n^T S_m} = \frac{\partial V}{\partial S_n^T\,\partial S_m}\,,\quad U_{S_n^T S_m^*} = \frac{\partial V}{\partial S_n^T\,\partial S_m^*}\,. \tag{A.37}$$

## A.2 $\mathbf{X_{SL}}$

<u>$\mathbf{U_{S_n f}}$</u>

$$U_{S_1\ell} = -(\lambda^{1\mathrm{L}}_{pr})\,\bar{q}^c_{pi\alpha}\epsilon^{\alpha\beta}\,, \qquad U_{S_1^\dagger\ell^c} = -(\lambda^{1\mathrm{L}}_{pr})^*\,\bar{q}_{pi\alpha}\epsilon^{\alpha\beta}\,, \tag{A.38}$$

$$U_{S_1^\dagger q} = 2(\lambda^{\not{B}L})^*\bar{q}^c_{pk\alpha}\epsilon^{\alpha\beta}\epsilon^{ijk}\,, \qquad U_{S_1^\dagger q^c} = (\lambda^{1\mathrm{L}}_{pr})^\dagger\delta_{ij}\bar{\ell}_{p\alpha}\epsilon^{\alpha\beta}\,, \tag{A.39}$$

$$U_{S_1 q} = (\lambda^{1\mathrm{L}}_{pr})^T\,\delta_{ij}\,\bar{\ell}^c_{p\alpha}\epsilon^{\alpha\beta}\,, \qquad U_{S_1 q^c} = 2(\lambda^{\not{B}L}_{pr})\epsilon^{ijk}\bar{q}_{pk\alpha}\epsilon^{\alpha\beta}\,, \tag{A.40}$$

$$U_{S_1^\dagger u} = (\lambda^{\not{B}R}_{pr})^*\,\bar{d}^c_{pk}\,\epsilon^{ijk}\,, \qquad U_{S_1^\dagger u^c} = -(\lambda^{1\mathrm{R}}_{pr})^\dagger\,\bar{e}_p\,\delta_{ij}\,, \tag{A.41}$$

$$U_{S_1 u} = -(\lambda^{1\mathrm{R}}_{pr})^T\bar{e}^c_p\,\delta_{ij}\,, \qquad U_{S_1 u^c} = (\lambda^{\not{B}R}_{pr})\epsilon^{ijk}\bar{d}_{pk}\,, \tag{A.42}$$

$$U_{S_1 e} = -(\lambda^{1\mathrm{R}}_{pr})\bar{u}^c_{pi}\,, \qquad U_{S_1^\dagger e^c} = -(\lambda^{1\mathrm{R}}_{pr})^*\,\bar{u}_{pi}\,, \tag{A.43}$$

$$U_{S_1^\dagger d} = -(\lambda^{\not{B}R}_{pr})^\dagger\,\bar{u}^c_{pk}\epsilon^{ijk}\,, \qquad U_{S_1 d^c} = -(\lambda^{\not{B}R}_{pr})^T\,\epsilon^{ijk}\bar{u}_{pk}\,, \tag{A.44}$$

$$U_{\tilde{S}_1^\dagger u} = -2(\tilde{\lambda}^{1\not{B}}_{pr})^\dagger\,\bar{u}^c_{pk}\,\epsilon^{ijk}\,, \qquad U_{\tilde{S}_1 u^c} = 2(\tilde{\lambda}^{1\not{B}}_{pr})\,\bar{u}_{pk}\,\epsilon^{ijk}\,, \tag{A.45}$$

$$U_{\tilde{S}_1 e} = -(\tilde{\lambda}^1_{pr})\,\bar{d}^c_{pi}\,, \qquad U_{\tilde{S}_1^\dagger e^c} = -(\tilde{\lambda}^1_{pr})^*\,\bar{d}_{pi}\,, \tag{A.46}$$

$$U_{\tilde{S}_1 d} = -(\tilde{\lambda}^1_{pr})^T\,\bar{e}^c_p\,\delta_{ij}\,, \qquad U_{\tilde{S}_1^\dagger d^c} = -(\tilde{\lambda}^1_{pr})^\dagger\,\bar{e}_p\,\delta_{ij}\,, \tag{A.47}$$

$$U_{S_2^T\ell} = -(\lambda^{2RL}_{pr})\,\bar{u}_{pi}\,\epsilon^{\alpha\beta}\,, \qquad U_{S_2^\dagger\ell^c} = -(\lambda^{2RL}_{pr})^*\,\epsilon^{\alpha\beta}\,\bar{u}^c_{pi}\,, \tag{A.48}$$

$$U_{S_2^\dagger q} = -(\lambda^{2LR}_{pr})^\dagger\,\delta_{\alpha\beta}\delta_{ij}\,\bar{e}_p\,, \qquad U_{S_2^T q^c} = -(\lambda^{2LR}_{pr})^T\,\delta_{\alpha\beta}\delta_{ij}\,\bar{e}^c_p\,, \tag{A.49}$$

$$U_{S_2^\dagger u} = (\lambda^{2RL}_{pr})^\dagger\,\delta_{ij}\,\bar{\ell}_{p\beta}\epsilon^{\beta\alpha}\,, \qquad U_{S_2^T u^c} = (\lambda^{2RL}_{pr})^T\,\delta_{ij}\,\bar{\ell}^c_{p\beta}\,\epsilon^{\beta\alpha}\,, \tag{A.50}$$

$$U_{S_2^T e} = -(\lambda^{2LR}_{pr})\,\bar{q}_{pi\alpha}\,, \qquad U_{S_2^\dagger e^c} = -(\lambda^{2LR}_{pr})^*\,\bar{q}^c_{pi\alpha}\,, \tag{A.51}$$

$$U_{\tilde{S}_2^T\ell} = -(\tilde{\lambda}_{pr})\,\bar{d}_{pi}\,\epsilon^{\alpha\beta}\,, \qquad U_{\tilde{S}_2^\dagger\ell^c} = -(\tilde{\lambda}_{pr})^*\,\bar{d}^c_{pi}\,\epsilon^{\alpha\beta}\,, \tag{A.52}$$

$$U_{\tilde{S}_2^\dagger d} = (\tilde{\lambda}_{pr})^\dagger\,\delta_{ij}\bar{\ell}_{p\beta}\,\epsilon^{\beta\alpha}\,, \qquad U_{\tilde{S}_2^T d^c} = (\tilde{\lambda}_{pr})^T\delta_{ij}\,\bar{\ell}^c_{p\beta}\,\epsilon^{\beta\alpha}\,, \tag{A.53}$$

$$U_{S_3^T\ell} = -(\lambda^{3L}_{pr})\,\bar{q}^c_{pi\alpha}\epsilon^{\alpha\gamma}\,\sigma^I_{\gamma\beta}\,, \qquad U_{S_3^\dagger\ell^c} = (\lambda^{3L}_{pr})^*\,\bar{q}_{pi\alpha}\epsilon^{\gamma\alpha}\,\sigma^I_{\beta\gamma}\,, \tag{A.54}$$

$$U_{S_3^T q} = -(\lambda^{3L}_{pr})^T\,\bar{\ell}^c_{p\alpha}\,\sigma^I_{\gamma\alpha}\,\epsilon^{\beta\gamma}\delta_{ij}\,, \qquad U_{S_3^\dagger q^c} = (\lambda^{3L}_{pr})^\dagger\,\bar{\ell}_{p\alpha}\,\sigma^I_{\alpha\gamma}\,\epsilon^{\gamma\beta}\delta_{ij}\,, \tag{A.55}$$

$$U_{S_3^\dagger q} = 2(\lambda^{3\not{B}}_{pr})^\dagger\,\epsilon^{ijk}\,(\bar{q}^c_{pk}\cdot\epsilon\cdot\sigma^I)_\beta\,, \qquad U_{S_3^T q^c} = 2(\lambda^{3\not{B}}_{pr})\,\epsilon^{ijk}\,(\bar{q}_{pk}\cdot\sigma^I\cdot\epsilon)_\beta\,. \tag{A.56}$$

<u>**Matrix Structure**</u>

$$\mathbf{U_{S_1\ell}} = \begin{pmatrix} 0 & U_{S_1^\dagger\ell^c} \\ U_{S_1\ell} & 0 \end{pmatrix}, \qquad \mathbf{U_{S_1q}} = \begin{pmatrix} U_{S_1^\dagger q} & U_{S_1^\dagger q^c} \\ U_{S_1 q} & U_{S_1 q^c} \end{pmatrix}, \tag{A.57}$$

$$\mathbf{U_{S_1u}} = \begin{pmatrix} U_{S_1^\dagger u} & U_{S_1^\dagger u^c} \\ U_{S_1 u} & U_{S_1 u^c} \end{pmatrix}, \ \mathbf{U_{S_1d}} = \begin{pmatrix} U_{S_1^\dagger d} & 0 \\ 0 & U_{S_1 d^c} \end{pmatrix}, \ \mathbf{U_{S_1e}} = \begin{pmatrix} 0 & U_{S_1^\dagger e^c} \\ U_{S_1 e} & 0 \end{pmatrix}, \tag{A.58}$$

$$\mathbf{U}_{\tilde{\mathbf{S}}_1\mathbf{u}} = \begin{pmatrix} U_{\tilde{S}_1^\dagger u} & 0 \\ 0 & U_{\tilde{S}_1 u^c} \end{pmatrix} , \mathbf{U}_{\tilde{\mathbf{S}}_1\mathbf{e}} = \begin{pmatrix} 0 & U_{\tilde{S}_1^\dagger e^c} \\ U_{\tilde{S}_1 e} & 0 \end{pmatrix} , \mathbf{U}_{\tilde{\mathbf{S}}_1\mathbf{d}} = \begin{pmatrix} 0 & U_{\tilde{S}_1^\dagger d^c} \\ U_{\tilde{S}_1 d} & \end{pmatrix} , \tag{A.59}$$

$$\mathbf{U}_{\mathbf{S}_2\ell} = \begin{pmatrix} 0 & U_{S_2^\dagger \ell^c} \\ U_{S_2^T \ell} & 0 \end{pmatrix} , \qquad \mathbf{U}_{\mathbf{S}_2\mathbf{d}} = \begin{pmatrix} U_{S_2^\dagger q} & 0 \\ 0 & U_{S_2^T q^c} \end{pmatrix} , \tag{A.60}$$

$$\mathbf{U}_{\mathbf{S}_2\mathbf{u}} = \begin{pmatrix} U_{S_2^\dagger u} & 0 \\ 0 & U_{S_2^T u^c} \end{pmatrix} , \qquad \mathbf{U}_{\mathbf{S}_2\mathbf{e}} = \begin{pmatrix} 0 & U_{S_2^\dagger e^c} \\ U_{S_2^T e} & 0 \end{pmatrix} , \tag{A.61}$$

$$\mathbf{U}_{\tilde{\mathbf{S}}_2\ell} = \begin{pmatrix} 0 & U_{\tilde{S}_2^\dagger \ell^c} \\ U_{\tilde{S}_2^T \ell} & 0 \end{pmatrix} , \qquad \mathbf{U}_{\tilde{\mathbf{S}}_2\mathbf{d}} = \begin{pmatrix} U_{\tilde{S}_2^\dagger d} & 0 \\ 0 & U_{\tilde{S}_2^T d^c} \end{pmatrix} , \tag{A.62}$$

$$\mathbf{U}_{\mathbf{S}_3\ell} = \begin{pmatrix} 0 & U_{S_3^\dagger \ell^c} \\ U_{S_3^T \ell} & 0 \end{pmatrix} , \qquad \mathbf{U}_{\mathbf{S}_3\mathbf{q}} = \begin{pmatrix} U_{S_3^\dagger q} & U_{S_3^\dagger q^c} \\ U_{S_3^T q} & U_{S_3^T q^c} \end{pmatrix} . \tag{A.63}$$

<u>$\mathbf{U}_{\mathbf{S_nH}}$</u>

$$U_{S_1^\dagger H} = \lambda_{H1} H_\beta^* S_{1i} + A_{\tilde{2}1}\, \tilde{S}_{2i\beta}^* + \lambda_{H13}^*\, S_{3i}^I\, (H^\dagger \cdot \sigma^I)_\beta \,, \tag{A.64}$$

$$U_{S_1^\dagger H^*} = \lambda_{H1} H_\beta S_{1i}^\dagger + \lambda_{H13}^*\, S_{3i}^I\, (\sigma^I \cdot H)_\beta^T \,, \tag{A.65}$$

$$U_{S_1 H} = \lambda_{H1} H_\beta^* S_{1i} + \lambda_{H13}\, S_{3i}^{I\dagger}\, (H^\dagger \cdot \sigma^I)_\beta \,, \tag{A.66}$$

$$U_{S_1 H^*} = \lambda_{H1} H_\beta S_{1i}^\dagger + A_{\tilde{2}1}^* \tilde{S}_{2i\beta} + \lambda_{H13}\, S_{3i}^{I\dagger}\, (\sigma^I \cdot H)_\beta^T \,. \tag{A.67}$$

$$U_{\tilde{S}_1^\dagger H} = \lambda_{H\tilde{1}}\, H_\beta^*\, \tilde{S}_{1i} - \lambda_{3\tilde{1}} \left[ (H^T \cdot \epsilon \cdot \sigma^I)_\beta - (\epsilon \cdot \sigma^I \cdot H)_\beta^T \right] S_{3i}^I \,, \tag{A.68}$$

$$U_{\tilde{S}_1^\dagger H^*} = \lambda_{H\tilde{1}}\, H_\beta\, \tilde{S}_{1i} \,, \tag{A.69}$$

$$U_{\tilde{S}_1 H} = \lambda_{H\tilde{1}}\, H_\beta^*\, \tilde{S}_{1i}^\dagger \,, \tag{A.70}$$

$$U_{\tilde{S}_1 H^*} = \lambda_{H\tilde{1}}\, H_\beta\, \tilde{S}_{1i}^\dagger - \lambda_{3\tilde{1}}^*\, S_{3i}^{I\dagger} \left[ (\sigma^I \cdot \epsilon \cdot H^*)_\beta^T - (H^\dagger \cdot \sigma^I \cdot \epsilon)_\beta \right] . \tag{A.71}$$

$$U_{S_2^\dagger H} = \lambda_{H2}\, H_\beta^*\, S_{2i\alpha}^* - \lambda_{2\tilde{2}}\, \delta_{\alpha\beta} (H^T \cdot \epsilon \cdot \tilde{S}_{2i}^*) - \lambda_{2\tilde{2}} H_\alpha (\epsilon \cdot \tilde{S}_{2i}^*)_\beta^T - \lambda_{22}\, (\epsilon \cdot S_{2i}^*)_\beta^T (\epsilon \cdot H^*)_\alpha^T \,, \tag{A.72}$$

$$U_{S_2^\dagger H^*} = \lambda_{H2}\, H_\beta\, S_{2i\alpha}^* - \lambda_{22}\, (H^T \cdot \epsilon \cdot S_{2i}^*)\, \epsilon^{\alpha\beta} \,, \tag{A.73}$$

$$U_{S_2^T H} = \lambda_{H2} H_\beta^*\, S_{2i\alpha} - \lambda_{22}\, \epsilon^{\beta\alpha}\, (S_{2i}^T \cdot \epsilon \cdot H^*) \,, \tag{A.74}$$

$$U_{S_2^T H^*} = \lambda_{H2}\, H_\beta\, S_{2i\alpha} + \lambda_{2\tilde{2}}^*\, \delta_{\alpha\beta}\, (\tilde{S}_{2i} \cdot \epsilon \cdot H^*) + \lambda_{2\tilde{2}}^*\, H_\alpha^*\, (\tilde{S}_{2i}^T \cdot \epsilon)_\beta - \lambda_{22}\, (H^T \cdot \epsilon)_\alpha\, (S_{2i}^T \cdot \epsilon)_\beta \,. \tag{A.75}$$

$$\begin{aligned} U_{\tilde{S}_2^\dagger H} &= \tilde{\lambda}_{H2} H_\beta^* \tilde{S}_{2i\alpha} + A_{\tilde{2}1} S_{1i}^\dagger \delta_{\alpha\beta} - A_{\tilde{2}3}\, S_{3i}^{I\dagger}\, \sigma_{\alpha\beta}^I - \lambda_{\tilde{2}\tilde{2}}\, \delta_{\alpha\beta} (H^\dagger \cdot \tilde{S}_{2i}) \\ &\quad + \frac{1}{3} \lambda_5 \epsilon^{ijk} \left( -2\epsilon^{\alpha\alpha_1} \tilde{S}_{2j\alpha_1} \tilde{S}_{2k\beta} + \tilde{S}_{2k}^T \cdot \epsilon \cdot \tilde{S}_{2j} \delta_{\alpha\beta} \right) , \end{aligned} \tag{A.76}$$

$$U_{\tilde{S}_2^\dagger H^*} = \tilde{\lambda}_{H2} H_\beta \tilde{S}_{2i\alpha} + \lambda_{2\tilde{2}}^*\, \epsilon^{\alpha\beta}\, (H^\dagger \cdot S_{2i}^*) + \lambda_{2\tilde{2}}^*\, S_{2i\beta}^*\, (\epsilon \cdot H^*)_\alpha^T - \lambda_{\tilde{2}\tilde{2}}\, \epsilon^{\alpha\beta}\, (H^T \cdot \epsilon \cdot \tilde{S}_{2i}^*) \,, \tag{A.77}$$

$$U_{\tilde{S}_2^T H} = \tilde{\lambda}_{H2} H^*_\beta \tilde{S}^*_{2i\alpha} - \lambda_{2\tilde{2}} (S^T_{2i} \cdot H) \epsilon^{\beta\alpha} - \lambda_{2\tilde{2}} S_{2i\beta} (H^T \cdot \epsilon)_\alpha - \lambda_{\tilde{2}\tilde{2}} \epsilon^{\beta\alpha} (\tilde{S}^T_{2i} \cdot \epsilon \cdot H^*) \,, \tag{A.78}$$

$$\begin{aligned} U_{\tilde{S}_2^T H^*} &= \tilde{\lambda}_{H2} H_\beta \tilde{S}^*_{2i\alpha} + A^*_{\tilde{2}1} \delta_{\alpha\beta} S_{1i} - A^*_{\tilde{2}3} \sigma^I_{\beta\alpha} S^I_{3i} - \lambda_{\tilde{2}\tilde{2}} (\tilde{S}^\dagger_{2i} \cdot H) \\ &+ \frac{1}{3} \lambda_5 \epsilon^{ijk} \left( -2 \epsilon^{\alpha\alpha_1} \tilde{S}^*_{2j\alpha_1} \tilde{S}^*_{2k\beta} + \tilde{S}^\dagger_{2k} \cdot \epsilon \cdot \tilde{S}^*_{2j} \delta_{\alpha\beta} \right) . \end{aligned} \tag{A.79}$$

$$U_{S_3^\dagger H} = \lambda_{H3} H^*_\beta S^I_{3i} + \lambda_{H13} (H^\dagger \cdot \sigma^I)_\beta S_{1i} - i \lambda_{\epsilon H3} \epsilon^{IJK} (H^\dagger \cdot \sigma^J)_\beta S^K_{3i} \,, \tag{A.80}$$

$$\begin{aligned} U_{S_3^\dagger H^*} &= \lambda_{H3} H_\beta S^I_{3i} + \lambda_{H13} (\sigma^I \cdot H)^T_\beta S_{1i} - i \lambda_{\epsilon H3} \epsilon^{IJK} (\sigma^J \cdot H)^T_\beta S^K_{3i} \\ &+ \lambda_{3\tilde{1}} \tilde{S}_{1i} \left[ (H^\dagger \cdot \sigma^I \cdot \epsilon) - (\sigma^I \cdot \epsilon \cdot H^*)^T \right]_\beta \,, \end{aligned} \tag{A.81}$$

$$\begin{aligned} U_{S_3^T H} &= \lambda_{H3} H^*_\beta S^{I*}_{3i} + \lambda^*_{H13} (H^\dagger \cdot \sigma^I)_\beta S^\dagger_{1i} - i \lambda_{\epsilon H3} \epsilon^{IJK} (H^\dagger \cdot \sigma^K)_\beta S^{J*}_{3i} \\ &- \lambda_{3\tilde{1}} \tilde{S}^\dagger_{1i} \left[ (H^T \cdot \epsilon \cdot \sigma^I) - (\epsilon \cdot \sigma^I \cdot H)^T \right]_\beta \,, \end{aligned} \tag{A.82}$$

$$U_{S_3^T H^*} = \lambda_{H3} H_\beta S^{I*}_{3i} + \lambda^*_{H13} S^\dagger_{1i} (\sigma^I \cdot H)^T_\beta - i \lambda_{\epsilon H3} \epsilon^{IJK} (\sigma^K \cdot H)^T_\beta S^{J*}_{3i} \tag{A.83}$$

**Matrix Structure**

$$\mathbf{U_{S_n H}} = \begin{pmatrix} U_{S_n^\dagger H} & U_{S_n^\dagger H^*} \\ U_{S_n^T H} & U_{S_n^T H^*} \end{pmatrix} . \tag{A.84}$$

## A.3 $\mathbf{X_{LS}}$

$\mathbf{U_{fS_n}}$

$$U_{\bar{\ell}^c S_1} = (\lambda^{1L}_{pr})^T \epsilon^{\alpha\beta} q_{rj\beta} \,, \qquad U_{\bar{\ell} S_1^\dagger} = (\lambda^{1L}_{pr})^\dagger \epsilon^{\alpha\beta} q^c_{rj\beta} \,, \tag{A.85}$$

$$U_{\bar{q} S_1} = 2(\lambda^{\not{B}L}_{pr}) \epsilon^{ijk} \epsilon^{\alpha\beta} q^c_{rj\beta} \,, \qquad U_{\bar{q} S_1^\dagger} = -(\lambda^{1L}_{pr})^* \epsilon^{\alpha\beta} \ell^c_{r\beta} \delta_{ij} \,, \tag{A.86}$$

$$U_{\bar{q}^c S_1} = -(\lambda^{1L}_{pr}) \epsilon^{\alpha\beta} \ell_{r\beta} \delta_{ij} \,, \qquad U_{\bar{q}^c S_1^\dagger} = 2(\lambda^{\not{B}L}_{pr})^* \epsilon^{ijk} \epsilon^{\alpha\beta} q_{rk\beta} \,, \tag{A.87}$$

$$U_{\bar{u} S_1} = -(\lambda^{\not{B}R}_{pr})^T \epsilon^{ijk} d^c_{rk} \,, \qquad U_{\bar{u} S_1^\dagger} = -(\lambda^{1R}_{pr})^* e^c_r \delta_{ij} \,, \tag{A.88}$$

$$U_{\bar{u}^c S_1} = -(\lambda^{1R}_{pr}) e_r \delta_{ij} \,, \qquad U_{\bar{u}^c S_1^\dagger} = -(\lambda^{\not{B}R}_{pr})^\dagger \epsilon^{ijk} d_{rk} \,, \tag{A.89}$$

$$U_{\bar{e}^c S_1} = -(\lambda^{1R}_{pr})^T u_{rj} \,, \qquad U_{\bar{e} S_1^\dagger} = -(\lambda^{1R}_{pr})^\dagger u^c_{rj} \,, \tag{A.90}$$

$$U_{\bar{d} S_1} = (\lambda^{\not{B}R}_{pr}) \epsilon^{ijk} u^c_{rk} \,, \qquad U_{\bar{d}^c S_1^\dagger} = (\lambda^{\not{B}R}_{pr})^* \epsilon_{ijk} u_{rk} \,, \tag{A.91}$$

$$U_{\bar{u} \tilde{S}_1} = 2(\tilde{\lambda}^{1\not{B}}_{pr}) \epsilon^{ijk} u^c_{rk} \,, \qquad U_{\bar{u}^c \tilde{S}_1^\dagger} = -2(\tilde{\lambda}^{1\not{B}}_{pr})^\dagger \epsilon^{ijk} u_{rk} \,, \tag{A.92}$$

$$U_{\bar{e}^c \tilde{S}_1} = -(\tilde{\lambda}^1_{pr})^T d_{rj} \,, \qquad U_{\bar{e} \tilde{S}_1^\dagger} = -(\tilde{\lambda}^1_{pr})^\dagger d^c_{rj} \,, \tag{A.93}$$

$$U_{\bar{d}^c \tilde{S}_1} = -(\tilde{\lambda}^1_{pr}) e_r \delta_{ij} \,, \qquad U_{\bar{d} \tilde{S}_1^\dagger} = -(\tilde{\lambda}^1_{pr})^* e^c_r \delta_{ij} \,, \tag{A.94}$$

$$U_{\bar{\ell}^c S_2} = -(\lambda^{2RL}_{pr})^T \epsilon^{\beta\alpha} u^c_{rj} \,, \qquad U_{\bar{\ell} S_2^*} = (\lambda^{2RL}_{pr})^\dagger \epsilon^{\alpha\beta} u_{rj} \,, \tag{A.95}$$

$$U_{\bar{q} S_2} = -(\lambda^{2LR}_{pr}) \delta_{\alpha\beta} \delta_{ij} e_r \,, \qquad U_{\bar{q}^c S_2^*} = -(\lambda^{2LR}_{pr})^* \delta_{\alpha\beta} \delta_{ij} e^c_r \,, \tag{A.96}$$

$$U_{\bar{u} S_2} = -(\lambda^{2RL}_{pr}) \delta_{ij} \epsilon^{\beta\alpha} \ell_{r\alpha} \alpha \,, \qquad U_{\bar{u}^c S_2^*} = (\lambda^{2RL}_{pr})^* \delta_{ij} \ell^c_{r\alpha} \epsilon^{\alpha\beta} \,, \tag{A.97}$$

$$U_{\bar{e}^c S_2} = -(\lambda^{2LR}_{pr})^T\, q^c_{pj\beta}\ , \qquad U_{\bar{e}S_2^*} = -(\lambda^{2LR}_{pr})^\dagger\, q_{rj\beta}\ , \tag{A.98}$$

$$U_{\bar{\ell}^c \tilde{S}_2} = (\tilde{\lambda}_{pr})^T d^c_{ri}\epsilon^{\alpha\beta}\ , \qquad U_{\bar{\ell}\tilde{S}_2^*} = (\tilde{\lambda}pr)^\dagger d_{rj}\epsilon^{\alpha\beta}\ , \tag{A.99}$$

$$U_{\bar{d}\tilde{S}_2} = -(\tilde{\lambda}_{pr})\delta_{ij}\epsilon^{\beta\alpha}\ell_{r\alpha}\ , \qquad U_{\bar{d}^c\tilde{S}_2^*} = (\tilde{\lambda}_{pr})^*\delta_{ij}\ell^c_{r\alpha}\epsilon^{\alpha\beta}\ , \tag{A.100}$$

$$U_{\bar{\ell}^c S_3} = -(\lambda^{3L}_{pr})^T\,(q_{rj}\cdot\epsilon\cdot\sigma^J)_\alpha\ , \qquad U_{\bar{\ell}S_3^*} = (\lambda^{3L}_{pr})^\dagger\,\sigma^J_{\alpha\alpha_1}\,\epsilon^{\alpha_1\alpha_2}\,q^c_{rj\alpha_2}\ , \tag{A.101}$$

$$U_{\bar{q}^c S_3} = -(\lambda^{3L}_{pr})\,\delta_{ij}\,\epsilon^{\alpha\alpha_1}\sigma^I_{\alpha_1\alpha_2}\ell_{r\alpha_2}\ , \qquad U_{\bar{q}S_3^*} = (\lambda^{3L}_{pr})^*\,(\ell^c_r\cdot\sigma^J\cdot\epsilon)_\alpha\ , \tag{A.102}$$

$$U_{\bar{q}S_3} = 2(\lambda^{3\not{B}}_{pr})\,\epsilon^{ijk}\,\sigma^J_{\alpha\alpha_1}\epsilon^{\alpha_1\alpha_2}\,q^c_{rk\alpha_2}\ , \qquad U_{\bar{q}^c S_3^*} = 2(\lambda^{3\not{B}}_{pr})^\dagger\,\epsilon^{ijk}\,\epsilon^{\alpha\alpha_1}\,\sigma^J_{\alpha_1\alpha_2}\,q_{rk\alpha_2}\ . \tag{A.103}$$

## Matrix Structure

$$\mathbf{U}_{\ell\mathbf{S_1}} = \begin{pmatrix} 0 & U_{\bar{\ell}S_1^\dagger} \\ U_{\bar{\ell}^c S_1} & 0 \end{pmatrix}, \qquad \mathbf{U}_{\mathbf{qS_1}} = \begin{pmatrix} U_{\bar{q}S_1} & U_{\bar{q}S_1^\dagger} \\ U_{\bar{q}^c S_1} & U_{\bar{q}^c S_1^\dagger} \end{pmatrix}, \tag{A.104}$$

$$\mathbf{U}_{\mathbf{uS_1}} = \begin{pmatrix} U_{\bar{u}S_1} & U_{\bar{u}S_1^\dagger} \\ U_{\bar{u}^c S_1} & U_{\bar{u}^c S_1^\dagger} \end{pmatrix}, \quad \mathbf{U}_{\mathbf{dS_1}} = \begin{pmatrix} U_{\bar{d}S_1} & 0 \\ 0 & U_{\bar{d}^c S_1^\dagger} \end{pmatrix}, \quad \mathbf{U}_{\mathbf{eS_1}} = \begin{pmatrix} 0 & U_{\bar{e}S_1^\dagger} \\ U_{\bar{e}^c S_1} & 0 \end{pmatrix}, \tag{A.105}$$

$$\mathbf{U}_{\mathbf{u\tilde{S}_1}} = \begin{pmatrix} U_{\bar{u}\tilde{S}_1} & 0 \\ 0 & U_{\bar{\ell}^c \tilde{S}_1^\dagger} \end{pmatrix}, \quad \mathbf{U}_{\mathbf{e\tilde{S}_1}} = \begin{pmatrix} 0 & U_{\bar{e}\tilde{S}_1^\dagger} \\ U_{\bar{e}^c \tilde{S}_1} & 0 \end{pmatrix}, \quad \mathbf{U}_{\mathbf{d\tilde{S}_1}} = \begin{pmatrix} 0 & U_{\bar{d}\tilde{S}_1^\dagger} \\ U_{\bar{d}^c \tilde{S}_1} & 0 \end{pmatrix}, \tag{A.106}$$

$$\mathbf{U}_{\ell\mathbf{S_2}} = \begin{pmatrix} 0 & U_{\bar{\ell}S_2^*} \\ U_{\bar{\ell}^c S_2} & 0 \end{pmatrix}, \quad \mathbf{U}_{\mathbf{qS_2}} = \begin{pmatrix} U_{\bar{q}S_2} & 0 \\ 0 & U_{\bar{q}^c S_2^*} \end{pmatrix}, \tag{A.107}$$

$$\mathbf{U}_{\mathbf{uS_2}} = \begin{pmatrix} U_{\bar{u}S_2} & 0 \\ 0 & U_{\bar{u}^c S_2^*} \end{pmatrix}, \qquad \mathbf{U}_{\mathbf{eS_2}} = \begin{pmatrix} 0 & U_{\bar{e}S_2^*} \\ U_{\bar{e}^c S_2} & 0 \end{pmatrix}, \tag{A.108}$$

$$\mathbf{U}_{\ell\mathbf{\tilde{S}_2}} = \begin{pmatrix} 0 & U_{\bar{\ell}\tilde{S}_2^*} \\ U_{\bar{\ell}^c \tilde{S}_2} & 0 \end{pmatrix}, \qquad \mathbf{U}_{\mathbf{d\tilde{S}_2}} = \begin{pmatrix} U_{\bar{d}\tilde{S}_2} & 0 \\ 0 & U_{\bar{d}^c \tilde{S}_2^*} \end{pmatrix}, \tag{A.109}$$

$$\mathbf{U}_{\ell\mathbf{S_3}} = \begin{pmatrix} 0 & U_{\bar{\ell}S_3^*} \\ U_{\bar{\ell}^c S_3} & 0 \end{pmatrix}, \qquad \mathbf{U}_{\mathbf{qS_3}} = \begin{pmatrix} U_{\bar{q}S_3} & U_{\bar{q}S_3^*} \\ U_{\bar{q}^c S_3} & U_{\bar{q}^c S_3^*} \end{pmatrix}. \tag{A.110}$$

## $\mathbf{U_{HS_n}}$

$$U_{H^\dagger S_1} = \lambda_{H1}H_\alpha S^\dagger_{1j} + A^*_{\tilde{2}1}\tilde{S}_{2j\alpha} + \lambda_{H13}\,S^{J\dagger}_{3j}\,(\sigma^J\cdot H)^T_\alpha\ , \tag{A.111}$$

$$U_{H^\dagger S_1^\dagger} = \lambda_{H1}H_\alpha S_{1j} + \lambda^*_{H13}\,S^J_{3j}\,(\sigma^J\cdot H)^T_\alpha\ , \tag{A.112}$$

$$U_{H^T S_1} = \lambda_{H1}H^*_\alpha S^\dagger_{1j} + \lambda_{H13}\,S^{J\dagger}_{3j}\,(H^\dagger\cdot\sigma^J)_\alpha\ , \tag{A.113}$$

$$U_{H^T S_1^\dagger} = \lambda_{H1}H^*_\alpha S_{1j} + A_{\tilde{2}1}\tilde{S}^*_{2j\alpha} + \lambda^*_{H13}\,(H^\dagger\cdot\sigma^J)\,S^J_{3j}\ , \tag{A.114}$$

$$U_{H^\dagger\tilde{S}_1} = \lambda_{H\tilde{1}}\,H_\alpha\,\tilde{S}^\dagger_{1j} + \lambda^*_{3\tilde{1}}\left[(\sigma^I\cdot\epsilon\cdot H^*) - (H^\dagger\cdot\sigma^I\cdot\epsilon)^T\right]_\alpha\,S^{I\dagger}_{3j}\ , \tag{A.115}$$

$$U_{H^\dagger \tilde{S}_1^\dagger} = \lambda_{H\tilde{1}}\, H_\alpha\, \tilde{S}_{1j}\,, \tag{A.116}$$
$$U_{H^T \tilde{S}_1} = \lambda_{H\tilde{1}}\, H^*_\alpha\, \tilde{S}^\dagger_{1j}\,, \tag{A.117}$$
$$U_{H^T \tilde{S}_1^\dagger} = \lambda_{H\tilde{1}}\, H^*_\alpha\, \tilde{S}_{1j} - \lambda_{3\tilde{1}}\left[(H^T\cdot\epsilon\cdot\sigma^I) - (\epsilon\cdot\sigma^I\cdot H)^T\right]_\alpha S^I_{3j}\,. \tag{A.118}$$

$$U_{H^\dagger S_2} = \lambda_{H2}\, H_\alpha\, S_{2j\beta} - \lambda^*_{2\tilde{2}}\left[H^*_\beta\,(\tilde{S}^T_{2j}\cdot\epsilon)_\alpha - \delta_{\alpha\beta}(\tilde{S}^T_{2j}\cdot\epsilon\cdot H^*)\right] - \lambda_{22}\,(S_{2j}\cdot\epsilon)^T_\alpha\,(H^T\cdot\epsilon)^T_\beta\,, \tag{A.119}$$
$$U_{H^\dagger S_2^*} = \lambda_{H2}\, H_\alpha\, S^*_{2j\beta} - \lambda_{22}\,\epsilon^{\beta\alpha}\,(H^T\cdot\epsilon\cdot S^*_{2j})\,, \tag{A.120}$$
$$U_{H^T S_2} = \lambda_{H2}\, H^*_\alpha\, S_{2j\beta} - \lambda_{22}\,\epsilon^{\alpha\beta}\,(S^T_{2j}\cdot\epsilon\cdot H^*)\,, \tag{A.121}$$
$$U_{H^T S_2^*} = \lambda_{H2}\, H_\alpha\, S^*_{2j\beta} - \lambda_{2\tilde{2}}\left[H_\beta\,(\epsilon\cdot\tilde{S}^*_{2i})_\alpha + (H^T\cdot\epsilon\cdot\tilde{S}^*_{2j})\delta_{\alpha\beta}\right] - \lambda_{22}\,(\epsilon\cdot S^*_{2j})_\alpha\,(\epsilon\cdot H^*)_\beta\,. \tag{A.122}$$

$$\begin{aligned} U_{H^\dagger \tilde{S}_2} &= \tilde{\lambda}_{H2} H_\alpha \tilde{S}^*_{2j\beta} + A^*_{\tilde{2}1}\delta_{\alpha\beta} S_{1j} - A^*_{\tilde{2}3}\, S^I_{3j}\,\sigma^I_{\alpha\beta} - \lambda_{\tilde{2}\tilde{2}}\,(\tilde{S}^\dagger_{2i}\cdot H) \\ &\quad + \frac{1}{3}\lambda_5\epsilon^{ijk}\left[-2\tilde{S}_{2i\alpha_1}\epsilon^{\alpha_1\beta}\tilde{S}_{2k\alpha} + \left(\tilde{S}_{2i}\cdot\epsilon\cdot\tilde{S}_{2k}\right)\delta_{\alpha\beta}\right]\,, \end{aligned} \tag{A.123}$$
$$U_{H^\dagger \tilde{S}_2^*} = \tilde{\lambda}_{H2} H_\alpha \tilde{S}_{2j\beta} + \lambda^*_{2\tilde{2}}\left[S^*_{2j\alpha}\,(\epsilon\cdot H^*)_\beta - \epsilon^{\alpha\beta}\,(H^\dagger\cdot S^*_{2j})\right] + \lambda_{\tilde{2}\tilde{2}}\,\epsilon^{\alpha\beta}\,(H^T\cdot\epsilon\cdot\tilde{S}^*_{2j})\,, \tag{A.124}$$
$$U_{H^T \tilde{S}_2} = \tilde{\lambda}_{H2} H^*_\alpha \tilde{S}^*_{2j\beta} - \lambda_{2\tilde{2}}\left[\epsilon^{\alpha\beta}\,(S^T_{2j}\cdot H) - S_{2j\alpha}\,(H^T\cdot\epsilon)^T_\beta\right] - \lambda_{\tilde{2}\tilde{2}}\,\epsilon^{\alpha\beta}\,(\tilde{S}_{2j}\cdot\epsilon\cdot H^*)\,, \tag{A.125}$$
$$\begin{aligned} U_{H^T \tilde{S}_2^*} &= \tilde{\lambda}_{H2} H^*_\alpha \tilde{S}_{2i\beta} + A_{\tilde{2}1} S^\dagger_{1j}\delta_{\alpha\beta} - A_{\tilde{2}3}\, S^{I\dagger}_{3j}\,\sigma^I_{\beta\alpha} - \lambda_{\tilde{2}\tilde{2}}\,(H^\dagger\cdot\tilde{S}_{2i}) \\ &\quad + \frac{1}{3}\lambda_5\epsilon^{ijk}\left[-2\tilde{S}^*_{2i\alpha_1}\epsilon^{\alpha_1\beta}\tilde{S}^*_{2k\alpha} + \left(\tilde{S}^\dagger_{2i}\cdot\epsilon\cdot\tilde{S}^*_{2k}\right)\delta_{\alpha\beta}\right]\,. \end{aligned} \tag{A.126}$$

$$U_{H^\dagger S_3} = \lambda_{H3}\, H_\alpha\, S^{J\dagger}_{3j} + \lambda^*_{H13}\,(\sigma^J\cdot H)_\alpha\, S^\dagger_{1j} - i\lambda_{\epsilon H3}\,\epsilon^{IJK}\,(H^\dagger\cdot\sigma^I)^T_\alpha\, S^{K\dagger}_{3j}\,, \tag{A.127}$$
$$\begin{aligned} U_{H^\dagger S_3^*} &= \lambda_{H3}\, H_\alpha\, S^J_{3j} + \lambda_{H13}\,(\sigma^J\cdot H)_\alpha\, S_{1j} + i\lambda_{\epsilon H3}\,\epsilon^{IJK}\,(\sigma^I\cdot H)_\alpha\, S^K_{3j} \\ &\quad + \lambda^*_{3\tilde{1}}\,\tilde{S}_{1j}\left[(\sigma^J\cdot\epsilon\cdot H^*) - (H^\dagger\cdot\sigma^J\cdot\epsilon)^T\right]_\alpha\,, \end{aligned} \tag{A.128}$$
$$\begin{aligned} U_{H^T S_3} &= \lambda_{H3}\, H^*_\alpha\, S^{J\dagger}_{3j} + \lambda^*_{H13}\,(\sigma^I\cdot H^*)_\alpha\, S^\dagger_{1j} - i\lambda_{\epsilon H3}\,\epsilon^{IJK}\,(H^\dagger\cdot\sigma^I)^T_\alpha\, S^{K\dagger}_{3j} \\ &\quad - \lambda_{3\tilde{1}}\,\tilde{S}^\dagger_{1j}\left[(\epsilon\cdot\sigma^J\cdot H) - (H^T\cdot\epsilon\cdot\sigma^J)^T\right]_\alpha\,, \end{aligned} \tag{A.129}$$
$$U_{H^T S_3^*} = \lambda_{H3}\, H^*_\alpha\, S^J_{3j} + \lambda_{H13}\,(H^\dagger\cdot\sigma^J)^T_\alpha\, S_{1j} + i\lambda_{\epsilon H3}\,\epsilon^{IJK}\,(H^\dagger\cdot\sigma^I)_\alpha\, S^K_{3j}\,. \tag{A.130}$$

**Matrix Structure**

$$\mathbf{U_{HS_n}} = \begin{pmatrix} U_{H^\dagger S_n} & U_{H^\dagger S_n^*} \\ U_{H^T S_n} & U_{H^T S_n^*} \end{pmatrix}\,. \tag{A.131}$$

## A.4 $\mathbf{X_{LL}}$

**$\mathbf{U_{ff}}$**

$$U_{\bar{\ell} q^c} = (\lambda^{1L}_{pr})^\dagger S^\dagger_{1j}\epsilon^{\alpha\beta} + (\lambda^{3L}_{pr})^\dagger\, S^J_{3j}\,\sigma^J_{\alpha\gamma}\,\epsilon^{\gamma\beta}\,, \qquad U_{\bar{\ell}^c q} = -(\lambda^{1L}_{pr})^T S_{1j}\epsilon^{\alpha\beta} + (\lambda^{3L}_{pr})^T\, S^J_{3j}\,\epsilon^{\beta\gamma}\,\sigma^J_{\gamma\alpha}\,, \tag{A.132}$$

$$U_{\bar{\ell}u} = (\lambda^{2RL}_{pr})^{\dagger}\,(\epsilon\cdot S^{*}_{2i})_{\alpha}\,, \qquad U_{\bar{\ell}^c u^c} = (\lambda^{2RL}_{pr})^{T}\,(\epsilon\cdot S_{2j})^{T}_{\alpha}\,, \tag{A.133}$$

$$U_{\bar{\ell}e} = (y_E)_{pr} H_{\alpha}\,, \qquad U_{\bar{\ell}^c e^c} = (y_E)^{*}_{pr} H^{*}_{\alpha}\,, \tag{A.134}$$

$$U_{\bar{\ell}d} = (\tilde{\lambda}_{pr})^{\dagger}\epsilon^{\alpha\beta}\tilde{S}^{*}_{2i\beta}\,, \qquad U_{\bar{\ell}^c d^c} = (\tilde{\lambda}_{pr})^{T}\epsilon^{\alpha\beta}\tilde{S}_{2j\beta}\,, \tag{A.135}$$

$$U_{\bar{q}\ell^c} = -(\lambda^{1L}_{pr})^{*} S^{\dagger}_{1i}\epsilon^{\alpha\beta} + (\lambda^{3L}_{pr})^{*} S^{I}_{3i}\sigma^{I}_{\beta\gamma}\,\epsilon^{\gamma\alpha}\,, \qquad U_{\bar{q}^c\ell} = -(\lambda^{1L}_{pr})\epsilon^{\alpha\beta} S_{1i} - (\lambda^{3L}_{pr}) S^{I}_{3i}\,\sigma^{I}_{\alpha\gamma}\epsilon^{\gamma\beta}\,, \tag{A.136}$$

$$\begin{aligned} U_{\bar{q}q^c} &= -2(\lambda^{\not{B}L}_{pr})\epsilon^{\alpha\beta}\epsilon^{ijk}S_{1k}\,, & U_{\bar{q}^c\bar{q}} &= -2(\lambda^{\not{B}L}_{pr})^{*}\epsilon^{\alpha\beta}\epsilon^{ijk}S^{\dagger}_{1k}\,, \\ &-2(\lambda^{3\not{B}}_{pr})\,\epsilon^{ijk}S^{K}_{3k}\,\sigma^{K}_{\alpha\gamma}\epsilon^{\gamma\beta}\,, & &-(\lambda^{3\not{B}}_{pr})^{\dagger}\epsilon^{ijk}\,\epsilon^{\alpha\gamma}\sigma^{K}_{\gamma\beta}S^{K\dagger}_{3k} \end{aligned} \tag{A.137}$$

$$U_{\bar{q}u} = (y_U)_{pr}\delta_{ij}\epsilon^{\alpha\beta}H^{*}_{\beta}\,, \qquad U_{\bar{q}^c u^c} = (y_U)^{*}_{pr}\delta_{ij}\epsilon^{\alpha\beta}H_{\beta}\,, \tag{A.138}$$

$$U_{\bar{q}e} = -(\lambda^{2LR}_{pr})\,S_{2i\alpha}\,, \qquad U_{\bar{q}^c e^c} = -(\lambda^{2LR}_{pr})^{*}\,S^{*}_{2i\alpha}\,, \tag{A.139}$$

$$U_{\bar{q}d} = (y_D)_{pr}H_{\alpha}\delta_{ij}\,, \qquad U_{\bar{q}^c d^c} = (y_D)^{*}_{pr}\delta_{ij}H^{*}_{\alpha}\,, \tag{A.140}$$

$$U_{\bar{u}\ell} = -(\lambda^{2RL}_{pr})\,S_{2i\gamma}\epsilon^{\gamma\beta}\,, \qquad U_{\bar{u}^c\ell^c} = (\lambda^{2RL}_{pr})^{*}\,\epsilon^{\beta\gamma}\,S^{*}_{2i\gamma}\,, \tag{A.141}$$

$$U_{\bar{u}q} = -(y_U)^{\dagger}_{pr}\epsilon^{\alpha\beta}H_{\alpha}\delta_{ij}\,, \qquad U_{\bar{u}^c\bar{q}^c} = -(y_U)^{T}_{pr}\epsilon^{\beta\alpha}H^{*}_{\alpha}\delta_{ij}\,, \tag{A.142}$$

$$U_{\bar{u}u^c} = -2(\tilde{\lambda}^{1\not{B}}_{pr})\,\epsilon^{ijk}\,\tilde{S}_{1k}\,, \qquad U_{\bar{u}^c u} = 2(\tilde{\lambda}^{1\not{B}}_{pr})^{\dagger}\,\epsilon^{ijk}\,\tilde{S}^{\dagger}_{1k}\,, \tag{A.143}$$

$$U_{\bar{u}e^c} = -(\lambda^{1R}_{pr})^{*}S^{\dagger}_{1i}\,, \qquad U_{\bar{u}^c e} = -(\lambda^{1R}_{pr})S_{1i}\,, \tag{A.144}$$

$$U_{\bar{u}d^c} = -(\lambda^{\not{B}R}_{pr})^{T}\epsilon^{ijk}S_{1k}\,, \qquad U_{\bar{u}^c d} = -(\lambda^{\not{B}R}_{pr})^{\dagger}\epsilon^{ijk}S^{\dagger}_{1k}\,, \tag{A.145}$$

$$U_{\bar{e}\ell} = (y_E)^{\dagger}_{pr}H^{*}_{\beta}\,, \qquad U_{\bar{e}^c\ell^c} = (y_E)^{T}_{pr}H_{\beta}\,, \tag{A.146}$$

$$U_{\bar{e}q} = -(\lambda^{2LR}_{pr})^{\dagger}\,S^{\dagger}_{2j\alpha}\,, \qquad U_{\bar{e}^c q^c} = -(\lambda^{2LR}_{pr})^{T}\,S_{2j\beta}\,, \tag{A.147}$$

$$U_{\bar{e}u^c} = (\lambda^{1R}_{pr})^{\dagger}S^{\dagger}_{1j}\,, \qquad U_{\bar{e}^c u} = -(\lambda^{1R}_{pr})^{T}S_{1j}\,, \tag{A.148}$$

$$U_{\bar{e}d^c} = -(\tilde{\lambda}_{pr})^{\dagger}\,\tilde{S}_{1j}\,, \qquad U_{\bar{e}^c d} = -(\tilde{\lambda}_{pr})^{T}\,\tilde{S}_{1j}\,, \tag{A.149}$$

$$U_{\bar{d}\ell} = -(\tilde{\lambda}_{pr})\tilde{S}_{2i\alpha}\epsilon^{\alpha\beta}\,, \qquad U_{\bar{d}^c\ell^c} = (\tilde{\lambda}_{pr})^{*}\epsilon^{\beta\alpha}\tilde{S}^{*}_{2i\alpha}\,, \tag{A.150}$$

$$U_{\bar{d}q} = (y_D)^{\dagger}_{pr}H^{*}_{\beta}\delta_{ij}\,, \qquad U_{\bar{d}^c q^c} = (y_D)^{T}_{pr}H_{\alpha}\delta_{ij}\,, \tag{A.151}$$

$$U_{\bar{d}u^c} = (\lambda^{\not{B}R}_{pr})\epsilon^{ijk}S_{1k}\,, \qquad U_{\bar{d}^c u} = (\lambda^{\not{B}R}_{pr})^{*}\epsilon^{ijk}S^{\dagger}_{1k}\,, \tag{A.152}$$

$$U_{\bar{d}e^c} = -(\tilde{\lambda}_{pr})^{*}\,\tilde{S}^{\dagger}_{1i}\,, \qquad U_{\bar{d}^c e} = -(\tilde{\lambda}_{pr})\,\tilde{S}_{1i}\,. \tag{A.153}$$

**Matrix Structure**

$$\mathbf{U_{\ell q}} = \begin{pmatrix} 0 & U_{\bar{\ell} q^c} \\ U_{\bar{\ell}^c q} & 0 \end{pmatrix}, \quad \mathbf{U_{\ell u}} = \begin{pmatrix} U_{\bar{\ell} u} & 0 \\ 0 & U_{\bar{\ell}^c u^c} \end{pmatrix}, \tag{A.154}$$

$$\mathbf{U_{\ell e}} = \begin{pmatrix} U_{\bar{\ell} e} & 0 \\ 0 & U_{\bar{\ell}^c e^c} \end{pmatrix}, \quad \mathbf{U_{\ell d}} = \begin{pmatrix} U_{\bar{\ell} d} & 0 \\ 0 & U_{\bar{\ell}^c d^c} \end{pmatrix}, \tag{A.155}$$

$$\mathbf{U_{q\ell}} = \begin{pmatrix} 0 & U_{\bar{q}\ell^c} \\ U_{\bar{q}^c \ell} & 0 \end{pmatrix}, \quad \mathbf{U_{qq}} = \begin{pmatrix} 0 & U_{\bar{q}q^c} \\ U_{\bar{q}^c q} & 0 \end{pmatrix}, \quad \mathbf{U_{qu}} = \begin{pmatrix} U_{\bar{q}u} & 0 \\ 0 & U_{\bar{q}^c u^c} \end{pmatrix}, \tag{A.156}$$

$$\mathbf{U_{qe}} = \begin{pmatrix} U_{\bar{q}e} & 0 \\ 0 & U_{\bar{q}^c e^c} \end{pmatrix}, \quad \mathbf{U_{qd}} = \begin{pmatrix} U_{\bar{q}d} & 0 \\ 0 & U_{\bar{q}^c d^c} \end{pmatrix}, \tag{A.157}$$

$$\mathbf{U_{u\ell}} = \begin{pmatrix} U_{\bar{u}\ell} & 0 \\ 0 & U_{\bar{u}^c \ell^c} \end{pmatrix}, \quad \mathbf{U_{uq}} = \begin{pmatrix} U_{\bar{u}q} & 0 \\ 0 & U_{\bar{u}^c q^c} \end{pmatrix}, \quad \mathbf{U_{uu}} = \begin{pmatrix} 0 & U_{\bar{u}u^c} \\ U_{\bar{u}^c u} & 0 \end{pmatrix}, \tag{A.158}$$

$$\mathbf{U_{ue}} = \begin{pmatrix} 0 & U_{\bar{u}e^c} \\ U_{\bar{u}^c e} & 0 \end{pmatrix}, \quad \mathbf{U_{ud}} = \begin{pmatrix} 0 & U_{\bar{u}d^c} \\ U_{\bar{u}^c d} & 0 \end{pmatrix}, \tag{A.159}$$

$$\mathbf{U_{d\ell}} = \begin{pmatrix} U_{\bar{d}\ell} & 0 \\ 0 & U_{\bar{d}^c \ell^c} \end{pmatrix}, \quad \mathbf{U_{dq}} = \begin{pmatrix} U_{\bar{d}q} & 0 \\ 0 & U_{\bar{d}^c q^c} \end{pmatrix}, \tag{A.160}$$

$$\mathbf{U_{du}} = \begin{pmatrix} 0 & U_{\bar{d}u^c} \\ U_{\bar{d}^c u} & 0 \end{pmatrix}, \quad \mathbf{U_{de}} = \begin{pmatrix} 0 & U_{\bar{d}e^c} \\ U_{\bar{d}^c e} & 0 \end{pmatrix}, \tag{A.161}$$

$$\mathbf{U_{e\ell}} = \begin{pmatrix} U_{\bar{e}\ell} & 0 \\ 0 & U_{\bar{e}^c \ell^c} \end{pmatrix}, \quad \mathbf{U_{eq}} = \begin{pmatrix} U_{\bar{e}q} & 0 \\ 0 & U_{\bar{e}^c q^c} \end{pmatrix}, \tag{A.162}$$

$$\mathbf{U_{eu}} = \begin{pmatrix} 0 & U_{\bar{e}u^c} \\ U_{\bar{e}^c u} & 0 \end{pmatrix}, \quad \mathbf{U_{ed}} = \begin{pmatrix} 0 & U_{\bar{e}d^c} \\ U_{\bar{e}^c d} & 0 \end{pmatrix}. \tag{A.163}$$

$$\mathbf{U_{\ell u}} = \mathbf{U_{\ell\ell}} = \mathbf{U_{qe}} = \mathbf{U_{u\ell}} = \mathbf{U_{uu}} = \mathbf{U_{dd}} = \mathbf{U_{de}} = \mathbf{U_{ee}} = \mathbf{U_{eq}} = \mathbf{U_{ed}} = \mathbf{0} \tag{A.164}$$

## $\underline{\mathbf{U_{Hf}}}$

$$U_{H^\dagger \ell} = (y_E)^\dagger_{pr} \bar{e}_p \delta_{\alpha\beta}, \quad U_{H^T \ell^c} = (y_E)^T_{pr} \bar{e}^c_p \delta_{\alpha\beta}, \tag{A.165}$$

$$U_{H^\dagger q} = (y_D)^\dagger_{pr} \bar{d}_{pj} \delta_{\alpha\beta}, \quad U_{H^\dagger q^c} = (y_U)^T_{pr} \bar{u}^c_{pj} \epsilon^{\beta\alpha}, \tag{A.166}$$

$$U_{H^T q} = (y_U)^\dagger_{pr} \epsilon^{\alpha\beta} \bar{u}_{pj}, \quad U_{H^T q^c} = (y_D)^T_{pr} \bar{d}^c_{pj} \delta_{\alpha\beta}, \tag{A.167}$$

$$U_{H^\dagger u} = (y_U)_{pr} \bar{q}_{pj\beta} \epsilon^{\beta\alpha}, \quad U_{H^T u^c} = (y_U)^*_{pr} \bar{q}^c_{pj\beta} \epsilon^{\alpha\beta}, \tag{A.168}$$

$$U_{H^T e} = (y_E)_{pr} \bar{\ell}_{p\alpha}, \quad U_{H^\dagger e^c} = (y_E)^*_{pr} \bar{\ell}^c_{p\alpha}, \tag{A.169}$$

$$U_{H^T d} = (y_D)_{pr} \bar{q}_{pj\alpha}, \quad U_{H^\dagger d^c} = (y_D)^*_{pr} \bar{q}^c_{pj\alpha}. \tag{A.170}$$

(A.171)

**Matrix Structure**

$$\mathbf{U_{H\ell}} = \begin{pmatrix} U_{H^\dagger \ell} & 0 \\ 0 & U_{H^T \ell^c} \end{pmatrix}, \qquad \mathbf{U_{Hq}} = \begin{pmatrix} U_{H^\dagger q} & U_{H^\dagger q^c} \\ U_{H^T q} & U_{H^T q^c} \end{pmatrix}, \tag{A.172}$$

$$\mathbf{U_{Hu}} = \begin{pmatrix} U_{H^\dagger u} & 0 \\ 0 & U_{H^T u^c} \end{pmatrix}, \quad \mathbf{U_{Hd}} = \begin{pmatrix} 0 & U_{H^\dagger d^c} \\ U_{H^T d} & 0 \end{pmatrix}, \quad \mathbf{U_{He}} = \begin{pmatrix} 0 & U_{H^\dagger e^c} \\ U_{H^T e} & 0 \end{pmatrix}. \tag{A.173}$$

$\mathbf{U_{fH}}$

$$U_{\bar{\ell}H} = (y_E)_{pr} e_r \delta_{\alpha\beta}\,, \qquad U_{\bar{\ell}^c H^*} = (y_E)^*_{pr} e^c_r \delta_{\alpha\beta}\,, \tag{A.174}$$

$$U_{\bar{q}H} = (y_D)_{pr} d_{ri} \delta_{\alpha\beta}\,, \qquad U_{\bar{q}H^*} = (y_U)_{pr} u_{ri} \epsilon^{\alpha\beta}\,, \tag{A.175}$$

$$U_{\bar{q}^c H} = (y_U)^*_{pr} \epsilon^{\alpha\beta} u^c_{ri}\,, \qquad U_{\bar{q}^c H^*} = (y_D)^*_{pr} d^c_{ri} \delta_{\alpha\beta}\,, \tag{A.176}$$

$$U_{\bar{u}H} = (y_U)^\dagger_{pr} \epsilon^{\beta\alpha} q_{ri\alpha}\,, \qquad U_{\bar{u}^c H^*} = (y_U)^T_{pr} \epsilon^{\alpha\beta} q^c_{ri\alpha}\,, \tag{A.177}$$

$$U_{\bar{d}^c H} = (y_D)^T_{pr} q^c_{ri\beta}\,, \qquad U_{\bar{d}H^*} = (y_D)^\dagger_{pr} q_{ri\beta}\,, \tag{A.178}$$

$$U_{\bar{e}^c H} = (y_E)^T_{pr} \ell^c_{r\beta}\,, \qquad U_{\bar{e}H^*} = (y_E)^\dagger_{pr} \ell_{r\beta}\,. \tag{A.179}$$

**Matrix Structure**

$$\mathbf{U_{\ell H}} = \begin{pmatrix} U_{\bar{\ell}H} & 0 \\ 0 & U_{\bar{\ell}^c H^*} \end{pmatrix}, \qquad \mathbf{U_{qH}} = \begin{pmatrix} U_{\bar{q}H} & U_{\bar{q}H^*} \\ U_{\bar{q}^c H} & U_{\bar{q}^c H^*} \end{pmatrix}, \tag{A.180}$$

$$\mathbf{U_{uH}} = \begin{pmatrix} U_{\bar{u}H} & 0 \\ 0 & U_{\bar{u}^c H^*} \end{pmatrix}, \quad \mathbf{U_{dH}} = \begin{pmatrix} 0 & U_{\bar{d}H^*} \\ U_{\bar{d}^c H} & 0 \end{pmatrix}, \quad \mathbf{U_{eH}} = \begin{pmatrix} 0 & U_{\bar{e}H^*} \\ U_{\bar{e}^c H} & 0 \end{pmatrix}. \tag{A.181}$$

$\mathbf{U_{Vf}}$

$$U_{B\ell} = -\bar{\ell}_{r\beta} g' Y_\ell \gamma^\mu\,, \qquad U_{B\ell^c} = \bar{\ell}^c_{r\beta} g' Y_\ell \gamma^\mu\,, \tag{A.182}$$

$$U_{W\ell} = -\frac{g}{2} \bar{\ell}_{r\alpha_1} \sigma^I_{\alpha_1\beta} \gamma^\mu\,, \qquad U_{W\ell^c} = \frac{g}{2} \bar{\ell}_{r\alpha_1} \sigma^I_{\beta\alpha_1} \gamma^\mu\,, \tag{A.183}$$

$$U_{Bq} = -\bar{q}_{rj\beta} g' Y_q \gamma^\mu\,, \qquad U_{Bq^c} = \bar{q}^c_{rj\beta} g' Y_q \gamma^\mu\,, \tag{A.184}$$

$$U_{Wq} = -\frac{g}{2} \bar{q}_{rj\alpha_1} \sigma^I_{\alpha_1\beta} \gamma^\mu\,, \qquad U_{Wq^c} = \frac{g}{2} \bar{\ell}_{rj\alpha_1} \sigma^I_{\beta\alpha_1} \gamma^\mu\,, \tag{A.185}$$

$$U_{Gq} = -g_s \bar{q}_{ri\beta} T^A_{ij} \gamma^\mu\,, \qquad U_{Gq^c} = g_s \bar{q}^c_{ri\beta} T^A_{ji} \gamma^\mu\,, \tag{A.186}$$

$$U_{Bu} = -\bar{u}_{rj} g' Y_u \gamma^\mu\,, \qquad U_{Bu^c} = \bar{u}^c_{ri} g' Y_u \gamma^\mu\,, \tag{A.187}$$

$$U_{Gu} = -g_s \bar{u}_{ri} T^A_{ij} \gamma^\mu\,, \qquad U_{Gu^c} = g_s \bar{u}_{ri} T^A_{ji} \gamma^\mu\,, \tag{A.188}$$

$$U_{Bd} = -\bar{d}_{rj} g' Y_d \gamma^\mu\,, \qquad U_{Bd^c} = \bar{d}^c_{rj} g' Y_d \gamma^\mu\,, \tag{A.189}$$

$$U_{Gd} = -g_s \bar{d}_{ri} T^A_{ij} \gamma^\mu\,, \qquad U_{Gd^c} = g_s \bar{d}^c_{ri} T^A_{ji} \gamma^\mu\,, \tag{A.190}$$

$$U_{Be} = -\bar{e}_r g' Y_e \gamma^\mu \,, \qquad U_{Be^c} = \bar{e}^c_r g' Y_e \gamma^\mu \,. \tag{A.191}$$

## Matrix Structure

$$\mathbf{U_{V\ell}} = \begin{pmatrix} U_{B\ell} & U_{B\ell^c} \\ U_{W\ell} & U_{W\ell^c} \\ 0 & 0 \end{pmatrix} , \qquad \mathbf{U_{Vq}} = \begin{pmatrix} U_{Bq} & U_{Bq^c} \\ U_{Wq} & U_{Wq^c} \\ U_{Gq} & U_{Gq^c} \end{pmatrix} , \tag{A.192}$$

$$\mathbf{U_{Vu}} = \begin{pmatrix} U_{Bu} & U_{Bu^c} \\ 0 & 0 \\ U_{Gu} & U_{Gu^c} \end{pmatrix} , \qquad \mathbf{U_{Vd}} = \begin{pmatrix} U_{Bd} & U_{Bd^c} \\ 0 & 0 \\ U_{Gd} & U_{Gd^c} \end{pmatrix} , \qquad \mathbf{U_{Ve}} = \begin{pmatrix} U_{Be} & U_{Be^c} \\ 0 & 0 \\ 0 & 0 \end{pmatrix} . \tag{A.193}$$

## $\mathbf{U_{fV}}$

$$U_{\bar{\ell}B} = -g' Y_\ell \gamma^\nu \ell_{p\alpha} \,, \qquad U_{\bar{\ell}^c B} = g' Y_\ell \gamma^\nu \ell^c_{p\alpha} \,, \tag{A.194}$$

$$U_{\bar{\ell}W} = -\frac{g}{2} \sigma^I_{\alpha\alpha_1} \gamma^\nu \ell_{p\alpha_1} \,, \qquad U_{\bar{\ell}^c W} = \frac{g}{2} \sigma^I_{\alpha_1\alpha} \gamma^\nu \ell^c_{p\alpha_1} \,, \tag{A.195}$$

$$U_{\bar{q}B} = -g' Y_q \gamma^\nu q_{pi\alpha} \,, \qquad U_{\bar{q}^c B} = g' Y_q \gamma^\nu q^c_{pi\alpha} \,, \tag{A.196}$$

$$U_{\bar{q}W} = -\frac{g}{2} \sigma^I_{\alpha\alpha_1} \gamma^\nu q_{pi\alpha_1} \,, \qquad U_{\bar{q}^c W} = \frac{g}{2} \sigma^I_{\alpha_1\alpha} \gamma^\nu q_{pi\alpha_1} \,, \tag{A.197}$$

$$U_{\bar{q}G} = -g_s \gamma^\mu T^B_{ij} q_{pj\alpha} \,, \qquad U_{\bar{q}^c G} = g_s \gamma^\mu T^B_{ji} q^c_{pj\alpha} \,, \tag{A.198}$$

$$U_{\bar{u}B} = -g' Y_u \gamma^\nu u_{pi} \,, \qquad U_{\bar{u}^c B} = g' Y_q \gamma^\nu u^c_{pi} \,, \tag{A.199}$$

$$U_{\bar{u}G} = -g_s \gamma^\mu T^B_{ij} u_{pj} \,, \qquad U_{\bar{u}^c G} = g_s \gamma^\mu T^B_{ji} q^c_{pj} \,, \tag{A.200}$$

$$U_{\bar{d}B} = -g' Y_d \gamma^\nu d_{pi} \,, \qquad U_{\bar{d}^c B} = g' Y_d \gamma^\nu d^c_{pi} \,, \tag{A.201}$$

$$U_{\bar{d}G} = -g_s \gamma^\mu T^B_{ij} d_{pj} \,, \qquad U_{\bar{d}^c G} = g_s \gamma^\mu T^B_{ji} d^c_{pj} \,, \tag{A.202}$$

$$U_{\bar{e}B} = -g' Y_e \gamma^\nu e_p \,, \qquad U_{\bar{e}^c B} = g' Y_e \gamma^\nu e_p \,. \tag{A.203}$$

## Matrix Structure

$$\mathbf{U_{\ell V}} = \begin{pmatrix} U_{\bar{\ell}B} & U_{\bar{\ell}W} & 0 \\ U_{\bar{\ell}^c B} & U_{\bar{\ell}^c W} & 0 \end{pmatrix} , \qquad \mathbf{U_{qV}} = \begin{pmatrix} U_{\bar{q}B} & U_{\bar{q}W} & U_{\bar{q}G} \\ U_{\bar{q}^c B} & U_{\bar{q}^c W} & U_{\bar{q}^c G} \end{pmatrix} , \tag{A.204}$$

$$\mathbf{U_{uV}} = \begin{pmatrix} U_{\bar{u}B} & 0 & U_{\bar{u}G} \\ U_{\bar{u}B} & 0 & U_{\bar{u}^c G} \end{pmatrix} , \quad \mathbf{U_{dV}} = \begin{pmatrix} U_{\bar{d}B} & 0 & U_{\bar{d}G} \\ U_{\bar{d}^c B} & 0 & U_{\bar{d}^c G} \end{pmatrix} , \quad \mathbf{U_{eV}} = \begin{pmatrix} U_{\bar{e}B} & 0 & 0 \\ U_{\bar{e}^c B} & 0 & 0 \end{pmatrix} . \tag{A.205}$$

## $\mathbf{Z_{S_n V}}$

$$Z^{\rho\nu}_{S_{(1,\tilde{1})}B} = -g^{\rho\nu} g' Y_{S_{(1,\tilde{1})}} S^{\dagger}_{(1,\tilde{1})i}\,, \qquad \bar{Z}^{\mu\kappa}_{BS_{(1,\tilde{1})}} = -g^{\mu\kappa} g' Y_{S_{(1,\tilde{1})}} S^{\dagger}_{(1,\tilde{1})j}\,, \tag{A.206}$$

$$Z^{\rho\nu}_{S^{\dagger}_{(1,\tilde{1})}B} = -g^{\rho\nu} g' Y_{S_{(1,\tilde{1})}} S_{(1,\tilde{1})i}\,, \qquad \bar{Z}^{\mu\kappa}_{BS^{\dagger}_{(1,\tilde{1})}} = -g^{\mu\kappa} g' Y_{S_{(1,\tilde{1})}} S_{(1,\tilde{1})j}\,, \tag{A.207}$$

$$Z^{\rho\nu}_{S_{(1,\tilde{1})}G} = -g^{\rho\nu} g_s S^{\dagger}_{(1,\tilde{1})k} T^{B}_{ik}\,, \qquad \bar{Z}^{\mu\kappa}_{GS_{(1,\tilde{1})}} = -g^{\mu\kappa} g_s S^{\dagger}_{(1,\tilde{1})k} T^{B}_{kj}\,, \tag{A.208}$$

$$Z^{\rho\nu}_{S^{\dagger}_{(1,\tilde{1})}G} = -g^{\rho\nu} g_s T^{B}_{ik} S_{(1,\tilde{1})k}\,, \qquad \bar{Z}^{\mu\kappa}_{GS^{\dagger}_{(1,\tilde{1})}} = -g^{\mu\kappa} g_s T^{B}_{kj} S_{(1,\tilde{1})k}\,, \tag{A.209}$$

$$Z^{\rho\nu}_{S^{T}_{(2,\tilde{2})}B} = -g^{\rho\nu} g' Y_{S_{(2,\tilde{2})}} S^{*}_{(2,\tilde{2})i\alpha}\,, \qquad \bar{Z}^{\mu\kappa}_{BS^{T}_{(2,\tilde{2})}} = -g^{\mu\kappa} g' Y_{S_{(2,\tilde{2})}} S_{(2,\tilde{2})j\beta}\,, \tag{A.210}$$

$$Z^{\rho\nu}_{S^{\dagger}_{(2,\tilde{2})}B} = -g^{\rho\nu} g' Y_{S_{(2,\tilde{2})}} S_{(2,\tilde{2})i\alpha}\,, \qquad \bar{Z}^{\mu\kappa}_{BS^{\dagger}_{(2,\tilde{2})}} = -g^{\mu\kappa} g' Y_{S_{(2,\tilde{2})}} S^{*}_{(2,\tilde{2})j\beta}\,, \tag{A.211}$$

$$Z^{\rho\nu}_{S^{T}_{(2,\tilde{2})}W} = -g^{\rho\nu} \frac{g}{2} \sigma^{J}_{\alpha\alpha_1} S^{*}_{(2,\tilde{2})i\alpha_1}\,, \qquad \bar{Z}^{\mu\kappa}_{WS^{T}_{(2,\tilde{2})}} = -g^{\mu\kappa} \frac{g}{2} \sigma^{I}_{\alpha_1\beta} S_{(2,\tilde{2})j\alpha_1}\,, \tag{A.212}$$

$$Z^{\rho\nu}_{S^{\dagger}_{(2,\tilde{2})}W} = -g^{\rho\nu} \frac{g}{2} \sigma^{J}_{\alpha\alpha_1} S_{(2,\tilde{2})i\alpha_1}\,, \qquad \bar{Z}^{\mu\kappa}_{WS^{\dagger}_{(2,\tilde{2})}} = -g^{\mu\kappa} \frac{g}{2} \sigma^{I}_{\alpha_1\beta} S^{*}_{(2,\tilde{2})j\alpha_1}\,, \tag{A.213}$$

$$Z^{\rho\nu}_{S^{T}_{(2,\tilde{2})}G} = -g^{\rho\nu} g_s T^{B}_{ik} S^{*}_{(2,\tilde{2})k\alpha}\,, \qquad \bar{Z}^{\mu\kappa}_{GS^{T}_{(2,\tilde{2})}} = -g^{\mu\kappa} g_s T^{B}_{kj} S_{(2,\tilde{2})k\beta}\,, \tag{A.214}$$

$$Z^{\mu\nu}_{S^{\dagger}_{(2,\tilde{2})}G} = -g^{\mu\nu} g_s T^{B}_{ik} S_{(2,\tilde{2})k\alpha}\,, \qquad \bar{Z}^{\mu\kappa}_{GS^{\dagger}_{(2,\tilde{2})}} = -g^{\mu\kappa} g_s T^{B}_{kj} S^{*}_{(2,\tilde{2})k\beta}\,, \tag{A.215}$$

$$Z^{\rho\nu}_{S^{T}_{3}B} = -g^{\rho\nu} g' Y_{S_3} S^{I*}_{3i}\,, \qquad \bar{Z}^{\mu\kappa}_{BS^{T}_{3}} = -g^{\mu\kappa} g' Y_{S_3} S^{J}_{3j}\,, \tag{A.216}$$

$$Z^{\rho\nu}_{S^{\dagger}_{3}B} = -g^{\rho\nu} g' Y_{S_3} S^{I}_{3i}\,, \qquad \bar{Z}^{\mu\kappa}_{BS^{\dagger}_{3}} = -g^{\mu\kappa} g' Y_{S_3} S^{J*}_{3j}\,, \tag{A.217}$$

$$Z^{\rho\nu}_{S^{T}_{3}W} = i g^{\rho\nu} g \epsilon^{LKJ} S^{K*}_{3l}\,, \qquad \bar{Z}^{\mu\kappa}_{WS^{T}_{3}} = -i g^{\mu\kappa} g \epsilon^{LKI} S^{K}_{3l}\,, \tag{A.218}$$

$$Z^{\rho\nu}_{S^{\dagger}_{3}W} = i g^{\rho\nu} g \epsilon^{LKJ} S^{K}_{3l}\,, \qquad \bar{Z}^{\mu\kappa}_{WS^{\dagger}_{3}} = -i g^{\mu\kappa} g \epsilon^{LKI} S^{K*}_{3j}\,, \tag{A.219}$$

$$Z^{\rho\nu}_{S^{T}_{3}G} = -g^{\rho\nu} g_s T^{B}_{ik} S^{*}_{3k\alpha}\,, \qquad \bar{Z}^{\mu\kappa}_{GS^{T}_{3}} = -g^{\mu\kappa} g_s T^{B}_{kj} S_{3k\beta}\,, \tag{A.220}$$

$$Z^{\mu\nu}_{S^{\dagger}_{3}G} = -g^{\mu\nu} g_s T^{B}_{ik} S_{3k\alpha}\,, \qquad \bar{Z}^{\mu\kappa}_{GS^{\dagger}_{3}} = -g^{\mu\kappa} g_s T^{B}_{kj} S^{*}_{3k\beta}\,. \tag{A.221}$$

# Appendix B

# Supertraces vs covariant diagrams

The construction of covariant diagrams precedes chronologically the method of Supertraces. The essential difference between these two techniques is the point at which the CDE is applied. In Supertraces one first makes superdiagrams from the distinct components of the interaction matrix **X** and then applies the CDE in the resulting Supertrace. In the Covariant diagrams approach the components of the interaction matrix are split explicitly into, *heavy-only*, *heavy-light* and *light-only* contributions. In the resulting trace the CDE is applied and the log-function is ultimately Taylor expanded. Finally, from the expanded formula one reads the components of the covariant diagrams in the same manner one would read of Feynman rules and the covariant diagrams are drawn. All in all Supertraces are a more compact way to present Covariant diagrams. One can also look at [35] for a more elaborate comparison between the two approaches.

In Tables B.1 and B.2 we present the relevant covariant diagrams for the Leptoquark Scalar Action. We have made combinations of matrices, and momentum insertions following the rules for constructing covariant diagrams in [26]. We have classified them in terms of $U$, $P$ and $Z$ insertions. In total we count 60 covariant diagrams.

| | | | |
|---|---|---|---|
| $\mathcal{O}(U^2)$ | 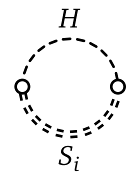 | $\mathcal{O}(U^3)$ | 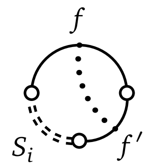 |
| $\mathcal{O}(U^4)$ | 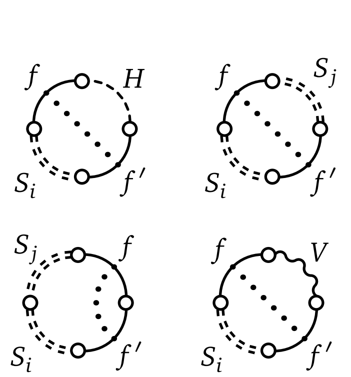 | $\mathcal{O}(U^5)$ | 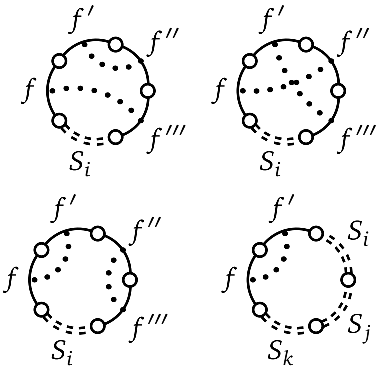 |
| $\mathcal{O}(Z^1)$ | 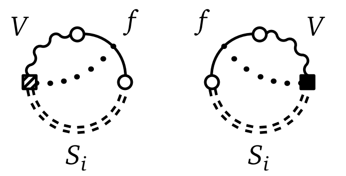 | $\mathcal{O}(Z^2)$ | 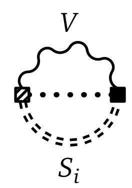 |

*Table B.1: U and Z only, heavy-light, covariant diagrams contributing to the construction of operators up to dimension 6. Where $S_i = S_1, \tilde{S}_2$, $f = \ell, q, u, e, d$ and $V = B, W, G$. In total we count 13 diagrams.*

| $\mathcal{O}(U^2P)$ | $\mathcal{O}(U^3P)$ |
|---|---|
| 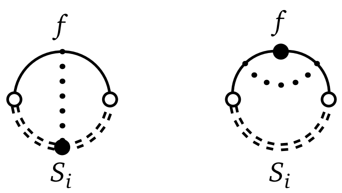 | 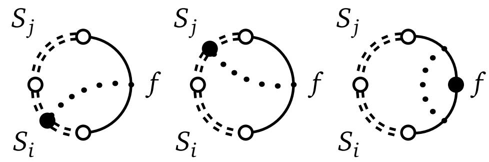 |

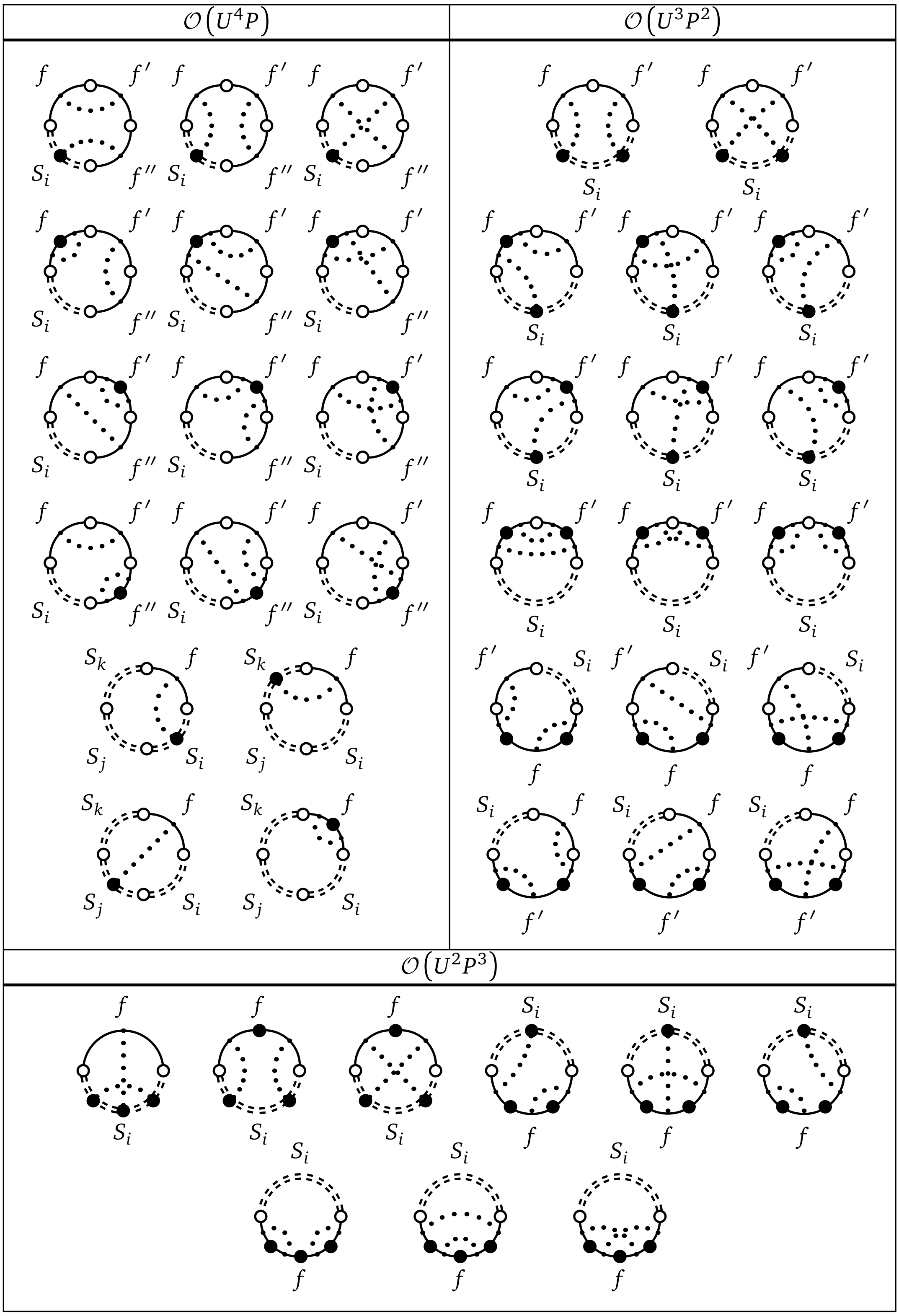


*Table B.2: Covariant diagrams containing powers of both U and P contributing to operators up to dimension 6. In total we have 47 diagrams.*

To summarize one can now clearly see the advantage of using the method of Supertraces. From 60 Covariant Diagrams we ended up with 15 Supertrace Diagrams calculated in Section 2.2.3.

# Appendix C

# Green Basis Operators

The Green basis has been initially developed in ref. [64] and serves as a middle result before the transition to the Warsaw basis by using the equations of motion of the SM fields. It is useful because in the Feynman diagrammatic approach it is this basis that the initial calculations are matched upon. The transition from Green to Warsaw has been also worked out in ref. [64].

In the tables that follow flavor indices are suppressed, greek letters $\alpha, \beta, \gamma$ denote $SU(2)_L$ fundamental indices while $I, J, K$ denote the $SU(2)_L$ adjoint representation. Small latin letters $i, j, k$ denote $SU(3)_c$ fundamental indices, while capital latin letters $A, B, C$ denote the adjoint representation of $SU(3)$.

The dimension-5 operator has the same definition in both Green and Warsaw basis:

| $H^2\psi^2$ | |
|---|---|
| $\mathcal{O}_{\nu\nu}$ | $\epsilon^{\alpha\beta}\epsilon^{\alpha_1\beta_1}H^{\alpha}H^{\alpha_1}\,\bar{\ell}^{c}_{p\beta}\,\ell_{r\beta_1}$ |

*Table C.1: Single dimension-5 operator giving rise to neutrino masses after EW symmetry breaking.*

The dimension-6 operators in Green basis are listed below. Shaded ones are included in Warsaw basis too presented in Tables 1.1 and 1.2 in the Introduction of this thesis.

| $X^3$ | | $X^2H^2$ | | $H^2D^4$ | |
|---|---|---|---|---|---|
| $\mathcal{O}_{3G}$ | $f^{ABC}G_\mu^{A\nu}G_\nu^{B\rho}G_\rho^{C\mu}$ | $\mathcal{O}_{HG}$ | $G^A_{\mu\nu}G^{A\mu\nu}(H^\dagger H)$ | $\mathcal{O}_{DH}$ | $(D_\mu D^\mu H)^\dagger(D_\nu D^\nu H)$ |
| $\mathcal{O}_{3\widetilde{G}}$ | $f^{ABC}\widetilde{G}_\mu^{A\nu}G_\nu^{B\rho}G_\rho^{C\mu}$ | $\mathcal{O}_{H\widetilde{G}}$ | $\widetilde{G}^A_{\mu\nu}G^{A\mu\nu}(H^\dagger H)$ | **$H^4D^2$** | |
| $\mathcal{O}_{3W}$ | $\epsilon^{IJK}W_\mu^{I\nu}W_\nu^{J\rho}W_\rho^{K\mu}$ | $\mathcal{O}_{HW}$ | $W^I_{\mu\nu}W^{I\mu\nu}(H^\dagger H)$ | $\mathcal{O}_{H\Box}$ | $(H^\dagger H)\Box(H^\dagger H)$ |
| $\mathcal{O}_{3\widetilde{W}}$ | $\epsilon^{IJK}\widetilde{W}_\mu^{I\nu}W_\nu^{J\rho}W_\rho^{K\mu}$ | $\mathcal{O}_{H\widetilde{W}}$ | $\widetilde{W}^I_{\mu\nu}W^{I\mu\nu}(H^\dagger H)$ | $\mathcal{O}_{HD}$ | $(H^\dagger D^\mu H)^\dagger(H^\dagger D_\mu H)$ |
| **$X^2D^2$** | | $\mathcal{O}_{HB}$ | $B_{\mu\nu}B^{\mu\nu}(H^\dagger H)$ | $\mathcal{O}'_{HD}$ | $(H^\dagger H)(D_\mu H)^\dagger(D^\mu H)$ |
| $\mathcal{O}_{2G}$ | $-\frac{1}{2}(D_\mu G^{A\mu\nu})(D^\rho G^A_{\rho\nu})$ | $\mathcal{O}_{H\widetilde{B}}$ | $\widetilde{B}_{\mu\nu}B^{\mu\nu}(H^\dagger H)$ | $\mathcal{O}''_{HD}$ | $(H^\dagger H)D_\mu(H^\dagger i\overleftrightarrow{D}^\mu H)$ |
| $\mathcal{O}_{2W}$ | $-\frac{1}{2}(D_\mu W^{I\mu\nu})(D^\rho W^I_{\rho\nu})$ | $\mathcal{O}_{HWB}$ | $W^I_{\mu\nu}B^{\mu\nu}(H^\dagger\sigma^I H)$ | **$H^6$** | |
| $\mathcal{O}_{2B}$ | $-\frac{1}{2}(\partial_\mu B^{\mu\nu})(\partial^\rho B_{\rho\nu})$ | $\mathcal{O}_{H\widetilde{W}B}$ | $\widetilde{W}^I_{\mu\nu}B^{\mu\nu}(H^\dagger\sigma^I H)$ | $\mathcal{O}_H$ | $(H^\dagger H)^3$ |
| | | **$H^2XD^2$** | | | |
| | | $\mathcal{O}_{WDH}$ | $D_\nu W^{I\mu\nu}(H^\dagger i\overleftrightarrow{D}^I_\mu H)$ | | |
| | | $\mathcal{O}_{BDH}$ | $\partial_\nu B^{\mu\nu}(H^\dagger i\overleftrightarrow{D}_\mu H)$ | | |

*Table C.2: Bosonic operators in the Green's basis.*

| Four-quark | | Four-lepton | | Semileptonic | |
|---|---|---|---|---|---|
| $\mathcal{O}^{(1)}_{qq}$ | $(\bar{q}\gamma^\mu q)(\bar{q}\gamma_\mu q)$ | $\mathcal{O}_{\ell\ell}$ | $(\bar{\ell}\gamma^\mu\ell)(\bar{\ell}\gamma_\mu\ell)$ | $\mathcal{O}^{(1)}_{\ell q}$ | $(\bar{\ell}\gamma^\mu\ell)(\bar{q}\gamma_\mu q)$ |
| $\mathcal{O}^{(3)}_{qq}$ | $(\bar{q}\gamma^\mu\sigma^I q)(\bar{q}\gamma_\mu\sigma^I q)$ | $\mathcal{O}_{ee}$ | $(\bar{e}\gamma^\mu e)(\bar{e}\gamma_\mu e)$ | $\mathcal{O}^{(3)}_{\ell q}$ | $(\bar{\ell}\gamma^\mu\sigma^I\ell)(\bar{q}\gamma_\mu\sigma^I q)$ |
| $\mathcal{O}_{uu}$ | $(\bar{u}\gamma^\mu u)(\bar{u}\gamma_\mu u)$ | $\mathcal{O}_{\ell e}$ | $(\bar{\ell}\gamma^\mu\ell)(\bar{e}\gamma_\mu e)$ | $\mathcal{O}_{eu}$ | $(\bar{e}\gamma^\mu e)(\bar{u}\gamma_\mu u)$ |
| $\mathcal{O}_{dd}$ | $(\bar{d}\gamma^\mu d)(\bar{d}\gamma_\mu d)$ | | | $\mathcal{O}_{ed}$ | $(\bar{e}\gamma^\mu e)(\bar{d}\gamma_\mu d)$ |
| $\mathcal{O}^{(1)}_{ud}$ | $(\bar{u}\gamma^\mu u)(\bar{d}\gamma_\mu d)$ | | | $\mathcal{O}_{qe}$ | $(\bar{q}\gamma^\mu q)(\bar{e}\gamma_\mu e)$ |
| $\mathcal{O}^{(8)}_{ud}$ | $(\bar{u}\gamma^\mu T^A u)(\bar{d}\gamma_\mu T^A d)$ | | | $\mathcal{O}_{\ell u}$ | $(\bar{\ell}\gamma^\mu\ell)(\bar{u}\gamma_\mu u)$ |
| $\mathcal{O}^{(1)}_{qu}$ | $(\bar{q}\gamma^\mu q)(\bar{u}\gamma_\mu u)$ | | | $\mathcal{O}_{\ell d}$ | $(\bar{\ell}\gamma^\mu\ell)(\bar{d}\gamma_\mu d)$ |
| $\mathcal{O}^{(8)}_{qu}$ | $(\bar{q}\gamma^\mu T^A q)(\bar{u}\gamma_\mu T^A u)$ | | | $\mathcal{O}_{\ell edq}$ | $(\bar{\ell}e)(\bar{d}q)$ |
| $\mathcal{O}^{(1)}_{qd}$ | $(\bar{q}\gamma^\mu q)(\bar{d}\gamma_\mu d)$ | | | $\mathcal{O}^{(1)}_{\ell equ}$ | $(\bar{\ell}^\alpha e)\epsilon_{\alpha\beta}(\bar{q}^\beta u)$ |
| $\mathcal{O}^{(8)}_{qd}$ | $(\bar{q}\gamma^\mu T^A q)(\bar{d}\gamma_\mu T^A d)$ | | | $\mathcal{O}^{(3)}_{\ell equ}$ | $(\bar{\ell}^\alpha\sigma^{\mu\nu}e)\epsilon_{\alpha\beta}(\bar{q}^\beta\sigma_{\mu\nu}u)$ |
| $\mathcal{O}^{(1)}_{quqd}$ | $(\bar{q}^\alpha u)\epsilon_{\alpha\beta}(\bar{q}^\beta d)$ | | | | |
| $\mathcal{O}^{(8)}_{quqd}$ | $(\bar{q}^\alpha T^A u)\epsilon_{\alpha\beta}(\bar{q}^\beta T^A d)$ | | | | |

*Table C.3: Four-fermion operators. Generation indices are suppressed.*

| $B$ and $L$ violating | |
|---|---|
| $\mathcal{O}_{duq}$ | $\varepsilon_{ijk}\epsilon_{\alpha\beta}\left[(d^i)^T C u^j\right]\left[(q^{k\alpha})^T C\ell^\beta\right]$ |
| $\mathcal{O}_{qqu}$ | $\varepsilon_{ijk}\epsilon_{\alpha\beta}\left[(q^{i\alpha})^T C q^{j\beta}\right]\left[(u^k)^T C e\right]$ |
| $\mathcal{O}_{qqq}$ | $\varepsilon_{ijk}\epsilon_{\alpha\beta}\epsilon_{\gamma\delta}\left[(q^{i\alpha})^T C q^{j\gamma}\right]\left[(q^{k\delta})^T C\ell^\beta\right]$ |
| $\mathcal{O}_{duu}$ | $\varepsilon_{ijk}\left[(d^i)^T C u^j\right]\left[(u^k)^T C e\right]$ |

*Table C.4: Baryon and lepton number violating four-fermion operators. Generation indices are suppressed and $C = i\gamma^2\gamma^0$ is the Dirac charge conjugation matrix.*

| $\psi^2 D^3$ | |
|---|---|
| $\mathcal{O}_{qD}$ | $\frac{i}{2}\bar{q}\left\{D_\mu D^\mu, \slashed{D}\right\} q$ |
| $\mathcal{O}_{uD}$ | $\frac{i}{2}\bar{u}\left\{D_\mu D^\mu, \slashed{D}\right\} u$ |
| $\mathcal{O}_{dD}$ | $\frac{i}{2}\bar{d}\left\{D_\mu D^\mu, \slashed{D}\right\} d$ |
| $\mathcal{O}_{\ell D}$ | $\frac{i}{2}\bar{\ell}\left\{D_\mu D^\mu, \slashed{D}\right\} \ell$ |
| $\mathcal{O}_{eD}$ | $\frac{i}{2}\bar{e}\left\{D_\mu D^\mu, \slashed{D}\right\} e$ |

| $\psi^2 H D^2 + \text{h.c.}$ | |
|---|---|
| $\mathcal{O}_{uHD1}$ | $(\bar{q}u)D_\mu D^\mu \widetilde{H}$ |
| $\mathcal{O}_{uHD2}$ | $(\bar{q}i\sigma_{\mu\nu}D^\mu u)D^\nu \widetilde{H}$ |
| $\mathcal{O}_{uHD3}$ | $(\bar{q}D_\mu D^\mu u)\widetilde{H}$ |
| $\mathcal{O}_{uHD4}$ | $(\bar{q}D_\mu u)D^\mu \widetilde{H}$ |
| $\mathcal{O}_{dHD1}$ | $(\bar{q}d)D_\mu D^\mu H$ |
| $\mathcal{O}_{dHD2}$ | $(\bar{q}i\sigma_{\mu\nu}D^\mu d)D^\nu H$ |
| $\mathcal{O}_{dHD3}$ | $(\bar{q}D_\mu D^\mu d)H$ |
| $\mathcal{O}_{dHD4}$ | $(\bar{q}D_\mu d)D^\mu H$ |
| $\mathcal{O}_{eHD1}$ | $(\bar{\ell}e)D_\mu D^\mu H$ |
| $\mathcal{O}_{eHD2}$ | $(\bar{\ell}i\sigma_{\mu\nu}D^\mu e)D^\nu H$ |
| $\mathcal{O}_{eHD3}$ | $(\bar{\ell}D_\mu D^\mu e)H$ |
| $\mathcal{O}_{eHD4}$ | $(\bar{\ell}D_\mu e)D^\mu H$ |

| $\psi^2 X H + \text{h.c.}$ | |
|---|---|
| $\mathcal{O}_{uG}$ | $(\bar{q}T^A\sigma^{\mu\nu}u)\widetilde{H}G^A_{\mu\nu}$ |
| $\mathcal{O}_{uW}$ | $(\bar{q}\sigma^{\mu\nu}u)\sigma^I\widetilde{H}W^I_{\mu\nu}$ |
| $\mathcal{O}_{uB}$ | $(\bar{q}\sigma^{\mu\nu}u)\widetilde{H}B_{\mu\nu}$ |
| $\mathcal{O}_{dG}$ | $(\bar{q}T^A\sigma^{\mu\nu}d)HG^A_{\mu\nu}$ |
| $\mathcal{O}_{dW}$ | $(\bar{q}\sigma^{\mu\nu}d)\sigma^I HW^I_{\mu\nu}$ |
| $\mathcal{O}_{dB}$ | $(\bar{q}\sigma^{\mu\nu}d)HB_{\mu\nu}$ |
| $\mathcal{O}_{eW}$ | $(\bar{\ell}\sigma^{\mu\nu}e)\sigma^I HW^I_{\mu\nu}$ |
| $\mathcal{O}_{eB}$ | $(\bar{\ell}\sigma^{\mu\nu}e)HB_{\mu\nu}$ |

| $\psi^2 X D$ | |
|---|---|
| $\mathcal{O}_{Gq}$ | $(\bar{q}T^A\gamma^\mu q)D^\nu G^A_{\mu\nu}$ |
| $\mathcal{O}'_{Gq}$ | $\frac{1}{2}(\bar{q}T^A\gamma^\mu i\overleftrightarrow{D}^\nu q)G^A_{\mu\nu}$ |
| $\mathcal{O}'_{\widetilde{G}q}$ | $\frac{1}{2}(\bar{q}T^A\gamma^\mu i\overleftrightarrow{D}^\nu q)\widetilde{G}^A_{\mu\nu}$ |
| $\mathcal{O}_{Wq}$ | $(\bar{q}\sigma^I\gamma^\mu q)D^\nu W^I_{\mu\nu}$ |
| $\mathcal{O}'_{Wq}$ | $\frac{1}{2}(\bar{q}\sigma^I\gamma^\mu i\overleftrightarrow{D}^\nu q)W^I_{\mu\nu}$ |
| $\mathcal{O}'_{\widetilde{W}q}$ | $\frac{1}{2}(\bar{q}\sigma^I\gamma^\mu i\overleftrightarrow{D}^\nu q)\widetilde{W}^I_{\mu\nu}$ |
| $\mathcal{O}_{Bq}$ | $(\bar{q}\gamma^\mu q)\partial^\nu B_{\mu\nu}$ |
| $\mathcal{O}'_{Bq}$ | $\frac{1}{2}(\bar{q}\gamma^\mu i\overleftrightarrow{D}^\nu q)B_{\mu\nu}$ |
| $\mathcal{O}'_{\widetilde{B}q}$ | $\frac{1}{2}(\bar{q}\gamma^\mu i\overleftrightarrow{D}^\nu q)\widetilde{B}_{\mu\nu}$ |
| $\mathcal{O}_{Gu}$ | $(\bar{u}T^A\gamma^\mu u)D^\nu G^A_{\mu\nu}$ |
| $\mathcal{O}'_{Gu}$ | $\frac{1}{2}(\bar{u}T^A\gamma^\mu i\overleftrightarrow{D}^\nu u)G^A_{\mu\nu}$ |
| $\mathcal{O}'_{\widetilde{G}u}$ | $\frac{1}{2}(\bar{u}T^A\gamma^\mu i\overleftrightarrow{D}^\nu u)\widetilde{G}^A_{\mu\nu}$ |
| $\mathcal{O}_{Bu}$ | $(\bar{u}\gamma^\mu u)\partial^\nu B_{\mu\nu}$ |
| $\mathcal{O}'_{Bu}$ | $\frac{1}{2}(\bar{u}\gamma^\mu i\overleftrightarrow{D}^\nu u)B_{\mu\nu}$ |
| $\mathcal{O}'_{\widetilde{B}u}$ | $\frac{1}{2}(\bar{u}\gamma^\mu i\overleftrightarrow{D}^\nu u)\widetilde{B}_{\mu\nu}$ |
| $\mathcal{O}_{Gd}$ | $(\bar{d}T^A\gamma^\mu d)D^\nu G^A_{\mu\nu}$ |
| $\mathcal{O}'_{Gd}$ | $\frac{1}{2}(\bar{d}T^A\gamma^\mu i\overleftrightarrow{D}^\nu d)G^A_{\mu\nu}$ |
| $\mathcal{O}'_{\widetilde{G}d}$ | $\frac{1}{2}(\bar{d}T^A\gamma^\mu i\overleftrightarrow{D}^\nu d)\widetilde{G}^A_{\mu\nu}$ |
| $\mathcal{O}_{Bd}$ | $(\bar{d}\gamma^\mu d)\partial^\nu B_{\mu\nu}$ |
| $\mathcal{O}'_{Bd}$ | $\frac{1}{2}(\bar{d}\gamma^\mu i\overleftrightarrow{D}^\nu d)B_{\mu\nu}$ |
| $\mathcal{O}'_{\widetilde{B}d}$ | $\frac{1}{2}(\bar{d}\gamma^\mu i\overleftrightarrow{D}^\nu d)\widetilde{B}_{\mu\nu}$ |
| $\mathcal{O}_{W\ell}$ | $(\bar{\ell}\sigma^I\gamma^\mu \ell)D^\nu W^I_{\mu\nu}$ |
| $\mathcal{O}'_{W\ell}$ | $\frac{1}{2}(\bar{\ell}\sigma^I\gamma^\mu i\overleftrightarrow{D}^\nu \ell)W^I_{\mu\nu}$ |
| $\mathcal{O}'_{\widetilde{W}\ell}$ | $\frac{1}{2}(\bar{\ell}\sigma^I\gamma^\mu i\overleftrightarrow{D}^\nu \ell)\widetilde{W}^I_{\mu\nu}$ |
| $\mathcal{O}_{B\ell}$ | $(\bar{\ell}\gamma^\mu \ell)\partial^\nu B_{\mu\nu}$ |
| $\mathcal{O}'_{B\ell}$ | $\frac{1}{2}(\bar{\ell}\gamma^\mu i\overleftrightarrow{D}^\nu \ell)B_{\mu\nu}$ |
| $\mathcal{O}'_{\widetilde{B}\ell}$ | $\frac{1}{2}(\bar{\ell}\gamma^\mu i\overleftrightarrow{D}^\nu \ell)\widetilde{B}_{\mu\nu}$ |
| $\mathcal{O}_{Be}$ | $(\bar{e}\gamma^\mu e)\partial^\nu B_{\mu\nu}$ |
| $\mathcal{O}'_{Be}$ | $\frac{1}{2}(\bar{e}\gamma^\mu i\overleftrightarrow{D}^\nu e)B_{\mu\nu}$ |
| $\mathcal{O}'_{\widetilde{B}e}$ | $\frac{1}{2}(\bar{e}\gamma^\mu i\overleftrightarrow{D}^\nu e)\widetilde{B}_{\mu\nu}$ |

| $\psi^2 D H^2$ | |
|---|---|
| $\mathcal{O}^{(1)}_{Hq}$ | $(\bar{q}\gamma^\mu q)(H^\dagger i\overleftrightarrow{D}_\mu H)$ |
| $\mathcal{O}'^{(1)}_{Hq}$ | $(\bar{q}i\overleftrightarrow{\slashed{D}}q)(H^\dagger H)$ |
| $\mathcal{O}''^{(1)}_{Hq}$ | $(\bar{q}\gamma^\mu q)\partial_\mu(H^\dagger H)$ |
| $\mathcal{O}^{(3)}_{Hq}$ | $(\bar{q}\sigma^I\gamma^\mu q)(H^\dagger i\overleftrightarrow{D}^I_\mu H)$ |
| $\mathcal{O}'^{(3)}_{Hq}$ | $(\bar{q}i\overleftrightarrow{\slashed{D}}^I q)(H^\dagger\sigma^I H)$ |
| $\mathcal{O}''^{(3)}_{Hq}$ | $(\bar{q}\sigma^I\gamma^\mu q)D_\mu(H^\dagger\sigma^I H)$ |
| $\mathcal{O}_{Hu}$ | $(\bar{u}\gamma^\mu u)(H^\dagger i\overleftrightarrow{D}_\mu H)$ |
| $\mathcal{O}'_{Hu}$ | $(\bar{u}i\overleftrightarrow{\slashed{D}}u)(H^\dagger H)$ |
| $\mathcal{O}''_{Hu}$ | $(\bar{u}\gamma^\mu u)\partial_\mu(H^\dagger H)$ |
| $\mathcal{O}_{Hd}$ | $(\bar{d}\gamma^\mu d)(H^\dagger i\overleftrightarrow{D}_\mu H)$ |
| $\mathcal{O}'_{Hd}$ | $(\bar{d}i\overleftrightarrow{\slashed{D}}d)(H^\dagger H)$ |
| $\mathcal{O}''_{Hd}$ | $(\bar{d}\gamma^\mu d)\partial_\mu(H^\dagger H)$ |
| $\mathcal{O}_{Hud}$ | $(\bar{u}\gamma^\mu d)(\widetilde{H}^\dagger iD_\mu H)$ |
| $\mathcal{O}^{(1)}_{H\ell}$ | $(\bar{\ell}\gamma^\mu \ell)(H^\dagger i\overleftrightarrow{D}_\mu H)$ |
| $\mathcal{O}'^{(1)}_{H\ell}$ | $(\bar{\ell}i\overleftrightarrow{\slashed{D}}\ell)(H^\dagger H)$ |
| $\mathcal{O}''^{(1)}_{H\ell}$ | $(\bar{\ell}\gamma^\mu \ell)\partial_\mu(H^\dagger H)$ |
| $\mathcal{O}^{(3)}_{H\ell}$ | $(\bar{\ell}\sigma^I\gamma^\mu \ell)(H^\dagger i\overleftrightarrow{D}^I_\mu H)$ |
| $\mathcal{O}'^{(3)}_{H\ell}$ | $(\bar{\ell}i\overleftrightarrow{\slashed{D}}^I \ell)(H^\dagger\sigma^I H)$ |
| $\mathcal{O}''^{(3)}_{H\ell}$ | $(\bar{\ell}\sigma^I\gamma^\mu \ell)D_\mu(H^\dagger\sigma^I H)$ |
| $\mathcal{O}_{He}$ | $(\bar{e}\gamma^\mu e)(H^\dagger i\overleftrightarrow{D}_\mu H)$ |
| $\mathcal{O}'_{He}$ | $(\bar{e}i\overleftrightarrow{\slashed{D}}e)(H^\dagger H)$ |
| $\mathcal{O}''_{He}$ | $(\bar{e}\gamma^\mu e)\partial_\mu(H^\dagger H)$ |

| $\psi^2 H^3 + \text{h.c.}$ | |
|---|---|
| $\mathcal{O}_{uH}$ | $(H^\dagger H)\bar{q}\widetilde{H}u$ |
| $\mathcal{O}_{dH}$ | $(H^\dagger H)\bar{q}Hd$ |
| $\mathcal{O}_{eH}$ | $(H^\dagger H)\bar{\ell}He$ |

*Table C.5: Two-fermion operators in the Green's basis. Generation indices are suppressed.*

# Appendix D

# Auxiliary expressions from the UOLEA

We append here expressions for the UOLEA coefficients found in eq. (2.49) that arise in case of possible LQs mass degeneracies. In the mass degeneracy limit, $M_i = M_j$, these are well defined functions, whose degenerate expressions can be found in the original UOLEA, ref. [24]. We split them as $f_n = \frac{i}{16\pi^2}\tilde{f}_n$ listing only $\tilde{f}_n$. We also adopt the notation $\Delta^2_{ij} = M_i^2 - M_j^2$ and wherever $S_i = \{S_1, \tilde{S}_2\}$. The coefficients then read,

$$\tilde{f}_{11}^{S_iS_jS_i} = \frac{2M_i^6 + M_j^6 + 3M_i^2M_j^2(M_i^2 - 2M_j^2) + M_i^4M_j^2\log M_j^2/M_i^2}{6M_i^2(\Delta_{ij})^4}\,, \tag{D.1}$$

$$\tilde{f}_{11}^{S_iS_iS_j} = \frac{M_i^4 + 4M_i^2M_j^2(1 + \log M_j^2/M_i^2) + 2M_j^4(\log M_j^2/M_i^2 - 5/2)}{2(\Delta_{ij})^4}\,, \tag{D.2}$$

$$\tilde{f}_{12}^{S_iS_j} = \frac{M_i^4 + 10M_i^2M_j^2 + M_j^4}{12(\Delta^2_{ij})^4} - \frac{M_i^2M_j^2(M_i^2 + M_j^2)\log M_i^2/M_j^2}{2(\Delta^2_{ij})^5}\,, \tag{D.3}$$

$$\tilde{f}_{13}^{S_iS_j} = \frac{2M_i^4 + 5M_i^2M_j^2 - M_j^4}{12M_i^2(\Delta^2_{ij})^3} - \frac{M_i^2M_j^2\log M_i^2/M_j^2}{(\Delta^2_{ij})^5} \tag{D.4}$$

$$\tilde{f}_{14}^{S_iS_j} = -\frac{M_i^4 + 10M_i^2M_j^2M_j^4}{6(\Delta^2_{ij})^4} + \frac{M_i^2M_j^2(M_i^2M_j^2)\log M_i^2/M_j^2}{(\Delta^2_{ij})^5}\,, \tag{D.5}$$

$$\tilde{f}_{17}^{S_iS_jS_iS_j} = \tilde{f}_{17}^{S_iS_j} = \frac{18M_j^2(M_i^4 + M_i^2M_j^2) - 2M_i^6 - 34M_j^6}{12M_j^2(\Delta^2_{ij})^5} + \frac{(M_j^4 + 3M_i^2M_j^2)}{M_j^2(\Delta^2_{ij})^5}\log\frac{M_j^2}{M_i^2}\,, \tag{D.6}$$

$$\tilde{f}_{18}^{S_iS_jS_iS_j} = \tilde{f}_{18}^{S_iS_j} = \frac{M_i^2 + M_j^2}{6(\Delta^2_{ij})^4} + \frac{M_j^8 - M_i^8}{12M_i^2M_j^2(\Delta^2_{ij})^5} + \frac{M_i^2M_j^2\log M_j^2/M_i^2}{(\Delta^2_{ij})^5}\,, \tag{D.7}$$

$$\tilde{f}_{19}^{S_iS_jS_iS_jS_iS_j} = \tilde{f}_{19}^{S_iS_j} = \frac{(M_i^6 - M_j^6) + 9M_i^2M_j^2(\Delta^2_{ij}) + 6M_i^2M_j^2(M_i^2 + M_j^2)\log M_j^2/M_i^2}{12M_i^2M_j^2(\Delta^2_{ij})^5} \tag{D.8}$$

# Appendix E

# Semi-numerical expressions of signal strengths

Here we provide the semi-numerical expressions of the signal strength corrections to the SM, in the decays and production channels of the Higgs boson, that we have used in this study. Apart from $\delta R_{h\to Z\gamma}$ and $\delta R_{h\to\gamma\gamma}$, which their one loop expressions are considered, found in [129, 130], all other formulas are taken to leading order from [137] and are computed in TeV$^{-2}$ units. All expressions are given in the input scheme $\{G_F, M_W, M_Z\}$, the numerical values used throughout Chapter 3 are,

$$G_F = 1.1663787 \times 10^{-5}\ \text{GeV}^{-2}\,, \tag{E.1}$$

$$M_W = 80.385\ \text{GeV}\,, \tag{E.2}$$

$$M_Z = 91.1876\ \text{GeV}\,, \tag{E.3}$$

$$M_H = 125.25\ \text{GeV}\,, \tag{E.4}$$

$$M_t = 172.57\ \text{GeV}\,. \tag{E.5}$$

## E.1 Decay channels

$$\delta R_{h\to b\bar{b}} = -5.050\, C_{33}^{d\phi} + 0.121\,(C^{\phi\Box} - \frac{1}{4}C^{\phi D}) + 0.0606\,(C_{1221}^{\ell\ell} - C_{11}^{\phi\ell(3)} - C_{22}^{\phi\ell(3)})\,, \tag{E.6}$$

$$\delta R_{h\to WW^*} = -0.0895\, C^{\phi W} + 0.121\,(C^{\phi\Box} - \frac{1}{4}C^{\phi D}) + 0.0606\,(C_{1221}^{\ell\ell} - C_{11}^{\phi\ell(3)} - C_{22}^{\phi\ell(3)})\,, \tag{E.7}$$

$$\delta R_{h\to\tau\bar{\tau}} = -11.88\, C_{33}^{e\phi} + 0.121\,(C^{\phi\Box} - \frac{1}{4}C^{\phi D}) + 0.0606\,(C_{1221}^{\ell\ell} - C_{11}^{\phi\ell(3)} - C_{22}^{\phi\ell(3)})\,, \tag{E.8}$$

$$\begin{aligned}\delta R_{h\to ZZ^*} &= 0.296\,(C^{\phi WB} - C^{\phi W}) - 0.197\, C^{\phi B} + 0.119\, C^{\phi\Box} + 0.005 C^{\phi D} + 0.181\, C_{1221}^{\ell\ell} \\ &- 0.117\,(C_{11}^{\phi\ell(3)} + C_{22}^{\phi\ell(3)})\,,\end{aligned} \tag{E.9}$$

$$\delta R_{h\to\mu\mu} = -199.79\, C_{22}^{e\phi} + 0.121\,(C^{\phi\Box} - \frac{1}{4}C^{\phi D})\,, \tag{E.10}$$

$$
\begin{aligned}
\delta R_{h\to Z\gamma} \simeq\, & 0.18\left(C^{\ell\ell}_{1221} - C^{\phi\ell(3)}_{11} - C^{\phi\ell(3)}_{22}\right) + 0.12\left(C^{\phi\Box} - C^{\phi D}\right) \\
& - 0.01\left(C^{d\phi}_{33} - C^{u\phi}_{33}\right) + 0.02\left(C^{\phi u}_{33} + C^{\phi q(1)}_{33} - C^{\phi q(3)}_{33}\right) \\
& + \left[14.99 - 0.35\log\frac{\mu^2}{M_W^2}\right]C^{\phi B} - \left[14.88 - 0.15\log\frac{\mu^2}{M_W^2}\right]C^{\phi W} + \left[9.44 - 0.26\log\frac{\mu^2}{M_W^2}\right]C^{\phi WB} \\
& + \left[0.10 - 0.20\log\frac{\mu^2}{M_W^2}\right]C^{W} - \left[0.11 - 0.04\log\frac{\mu^2}{M_W^2}\right]C^{uB}_{33} + \left[0.71 - 0.28\log\frac{\mu^2}{M_W^2}\right]C^{uW}_{33} \\
& - 0.01\, C^{uW}_{22} - 0.01\, C^{dW}_{33} + \dots\,,
\end{aligned} \tag{E.11}
$$

$$
\begin{aligned}
\delta R_{h\to\gamma\gamma} \simeq\, & 0.18\left(C^{\ell\ell}_{1221} - C^{\phi\ell(3)}_{11} - C^{\phi\ell(3)}_{22}\right) + 0.12\left(C^{\phi\Box} - 2C^{\phi D}\right) \\
& - 0.01\left(C^{e\phi}_{22} + 4C^{e\phi}_{33} + 5C^{u\phi}_{22} + 2C^{d\phi}_{33} - 3C^{u\phi}_{33}\right) \\
& - \left[48.04 - 1.07\log\frac{\mu^2}{M_W^2}\right]C^{\phi B} - \left[14.29 - 0.12\log\frac{\mu^2}{M_W^2}\right]C^{\phi W} + \left[26.17 - 0.52\log\frac{\mu^2}{M_W^2}\right]C^{\phi WB} \\
& + \left[0.16 - 0.22\log\frac{\mu^2}{M_W^2}\right]C^{W} + \left[2.11 - 0.84\log\frac{\mu^2}{M_W^2}\right]C^{uB}_{33} + \left[1.13 - 0.45\log\frac{\mu^2}{M_W^2}\right]C^{uW}_{33} \\
& - \left[0.03 - 0.01\log\frac{\mu^2}{M_W^2}\right]C^{uB}_{22} - \left[0.01 - 0.00\log\frac{\mu^2}{M_W^2}\right]C^{uW}_{22} + \left[0.03 - 0.01\log\frac{\mu^2}{M_W^2}\right]C^{dB}_{33} \\
& - \left[0.02 - 0.01\log\frac{\mu^2}{M_W^2}\right]C^{dW}_{33} + \left[0.02 - 0.00\log\frac{\mu^2}{M_W^2}\right]C^{eB}_{33} - \left[0.01 - 0.00\log\frac{\mu^2}{M_W^2}\right]C^{eW}_{33} + \dots\,.
\end{aligned} \tag{E.12}
$$

## E.2 Production channels

$$
\delta R_{\mathrm{ggF}} = 0.249\, C^{d\phi}_{33} + 0.121\, C^{\phi\Box} - 0.303\, C^{\phi D} - 0.129\, C^{u\phi}_{33} - 0.0606(C^{\phi\ell(3)}_{11} + C^{\phi\ell(3)}_{22} - C^{\ell\ell}_{1221})\,, \tag{E.13}
$$

$$
\begin{aligned}
\delta R_{\mathrm{VBF}} =\, & -0.423\, C^{\phi q(3)}_{11} - 0.347\, C^{\phi q(1)}_{11} + 0.1005 C^{\phi\Box} + 0.0826\, C^{\ell\ell}_{1221} - 0.0670\, C^{\phi W} \\
& - 0.0150\, C^{\phi D} + 0.0126 C^{\phi WB} - 0.0107 C^{\phi B}\,,
\end{aligned} \tag{E.14}
$$

$$
\delta R_{Wh} = 1.950\, C^{\phi q(3)}_{11} + 0.887\, C^{\phi W} + 0.127\, C^{\phi\Box} + 0.0606\, C^{\ell\ell}_{1221} - 0.0303\, C^{\phi D}\,, \tag{E.15}
$$

$$
\begin{aligned}
\delta R_{Zh} =\, & 1.716\, C^{\phi q(3)}_{11} + 0.721\, C^{\phi W} + 0.426\, C^{\phi u}_{11} - 0.173\, C^{\phi q(1)}_{11} - 0.142\, C^{\phi d}_{11} + 0.121\, C^{\phi\Box} \\
& + 0.0865\, C^{\phi B} + 0.0375\, C^{\phi D} + 0.314\, C^{\phi WB} + 0.06045\, C^{\ell\ell}_{1221}\,,
\end{aligned} \tag{E.16}
$$

$$
\delta R_{t\bar{t}h} = 0.121\, C^{\phi\Box} - 0.122\, C^{u\phi}_{33} - 0.0606(C^{\phi\ell(3)}_{11} + C^{\phi\ell(3)}_{22} - C^{\ell\ell}_{1221}) - 0.0303\, C^{\phi D}\,. \tag{E.17}
$$

# Appendix F

# MSSM Photon-Penguin anatomy

The photon penguin MSSM contributions to the Wilson coefficients, $C_{VLL}$, $C_{VLR}$, $C_{VRL}$ and $C_{VRR}$, defined in (4.7) are

$$C^{IJKL}_{\gamma,VLL} = C^{IJKL}_{\gamma,VLR} = e^2 F^{JI}_{\gamma L}\,\delta^{KL}\,, \tag{F.1}$$

$$C^{IJKL}_{\gamma,VRR} = C^{IJKL}_{\gamma,VRL} = e^2 F^{JI}_{\gamma R}\,\delta^{KL}\,. \tag{F.2}$$

These are the last terms in the rhs of eqs. (4.17) - (4.20). Of course the photon penguin does not contribute to $C_{10}$ and only gives a lepton flavour universal contribution to $C_9$ through eqs. (4.10)

$$\lambda C^{IJKL(\prime)}_{9\gamma} = e^2 F^{JI}_{\gamma L(R)}\,\delta^{KL}\,, \qquad \lambda C^{IJKL(\prime)}_{10\gamma} = 0\,, \tag{F.3}$$

where in mass-basis

$$\begin{aligned}
F^{JI}_{\gamma L} =& - V^{Jij*}_{dUC,L} V^{Iij}_{dUC,L}\left[C_{01}(m^2_{C_j}, m^2_{U_i}) + \frac{2}{3}C_{02}(m^2_{C_j}, m^2_{U_i})\right] \\
&+ \frac{1}{3}V^{Jij*}_{dDN,L}V^{Iij}_{dDN,L}C_{02}(m^2_{N_j}, m^2_{D_i}) + \frac{2g_3^2}{3}C_F\, V^{Ji*}_{dD,L}V^{Ii}_{dD,L}C_{02}(m^2_G, m^2_{D_i}) \\
&- \frac{1}{6}Y^{I*}_d Y^I_d \delta^{IJ}\left\{Z^{1i*}_{1R}Z^{1i}_{1R}C_{01}(m^2_{d_I}, m^2_{H^0_i}) + Z^{1i*}_{1H}Z^{1i}_{1H}C_{01}(m^2_{d_I}, m^2_{A^0_i})\right\} \\
&- Y^{J*}_d Y^I_d K^{NJ}K^{NI*}Z^{1i*}_H Z^{1i}_H\left[C_{02}(m^2_{u_N}, m^2_{H^-_i}) - \frac{2}{3}C_{01}(m^2_{u_N}, m^2_{H^-_i})\right],
\end{aligned} \tag{F.4}$$

$$\begin{aligned}
F^{JI}_{\gamma R} =& - V^{Jij*}_{dUC,R} V^{Iij}_{dUC,R}\left[C_{01}(m^2_{C_j}, m^2_{U_i}) + \frac{2}{3}C_{02}(m^2_{C_j}, m^2_{U_i})\right] \\
&+ \frac{1}{3}V^{Jij*}_{dDN,R}V^{Iij}_{dDN,R}C_{02}(m^2_{N_j}, m^2_{D_i}) + \frac{2g_3^2}{3}C_F\, V^{Ji*}_{dD,R}V^{Ii}_{dD,R}C_{02}(m^2_G, m^2_{D_i})\,, \\
&- \frac{1}{6}Y^{J*}_d Y^I_d \delta^{IJ}\left[Z^{1i*}_{1R}Z^{1i}_{1R}C_{01}(m^2_{d_I}, m^2_{H^0_i}) + Z^{1i*}_{1H}Z^{1i}_{1H}C_{01}(m^2_{d_I}, m^2_{A^0_i})\right] \\
&- Y^{N*}_u Y^N_u K^{NJ}K^{NI*}Z^{2i*}_H Z^{2i}_H\left[C_{02}(m^2_{u_N}, m^2_{H^-_i}) - \frac{2}{3}C_{01}(m^2_{u_N}, m^2_{H^-_i})\right],
\end{aligned} \tag{F.5}$$

and $C_F = 4/3$. The corresponding Feynman rules in the MSSM are [200]:

$$V^{Iij}_{dUC,L} = \frac{-e}{s_W}K^{JI}Z^{Ji*}_U Z^{1j}_+ + K^{JI}Y^J_u Z^{(J+3)i*}_U Z^{2j}_+\,, \tag{F.6}$$

$$V^{Iij}_{dUC,R} = -K^{JI} Y^I_d Z^{Ji*}_U Z^{2j*}_- \,, \tag{F.7}$$

$$V^{Iij}_{dDN,L} = \frac{-e}{\sqrt{2} s_W c_W} Z^{Ii}_D \left( \frac{1}{3} Z^{1j}_N s_W - Z^{2j}_N c_W \right) + Y^I_d Z^{(I+3)i}_D Z^{3j}_N \,, \tag{F.8}$$

$$V^{Iij}_{dDN,R} = \frac{-e\sqrt{2}}{3c_W} Z^{(I+3)i}_D Z^{1j*}_N + Y^I_d Z^{Ii}_D Z^{3j*}_N \,, \tag{F.9}$$

$$V^{Ii}_{dD,L} = -Z^{Ii}_D \,, \tag{F.10}$$

$$V^{Ii}_{dD,R} = Z^{(I+3)i}_D \,. \tag{F.11}$$

The loop functions $C_{01}$ and $C_{02}$ are defined as,

$$C_{01}(m_1^2, m_2^2) = \frac{7m_1^4 - 29m_1^2 m_2^2 + 16m_2^4}{36(m_1^2 - m_2^2)^3} + \frac{m_2^4(2m_2^2 - 3m_1^2)}{6(m_1^2 - m_2^2)^4} \log \frac{m_2^2}{m_1^2} \,, \tag{F.12}$$

$$C_{02}(m_1^2, m_2^2) = \frac{11m_1^4 - 7m_1^2 m_2^2 + 2m_2^4}{36(m_1^2 - m_2^2)^3} + \frac{m_1^6}{6(m_1^2 - m_2^2)^4} \log \frac{m_2^2}{m_1^2} \,. \tag{F.13}$$

Our result when translated from external quarks to external leptons agrees with the result of Ref. [203]. Furthermore, it has been added in the current working version of `SUSY_FLAVOR` code. It is very useful to exploit the FET in eqs. (F.4)-(F.5) in order to understand the dominant contributions.

## F.1 FET in chargino diagrams

Expanding the chargino-up squark contribution and keeping terms up to $1/M^2_{\rm SUSY}$, and single powers of quark masses as well as single powers of $M_W$ we get,

$$\begin{aligned} \left(F^{JI}_{\gamma L}\right)_C = & -\frac{e^2}{s_W^2} K^{NJ*} K^{MI} (\mathcal{M}^2_U)^{NM}_{LL} \Big[ C_{01}(|M_2|^2, \{(\mathcal{M}^2_U)^N_{LL}, (\mathcal{M}^2_U)^M_{LL}\}) \\ & + \frac{2}{3} C_{02}(|M_2|^2, \{(\mathcal{M}^2_U)^N_{LL}, (\mathcal{M}^2_U)^M_{LL}\}) \Big] , \end{aligned} \tag{F.14}$$

while the right-handed $(F^{JI}_{\gamma R})_C$ part is of higher order. The abbreviation $\{x, y\}$ inside a function denotes a first order divided difference e.g. $f(x, \{y, z\}) = \frac{f(x,y) - f(x,z)}{y - z}$ (see Refs. [186, 203] for further details and properties).

## F.2 FET in neutralino diagrams

Expanding the neutralino-down squark diagram to leading order we obtain,

$$\begin{aligned} \left(F^{JI}_{\gamma L}\right)_N = & \frac{e^2}{6 s_W^2 c_W^2} (\widehat{\mathcal{M}^2_D})^{IJ}_{LL} \Big[ c_W^2 C_{02}(|M_2|^2, \{(\mathcal{M}^2_D)^I_{LL}, (\mathcal{M}^2_D)^J_{LL}\}) \\ & + \frac{s_W^2}{9} C_{02}(|M_1|^2, \{(\mathcal{M}^2_D)^I_{LL}, (\mathcal{M}^2_D)^J_{LL}\}) \Big] , \end{aligned} \tag{F.15}$$

$$\left(F^{JI}_{\gamma R}\right)_N = \frac{2e^2}{27 c_W^2} (\widehat{\mathcal{M}^2_D})^{IJ}_{RR} \, C_{02}(|M_1|^2, \{(\mathcal{M}^2_D)^I_{RR}, (\mathcal{M}^2_D)^J_{RR}\}) \,. \tag{F.16}$$

## F.3 FET in gluino diagrams

Finally, expanding the gluino-down squark amplitude to leading order we get,

$$\left(F^{JI}_{\gamma L}\right)_G = \frac{2}{3} g_3^2 C_F\, (\widehat{\mathcal{M}^2_D})^{IJ}_{LL}\, C_{02}(m_G^2, \{(\mathcal{M}^2_D)^I_{LL}, (\mathcal{M}^2_D)^J_{LL}\})\,, \tag{F.17}$$

$$\left(F^{JI}_{\gamma R}\right)_G = \frac{2}{3} g_3^2 C_F\, (\widehat{M^2_D})^{IJ}_{RR}\, C_{02}(m_G^2, (\mathcal{M}^2_D)^I_{RR}, (\mathcal{M}^2_D)^J_{RR}\})\,. \tag{F.18}$$

where $C_F = 4/3$.

## F.4 Charged Higgs diagrams

Substituting the rotation matrices into the charged Higgs contributions, which are the last terms in (F.4) and (F.5), respectively, we get,

$$(F^{JI}_{\gamma L})_{H^-} = -\frac{e^2\, m_d^I\, m_d^J}{2 s_W^2 M_W^2} K^{NJ} K^{NI*} \tan^2\beta \left[ C_{02}(m^2_{u_N}, m^2_{H_1^-}) - \frac{2}{3} C_{01}(m^2_{u_N}, m^2_{H_1^-}) \right], \tag{F.19}$$

$$(F^{JI}_{\gamma R})_{H^-} = -\frac{e^2\, m_u^N\, m_u^N}{2 s_W^2 M_W^2} K^{NJ} K^{NI*} \cot^2\beta \left[ C_{02}(m^2_{u_N}, m^2_{H_1^-}) - \frac{2}{3} C_{01}(m^2_{u_N}, m^2_{H_1^-}) \right], \tag{F.20}$$

where, $m^2_{H_1^-} = M_W^2 + m^2_{H_1} + m^2_{H_2} + 2|\mu|^2$.

# Appendix G

# Auxiliary Functions

We append here relevant loop functions appeared in the text:

$$D_0(m_1, m_2, m_3, m_4) = -\sum_{j=2}^{4} \frac{m_j^2 \log \frac{m_j^2}{m_1^2}}{\prod_{k=1,k\neq j}^{4}(m_j^2 - m_k^2)} \,, \tag{G.1}$$

$$D_2(m_1, m_2, m_3, m_4) = \sum_{j=2}^{4} \frac{m_j^4 \log \frac{m_j^2}{m_1^2}}{\prod_{k=1,k\neq j}^{4}(m_j^2 - m_k^2)} \,, \tag{G.2}$$

$$E_2(m_1, m_2, m_3, m_4, m_5) = \sum_{j=2}^{5} \frac{m_j^4 \log \frac{m_j^2}{m_1^2}}{\prod_{k=1,k\neq j}^{5}(m_j^2 - m_k^2)} \,. \tag{G.3}$$

# References


[1] S.L. Glashow. "Partial Symmetries of Weak Interactions". In: *Nucl.Phys.* 22 (1961), pp. 579–588. DOI: 10.1016/0029-5582(61)90469-2.

[2] Steven Weinberg. "A Model of Leptons". In: *Phys.Rev.Lett.* 19 (1967), pp. 1264–1266. DOI: 10.1103/PhysRevLett.19.1264.

[3] Abdus Salam. "in *Proceedings of the Eighth Nobel Symposium*, edited by N. Svartholm (Wiley, New York, 1968), p.367." In: ().

[4] Michael E. Peskin and Daniel V. Schroeder. *An Introduction to quantum field theory*. Reading, USA: Addison-Wesley, 1995. ISBN: 978-0-201-50397-5, 978-0-429-50355-9, 978-0-429-49417-8. DOI: 10.1201/9780429503559.

[5] Matthew D. Schwartz. *Quantum Field Theory and the Standard Model*. Cambridge University Press, Mar. 2014. ISBN: 978-1-107-03473-0, 978-1-107-03473-0.

[6] F. Halzen and Alan D. Martin. *QUARKS AND LEPTONS: AN INTRODUCTORY COURSE IN MODERN PARTICLE PHYSICS*. 1984. ISBN: 978-0-471-88741-6.

[7] Stephen P. Martin. "A Supersymmetry primer". In: *Adv. Ser. Direct. High Energy Phys.* 18 (1998). Ed. by Gordon L. Kane, pp. 1–98. DOI: 10.1142/9789812839657_0001. arXiv: hep-ph/9709356.

[8] Aneesh V. Manohar. "Introduction to Effective Field Theories". In: *Les Houches Lect. Notes* 108 (2020). Ed. by Sacha Davidson et al. DOI: 10.1093/oso/9780198855743.003.0002. arXiv: 1804.05863 [hep-ph].

[9] Timothy Cohen. "As Scales Become Separated: Lectures on Effective Field Theory". In: *PoS* TASI2018 (2019), p. 011. arXiv: 1903.03622 [hep-ph].

[10] A. V. Manohar. "Effective field theories". In: *Lect. Notes Phys.* 479 (1997). Ed. by H. Latal and W. Schweiger, pp. 311–362. DOI: 10.1007/BFb0104294. arXiv: hep-ph/9606222.

[11] Matthias Neubert. "Renormalization Theory and Effective Field Theories". In: (Jan. 2019). Ed. by Sacha Davidson et al. DOI: 10.1093/oso/9780198855743.003.0001. arXiv: 1901.06573 [hep-ph].

[12] W. Buchmuller and D. Wyler. "Effective Lagrangian Analysis of New Interactions and Flavor Conservation". In: *Nucl. Phys. B* 268 (1986), pp. 621–653. DOI: 10.1016/0550-3213(86)90262-2.

[13] B. Grzadkowski et al. "Dimension-Six Terms in the Standard Model Lagrangian". In: *JHEP* 10 (2010), p. 085. DOI: 10.1007/JHEP10(2010)085. arXiv: 1008.4884 [hep-ph].

[14] Landon Lehman. "Extending the Standard Model Effective Field Theory with the Complete Set of Dimension-7 Operators". In: *Phys. Rev. D* 90.12 (2014), p. 125023. DOI: 10.1103/PhysRevD.90.125023. arXiv: 1410.4193 [hep-ph].

[15] Christopher W. Murphy. “Dimension-8 operators in the Standard Model Effective Field Theory”. In: *JHEP* 10 (2020), p. 174. DOI: 10.1007/JHEP10(2020)174. arXiv: 2005.00059 [hep-ph].

[16] Steven Weinberg. “Baryon and Lepton Nonconserving Processes”. In: *Phys. Rev. Lett.* 43 (1979), pp. 1566–1570. DOI: 10.1103/PhysRevLett.43.1566.

[17] A. Dedes et al. “Feynman rules for the Standard Model Effective Field Theory in $R_\xi$ -gauges”. In: *JHEP* 06 (2017), p. 143. DOI: 10.1007/JHEP06(2017)143. arXiv: 1704.03888 [hep-ph].

[18] Elizabeth E. Jenkins, Aneesh V. Manohar, and Michael Trott. “Renormalization Group Evolution of the Standard Model Dimension Six Operators I: Formalism and lambda Dependence”. In: *JHEP* 10 (2013), p. 087. DOI: 10.1007/JHEP10(2013)087. arXiv: 1308.2627 [hep-ph].

[19] Elizabeth E. Jenkins, Aneesh V. Manohar, and Michael Trott. “Renormalization Group Evolution of the Standard Model Dimension Six Operators II: Yukawa Dependence”. In: *JHEP* 01 (2014), p. 035. DOI: 10.1007/JHEP01(2014)035. arXiv: 1310.4838 [hep-ph].

[20] Rodrigo Alonso et al. “Renormalization Group Evolution of the Standard Model Dimension Six Operators III: Gauge Coupling Dependence and Phenomenology”. In: *JHEP* 04 (2014), p. 159. DOI: 10.1007/JHEP04(2014)159. arXiv: 1312.2014 [hep-ph].

[21] Ilaria Brivio and Michael Trott. “The Standard Model as an Effective Field Theory”. In: *Phys. Rept.* 793 (2019), pp. 1–98. DOI: 10.1016/j.physrep.2018.11.002. arXiv: 1706.08945 [hep-ph].

[22] Yi Liao and Xiao-Dong Ma. “Renormalization Group Evolution of Dimension-seven Baryon- and Lepton-number-violating Operators”. In: *JHEP* 11 (2016), p. 043. DOI: 10.1007/JHEP11(2016)043. arXiv: 1607.07309 [hep-ph].

[23] Hao-Lin Li et al. “Complete set of dimension-eight operators in the standard model effective field theory”. In: *Phys. Rev. D* 104.1 (2021), p. 015026. DOI: 10.1103/PhysRevD.104.015026. arXiv: 2005.00008 [hep-ph].

[24] Aleksandra Drozd et al. “The Universal One-Loop Effective Action”. In: *JHEP* 03 (2016), p. 180. DOI: 10.1007/JHEP03(2016)180. arXiv: 1512.03003 [hep-ph].

[25] James D. Wells and Zhengkang Zhang. “Effective field theory approach to trans-TeV supersymmetry: covariant matching, Yukawa unification and Higgs couplings”. In: *JHEP* 05 (2018), p. 182. DOI: 10.1007/JHEP05(2018)182. arXiv: 1711.04774 [hep-ph].

[26] Zhengkang Zhang. “Covariant diagrams for one-loop matching”. In: *JHEP* 05 (2017), p. 152. DOI: 10.1007/JHEP05(2017)152. arXiv: 1610.00710 [hep-ph].

[27] Sebastian A. R. Ellis et al. “Mixed heavy–light matching in the Universal One-Loop Effective Action”. In: *Phys. Lett. B* 762 (2016), pp. 166–176. DOI: 10.1016/j.physletb.2016.09.016. arXiv: 1604.02445 [hep-ph].

[28] Sebastian A. R. Ellis et al. “Extending the Universal One-Loop Effective Action: Heavy-Light Coefficients”. In: *JHEP* 08 (2017), p. 054. DOI: 10.1007/JHEP08(2017)054. arXiv: 1706.07765 [hep-ph].

[29] Sebastian A.R. Ellis et al. “The Fermionic Universal One-Loop Effective Action”. In: *JHEP* 11 (2020), p. 078. DOI: 10.1007/JHEP11(2020)078. arXiv: 2006.16260 [hep-ph].

[30] Andrei Angelescu and Peisi Huang. “Integrating Out New Fermions at One Loop”. In: (June 2020). arXiv: 2006.16532 [hep-ph].

[31] Benjamin Summ. “One Formula To Match Them All: The Bispinor Universal One-Loop Effective Action”. PhD thesis. RWTH Aachen U., 2020. DOI: 10.18154/RWTH-2021-00828. arXiv: 2103.02487 [hep-ph].

[32] Brian Henning, Xiaochuan Lu, and Hitoshi Murayama. “One-loop Matching and Running with Covariant Derivative Expansion”. In: *JHEP* 01 (2018), p. 123. DOI: 10.1007/JHEP01(2018)123. arXiv: 1604.01019 [hep-ph].

[33] Javier Fuentes-Martin, Jorge Portoles, and Pedro Ruiz-Femenia. “Integrating out heavy particles with functional methods: a simplified framework”. In: *JHEP* 09 (2016), p. 156. DOI: 10.1007/JHEP09(2016)156. arXiv: 1607.02142 [hep-ph].

[34] Javier Fuentes-Martín, Ajdin Palavrić, and Anders Eller Thomsen. “Functional matching and renormalization group equations at two-loop order”. In: *Phys. Lett. B* 851 (2024), p. 138557. DOI: 10.1016/j.physletb.2024.138557. arXiv: 2311.13630 [hep-ph].

[35] Timothy Cohen, Xiaochuan Lu, and Zhengkang Zhang. “Functional Prescription for EFT Matching”. In: (Nov. 2020). arXiv: 2011.02484 [hep-ph].

[36] Juan C. Criado. “MatchingTools: a Python library for symbolic effective field theory calculations”. In: *Comput. Phys. Commun.* 227 (2018), pp. 42–50. DOI: 10.1016/j.cpc.2018.02.016. arXiv: 1710.06445 [hep-ph].

[37] Supratim Das Bakshi, Joydeep Chakrabortty, and Sunando Kumar Patra. “CoDEx: Wilson coefficient calculator connecting SMEFT to UV theory”. In: *Eur. Phys. J. C* 79.1 (2019), p. 21. DOI: 10.1140/epjc/s10052-018-6444-2. arXiv: 1808.04403 [hep-ph].

[38] Timothy Cohen, Xiaochuan Lu, and Zhengkang Zhang. “STrEAMlining EFT Matching”. In: (Dec. 2020). arXiv: 2012.07851 [hep-ph].

[39] Javier Fuentes-Martin et al. “SuperTracer: A Calculator of Functional Supertraces for One-Loop EFT Matching”. In: (Dec. 2020). arXiv: 2012.08506 [hep-ph].

[40] Adrian Carmona et al. “Matchmakereft: automated tree-level and one-loop matching”. In: *SciPost Phys.* 12.6 (2022), p. 198. DOI: 10.21468/SciPostPhys.12.6.198. arXiv: 2112.10787 [hep-ph].

[41] Javier Fuentes-Martín et al. “A proof of concept for matchete: an automated tool for matching effective theories”. In: *Eur. Phys. J. C* 83.7 (2023), p. 662. DOI: 10.1140/epjc/s10052-023-11726-1. arXiv: 2212.04510 [hep-ph].

[42] John Ellis et al. “Top, Higgs, Diboson and Electroweak Fit to the Standard Model Effective Field Theory”. In: *JHEP* 04 (2021), p. 279. DOI: 10.1007/JHEP04(2021)279. arXiv: 2012.02779 [hep-ph].

[43] Jason Aebischer et al. “A Global Likelihood for Precision Constraints and Flavour Anomalies”. In: *Eur. Phys. J. C* 79.6 (2019), p. 509. DOI: 10.1140/epjc/s10052-019-6977-z. arXiv: 1810.07698 [hep-ph].

[44] Athanasios Dedes and Kostas Mantzaropoulos. “Universal scalar leptoquark action for matching”. In: *JHEP* 11 (2021), p. 166. DOI: 10.1007/JHEP11(2021)166. arXiv: 2108.10055 [hep-ph].

[45] Steven Weinberg. “Effective Gauge Theories”. In: *Phys. Lett.* B91 (1980), pp. 51–55. DOI: 10.1016/0370-2693(80)90660-7.

[46] Curtis G. Callan Jr. et al. “Structure of phenomenological Lagrangians. 2.” In: *Phys. Rev.* 177 (1969), pp. 2247–2250. DOI: 10.1103/PhysRev.177.2247.

[47] Sidney R. Coleman, J. Wess, and Bruno Zumino. "Structure of phenomenological Lagrangians. 1." In: *Phys. Rev.* 177 (1969), pp. 2239–2247. DOI: 10.1103/PhysRev.177.2239.

[48] Thomas Appelquist and J. Carazzone. "Infrared Singularities and Massive Fields". In: *Phys. Rev.* D11 (1975), p. 2856. DOI: 10.1103/PhysRevD.11.2856.

[49] M.K. Gaillard. "The Effective One Loop Lagrangian With Derivative Couplings". In: *Nucl. Phys. B* 268 (1986), pp. 669–692. DOI: 10.1016/0550-3213(86)90264-6.

[50] Oren Cheyette. "Effective Action for the Standard Model With Large Higgs Mass". In: *Nucl. Phys. B* 297 (1988), pp. 183–204. DOI: 10.1016/0550-3213(88)90205-2.

[51] Lai-Him Chan. "Derivative Expansion for the One Loop Effective Actions With Internal Symmetry". In: *Phys. Rev. Lett.* 57 (1986), p. 1199. DOI: 10.1103/PhysRevLett.57.1199.

[52] Brian Henning, Xiaochuan Lu, and Hitoshi Murayama. "How to use the Standard Model effective field theory". In: *JHEP* 01 (2016), p. 023. DOI: 10.1007/JHEP01(2016)023. arXiv: 1412.1837 [hep-ph].

[53] Michael Kramer, Benjamin Summ, and Alexander Voigt. "Completing the scalar and fermionic Universal One-Loop Effective Action". In: *JHEP* 01 (2020), p. 079. DOI: 10.1007/JHEP01(2020)079. arXiv: 1908.04798 [hep-ph].

[54] M. Beneke and Vladimir A. Smirnov. "Asymptotic expansion of Feynman integrals near threshold". In: *Nucl. Phys. B* 522 (1998), pp. 321–344. DOI: 10.1016/S0550-3213(98)00138-2. arXiv: hep-ph/9711391.

[55] Bernd Jantzen. "Foundation and generalization of the expansion by regions". In: *JHEP* 12 (2011), p. 076. DOI: 10.1007/JHEP12(2011)076. arXiv: 1111.2589 [hep-ph].

[56] Stefan Dittmaier and Carsten Grosse-Knetter. "Deriving nondecoupling effects of heavy fields from the path integral: A Heavy Higgs field in an SU(2) gauge theory". In: *Phys. Rev. D* 52 (1995), pp. 7276–7293. DOI: 10.1103/PhysRevD.52.7276. arXiv: hep-ph/9501285.

[57] Stefan Dittmaier and Carsten Grosse-Knetter. "Integrating out the standard Higgs field in the path integral". In: *Nucl. Phys. B* 459 (1996), pp. 497–536. DOI: 10.1016/0550-3213(95)00551-X. arXiv: hep-ph/9505266.

[58] Kieran Finn, Sotirios Karamitsos, and Apostolos Pilaftsis. "Frame Covariant Formalism for Fermionic Theories". In: *Eur. Phys. J. C* 81 (2021), p. 572. DOI: 10.1140/epjc/s10052-021-09360-w. arXiv: 2006.05831 [hep-th].

[59] W. Buchmuller, R. Ruckl, and D. Wyler. "Leptoquarks in Lepton - Quark Collisions". In: *Phys. Lett. B* 191 (1987). [Erratum: Phys.Lett.B 448, 320–320 (1999)], pp. 442–448. DOI: 10.1016/0370-2693(87)90637-X.

[60] Di Zhang and Shun Zhou. "Complete One-loop Matching of the Type-I Seesaw Model onto the Standard Model Effective Field Theory". In: (July 2021). arXiv: 2107.12133 [hep-ph].

[61] Ilaria Brivio et al. "From Models to SMEFT and Back?" In: (Aug. 2021). arXiv: 2108.01094 [hep-ph].

[62] Supratim Das Bakshi, Joydeep Chakrabortty, and Michael Spannowsky. "Classifying Standard Model Extensions Effectively with Precision Observables". In: *Phys. Rev. D* 103.5 (2021), p. 056019. DOI: 10.1103/PhysRevD.103.056019. arXiv: 2012.03839 [hep-ph].

[63] Minyuan Jiang et al. "Complete one-loop matching for a singlet scalar in the Standard Model EFT". In: *JHEP* 02 (2019). [Erratum: JHEP 01, 135 (2021)], p. 031. DOI: 10.1007/JHEP02(2019)031. arXiv: 1811.08878 [hep-ph].
[64] Valerio Gherardi, David Marzocca, and Elena Venturini. "Matching scalar leptoquarks to the SMEFT at one loop". In: *JHEP* 07 (2020), p. 225. DOI: 10.1007/JHEP07(2020)225. arXiv: 2003.12525 [hep-ph].
[65] Mikhail S. Bilenky and Arcadi Santamaria. "One loop effective Lagrangian for a standard model with a heavy charged scalar singlet". In: *Nucl. Phys. B* 420 (1994), pp. 47–93. DOI: 10.1016/0550-3213(94)90375-1. arXiv: hep-ph/9310302.
[66] Konstantinos Mantzaropoulos. "Effective Field Theories and One-Loop Matching, MSc thesis, University of Ioannina, 2019". In: (2019).
[67] J. de Blas et al. "Effective description of general extensions of the Standard Model: the complete tree-level dictionary". In: *JHEP* 03 (2018), p. 109. DOI: 10.1007/JHEP03(2018)109. arXiv: 1711.10391 [hep-ph].
[68] I. Doršner et al. "Physics of leptoquarks in precision experiments and at particle colliders". In: *Phys. Rept.* 641 (2016), pp. 1–68. DOI: 10.1016/j.physrep.2016.06.001. arXiv: 1603.04993 [hep-ph].
[69] Martin Bauer and Matthias Neubert. "Minimal Leptoquark Explanation for the $R_{D^{(*)}}$, $R_K$, and $(g-2)_g$ Anomalies". In: *Phys. Rev. Lett.* 116.14 (2016), p. 141802. DOI: 10.1103/PhysRevLett.116.141802. arXiv: 1511.01900 [hep-ph].
[70] Andrei Angelescu et al. "On the single leptoquark solutions to the $B$-physics anomalies". In: (Mar. 2021). arXiv: 2103.12504 [hep-ph].
[71] Andreas Crivellin et al. "Scalar Leptoquarks in Leptonic Processes". In: *JHEP* 02 (2021), p. 182. DOI: 10.1007/JHEP02(2021)182. arXiv: 2010.06593 [hep-ph].
[72] Valerio Gherardi, David Marzocca, and Elena Venturini. "Low-energy phenomenology of scalar leptoquarks at one-loop accuracy". In: *JHEP* 01 (2021), p. 138. DOI: 10.1007/JHEP01(2021)138. arXiv: 2008.09548 [hep-ph].
[73] Lina Alasfar et al. "$B$ anomalies under the lens of electroweak precision". In: *JHEP* 12 (2020), p. 016. DOI: 10.1007/JHEP12(2020)016. arXiv: 2007.04400 [hep-ph].
[74] Marzia Bordone et al. "Constraining flavour patterns of scalar leptoquarks in the effective field theory". In: *JHEP* 03 (2021), p. 122. DOI: 10.1007/JHEP03(2021)122. arXiv: 2010.03297 [hep-ph].
[75] Michael J. Dugan and Benjamin Grinstein. "On the vanishing of evanescent operators". In: *Phys. Lett. B* 256 (1991), pp. 239–244. DOI: 10.1016/0370-2693(91)90680-O.
[76] Stefan Herrlich and Ulrich Nierste. "Evanescent operators, scheme dependences and double insertions". In: *Nucl. Phys. B* 455 (1995), pp. 39–58. DOI: 10.1016/0550-3213(95)00474-7. arXiv: hep-ph/9412375.
[77] Wouter Dekens and Peter Stoffer. "Low-energy effective field theory below the electroweak scale: matching at one loop". In: *JHEP* 10 (2019), p. 197. DOI: 10.1007/JHEP10(2019)197. arXiv: 1908.05295 [hep-ph].
[78] Jason Aebischer et al. "SMEFT ATLAS of $\Delta F = 2$ transitions". In: *JHEP* 12 (2020), p. 187. DOI: 10.1007/JHEP12(2020)187. arXiv: 2009.07276 [hep-ph].
[79] Ilja Dorsner. "A scalar leptoquark in SU(5)". In: *Phys. Rev. D* 86 (2012), p. 055009. DOI: 10.1103/PhysRevD.86.055009. arXiv: 1206.5998 [hep-ph].
[80] Ilja Doršner, Svjetlana Fajfer, and Nejc Košnik. "Leptoquark mechanism of neutrino masses within the grand unification framework". In: *Eur. Phys. J. C* 77.6 (2017), p. 417. DOI: 10.1140/epjc/s10052-017-4987-2. arXiv: 1701.08322 [hep-ph].

[81] Ilja Dorsner, Svjetlana Fajfer, and Nejc Kosnik. "Heavy and light scalar leptoquarks in proton decay". In: *Phys. Rev. D* 86 (2012), p. 015013. DOI: 10.1103/PhysRevD.86.015013. arXiv: 1204.0674 [hep-ph].

[82] Julian Heeck and Volodymyr Takhistov. "Inclusive Nucleon Decay Searches as a Frontier of Baryon Number Violation". In: *Phys. Rev. D* 101.1 (2020), p. 015005. DOI: 10.1103/PhysRevD.101.015005. arXiv: 1910.07647 [hep-ph].

[83] Uma Mahanta. "Neutrino masses and mixing angles from leptoquark interactions". In: *Phys. Rev. D* 62 (2000), p. 073009. DOI: 10.1103/PhysRevD.62.073009. arXiv: hep-ph/9909518.

[84] Di Zhang. "Radiative neutrino masses, lepton flavor mixing and muon $g-2$ in a leptoquark model". In: (May 2021). arXiv: 2105.08670 [hep-ph].

[85] Andreas Crivellin and Martin Hoferichter. "Consequences of chirally enhanced explanations of $(g-2)_\mu$ for $h \to \mu\mu$ and $Z \to \mu\mu$". In: (Apr. 2021). arXiv: 2104.03202 [hep-ph].

[86] Peter Athron et al. "New physics explanations of $a_\mu$ in light of the FNAL muon $g-2$ measurement". In: (Apr. 2021). arXiv: 2104.03691 [hep-ph].

[87] Jonathan M. Arnold, Bartosz Fornal, and Mark B. Wise. "Phenomenology of scalar leptoquarks". In: *Phys. Rev. D* 88 (2013), p. 035009. DOI: 10.1103/PhysRevD.88.035009. arXiv: 1304.6119 [hep-ph].

[88] Clara Murgui and Mark B. Wise. "Scalar Leptoquarks, Baryon Number Violation and Pati-Salam Symmetry". In: (May 2021). arXiv: 2105.14029 [hep-ph].

[89] Andrew Kobach. "Baryon Number, Lepton Number, and Operator Dimension in the Standard Model". In: *Phys. Lett. B* 758 (2016), pp. 455–457. DOI: 10.1016/j.physletb.2016.05.050. arXiv: 1604.05726 [hep-ph].

[90] Andreas Helset and Andrew Kobach. "Baryon Number, Lepton Number, and Operator Dimension in the SMEFT with Flavor Symmetries". In: *Phys. Lett. B* 800 (2020), p. 135132. DOI: 10.1016/j.physletb.2019.135132. arXiv: 1909.05853 [hep-ph].

[91] Andrzej J. Buras and Peter H. Weisz. "QCD nonleading corrections to weak decays in dimensional regularization and 't Hooft-Veltman schemes". In: *Nuclear Physics B* 333.1 (1990), pp. 66–99. ISSN: 0550-3213. DOI: https://doi.org/10.1016/0550-3213(90)90223-Z. URL: https://www.sciencedirect.com/science/article/pii/055032139090223Z.

[92] Alejandro Celis et al. "DsixTools: The Standard Model Effective Field Theory Toolkit". In: *Eur. Phys. J. C* 77.6 (2017), p. 405. DOI: 10.1140/epjc/s10052-017-4967-6. arXiv: 1704.04504 [hep-ph].

[93] B. Abi et al. "Measurement of the Positive Muon Anomalous Magnetic Moment to 0.46 ppm". In: *Phys. Rev. Lett.* 126.14 (2021), p. 141801. DOI: 10.1103/PhysRevLett.126.141801. arXiv: 2104.03281 [hep-ex].

[94] G. W. Bennett et al. "Final Report of the Muon E821 Anomalous Magnetic Moment Measurement at BNL". In: *Phys. Rev. D* 73 (2006), p. 072003. DOI: 10.1103/PhysRevD.73.072003. arXiv: hep-ex/0602035.

[95] Jason Aebischer et al. "Effective field theory interpretation of lepton magnetic and electric dipole moments". In: (Feb. 2021). arXiv: 2102.08954 [hep-ph].

[96] V. Andreev et al. "Improved limit on the electric dipole moment of the electron". In: *Nature* 562.7727 (2018), pp. 355–360. DOI: 10.1038/s41586-018-0599-8.

[97] Athanasios Dedes, Howard E. Haber, and Janusz Rosiek. “Seesaw mechanism in the sneutrino sector and its consequences”. In: *JHEP* 11 (2007), p. 059. DOI: 10.1088/1126-6708/2007/11/059. arXiv: 0707.3718 [hep-ph].
[98] Giuliano Panico, Alex Pomarol, and Marc Riembau. “EFT approach to the electron Electric Dipole Moment at the two-loop level”. In: *JHEP* 04 (2019), p. 090. DOI: 10.1007/JHEP04(2019)090. arXiv: 1810.09413 [hep-ph].
[99] W. Dekens et al. “The phenomenology of electric dipole moments in models of scalar leptoquarks”. In: *JHEP* 01 (2019), p. 069. DOI: 10.1007/JHEP01(2019)069. arXiv: 1809.09114 [hep-ph].
[100] K. Abe et al. “Search for proton decay via $p \to e^+\pi^0$ and $p \to \mu^+\pi^0$ in 0.31 megaton·years exposure of the Super-Kamiokande water Cherenkov detector”. In: *Phys. Rev. D* 95.1 (2017), p. 012004. DOI: 10.1103/PhysRevD.95.012004. arXiv: 1610.03597 [hep-ex].
[101] K. Abe et al. “Search for proton decay via $p \to \nu K^+$ using 260 kiloton·year data of Super-Kamiokande”. In: *Phys. Rev. D* 90.7 (2014), p. 072005. DOI: 10.1103/PhysRevD.90.072005. arXiv: 1408.1195 [hep-ex].
[102] Pran Nath and Pavel Fileviez Perez. “Proton stability in grand unified theories, in strings and in branes”. In: *Phys. Rept.* 441 (2007), pp. 191–317. DOI: 10.1016/j.physrep.2007.02.010. arXiv: hep-ph/0601023.
[103] Iason Baldes, Nicole F. Bell, and Raymond R. Volkas. “Baryon Number Violating Scalar Diquarks at the LHC”. In: *Phys. Rev. D* 84 (2011), p. 115019. DOI: 10.1103/PhysRevD.84.115019. arXiv: 1110.4450 [hep-ph].
[104] Thomas Hambye and Julian Heeck. “Proton decay into charged leptons”. In: *Phys. Rev. Lett.* 120.17 (2018), p. 171801. DOI: 10.1103/PhysRevLett.120.171801. arXiv: 1712.04871 [hep-ph].
[105] Juan Carlos Helo, Martin Hirsch, and Toshihiko Ota. “Proton decay at one loop”. In: *Phys. Rev. D* 99.9 (2019), p. 095021. DOI: 10.1103/PhysRevD.99.095021. arXiv: 1904.00036 [hep-ph].
[106] Kostas Mantzaropoulos. “Disentangling SMEFT and UV contributions in h$\to$Z$\gamma$ and h$\to\gamma\gamma$ decays”. In: *Phys. Rev. D* 110.5 (2024), p. 055041. DOI: 10.1103/PhysRevD.110.055041. arXiv: 2407.09145 [hep-ph].
[107] Georges Aad et al. “Observation of a new particle in the search for the Standard Model Higgs boson with the ATLAS detector at the LHC”. In: *Phys. Lett. B* 716 (2012), pp. 1–29. DOI: 10.1016/j.physletb.2012.08.020. arXiv: 1207.7214 [hep-ex].
[108] Serguei Chatrchyan et al. “Observation of a New Boson at a Mass of 125 GeV with the CMS Experiment at the LHC”. In: *Phys. Lett. B* 716 (2012), pp. 30–61. DOI: 10.1016/j.physletb.2012.08.021. arXiv: 1207.7235 [hep-ex].
[109] Gino Isidori, Felix Wilsch, and Daniel Wyler. “The standard model effective field theory at work”. In: *Rev. Mod. Phys.* 96.1 (2024), p. 015006. DOI: 10.1103/RevModPhys.96.015006. arXiv: 2303.16922 [hep-ph].
[110] Morad Aaboud et al. “Measurements of gluon-gluon fusion and vector-boson fusion Higgs boson production cross-sections in the $H \to WW^* \to e\nu\mu\nu$ decay channel in $pp$ collisions at $\sqrt{s} = 13$ TeV with the ATLAS detector”. In: *Phys. Lett. B* 789 (2019), pp. 508–529. DOI: 10.1016/j.physletb.2018.11.064. arXiv: 1808.09054 [hep-ex].
[111] Georges Aad et al. “Measurement of the production cross section for a Higgs boson in association with a vector boson in the $H \to WW^* \to \ell\nu\ell\nu$ channel in $pp$ collisions at

$\sqrt{s} = 13$ TeV with the ATLAS detector". In: *Phys. Lett. B* 798 (2019), p. 134949. DOI: 10.1016/j.physletb.2019.134949. arXiv: 1903.10052 [hep-ex].

[112] Albert M. Sirunyan et al. "Measurements of properties of the Higgs boson decaying to a W boson pair in pp collisions at $\sqrt{s} = 13$ TeV". In: *Phys. Lett. B* 791 (2019), p. 96. DOI: 10.1016/j.physletb.2018.12.073. arXiv: 1806.05246 [hep-ex].

[113] Albert M Sirunyan et al. "Measurement of the inclusive and differential Higgs boson production cross sections in the leptonic WW decay mode at $\sqrt{s} = 13$ TeV". In: *JHEP* 03 (2021), p. 003. DOI: 10.1007/JHEP03(2021)003. arXiv: 2007.01984 [hep-ex].

[114] Albert M Sirunyan et al. "Measurement and interpretation of differential cross sections for Higgs boson production at $\sqrt{s} = 13$ TeV". In: *Phys. Lett. B* 792 (2019), pp. 369–396. DOI: 10.1016/j.physletb.2019.03.059. arXiv: 1812.06504 [hep-ex].

[115] Georges Aad et al. "Measurements of Higgs boson production and couplings in diboson final states with the ATLAS detector at the LHC". In: *Phys. Lett. B* 726 (2013). [Erratum: Phys.Lett.B 734, 406–406 (2014)], pp. 88–119. DOI: 10.1016/j.physletb.2014.05.011. arXiv: 1307.1427 [hep-ex].

[116] Morad Aaboud et al. "Measurements of Higgs boson properties in the diphoton decay channel with 36 fb$^{-1}$ of $pp$ collision data at $\sqrt{s} = 13$ TeV with the ATLAS detector". In: *Phys. Rev. D* 98 (2018), p. 052005. DOI: 10.1103/PhysRevD.98.052005. arXiv: 1802.04146 [hep-ex].

[117] Armen Tumasyan et al. "A portrait of the Higgs boson by the CMS experiment ten years after the discovery." In: *Nature* 607.7917 (2022), pp. 60–68. DOI: 10.1038/s41586-022-04892-x. arXiv: 2207.00043 [hep-ex].

[118] Georges Aad et al. "A detailed map of Higgs boson interactions by the ATLAS experiment ten years after the discovery". In: *Nature* 607.7917 (2022). [Erratum: Nature 612, E24 (2022)], pp. 52–59. DOI: 10.1038/s41586-022-04893-w. arXiv: 2207.00092 [hep-ex].

[119] Georges Aad et al. "Evidence for the Higgs Boson Decay to a Z Boson and a Photon at the LHC". In: *Phys. Rev. Lett.* 132 (2024), p. 021803. DOI: 10.1103/PhysRevLett.132.021803. arXiv: 2309.03501 [hep-ex].

[120] Benjamin Summ and Alexander Voigt. "Extending the Universal One-Loop Effective Action by Regularization Scheme Translating Operators". In: *JHEP* 08 (2018), p. 026. DOI: 10.1007/JHEP08(2018)026. arXiv: 1806.05171 [hep-ph].

[121] Guilherme Guedes, Pablo Olgoso, and José Santiago. "Towards the one loop IR/UV dictionary in the SMEFT: One loop generated operators from new scalars and fermions". In: *SciPost Phys.* 15.4 (2023), p. 143. DOI: 10.21468/SciPostPhys.15.4.143. arXiv: 2303.16965 [hep-ph].

[122] Xiao-Gang He et al. "The SM expected branching ratio for $h \to \gamma\gamma$ and an excess for $h \to Z\gamma$". In: (Feb. 2024). arXiv: 2402.08190 [hep-ph].

[123] Rafael Boto et al. "New physics interpretations for nonstandard values of $h \to Z\gamma$". In: (Dec. 2023). arXiv: 2312.13050 [hep-ph].

[124] T. T. Hong et al. "Decays of Standard Model like Higgs boson $h \to \gamma\gamma, Z\gamma$ in a minimal left-right symmetric model". In: (Dec. 2023). arXiv: 2312.11045 [hep-ph].

[125] Daniele Barducci et al. "Closing in on new chiral leptons at the LHC". In: *JHEP* 12 (2023), p. 154. DOI: 10.1007/JHEP12(2023)154. arXiv: 2311.10130 [hep-ph].

[126] Christophe Grojean et al. "A log story short: running contributions to radiative Higgs decays in the SMEFT". In: (May 2024). arXiv: 2405.20371 [hep-ph].

[127] Sajid Israr and Muhammad Rehman. “Higgs Decay to $Z\gamma$ in the Minimal Supersymmetric Standard Model and Its Nonholomorphic Extension”. In: (July 2024). arXiv: 2407.01210 [hep-ph].

[128] Qing-Hong Cao et al. “Signature of pseudo Nambu–Goldstone Higgs boson in its decay”. In: *Phys. Lett. B* 789 (2019), pp. 233–237. DOI: 10.1016/j.physletb.2018.12.040. arXiv: 1810.07661 [hep-ph].

[129] A. Dedes et al. “The decay $h \to \gamma\gamma$ in the Standard-Model Effective Field Theory”. In: *JHEP* 08 (2018), p. 103. DOI: 10.1007/JHEP08(2018)103. arXiv: 1805.00302 [hep-ph].

[130] A. Dedes, K. Suxho, and L. Trifyllis. “The decay $h \to Z\gamma$ in the Standard-Model Effective Field Theory”. In: *JHEP* 06 (2019), p. 115. DOI: 10.1007/JHEP06(2019)115. arXiv: 1903.12046 [hep-ph].

[131] Sally Dawson and Pier Paolo Giardino. “Higgs decays to $ZZ$ and $Z\gamma$ in the standard model effective field theory: An NLO analysis”. In: *Phys. Rev. D* 97.9 (2018), p. 093003. DOI: 10.1103/PhysRevD.97.093003. arXiv: 1801.01136 [hep-ph].

[132] Sébastien Descotes-Genon et al. “The CKM parameters in the SMEFT”. In: *JHEP* 05 (2019), p. 172. DOI: 10.1007/JHEP05(2019)172. arXiv: 1812.08163 [hep-ph].

[133] R. L. Workman et al. “Review of Particle Physics”. In: *PTEP* 2022 (2022), p. 083C01. DOI: 10.1093/ptep/ptac097.

[134] Geoffrey T. Bodwin and Hee Sok Chung. “New method for fitting coefficients in standard model effective theory”. In: *Phys. Rev. D* 101.11 (2020), p. 115039. DOI: 10.1103/PhysRevD.101.115039. arXiv: 1912.09843 [hep-ph].

[135] Jacob J. Ethier et al. “Combined SMEFT interpretation of Higgs, diboson, and top quark data from the LHC”. In: *JHEP* 11 (2021), p. 089. DOI: 10.1007/JHEP11(2021)089. arXiv: 2105.00006 [hep-ph].

[136] Xu-Xiang Li, Zhe Ren, and Jiang-Hao Yub. “Complete tree-level dictionary between simplified BSM models and SMEFT d≤7 operators”. In: *Phys. Rev. D* 109.9 (2024), p. 095041. DOI: 10.1103/PhysRevD.109.095041. arXiv: 2307.10380 [hep-ph].

[137] Supratim Das Bakshi et al. “Relevance of one-loop SMEFT matching in the 2HDM”. In: (Jan. 2024). arXiv: 2401.12279 [hep-ph].

[138] S. L. Glashow, J. Iliopoulos, and L. Maiani. “Weak Interactions with Lepton-Hadron Symmetry”. In: *Phys. Rev. D* 2 (1970), pp. 1285–1292. DOI: 10.1103/PhysRevD.2.1285.

[139] Sebastien Descotes-Genon et al. “Implications from clean observables for the binned analysis of $B -> K * \mu^+\mu^-$ at large recoil”. In: *JHEP* 01 (2013), p. 048. DOI: 10.1007/JHEP01(2013)048. arXiv: 1207.2753 [hep-ph].

[140] Roel Aaij et al. “Angular analysis of the $B^0 \to K^{*0}\mu^+\mu^-$ decay using 3 fb$^{-1}$ of integrated luminosity”. In: *JHEP* 02 (2016), p. 104. DOI: 10.1007/JHEP02(2016)104. arXiv: 1512.04442 [hep-ex].

[141] Roel Aaij et al. “Measurement of $CP$-Averaged Observables in the $B^0 \to K^{*0}\mu^+\mu^-$ Decay”. In: *Phys. Rev. Lett.* 125.1 (2020), p. 011802. DOI: 10.1103/PhysRevLett.125.011802. arXiv: 2003.04831 [hep-ex].

[142] Roel Aaij et al. “Angular Analysis of the $B^+ \to K^{*+}\mu^+\mu^-$ Decay”. In: *Phys. Rev. Lett.* 126.16 (2021), p. 161802. DOI: 10.1103/PhysRevLett.126.161802. arXiv: 2012.13241 [hep-ex].

[143] R Aaij et al. “Differential branching fraction and angular analysis of the decay $B_s^0 \to \phi\mu^+\mu^-$”. In: *JHEP* 07 (2013), p. 084. DOI: 10.1007/JHEP07(2013)084. arXiv: 1305.2168 [hep-ex].

[144] Roel Aaij et al. “Angular analysis and differential branching fraction of the decay $B_s^0 \to \phi\mu^+\mu^-$”. In: *JHEP* 09 (2015), p. 179. DOI: 10.1007/JHEP09(2015)179. arXiv: 1506.08777 [hep-ex].

[145] Roel Aaij et al. “Branching Fraction Measurements of the Rare $B_s^0 \to \phi\mu^+\mu^-$ and $B_s^0 \to f_2'(1525)\mu^+\mu^-$- Decays”. In: *Phys. Rev. Lett.* 127.15 (2021), p. 151801. DOI: 10.1103/PhysRevLett.127.151801. arXiv: 2105.14007 [hep-ex].

[146] Roel Aaij et al. “Angular analysis of the rare decay $B_s^0 \to \phi\mu^+\mu^-$”. In: *JHEP* 11 (2021), p. 043. DOI: 10.1007/JHEP11(2021)043. arXiv: 2107.13428 [hep-ex].

[147] “Measurement of lepton universality parameters in $B^+ \to K^+\ell^+\ell^-$ and $B^0 \to K^{*0}\ell^+\ell^-$ decays”. In: (Dec. 2022). arXiv: 2212.09153 [hep-ex].

[148] “Test of lepton universality in $b \to s\ell^+\ell^-$ decays”. In: (Dec. 2022). arXiv: 2212.09152 [hep-ex].

[149] “Measurement of the $\mathrm{B_S^0}\to\mu^+\mu^-$ decay properties and search for the $\mathrm{B^0}\to\mu^+\mu^-$ decay in proton-proton collisions at $\sqrt{s} = 13$ TeV”. In: (Dec. 2022). arXiv: 2212.10311 [hep-ex].

[150] Martin Beneke, Christoph Bobeth, and Robert Szafron. “Power-enhanced leading-logarithmic QED corrections to $B_q \to \mu^+\mu^-$”. In: *JHEP* 10 (2019). [Erratum: JHEP 11, 099 (2022)], p. 232. DOI: 10.1007/JHEP10(2019)232. arXiv: 1908.07011 [hep-ph].

[151] Marcel Algueró et al. “Disentangling lepton flavor universal and lepton flavor universality violating effects in b→sℓ+ℓ- transitions”. In: *Phys. Rev. D* 105.11 (2022), p. 113007. DOI: 10.1103/PhysRevD.105.113007. arXiv: 2205.15212 [hep-ph].

[152] Nico Gubernari et al. “Improved theory predictions and global analysis of exclusive $b \to s\mu^+\mu^-$ processes”. In: *JHEP* 09 (2022), p. 133. DOI: 10.1007/JHEP09(2022)133. arXiv: 2206.03797 [hep-ph].

[153] Marco Ciuchini et al. “Constraints on lepton universality violation from rare B decays”. In: *Phys. Rev. D* 107.5 (2023), p. 055036. DOI: 10.1103/PhysRevD.107.055036. arXiv: 2212.10516 [hep-ph].

[154] Marcel Algueró et al. “To (b)e or not to (b)e: no electrons at LHCb”. In: *Eur. Phys. J. C* 83.7 (2023), p. 648. DOI: 10.1140/epjc/s10052-023-11824-0. arXiv: 2304.07330 [hep-ph].

[155] Andrzej J. Buras and Jennifer Girrbach. “Left-handed $Z'$ and $Z$ FCNC quark couplings facing new $b \to s\mu^+\mu^-$ data”. In: *JHEP* 12 (2013), p. 009. DOI: 10.1007/JHEP12(2013)009. arXiv: 1309.2466 [hep-ph].

[156] Rhorry Gauld, Florian Goertz, and Ulrich Haisch. “On minimal $Z'$ explanations of the $B \to K^*\mu^+\mu^-$ anomaly”. In: *Phys. Rev. D* 89 (2014), p. 015005. DOI: 10.1103/PhysRevD.89.015005. arXiv: 1308.1959 [hep-ph].

[157] Wolfgang Altmannshofer et al. “Quark flavor transitions in $L_\mu - L_\tau$ models”. In: *Phys. Rev. D* 89 (2014), p. 095033. DOI: 10.1103/PhysRevD.89.095033. arXiv: 1403.1269 [hep-ph].

[158] Andreas Crivellin, Giancarlo D’Ambrosio, and Julian Heeck. “Explaining $h \to \mu^\pm\tau^\mp$, $B \to K^*\mu^+\mu^-$ and $B \to K\mu^+\mu^-/B \to Ke^+e^-$ in a two-Higgs-doublet model with gauged $L_\mu - L_\tau$”. In: *Phys. Rev. Lett.* 114 (2015), p. 151801. DOI: 10.1103/PhysRevLett.114.151801. arXiv: 1501.00993 [hep-ph].

[159] Andreas Crivellin, Giancarlo D'Ambrosio, and Julian Heeck. "Addressing the LHC flavor anomalies with horizontal gauge symmetries". In: *Phys. Rev. D* 91.7 (2015), p. 075006. DOI: 10.1103/PhysRevD.91.075006. arXiv: 1503.03477 [hep-ph].
[160] Christoph Niehoff, Peter Stangl, and David M. Straub. "Violation of lepton flavour universality in composite Higgs models". In: *Phys. Lett. B* 747 (2015), pp. 182–186. DOI: 10.1016/j.physletb.2015.05.063. arXiv: 1503.03865 [hep-ph].
[161] Gudrun Hiller and Martin Schmaltz. "$R_K$ and future $b \to s\ell\ell$ physics beyond the standard model opportunities". In: *Phys. Rev. D* 90 (2014), p. 054014. DOI: 10.1103/PhysRevD.90.054014. arXiv: 1408.1627 [hep-ph].
[162] Rodrigo Alonso, Benjamín Grinstein, and Jorge Martin Camalich. "Lepton universality violation and lepton flavor conservation in $B$-meson decays". In: *JHEP* 10 (2015), p. 184. DOI: 10.1007/JHEP10(2015)184. arXiv: 1505.05164 [hep-ph].
[163] Lorenzo Calibbi, Andreas Crivellin, and Toshihiko Ota. "Effective Field Theory Approach to $b \to s\ell\ell^{(\prime)}$, $B \to K^{(*)}\nu\overline{\nu}$ and $B \to D^{(*)}\tau\nu$ with Third Generation Couplings". In: *Phys. Rev. Lett.* 115 (2015), p. 181801. DOI: 10.1103/PhysRevLett.115.181801. arXiv: 1506.02661 [hep-ph].
[164] Ben Gripaios, M. Nardecchia, and S. A. Renner. "Linear flavour violation and anomalies in B physics". In: *JHEP* 06 (2016), p. 083. DOI: 10.1007/JHEP06(2016)083. arXiv: 1509.05020 [hep-ph].
[165] Pere Arnan et al. "Loop effects of heavy new scalars and fermions in $b \to s\mu^+\mu^-$". In: *JHEP* 04 (2017), p. 043. DOI: 10.1007/JHEP04(2017)043. arXiv: 1608.07832 [hep-ph].
[166] B. Grinstein, S. Pokorski, and G. G. Ross. "Lepton non-universality in $B$ decays and fermion mass structure". In: *JHEP* 12 (2018), p. 079. DOI: 10.1007/JHEP12(2018)079. arXiv: 1809.01766 [hep-ph].
[167] Pere Arnan et al. "Generic Loop Effects of New Scalars and Fermions in $b \to s\ell^+\ell^-$, $(g-2)_\mu$ and a Vector-like 4$^{\text{th}}$ Generation". In: *JHEP* 06 (2019), p. 118. DOI: 10.1007/JHEP06(2019)118. arXiv: 1904.05890 [hep-ph].
[168] Quan-Yi Hu, Ya-Dong Yang, and Min-Di Zheng. "Revisiting the $B$-physics anomalies in $R$-parity violating MSSM". In: *Eur. Phys. J. C* 80.5 (2020), p. 365. DOI: 10.1140/epjc/s10052-020-7940-8. arXiv: 2002.09875 [hep-ph].
[169] Min-Di Zheng and Hong-Hao Zhang. "Studying the $b \to s\ell^+\ell^-$ anomalies and $(g-2)_\mu$ in $R$-parity violating MSSM framework with the inverse seesaw mechanism". In: *Phys. Rev. D* 104.11 (2021), p. 115023. DOI: 10.1103/PhysRevD.104.115023. arXiv: 2105.06954 [hep-ph].
[170] P. S. Bhupal Dev, Amarjit Soni, and Fang Xu. "Hints of Natural Supersymmetry in Flavor Anomalies?" In: (June 2021). arXiv: 2106.15647 [hep-ph].
[171] Weicong Huang and Yi-Lei Tang. "Flavor anomalies at the LHC and the R-parity violating supersymmetric model extended with vectorlike particles". In: *Phys. Rev. D* 92.9 (2015), p. 094015. DOI: 10.1103/PhysRevD.92.094015. arXiv: 1509.08599 [hep-ph].
[172] Diganta Das et al. "Scrutinizing $R$-parity violating interactions in light of $R_{K^{(*)}}$ data". In: *Phys. Rev. D* 96.9 (2017), p. 095033. DOI: 10.1103/PhysRevD.96.095033. arXiv: 1705.09188 [hep-ph].
[173] Guang Hua Duan et al. "A minimal $U(1)'$ extension of MSSM in light of the B decay anomaly". In: *Phys. Lett. B* 789 (2019), pp. 54–58. DOI: 10.1016/j.physletb.2018.12.005. arXiv: 1808.04116 [hep-ph].

[174] Alexander Bednyakov and Alfiia Mukhaeva. "Flavour Anomalies in a $U(1)$ SUSY Extension of the SM". In: *Symmetry* 13.2 (2021), p. 191. DOI: 10.3390/sym13020191.
[175] Min-Di Zheng, Feng-Zhi Chen, and Hong-Hao Zhang. "Explaining anomalies of B-physics, muon $g-2$ and W mass in R-parity violating MSSM with seesaw mechanism". In: *Eur. Phys. J. C* 82.10 (2022), p. 895. DOI: 10.1140/epjc/s10052-022-10822-y. arXiv: 2207.07636 [hep-ph].
[176] Shaaban Khalil. "Explaining the $R_K$ and $R_{K^*}$ Anomalies With Right-handed Sneutrino". In: *J. Phys. G* 45.12 (2018), p. 125004. DOI: 10.1088/1361-6471/aaeba3. arXiv: 1706.07337 [hep-ph].
[177] Georges Aad et al. "Observation of a new particle in the search for the Standard Model Higgs boson with the ATLAS detector at the LHC". In: *Phys. Lett.* B716 (2012), pp. 1–29. DOI: 10.1016/j.physletb.2012.08.020. arXiv: 1207.7214 [hep-ex].
[178] Serguei Chatrchyan et al. "Observation of a new boson at a mass of 125 GeV with the CMS experiment at the LHC". In: *Phys. Lett.* B716 (2012), pp. 30–61. DOI: 10.1016/j.physletb.2012.08.021. arXiv: 1207.7235 [hep-ex].
[179] Hans Peter Nilles. "Supersymmetry, Supergravity and Particle Physics". In: *Phys. Rept.* 110 (1984), pp. 1–162. DOI: 10.1016/0370-1573(84)90008-5.
[180] Howard E. Haber and Gordon L. Kane. "The Search for Supersymmetry: Probing Physics Beyond the Standard Model". In: *Phys. Rept.* 117 (1985), pp. 75–263. DOI: 10.1016/0370-1573(85)90051-1.
[181] Wolfgang Altmannshofer and David M. Straub. "New Physics in $B \to K^*\mu\mu$?" In: *Eur. Phys. J. C* 73 (2013), p. 2646. DOI: 10.1140/epjc/s10052-013-2646-9. arXiv: 1308.1501 [hep-ph].
[182] M. A. Boussejra, F. Mahmoudi, and G. Uhlrich. "Flavor anomalies in supersymmetric scenarios with nonminimal flavor violation". In: *Phys. Rev. D* 106.1 (2022), p. 015018. DOI: 10.1103/PhysRevD.106.015018. arXiv: 2201.04659 [hep-ph].
[183] Janusz Rosiek et al. "SUSY_FLAVOR: A Computational Tool for FCNC and CP-violating Processes in the MSSM". In: *Comput. Phys. Commun.* 181 (2010), pp. 2180–2205. DOI: 10.1016/j.cpc.2010.07.047. arXiv: 1003.4260 [hep-ph].
[184] A. Crivellin et al. "SUSY_FLAVOR v2: A Computational tool for FCNC and CP-violating processes in the MSSM". In: *Comput. Phys. Commun.* 184 (2013), pp. 1004–1032. DOI: 10.1016/j.cpc.2012.11.007. arXiv: 1203.5023 [hep-ph].
[185] Janusz Rosiek. "SUSY FLAVOR v2.5: a computational tool for FCNC and CP-violating processes in the MSSM". In: *Comput. Phys. Commun.* 188 (2015), pp. 208–210. DOI: 10.1016/j.cpc.2014.10.003. arXiv: 1410.0606 [hep-ph].
[186] A. Dedes et al. "Mass Insertions vs. Mass Eigenstates calculations in Flavour Physics". In: *JHEP* 06 (2015), p. 151. DOI: 10.1007/JHEP06(2015)151. arXiv: 1504.00960 [hep-ph].
[187] Wolfgang Adam and Iacopo Vivarelli. "Status of searches for electroweak-scale supersymmetry after LHC Run 2". In: *Int. J. Mod. Phys. A* 37.02 (2022), p. 2130022. DOI: 10.1142/S0217751X21300222. arXiv: 2111.10180 [hep-ex].
[188] Gerhard Buchalla, Andrzej J. Buras, and Markus E. Lautenbacher. "Weak decays beyond leading logarithms". In: *Rev. Mod. Phys.* 68 (1996), pp. 1125–1144. DOI: 10.1103/RevModPhys.68.1125. arXiv: hep-ph/9512380.
[189] Gudrun Hiller and Martin Schmaltz. "Diagnosing lepton-nonuniversality in $b \to s\ell\ell$". In: *JHEP* 02 (2015), p. 055. DOI: 10.1007/JHEP02(2015)055. arXiv: 1411.4773 [hep-ph].

[190] Wolfgang Altmannshofer, Peter Stangl, and David M. Straub. "Interpreting Hints for Lepton Flavor Universality Violation". In: *Phys. Rev. D* 96.5 (2017), p. 055008. DOI: 10.1103/PhysRevD.96.055008. arXiv: 1704.05435 [hep-ph].

[191] David London and Joaquim Matias. "$B$ Flavour Anomalies: 2021 Theoretical Status Report". In: (Oct. 2021). DOI: 10.1146/annurev-nucl-102020-090209. arXiv: 2110.13270 [hep-ph].

[192] C. Bobeth et al. "Analysis of neutral Higgs boson contributions to the decays $\bar{B}(\ s^{)} \to \ell^+\ell^-$ and $\bar{B} \to K\ell^+\ell^-$". In: *Phys. Rev. D* 64 (2001), p. 074014. DOI: 10.1103/PhysRevD.64.074014. arXiv: hep-ph/0104284.

[193] Athanasios Dedes, Herbert K. Dreiner, and Ulrich Nierste. "Correlation of $B_s \to \mu^+\mu^-$ and (g-2) ($\mu$) in minimal supergravity". In: *Phys. Rev. Lett.* 87 (2001), p. 251804. DOI: 10.1103/PhysRevLett.87.251804. arXiv: hep-ph/0108037.

[194] Athanasios Dedes and Apostolos Pilaftsis. "Resummed Effective Lagrangian for Higgs Mediated FCNC Interactions in the CP Violating MSSM". In: *Phys. Rev. D* 67 (2003), p. 015012. DOI: 10.1103/PhysRevD.67.015012. arXiv: hep-ph/0209306.

[195] Andrzej J. Buras et al. "$\Delta M_{d,s}, B^0 d, s \to \mu^+\mu^-$ and $B \to X_s\gamma$ in supersymmetry at large $\tan\beta$". In: *Nucl. Phys. B* 659 (2003), p. 3. DOI: 10.1016/S0550-3213(03)00190-1. arXiv: hep-ph/0210145.

[196] Damir Becirevic et al. "Complementarity of the constraints on New Physics from $B_s \to \mu^+\mu^-$ and from $B \to Kl^+l^-$ decays". In: *Phys. Rev. D* 86 (2012), p. 034034. DOI: 10.1103/PhysRevD.86.034034. arXiv: 1205.5811 [hep-ph].

[197] Athanasios Dedes, Janusz Rosiek, and Philip Tanedo. "Complete One-Loop MSSM Predictions for $B \to \ell\ell'$ at the Tevatron and LHC". In: *Phys. Rev. D* 79 (2009), p. 055006. DOI: 10.1103/PhysRevD.79.055006. arXiv: 0812.4320 [hep-ph].

[198] Christoph Bobeth, Gudrun Hiller, and Giorgi Piranishvili. "CP Asymmetries in bar $B \to \bar{K}^*(\to \bar{K}\pi)\bar{\ell}\ell$ and Untagged $\bar{B}_s$, $B_s \to \phi(\to K^+K^-)\bar{\ell}\ell$ Decays at NLO". In: *JHEP* 07 (2008), p. 106. DOI: 10.1088/1126-6708/2008/07/106. arXiv: 0805.2525 [hep-ph].

[199] Janusz Rosiek. "Complete Set of Feynman Rules for the Minimal Supersymmetric Extension of the Standard Model". In: *Phys. Rev. D* 41 (1990), p. 3464. DOI: 10.1103/PhysRevD.41.3464.

[200] Janusz Rosiek. "Complete set of Feynman rules for the MSSM: Erratum". In: (Nov. 1995). arXiv: hep-ph/9511250.

[201] Athanasios Dedes, John R. Ellis, and Martti Raidal. "Higgs mediated $B^0_{s,d} \to \mu\tau, e\tau$ and $\tau \to 3\mu, e\mu\mu$ decays in supersymmetric seesaw models". In: *Phys. Lett. B* 549 (2002), pp. 159–169. DOI: 10.1016/S0370-2693(02)02900-3. arXiv: hep-ph/0209207.

[202] Sheldon L. Glashow, Diego Guadagnoli, and Kenneth Lane. "Lepton Flavor Violation in $B$ Decays?" In: *Phys. Rev. Lett.* 114 (2015), p. 091801. DOI: 10.1103/PhysRevLett.114.091801. arXiv: 1411.0565 [hep-ph].

[203] Andreas Crivellin et al. "Lepton flavour violation in the MSSM: exact diagonalization vs mass expansion". In: *JHEP* 06 (2018), p. 003. DOI: 10.1007/JHEP06(2018)003. arXiv: 1802.06803 [hep-ph].

[204] Marzia Bordone, Gino Isidori, and Andrea Pattori. "On the Standard Model predictions for $R_K$ and $R_{K^*}$". In: *Eur. Phys. J. C* 76.8 (2016), p. 440. DOI: 10.1140/epjc/s10052-016-4274-7. arXiv: 1605.07633 [hep-ph].

[205] Janusz Rosiek. "MassToMI —A Mathematica package for an automatic Mass Insertion expansion". In: *Comput. Phys. Commun.* 201 (2016), pp. 144–158. DOI: 10.1016/j.cpc.2015.12.011. arXiv: 1509.05030 [hep-ph].

[206] Georges Aad et al. "Search for long-lived charginos based on a disappearing-track signature using 136 fb$^{-1}$ of pp collisions at $\sqrt{s}$ = 13 TeV with the ATLAS detector". In: *Eur. Phys. J. C* 82.7 (2022), p. 606. DOI: 10.1140/epjc/s10052-022-10489-5. arXiv: 2201.02472 [hep-ex].

[207] "Search for chargino-neutralino production with mass splittings near the electroweak scale in three-lepton final states in $\sqrt{s}$ = 13 TeV $pp$ collisions with the ATLAS detector". In: (2019). URL: http://cds.cern.ch/record/2676597.

[208] Tamas Almos Vami. "Searches for gluinos and squarks". In: *PoS* LHCP2019 (2019). Ed. by Pablo Roig Garcés et al., p. 168. DOI: 10.22323/1.350.0168. arXiv: 1909.11753 [hep-ex].

[209] Georges Aad et al. "Search for direct production of charginos, neutralinos and sleptons in final states with two leptons and missing transverse momentum in $pp$ collisions at $\sqrt{s}$ = 8 TeV with the ATLAS detector". In: *JHEP* 05 (2014), p. 071. DOI: 10.1007/JHEP05(2014)071. arXiv: 1403.5294 [hep-ex].

[210] Georges Aad et al. "Summary of the ATLAS experiment's sensitivity to supersymmetry after LHC Run 1 — interpreted in the phenomenological MSSM". In: *JHEP* 10 (2015), p. 134. DOI: 10.1007/JHEP10(2015)134. arXiv: 1508.06608 [hep-ex].

[211] Albert M Sirunyan et al. "Search for top squark production in fully-hadronic final states in proton-proton collisions at $\sqrt{s}$ = 13 TeV". In: *Phys. Rev. D* 104.5 (2021), p. 052001. DOI: 10.1103/PhysRevD.104.052001. arXiv: 2103.01290 [hep-ex].

[212] Sezen Sekmen. "Highlights on Supersymmetry and Exotic Searches at the LHC". In: *32nd Rencontres de Blois on Particle Physics and Cosmology*. Apr. 2022. arXiv: 2204.03053 [hep-ex].

[213] Georges Aad et al. "Search for new phenomena in final states with $b$-jets and missing transverse momentum in $\sqrt{s}$ = 13 TeV $pp$ collisions with the ATLAS detector". In: *JHEP* 05 (2021), p. 093. DOI: 10.1007/JHEP05(2021)093. arXiv: 2101.12527 [hep-ex].

[214] Georges Aad et al. "Search for bottom-squark pair production in $pp$ collision events at $\sqrt{s}$ = 13 TeV with hadronically decaying $\tau$-leptons, $b$-jets and missing transverse momentum using the ATLAS detector". In: *Phys. Rev. D* 104.3 (2021), p. 032014. DOI: 10.1103/PhysRevD.104.032014. arXiv: 2103.08189 [hep-ex].

[215] Andreas Crivellin, Lars Hofer, and Janusz Rosiek. "Complete resummation of chirally-enhanced loop-effects in the MSSM with non-minimal sources of flavor-violation". In: *JHEP* 07 (2011), p. 017. DOI: 10.1007/JHEP07(2011)017. arXiv: 1103.4272 [hep-ph].

[216] P.A. Zyla et al. "Review of Particle Physics". In: *PTEP* 2020.8 (2020). and 2021 update, p. 083C01. DOI: 10.1093/ptep/ptaa104.

[217] S. Bertolini, Francesca Borzumati, and A. Masiero. "QCD Enhancement of Radiative b Decays". In: *Phys. Rev. Lett.* 59 (1987), p. 180. DOI: 10.1103/PhysRevLett.59.180.

[218] John S. Hagelin, S. Kelley, and Toshiaki Tanaka. "Supersymmetric flavor changing neutral currents: Exact amplitudes and phenomenological analysis". In: *Nucl. Phys. B* 415 (1994), pp. 293–331. DOI: 10.1016/0550-3213(94)90113-9.

[219] F. Gabbiani et al. "A Complete analysis of FCNC and CP constraints in general SUSY extensions of the standard model". In: *Nucl. Phys. B* 477 (1996), pp. 321–352. DOI: 10.1016/0550-3213(96)00390-2. arXiv: hep-ph/9604387.

[220] Helmut Eberl et al. “Imprint of SUSY in radiative B-meson decays”. In: *Phys. Rev. D* 104.7 (2021), p. 075025. DOI: 10.1103/PhysRevD.104.075025. arXiv: 2106.15228 [hep-ph].

[221] G. Passarino and M. J. G. Veltman. “One Loop Corrections for e+ e- Annihilation Into mu+ mu- in the Weinberg Model”. In: *Nucl. Phys. B* 160 (1979), pp. 151–207. DOI: 10.1016/0550-3213(79)90234-7.

[222] Lisa L. Everett et al. “Alternative approach to b —> s gamma in the uMSSM”. In: *JHEP* 01 (2002), p. 022. DOI: 10.1088/1126-6708/2002/01/022. arXiv: hep-ph/0112126.

[223] B. Abi et al. “Measurement of the Positive Muon Anomalous Magnetic Moment to 0.46 ppm”. In: *Phys. Rev. Lett.* 126.14 (2021), p. 141801. DOI: 10.1103/PhysRevLett.126.141801. arXiv: 2104.03281 [hep-ex].

[224] Francesca Borzumati et al. “Gluino contribution to radiative B decays: Organization of QCD corrections and leading order results”. In: *Phys. Rev. D* 62 (2000), p. 075005. DOI: 10.1103/PhysRevD.62.075005. arXiv: hep-ph/9911245.

[225] Andreas Crivellin and Luc Schnell. “Complete Set of Feynman Rules for Scalar Leptoquarks”. In: (May 2021). arXiv: 2105.04844 [hep-ph].